# THE IMPACT OF VANADYL SULFATE-ENHANCED ONCOLYTIC VIRUS IMMUNOTHERAPY ON THE ANTITUMOR IMMUNE RESPONSE

**NOUF ALLUQMANI**

Thesis submitted to the University of Ottawa
in partial Fulfillment of the requirements for the
Doctor of Philosophy in Microbiology and Immunology

Department of Biochemistry, Microbiology & Immunology
Faculty of Medicine
University of Ottawa

**Abstract**

Oncolytic viruses (OVs) are promising tumor-selective treatments, and the efficacy of OV therapies has been shown to depend heavily on the successful delivery and spread of these agents within the tumor mass to generate profound immunostimulatory effects. We have previously reported the potential of vanadium-based compounds such as vanadyl sulfate (VS) as immune-stimulatory enhancers of OV immunotherapy. These compounds, in conjunction with RNA-based OVs such as oncolytic VSVΔ51, improve viral spread and oncolysis, leading to long-term antitumor immunity and prolonged survival in resistant tumor models as previously reported. This effect is associated with a virus-induced antiviral type I IFN response shifting towards a type II IFN response. Here, the systemic impact and the relevant immunological changes following VS/VSVΔ51 combination therapy were investigated to understand the immunological mechanism of action leading to improved antitumor responses. We screened for the secretion of chemokines and cytokines in vivo to understand the mechanism of action regulating the recruitment of immune cells to the tumor in the CT26WT tumor model following treatment. Additionally, the antigen-specific immune response was investigated to further identify the relevant immunological changes following treatment with the VS+VSVΔ51 combination. Our data revealed that VS+VSVΔ51 combination therapy significantly increased the levels of IFN-γ and IL-6, and other key important pro-inflammatory cytokines and chemokines. Improved tumor antigen-specific T-cell responses were observed following the combined therapy. Supported by relevant immunological changes and as a proof of concept for the design of more effective therapeutic regimens, we found that local delivery of VSVΔ51 encoded with IL-12 or with other transgenes in combination with VS further improved therapeutic outcomes in a syngeneic CT26WT colon cancer model. We found that CD8+ T cells and Natural Killer (NK) cells play significant roles in establishing the therapeutic efficacy that we observed; Furthermore, engineering new and targeted therapeutic platforms to impact the antitumor immune response further improves the therapeutic benefits of the combined therapy.

I dedicate my Ph.D. to

To the whole world

To the science world

To all immunologist

To the immunotherapy world

To all cancer patients

To my cousin Salema (breast cancer patient)

To the Kingdom of Saudi Arabia

To King Faisal Specialist Hospital and Research Centre

To my beloved mother, father, and siblings

To my beloved nieces and nephews

To my close friends

To my supporters

To myself

**Acknowledgements**

In the name of Allah, the most gracious, the most merciful, all praise of gratitude and thankfulness are due to Allah, for enabling me to complete this work, and making my dream come true and peace and blessings of Allah be upon His Messenger Muhammad, who says: "Whoever does not thank people (for their favours) is not thankful to Allah". This research would not have been possible without the support and assistance of several people. I want to thank them all, and I ask Allah to reward them on my behalf.

First and foremost, a special thanks to King Faisal Specialist Hospital and Research Centre for believing in me and allowing me to come abroad and complete my graduate studies at one of the best universities. Special thanks to Dr. Khalid Abu Khabar for being the first one to make this possible and for believing in me. Thank you to all the personnel at the academic and training affairs, scholarship and training section at KFSHRC for all their guidance, assistance, and for everything. I have been chosen to receive a full-covered scholarship to pursue my higher education. This support allowed me to pursue my ambitions wholeheartedly, driving me forward in my pursuit of becoming an expert in the field of oncolytic immunotherapy. I dedicate this achievement to them and my beloved country, Saudi Arabia.

I have been given a great opportunity that is life-changing for me. My journey has things that I chose and fought hard for and things that were on my way as part of my experience known as challenges, I have enjoyed every single moment of it the sad, the stressed, the hard, and the happy moments and my time was incredibly so unique and special that my whole future will be built based on it. As I know this is not enough to describe how amazing my whole journey was, I am so grateful for everything.

I would like to express my sincere gratitude and hearty thanks to my supervisor Dr. Jean-Simon Diallo for believing in me, for his continuous support during my Ph.D. studies and

for his patience, motivation, and immense knowledge. His guidance helped me in all the time of research and writing of this thesis. I could not have imagined having a better advisor and mentor for my Ph.D. studies. His invaluable help of constructive comments and suggestions throughout the experimental and thesis works have contributed to the success of this research. Thank you to him for making me feel that I have another family, who are always there with their support and care. He makes not just every day in my life, but also every moment in my graduate study a learning process that provides me with precious knowledge and many professional skills and techniques that are going to be part of my success and achievements in the future.

Besides my supervisor, I would like to thank the rest of my thesis committee: Dr. Alain Stintzi, and Dr. Douglas Gray, Dr. Michele Ardolino, Dr. Rebecca Auer for their insightful comments and encouragement, but also for their questions which encouraged me to widen my research from various perspectives. Thank you for believing in me and thank you for always giving me chances to do better and to achieve more.

I would like to thank Dr. Almohanad Alkayyal for helping me during my Ph.D. and for his guidance and for believing in me.

I would also like to thank my lab members, who shared with me most of my time during my Ph.D. Thank you to all the current Diallo lab members thank you to Dr. Rozanne Arulanandam, Dr. Elena Godbout, Andrew Chen, Anne Landry, Zaid Taha, Anna Jirovec, Boaz Wong, Akram Alwithenani, Glib Maznyi, Judy Sobh, Marcus Spinelli, Max Thomson and the former Diallo lab members for their encouragement, kindness and support.

Special Thanks to my best friend Zaid Taha for working with me as a team, supporting me and inspiring me in many ways. We have shared a lot of great moments starting from coffee time, our discussion, time at the gym, spinning classes, food, and shopping times to the flow

cytometry obsessions and animal workaholic. We have built a strong bond that will be part of our successes in the future. I cannot thank you enough for everything, thank you for always being there and for everything.

During my time here and working in one of the biggest research centers for the cancer therapeutic program that focuses on immunotherapies (OHRI- Cancer Center 3rd floor), I have met amazing people who made my time here remarkable and incredible. I would like to thank all the OHRI members including Scientists, the personnel of the administration office, members, and students. Thank you so much for everything, you contributed to all my achievements. I would like to give a special thanks to Carole Dore for managing the whole floor and making my lab work easy and professional, thank you so much for your invaluable contributions to this work. Thank you for everyone that I have met during my time there.

I would like to acknowledge my family for believing in me and their support. First and foremost, thank you to my mother of joy, who always supports and says to me that you have all the abilities to do anything, you are the hope for so many people, who wait for your success and accomplishments. Thank you, my mother, for your endless care and love. Thank you for my father, who is my ideal person in this life. Looking into how he builds his life from zero always motivates me to work hard and achieve my goals in a productive way. He is the reason I can do all of this and for empowering me as a woman. He is one of the milestones in the educational world. I dedicate this accomplishment to him, and I hope he recovers soon from the heart stroke that has major impact on his health and our hearts since the beginning of 2023, may Allah grant him good health and long life. I will not forget to thank my sisters and brothers for their prayers and warm wishes, especially my brother Abdul-Aziz, who is my biggest support and my friend. Thank you to all my nieces and nephews for their care and love and

special thanks to my niece Hala and my nephew Feras for their unconditioned love and precious words.

I also dedicated this work to my cousin Salema who got recently diagnosed with breast cancer, I hope this work contribute to the cancer therapy research where because of it significant changes could be made to this filed.

To all my friends thank you so much for your endless support and care. A special thanks to my friends Halah Al-Zawawi and Nedaa Osama, I am so lucky to have such great friends who despite the long distance always there for me. I thank you for your unconditional friendship, love, unyielding support. Thank you to my friend Nawal Alsadi for her care and support and for making my travel adventures more exciting and full of great memories. A special thanks go to my social media friends for their support, prayers, and wishes.

I would like to acknowledge the Saudi Arabian Culture Bureau (SACB) in Canada for their support during my Ph.D. studies and for making this journey full of incredible opportunities to explore, learn, and expand my horizons. Thank you to my supervisor there Dr. Ali Elghirani for his support and guidance. Thank you to all the personnel of SACB and KFSHRC, who are always there to provide me with the great support and assistance to achieve all of these accomplishments.

Finally, I would like to thank Dr. Vera Tang for training and assisting me during my work at uOttawa Flow Cytometry & Virometry Core Facility and Fernando Ortiz for training and assisting me during my work at Cell Sorting and Flow Cytometry Core Facility at the OHRI facility. Thank you to all the personnel of the Animal Care and Veterinary Service of the Faculty of Medicine at the University of Ottawa for their support. Thank you to all the mice that have been sacrificed during this work for their significant contributions.

I would like to thank my cats EmmaRose, Gucci, and Sky for brining joy to my life and for their companies. You have been such a blessing addition to my life.

To each of these individuals, I extend my deepest appreciation.

**Table of Contents**

**List of Abbreviations**

| | |
|---|---|
| 4T1 | tumor-bearing mice breast carcinoma cell line |
| 786-0 | human renal adenocarcinoma cell line |
| ACK | Ammonium-Chloride-Potassium. |
| ADCC | antibody-dependent cellular cytotoxicity. |
| AML | Acute Myeloid Leukemia. |
| APCs | Antigen Presenting Cells. |
| Asialo GM1 | Asialo ganglio-N-tetraosylceramide |
| ANOVA | Analysis of variance |
| B16F10 | murine melanoma cell line |
| BMOV | Bismaltolato oxovanadium (IV). |
| CARs | Chimeric Antigen Receptors |
| CD | Cluster of differentiation |
| cDNA | complementary DNA |
| CFSE | carboxyfluorescein succinimidyl ester. |
| CFSEHi | carboxyfluorescein succinimidyl ester High |
| CFSELo | carboxyfluorescein succinimidyl ester Low |
| CT26WT | tumor-bearing mice colon carcinoma CT26 wild type cell line |
| CTLA4 | Cytotoxic T Lymphocyte-Associated Antigen-4 |
| CTL | Cytotoxic T Lymphocyte |
| DAMPs | Damage Associated Molecular Patterns. |
| DBT | tumor-bearing mice glioma cell line |
| DC- | Dendritic cells |
| DNA | deoxyribonucleic acid |
| DMEM | Dulbecco's Modified Eagle Medium |
| EGFR | Epidermal Growth Factor Receptor |
| ELISA | Enzyme-linked immunosorbent assay |
| ELISPOT | enzyme-linked immune absorbent spot |
| FACS | fluorescence-activated cell sorting |
| FBS | Fetal Bovine Serum |
| FDA | Food and Drug Administration |
| G-CSF | Granulocyte Colony Stimulating Factor |
| GDP | Guanosine diphosphate |
| GM-CSF | Granulocyte Macrophage Colony Stimulating Factor. |
| GLUT4 | Glucose transporter type 4 |
| GP- | Glycoprotein. |
| GPCRs | G protein-coupled receptors. |
| gp70 | endogenous murine leukemia virus envelope glycoprotein 70 |
| GTP | Guanosine triphosphate |
| HDAC | Histone deacetylase. |
| HDIL-2 | high-dose Iinterlukin-2 |
| HEPES | 4-(2-hydroxyethyl)-1-piperazineethane sulfonic acid buffering agent |
| hpi | hours post-infection |
| HSV | Herpes Simplex Virus, type 1. |
| IA/IE | both I-A and I-E are subregion-encoded glycoproteins of MHC II |
| ICIs | Immune Checkpoint Inhibitors |

| | |
|---|---|
| ICV | Infected cell vaccine. |
| IFN I | Interferon type I |
| IFN II | Interferon type II |
| IFN-β | Interferon Beta |
| IFN-γ | Interferon gamma |
| IgG1 | Immunoglobulin G1 |
| IL1 β | Interleukin 1 beta |
| IL-2 | Interleukin 2 |
| IL4 | Interleukin 4 |
| IL5 | Interleukin 5 |
| IL-6 | Interleukin 6 |
| IL7¬ ¬ | Interleukin 7 |
| IL10 | Interleukin 10 |
| IL12 | Interleukin 12 |
| IL15 | Interleukin 15 |
| IL18 | Interleukin 18 |
| IL21 | Interleukin 21 |
| IL24 | Interleukin 24 |
| IL-12R-β1 | Interleukin 12 receptor beta 1 |
| IL-12R-β2 | Interleukin 12 receptor beta 2 |
| iNOS | Nitric Oxide |
| I.P./i.p. | Intraperitoneal |
| IP-10 | Interferon gamma-induced protein 10, also called CXCL10 |
| I.T./i.t. | Intratumoral |
| I.V./i.v. | Intravenous |
| JAK- | Janus kinase |
| LDL | Low-density lipoprotein |
| LL/2c | Lewis lung carcinoma |
| MDA5 | Melanoma Differentiation Associated Protein 5 |
| MDSCs | Myeloid Derived Suppressor Cells |
| MHC | Major Histocompatibility Complex. |
| MIG | Monokine Induced by Gamma Interferon, also called CXCL9 |
| MG1 | Maraba virus |
| mg/kg | milligram per kilogram |
| µl | microliter |
| ml | millilitre |
| MM | Metastatic Melanoma |
| µM | micromolar |
| mm | millimetre |
| mm3 | a cubic millimetre or microlitre |
| MOI | Multiplicity of infection |
| MY88 | myeloid differentiation primary response protein 88. |
| NF-κB | Nuclear Factor κappa B |
| NK | Natural Killer cells |
| NKp30 | Natural Killer p30 |
| NKp44 | Natural Killer p44 |
| NIS | Sodium Iodine Symporter |

| | |
|---|---|
| NDV | Newcastle disease virus |
| OAS | oligoadenylate synthase |
| OV | Oncolytic Virus |
| PAMPs | Pathogen Associated Molecular Patterns. |
| PBS | Phosphate-buffered saline buffer |
| PCR | Polymerase Chain Reaction |
| PD-1 | Programmed Death Receptor-1 |
| PDL1 | Programmed Death Ligand 1 |
| PFU | Plaque Forming Unit |
| PKR | Protein Kinase R |
| PMA | Phorbol 12-myristate 13-acetate |
| PRRs | Pattern Recognition Receptors |
| P21 | cyclin-dependent kinase inhibitor |
| PTPs | Tyrosine Protein Phosphatases. |
| P53 | Tumor protein P53 |
| qPCR | Quantitative real-time PCR |
| RANTES | regulated upon activation, normal T cell expressed and secreted, also called CCL 5 |
| RdRP | RNA-dependent RNA polymerase |
| RIG-1 | Retinoic Acid-Inducible Gene 1 |
| RNA | Ribonucleic acid |
| ROS | Reactive Oxygen Species |
| RPMI | Roswell Park Memorial Institute (RPMI) medium |
| S.C./s.c. | Subcutaneous |
| SFV | Semliki Forest Virus |
| SINV | Sindbis virus |
| SMCs | Smac Mimetic Compounds |
| STAT | Signal Transducer and Activator of Transcription. |
| STAT2 | Signal Transducer and Activator of Transcription 2 |
| TAAs | Tumor-Associated antigens |
| TAMs | Tumor Associated Macrophages |
| TANs | Tumor Associated Neoantigens |
| TAP-1 | Transporter associated with antigen processing 1 |
| TCR | T-cell receptors |
| TdLNs | Tumor draining Lymph Nodes |
| TH1 | T helper 1 T cells |
| TiLs | Tumor Infiltrating Lymphocytes |
| TME | Tumor Microenvironment. |
| TLRs | Toll-like receptors |
| TNFα | Tumor necrosis Factor alpha |
| TRAIL | TNF-related apoptosis-inducing ligand |
| T-VEC | Talimogene laherparepvec |
| Vero | Kidney epithelial cells of the African green monkey |
| VSV | Vesicular stomatitis virus |
| VSVΔ51 | Vesicular stomatitis virus delta 51 |
| VV | Vaccinia Virus |
| VSV-GP | Vesicular stomatitis virus-glycoprotein |

| | |
|---|---|
| VSV N | Vesicular stomatitis virus N protein |
| VS | Vanadyl Sulfate |

## List of Figures

# Chapter 1: Introduction

## 1.1. Cancer

Cancer is initiated by abnormal cell growth and tissue invasion, which may be benign or malignant (1). Many cancer types have been recognized with three main categories: carcinomas, sarcomas, and leukemias or lymphomas (1). They share similar characteristics, including self-sufficient proliferative signalling, resistance to growth suppressors and cell death, replicative immortality, and ability to induce angiogenesis, evasion of immune destruction, metastasis, reprogramming of energy metabolism, and invasion of immune destruction (2, 3).

Cancer has been intensively studied, providing an in-depth understanding of the processes that are involved in cancer initiation and progression. As a result, researchers are constantly developing new therapeutic approaches that contribute to cancer treatment and prevention. The most used therapies for cancer are chemotherapy, radiotherapy, and surgical excision (4), which directly remove tumors or target cancer cell proliferation among others. While they are effective in some cases, these historical cancer treatments still face several challenges and limitations, including cancer recurrence, tumor resistance (5) and off-target toxicity (6).

## 1.2. Tumor immunosuppressive microenvironment:

The tumor microenvironment (TME) plays a crucial role in shaping the progression and fate of cancer. Consisting of an array of cellular and non-cellular components that actively participate in shaping tumor response, angiogenesis,

immune evasion, and metastasis (Figure 1). One critical component of the TME is the immunosuppressive microenvironment, which hinders effective anti-tumor immune responses and supports tumor growth and metastasis. Understanding the mechanisms behind this immunosuppression is essential for developing novel therapeutic strategies to overcome immune evasion in cancer.

## 1. Cellular Components of the Tumor Microenvironment

The TME comprises tumor-infiltrating immune cells, cancer-associated fibroblasts (CAFs), endothelial cells, and mesenchymal stem cells (MSCs) (Figure 1). Tumor-infiltrating lymphocytes (TILs), including cytotoxic T cells, natural killer (NK) cells, and regulatory T cells (Tregs), each one of these immune cells significantly impacts tumor development (7).

CAFs are heterogeneous cells that originate from different cell types such as mesenchyme, epithelial cells, mesothelial cells, fibrocytes, endothelial-mesenchymal transition (EndMT) and epithelial-mesenchymal transition (EMT). They promote tumor growth, angiogenesis, and metastasis through paracrine signaling and extracellular matrix remodelling (8). The crosstalk between cancer cells and CAFs creates a supportive niche that facilitates cancer progression and therapeutic resistance (8). In addition, the interaction between CAFs and immune cells also contributes to cancer resistance by secreting TGF-β and IL-10. As a result, the secretion of TGF-β and IL-10 converts T cells into iTregs, induces tolerogenic DCs, eliminates APCs by reducing signal activity, inhibits T cell and NK cell function, and activates M2 macrophages (9).

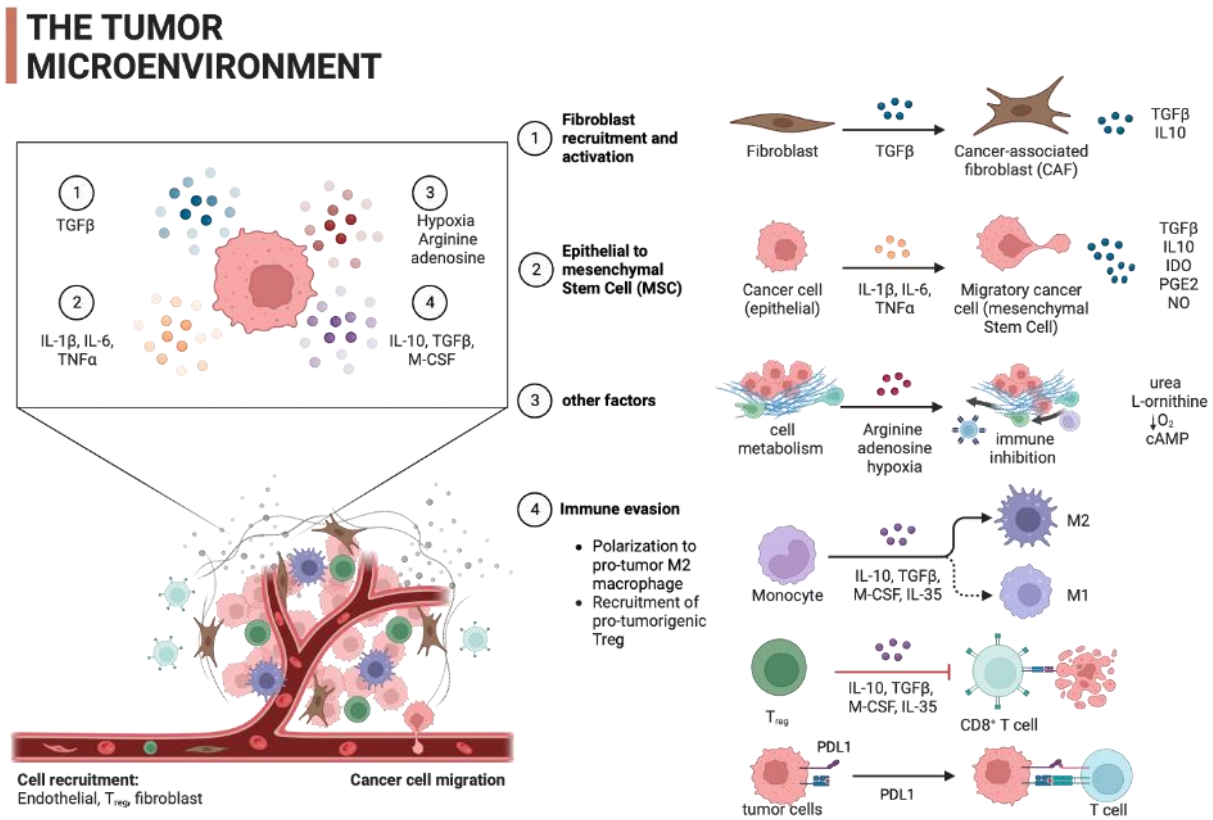


**Figure 1: Tumor immunosuppressive microenvironment components and mechanism of actions.**

The tumor microenvironment (TME) consists of cellular components including tumor-infiltrating immune cells, cancer-associated fibroblasts (CAFs), endothelial cells, mesenchymal stem cells (MSCs), non-cellular components, and released molecules. Each one of these components plays critical role in shaping the tumor microenvironment and promoting tumor resistance, figure was generated using Biorender.

MSCs are multipotent cells that differentiate and regenerate into many cell types, including bone, cartilage, and adipocytes. Besides their regenerative potential, they play a crucial role in tissue repair and immune regulation. However, when recruited to the TME, MSCs can also contribute to tumor progression and therapy resistance by promoting tumor growth, angiogenesis, and immunosuppression. They can suppress the proliferation and activation of T cells, B cells, natural killer (NK) cells, and dendritic cells (DCs) (10). MSCs collectively create an immunosuppressive milieu through the secretion of soluble factors like transforming growth factor-beta (TGF-β), interleukin-10 (IL-10), indoleamine 2,3-dioxygenase (IDO), prostaglandin E2 (PGE2), and nitric oxide (NO). In addition, they promote the expansion of cells that could further induce the tumor immune evasion including T regulatory cells (Tregs) and Myeloid-Derived Suppressor Cells (MDSCs) (11)

Tregs are a specialized subset of T cells that play a crucial role in maintaining immune tolerance and preventing autoimmunity. Both of MSCs and CAFs have been shown to promote the expansion and function of Tregs through direct cell-to-cell contact and the secretion of immunomodulatory cytokines like TGF-β and IL-10 (11, 12). Whereas MDSCs are a heterogeneous population of immature myeloid cells that play a role in inhibiting T cell activation and proliferation. MSCs induce the expansion and the recruitment of MDSCs in the TME through the secretion of factors like IL-6, IL-1β, and granulocyte-macrophage colony-stimulating factor (GM-CSF) (13). CAFs also mediate the recruitment and expansion of MDSCs through the secretion of GM-CSF and IL-6, further contributing to immune suppression (14).

## 2. Non- Cellular Components of the Tumor Microenvironment:

The non-cellular components of the tumor microenvironment consist of the structure of the extracellular matrix (ECM) and secreted factors within the TME that significantly impact cancer cell behaviour and modulate the tumor microenvironment (Figure 1). Here are some of the factors that influence the behaviour of tumor cells and promote the generation of tumor immunosuppressive microenvironment.

The secretion of immunosuppressive molecules hampers the antitumor immune response and generates an environment in favour of tumor growth. For instance, Indoleamine 2,3-dioxygenase (IDO) is an enzyme that plays a significant role in creating an immunosuppressive microenvironment within the tumor. It is involved in the degradation of tryptophan, an essential amino acid, into kynurenine and other metabolites that tumor cells need to promote their growth and evade host defences (15). PGE2 is a bioactive lipid molecule derived from arachidonic acid, in the TME, PGE2 is produced by various cells, including tumor cells, stromal cells, and immune cells. It suppresses immune responses through a series of intracellular signalling of the prostanoid E (EP) receptor pathway (16). Whereas Nitric oxide (NO) is a gaseous molecule that involves in various physiological and pathological processes, including cancer. In the TME, NO is mainly produced by inducible nitric oxide synthase (iNOS) expressed in tumor cells, immune cells, and stromal cells. NO can promote tumor growth and immune escape by inhibiting T cell activation (its production stimulates the production of superoxide by iNOS which then reacts with

NO to form ONOO- and other forms of RNS that cause T cell apoptosis (17).

Additionally, other secreted molecules such as Growth factor-beta (TGF-β) and interleukin-10 (IL-10) are key immunosuppressive factors that play critical roles in shaping an immunosuppressive milieu that promotes tumor growth, invasion, and immune evasion. TGF-β is secreted by both tumor cells and stromal cells and suppresses immune responses by inhibiting the activation and proliferation of effector T cells, promoting the expansion and function of regulatory T cells (Tregs), and impairing the function of natural killer (NK) cells and dendritic cells (DCs) (18). While, IL-10 is an anti-inflammatory cytokine secreted by Tregs, macrophages, and tumor-infiltrating lymphocytes. IL-10 mediates immunosuppressive effects by suppressing the function of effector T cells, DCs, and NK cells and on the other hand promoting the differentiation and expansion of MDSCs (19).

Other cytokines including IL-6, IL-1β, and granulocyte-macrophage colony-stimulating factor (GM-CSF) are also secreted in the tumor microenvironment (TME). They contribute to promoting an immunosuppressive microenvironment and modulating immune responses. IL-6 is a pro-inflammatory cytokine secreted by various cells, including tumor cells and immune cells in the TME. It promotes the expansion and activation of regulatory T cells (Tregs) and myeloid-derived suppressor cells (MDSCs) (20). The second cytokine is IL-1β is a pro-inflammatory cytokine secreted primarily by immune cells in response to infection,

injury, or inflammation. In the TME, IL-1β can promote the production of other immunosuppressive factors, such as IL-6 and IL-10 (21). Lastly, GM-CSF is a cytokine that mediates the production and maturation of granulocytes and macrophages including MDSCs and tumor-associated macrophages (TAMs) (22).

3. **Other Components of the Tumor Microenvironment:**

During malignancy transformation, the cell metabolism undergoes changes to support the progressing tumor. Tumor hypoxia, for instance, is a biochemical reaction in the organism, caused by an insufficient oxygen supply, and is a hallmark feature of the TME. As a result, this metabolic alteration in the TME has a major impact on the immune system and leads to drug resistance, angiogenesis, stimulation of metastasis, and tumor invasion as well as immune suppression (9, 23). Additionally, there are other metabolites that contribute to the generation of immunosuppressive microenvironment including Arginine and adenosine. Arginine is important for T cell TCR signaling and cytotoxicity. A high level of arginase that is released by TAMs, N2 neutrophils and monocytic MDSCs in the TME subsequently metabolizes L-Arg into urea and L-ornithine and as a result, impairs immune cell function (24). Whereas high adenosine concentration inhibits CTLs and NK cells by diminishing their cytotoxic capabilities due to a cAMP build-up which leads to protein kinase A (PKA) activity (25).

In addition to all these factors that contribute to the immunosuppressive microenvironment enabling tumors to evade immune surveillance, the TME can orchestrate various immune evasion mechanisms. One of which is the

expression of immune checkpoint receptors and ligands on tumor cells and other immune-suppressive molecules to impair effective antitumor immune responses (26). In a normal immune response, immune cells undergo multiple sequential steps following a stimulus that is regulated by counterbalancing stimulatory and inhibitory signals where the expression of several membrane receptors is induced as an indication of their functional status (27). These signals are triggered by the binding of these receptors to their ligands on other cells, that either initiate stimulatory or inhibitory signals (27, 28). For instance, T cells get activated upon receiving several signals from antigen-presenting cells, and when activated, they express inhibitory molecules, including cytotoxic T lymphocyte-associated antigen-4 (CTLA4), programmed death receptor-1 (PD-1) as part of the immunosurveillance process (29). Cancer cells escape the immune response by overexpressing immune checkpoint regulators such as PDL-1 which inhibits T-cells (30).

4. **Therapeutic implications:**

Understanding the dynamic and multifaceted nature of the TME is vital for designing effective therapeutic strategies. A lot of effort has been made to overcome some of these limitations by targeting specific components of the TME, such as immune checkpoint inhibitors, anti-angiogenic agents, and stromal modulators, which have shown promising results in preclinical and clinical studies (31). Strategies to selectively target and inhibit Tregs (32), and delete or reprogram MDSC (33), hold promise for restoring antitumor immunity. Depletion or functional inhibition of Tregs in

combination with other immunotherapies is being explored as a potential approach. Additionally, the inhibition of specific immunosuppressive factors produced by the tumor and stromal cells, such as TGF-β, IL-10, and IDO, have been investigated as potential therapeutic agents to enhance antitumor immune responses and reprogram the immunosuppressive TME (34).

One attractive approach to surmount TME barriers is Immune checkpoint inhibitors (ICI) which have been widely used as cancer therapy and have seen widespread clinical approvals. Immune checkpoints are regulatory signaling pathways that modulate the amplitude and duration of immune responses (27). Anti-cytotoxic T cell lymphocyte antigen 4 (CTLA4) antibodies and anti-programmed death 1 (PD1) receptor/ligand (PDL1) antibodies have been designed to overcome the negative effect of these immune suppressor regulatory mechanisms. ICI therapies have been approved as part of the standard of care for multiple malignancies and as monotherapies cannot effectively control the cancers in most treated patients (27, 28).

However, the complexity and heterogeneity of the TME present significant challenges in developing precise and personalized therapies. The importance of unravelling the complexities of the TME offers unprecedented opportunities to develop innovative therapeutic approaches that can exploit vulnerabilities within the tumor ecosystem. Continued research in this field holds the potential to transform cancer treatment and improve patient outcomes.

### 1.3. Oncolytic virotherapy:

Oncolytic virotherapy has been identified as an innovative and hybrid cancer gene therapy / immunotherapy approach to treating cancer that aims in part to stimulate the body's immune system to recognize and attack cancer cells. Over the past decade, significant progress has been made in the preclinical and clinical development of oncolytic virotherapy and many promising agents have been identified. Oncolytic virotherapy utilizes specially engineered viruses to selectively target and destroy cancer cells, offering a tumor-specific therapeutic platform. The impact of OVs therapies on the immune response has been studied and the generation of a robust antitumor immune response is identified as a key contributing mechanism. This is supported by accumulating evidence pointing to the importance of the immune response in generating long term immunity against the tumor, which has been demonstrated in many animal models (35). Generally, there is a correlation between the presence of effector T cells and improved prognosis and long-term survival in many solid tumours (36-44). The success of oncolytic virotherapy can be further augmented by implementing various strategies to amplify its anticancer effects. Therefore, several approaches have been tested to optimize viral replication and spread within the tumor, induce the immune response against cancer cells, and overcome potential challenges caused by the tumor microenvironment.

### 1.4. OVs as a versatile cancer therapeutic platform

Oncolytic virotherapy is an immunotherapy based on using replication viruses that specifically target malignant cells leading to their killing and inciting an

antitumor adaptive immune response (45-47). Oncolytic Viruses (OVs) have been extensively tested as anti-cancer therapies. They have a natural tropism for cells that have defects in antiviral defences, are able to evade immune cell detection and killing, and that divide rapidly, as is the case for many cancer cells (46). Therefore, tumors are considered an ideal substrate for the virus, which is used as machinery for effective virus replication.

There is a broad spectrum of viruses that have been tested clinically as anticancer therapy including DNA and RNA viruses namely adenovirus, measles virus, parvovirus, reovirus, vesicular stomatitis virus, and coxsackievirus (46). Despite the diversity and overall significant improvements in viral oncolysis associated to these viruses, few have been translated to clinical use.

### 1.4.1 Current Status of OV therapy:

To date, four OVs have reached regulatory approval throughout the world for the treatment of advanced cancers and since then, the number of clinical trials is increasing every year. The first one was in 2004, an RNA virus derived from the native ECHO-7 strain of a picornavirus, called Rigvir, and was approved for melanoma treatment in Latvia (48). Then, in 2005, a genetically modified adenovirus, H101 was approved for the treatment of nasopharyngeal carcinoma in combination with cytotoxic chemotherapy in China (49). More recently, Talimogene laherparepvec (T-VEC), an attenuated herpes simplex virus, type 1 (HSV-1) encoding granulocyte-macrophage colony-stimulating factor (GM-CSF) was approved in 2015 by the U.S. Food and Drug Administration for the local treatment of unresectable cutaneous, subcutaneous and nodal lesions in patients with recurrent melanoma after initial surgery (50). The most recently approved OV

is a modified HSV-1, named teserpaturev or G47Δ (DELYTACT®), for the treatment of malignant gliomas which received conditional and time-limited approval in June 2021 in Japan (51, 52). 97 clinical trials were reported from 2000 to 2020 including a wide range of clinical trial phases under study spanning many different viruses, cancer populations, routes of delivery, and combination treatment strategies, as well as evaluating immune responses (53).

Although the clinical trial results support the potential therapeutic benefit of OVs, oncolytic virotherapy experienced many barriers to translation in addition to the time it takes to reach the final FDA approval (54-57). A lot of efforts have been made to fill the gap to improve the clinical outcome of OVs therapy (58, 59). One of which by increasing the need for better-targeted therapies armed to be effectively targeted to the tumors (60). In addition, the development of animal models for preclinical testing is needed to address the toxicities including off-target toxicities observed in early clinical studies and test the efficacy of therapies before translation (60).

**1.4.2 OV therapy mediated immune response:**

Oncolytic viruses have emerged as a promising cancer therapy with a lot of potential to incite a sustainable immune response. Because of this, they are often categorized as immunotherapy because they naturally trigger immune responses towards tumors (61-63). OVs however have multiple mechanisms of action and their antitumor effects depend on 1) the direct tumor-selective oncolysis, 2) therapeutic transgene expression and 3) immune activation leading to anti-tumor immunity (Figure 2).

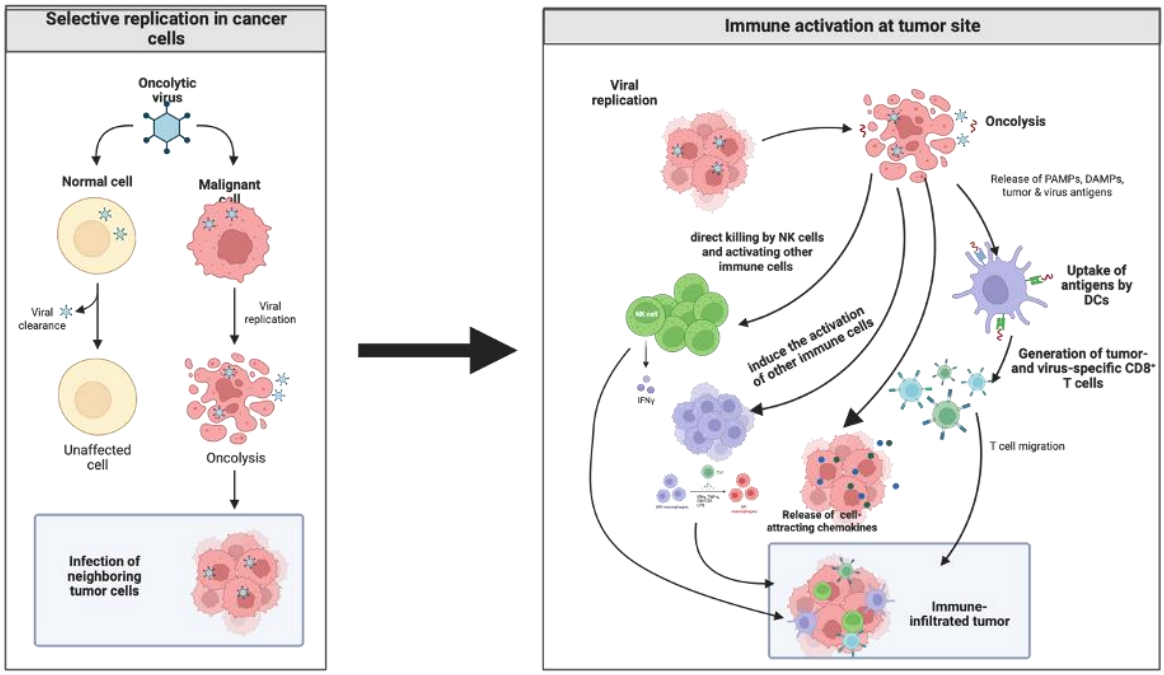


**Figure 2: OV therapy mediated immune response.**

OVs specifically target malignant cells and induce the release of danger signals, such as pathogen-associated molecular patterns (PAMPs) and damage-associated molecular patterns (DAMPs), from infected cancer cells which are recognized by pattern recognition receptors (PRRs) on immune cells. The recognition of these molecules contributes to the stimulation of the innate and adaptive anti-cancer immune responses and triggers the release of pro-inflammatory cytokines which are important to recruit, activate and stimulate multiple immune cells including dendritic cells, Natural killer cells, macrophages and T cells. Those cells facilitate cancer clearance through many mechanisms, figure was generated using Biorender.

In this regard, OVs activate the immune system through several mechanisms. One of which is through the release of danger signals, such as pathogen-associated molecular patterns (PAMPs) and damage-associated molecular patterns (DAMPs), from infected cancer cells (62). Subsequently, the release of damage-associated molecular patterns (DAMPs), as well as the release of infectious viral progeny that spread to surrounding tumor cells (64, 65) which are recognized by pattern recognition receptors (PRRs) on immune cells also contribute to the stimulation of the innate and adaptive anti-cancer immune responses and trigger the release of pro-inflammatory cytokines locally and systemically (66).

This process also activates other key regulators of the innate immune response to shift the TME towards an immunostimulatory phenotype, and recruitment of macrophages and NK cells as well as other immune cells that mediated adaptive immune response including Dendritic cells and T cells.

**1.4.2.1 Macrophage:**

As the first line of innate immune response defence, macrophages mediate anti-viral and anti-tumoral responses by releasing IFN-γ, followed by the expression of CCL20, CXCL10, CXCL11, CCL15, and CXCL9 and the secretion of TNF and IL-12 to attract and activate NK cells, T cells, and DCs (cytokine details presented in Table 1) (67). For instance, during viral infection, macrophages have a variety of antiviral properties that limit viral spread and replication through cellular mechanisms (68) or through the secretion of pro-inflammatory cytokines such as IFN-γ, TNFα, IL1ß, IL6, IL12 that mediate T cells, NK cells and DCs activation (Table A). The production of reactive oxygen species (ROS**)**, expression

## Table 1: the cytokines and chemokines

| Cytokine/ chemokine | Receptor | Secreted cells | Targeted cells | Biological function |
|---|---|---|---|---|
| IFN-gamma | IFNγR1, IFNγR2 | Th1 cells<br>NK cells<br>CD8 T cells | Macrophages, NK cells, T cells, others | Cell activation<br>Cytotoxic effect |
| G-CSF | GCSFRdimer | Macrophages<br>Fibroblasts<br>other tissues | Granulocytes | Cell expansion |
| IP-10/CXCL10 | CXCR3 | Endothelial cells<br>Antigen presenting cells | T cells<br>NK cells | Cell recruitment |
| MCP-1/CCL2 | CCR2 | monocytes<br>macrophages<br>dendritic cells | inflammatory monocytes | Cell recruitment |
| MIP-1a/CCL3 | CCR1, 5 | lymphocytes, fibroblasts, and epithelial cells, monocytes and macrophages | Monocytes<br>T cells<br>Basophils<br>NK cells<br>Eosinophils | Cell recruitment |
| MIP-1b/CCL4 | CCR5 | monocytes, T/B lymphocytes<br>Neutrophils<br>fibroblasts<br>endothelial/epithelial cells | Monocytes<br>T cells<br>Dendritic cells<br>Nk cells | Cell recruitment. |
| MIG/CXCL9 | CXCR3 | monocytes<br>endothelial cells<br>fibroblasts<br>cancer cells | T cells<br>NK cells | Cell recruitment |
| Rantes/CCL5 | CCR1,3,5 | Tumor cells<br>Monocytes | T cell<br>Eosinophils<br>Basophils<br>Dendritic cells | Cell recruitment |
| CCL20 | CCR6 | Endothelial cells<br>epithelial cells<br>monocyte<br>macrophage<br>neutrophils | immature dendritic cells (DC)<br>effector/memory T-cells and B-cells | Cell recruitment |
| CCL15 | | Macrophages | Monocytes<br>dendritic cells<br>T lymphocytes<br>eosinophils | Cell recruitment |
| TNF-alpha | TNFR,p55; TNF R,p75 | Macrophages<br>Monocytes<br>T cells<br>others | Macrophages<br>Monocytes<br>T cells<br>others | Cell activation |
| IL-2 | IL2Rα, IL2Rb, and IL2Rγ | activated T cells | CD 4+ T cells<br>CD 8+ T cells<br>NK cells<br>T reg | Cell activation |
| IL-5 | IL5Rα and IL3Rb | Th2 cells | Eosinophils<br>B cells | Cell maturation, activation, survival |
| IL-6 | IL6Rα and gp130 | Macrophages<br>endothelial cells<br>some activated T cells | B cells<br>T cells<br>Thymocytes<br>myeloid cells<br>osteoclasts | Cell proliferation |
| IL-7 | IL7Rα and IL2Rγ | hematopoietic cells<br>stromal cells | CD8+ T cells<br>B cells | Cell activation |
| IL-12 | IL12Rb1 and IL 12Rb2 | Macrophages<br>dendritic cells<br>B cells<br>neutrophils | T cells<br>NK cells | Cell activation |
| IL-17 A /CTLA8 | IL17RA orIL17R C | Th17 cells<br>and others | T cells | Cell activation |
| IL-15 | IL15Rα, IL2Rb, and IL2Rγ | DC<br>Macrophages<br>monocytes) | Memory T cells<br>CD8+ T cells<br>NK cells | The activation and proliferation of T and natural killer (NK) cells |

of nitric oxide (iNOS) and increased Major Histocompatibility Complex class II (MHC-II) expression on antigen presenting cells and phagocytosis are part of the cellular mechanisms that prevent the spread of the virus (67). Although macrophages have been shown to induce an antiviral immune response, macrophages also contribute to the antitumor immune response of OVs by acting as antigen-presenting cells or the secretion of pro-inflammatory molecules.

The increase in macrophage infiltration in the context of OV infection has been reported to be associated with enhanced antitumor effects (69). In line with this notion, treatment with oncolytic adenovirus (Delta24-RGD) increased the antitumor effect and improved survival and that is associated with enhanced macrophage infiltration and macrophage-stimulating cytokines such as IFN-γ and other pro-inflammatory cytokines including CCL3, IL1β, and IL6 (Table 1) (70). Macrophages are an important element in bridging innate and adaptive immune responses toward tumor cells. In addition, they have an antigen-presenting ability which contributes to enhancing the antitumor subsequently by stimulating tumor-specific T-cell response (71, 72, 73).

**1.4.2.2 Natural killer cells (NK cells):**

While NK cells are also one of the first defences during the innate immune response. The ability of NK cells to recognize "self" by detecting MHC-I through Killer Cell Immunoglobulin-like receptors (KIRs) in humans and Ly49 in mice prevents harm to the host's cells (74,75). NK cells also get stimulated through the interactions of activating receptors such as NKG2D and natural cytotoxicity receptors (NCRs) with their cognate ligands (for example, H60, Mult-1) as well as CD27-CD70 interactions (74, 75). They are responsible for both direct cytotoxicity

and significant cytokine production (76). For instance, they mediate their cellular cytotoxicity through the release of controlled degranulation of perforin and granzyme-B and the release of pro-inflammatory cytokines IFN-γ and TNF-related apoptosis-inducing ligand (TRAIL) (46) that facilitate the direct killing of target cells. NK cells also play an important role in combating transformed cells by antibody-dependent cellular cytotoxicity (ADCC), where antibody-coated cells are recognized through FcγRIIIa (CD16), which recognizes the Fc portion of IgG1 produced by B or plasma cells (77).

Their intrinsic ability to kill tumor cells without prior sensitization has made NK cells a very promising target for immunotherapy. Additionally, this early response of NK cells has been shown to be important for the generation and activity of other immune cells including dendritic cells that eventually play a critical role in priming an efficient T-cell response, which is required for generating effective therapeutic outcomes (78, 79). NK recruitment to tumors is associated with an increase in their activity following reovirus treatment (80), and HSV treatment (81). NK cells mediate direct cytotoxicity to tumor through the binding of their cytotoxicity receptors NKp30 to Bcl-2-associated athanogene 6 (BAG6) and B7-H6 and NKp44 to NKp44L on OV-infected tumor cells (82) as well as the release of perforin and granzyme release (81).

**1.4.2.3 Dendritic cells:**

In addition, antigen-presenting cells (APCs) bridge innate and adaptive immune responses. They uptake the released TAAs or tumor-associated neoantigens (TANs) and present them as antigens via MHC class I to T cells to activate T cells and recruit them to tumor site (83, 84). Dendritic cells are antigen-

presenting cells, they uptake and process antigens upon encountering tissue damage, infection, or transformed cells. That leads to their maturation and migration to lymphoid structures to present those antigens through the Major Histocompatibility Complex (MHC)-I/II expressed on their surface (85) to T-cell receptors (TCR) on CD8+ and CD4+ T-cells respectively to mediate their activation and differentiation to antigen-specific T-cells (86–89). They also release immunostimulatory molecules (87, 89, 91,91).

Treatment with reovirus or HSV induces DC recruitment to the tumor, and that is mediated by the increase in the secretion of a variety of cytokines including IL6, RANTES, and IFNγ (92, 93). OV treatment also induces the maturation of DCs by enhancing the expression of costimulatory proteins such as CD80, CD83, and CD86, as well as Transporter associated with antigen processing 1 (TAP-1) and MHC and generally boosts their antigen-presenting ability. As a result, this improves tumor-specific T-cell activation (92, 94). DCs also contribute to generating pro-inflammatory TME by releasing a variety of cytokines such as TNFα, IL1ß, IL6, IL12 (Table 1), and IFN, and reduced inhibitory signals, such as via IL10 (94).

**1.4.2.4 T cells:**

One of the critical components of the adaptive immune response is T cell-mediated immunity. T cells play a central role in recognizing and eliminating tumor cells. CD8+ cells recognize antigen that is presented by APC through MHC class I molecules to T cell receptor (TCR) and that initiates an intracellular signaling cascade leading to activation of these cells. In contrast, CD4+ T cells recognize tumor antigens presented on MHC class II molecules. As a result, activated CD8+

T cells and CD4+ T cells migrate to the tumor site and facilitate tumor clearance (95). Effector CD8+ T cells recognize tumor cells based on the expression of altered proteins that are presented via MHC class I that trigger apoptosis of tumor cells via secretion and release of perforin and granzymes or via the Fas-FasL axis, subsequently activating the caspase cascade in target cells (95, 96). Furthermore, both CD4+ and CD8+ T-cells secrete cytokines to promote host defense, particularly IFN-γ, which stimulates both innate and adaptive immune responses (95, 97). This cytokine not only targets tumor cells but also has other regulatory properties. It has been shown to increase MHC class I expression (98, 99), induces the secretion of chemokines such as CXCL9 and CXCL10 that elicit T cell recruitment, NK cell, DC, and macrophages infiltration (100), and shift the immune response toward pro-inflammatory phenotype (101).

The generation of specific anti-tumor CD8+ T-cell immune response is considered an important target for the efficacy of immunotherapies and several immunotherapies that have reached clinical trials demonstrated that the generation of such a response is correlated with improved outcomes (102, 103, 104). The improvement in clinical outcomes following treatment with HSV, VV, or VSV has been reported to be associated with an increase in T cell infiltration (105, 106, 107).

## 1.5. VSVΔ51

Many of the effects of OVs that contribute to generating long-lasting anti-tumor responses result from selective viral replication in the tumor. Some oncolytic viruses have a natural tropism for cancer cells, while other viruses have a genetic modification that leads to preferential targeting of cancer cells (46). Vesicular

stomatitis virus (VSV) is of particular interest due to its selective tumor killing properties and translational potential. VSV, a member of the Vesiculovirus genus, is a negative sense, single-stranded RNA virus. It mainly infects rodents, cattle, swine, and horses, and causes a relatively localized and non-fatal illness, and human infection is considerably rare and asymptomatic. Its genome consists of 5 genes of 3′-N-P-M-G-L-5′ (Figure 3) (108, 109).

The nucleoprotein (N) binds to the phosphoprotein (P) which is also bound to the viral RNA-dependent RNA polymerase, and the large (L) protein. The nucleocapsid complex and the viral polymerase complex (P and L proteins) form the ribonucleoprotein responsible for genome replication and transcription, which then is enveloped in a lipid bilayer generated from the host cell membrane during the budding process. The membrane-associated proteins comprise the glycoprotein (G) and the matrix protein (M). The matrix protein (M) is associated with the nucleocapsid and the lipid bilayer to maintain the compact structure of the virion and it also blocks transcript transport from the nucleus into the cytosol and facilitates VSV budding from the membrane. The glycoprotein (G), the integral membrane protein, controls viral entry, through cell attachment via the low-density lipoprotein (LDL) receptor and membrane fusion (110, 111, 112).

The VSV life cycle as described in Figure 4 begins when VSV-G binds to LDL receptors on the cell surface of the targeted cells, and subsequent receptor-mediated endocytosis occurs (113) resulting in the fusion of the viral and endosome membranes and the release of the ribonucleic core into the cytoplasm (114). The viral RNA-dependent RNA polymerase (RdRp) complex, composed of the L and P proteins, synthesizes the viral RNA.

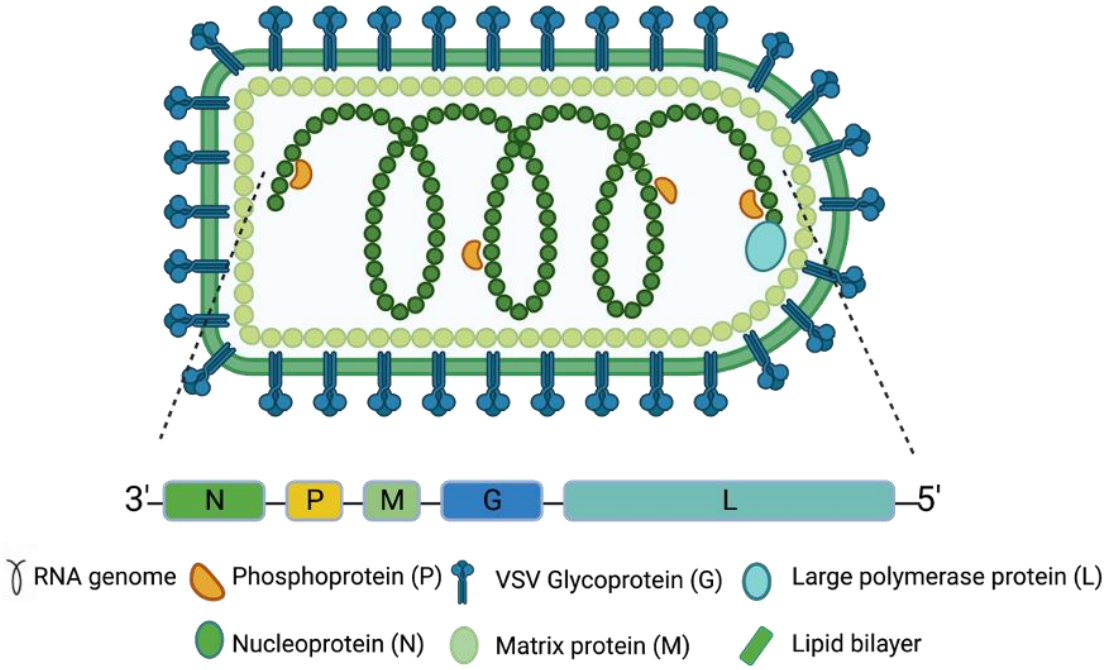


***Figure 3: VSV structure***

VSV, a member of the Vesiculovirus genus, is a negative sense, single-stranded RNA virus. VSV genome consists of 5 genes of The nucleoprotein (N) binds to the phosphoprotein (P) which is also bound to the viral RNA-dependent RNA polymerase, and the large (L) protein. The nucleocapsid complex and the viral polymerase complex (P and L proteins) form the ribonucleoprotein responsible for genome replication and transcription, which then is enveloped in a lipid bilayer generated from the host cell membrane during the budding process. The membrane-associated proteins comprise the glycoprotein (G) and the matrix protein (M). The matrix protein (M) is associated with the nucleocapsid and the lipid bilayer to maintain the compact structure of the virion and it also blocks transcript transport from the nucleus into the cytosol and facilitates VSV budding from the membrane. The glycoprotein (G), the integral membrane protein, controls viral entry, through cell attachment via the low-density lipoprotein (LDL) receptor and membrane fusion. Figure was generated using biorender.

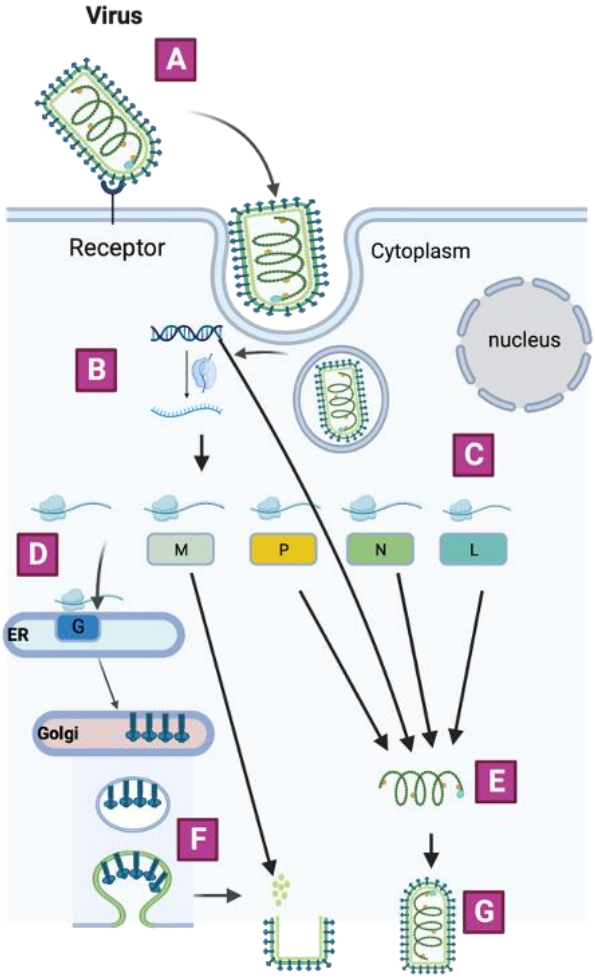


**Figure 4: VSV life cycle.**

**(A)** VSV-G binds to LDL receptors on the cell surface of the targeted cells and enters the cell via receptor-mediated endocytosis. **(B)** the ribonucleic core is released into the cytoplasm, the viral RNA-dependent RNA polymerase (RdRp) complex, composed of the L and P proteins, synthesizes the viral RNA. **(C)** The (−) strand RNA serves as the template for the transcription of five subgenomic mRNAs by the L and P proteins. The mRNAs encoding the N, P, M, and L proteins are translated by free cytoplasmic ribosomes. **(D)** The mRNA encoding the G protein is translated by ribosomes bound to the endoplasmic reticulum as to generate new synthesized G protein. **(E)** the formation of n nucleocapsids begins with the synthesis of a complementary full-length (+) strand, which is also in the form of a ribonucleoprotein containing the N, L, and P proteins. This RNA in turn serves as a template for the synthesis of progeny (−) strand RNAs. **(F)** Newly synthesized G proteins enter the secretory pathway, where they are glycosylated, oligomerized, and transported to the plasma membrane. **(G)** Progeny nucleocapsids and M proteins are transported to the plasma membrane, where the association with regions containing the G proteins initiates assembly and budding of progeny virions

The RdRp transcribes the leader RNA and the 5 mRNAs creating a gradient of RNA beginning with an abundance of leader RNA followed by decreasing mRNA levels moving towards the 5' end of the genome (N>P>M>G>L) (115, 116) where the polymerase binds only at the leader RNA (116). The N, P, M, G, and L mRNA transcripts then utilize the host cell machinery for translation of the 5 VSV proteins (116). Upon the production of sufficient N, P, and L proteins, the replication of the VSV genome is carried out by the RdRP. That results in the formation of a full-length (+) sense RNA genome which acts as a template for further replication and amplification of the (–) sense genome (117). Both copies of the genome are covered by N protein, and only the (–) sense genome is packaged into budding progeny virions which acquire an envelope from the host cell. VSV M protein associates with the RNP, condenses the RNP complex, and recruits host factors to facilitate budding (118, 119). From each infected cell, 1,000-10,000 progeny virions can be released (119).

### 1.5.1 Therapeutic properties of VSV:

VSV is known for preventing the anti-viral type I interferons (IFN) through its M protein by blocking the host mRNA export from the nucleus, thereby shutting off IFN production (120). As this is interfering with the host antiviral response, an attenuated version of VSV with a complete deletion of methionine at amino acid position 51 (Δ51) was engineered to generate VSV variant that is sensitive to an IFN-mediated antiviral response (120). This mutated variant of VSV can provide therapeutic benefit for interferon-signaling-deficient cancers, while not causing harm to normal cells with robust type I IFN responses (120, 121). VSV has a fast replication cycle which also can lead to substantial tumor destruction in a short

amount of time and release significant infectious virus progeny in the tumor micro-environment and bloodstream, where it can propagate to infect un-injected metastases (122). VSV can be readily manufactured to high titers, can be injected intravenously, and engineered with transgenes to enhance immunostimulatory and other properties (121,122, 123).

Based on preclinical and clinical evidence, VSVΔ51 has long been considered a safe therapeutic approach. This is due to its cytoplasmic replication preventing the risk of gene integration, its lack of pathogenicity in humans in contrast with the wild-type virus, and its mode of transmission. In addition, it has been reported to have a safety profile in clinical trials, especially for intravenous administration (124). VSV has been shown to effectively induce significant tumor regression and prolonged survival as well as stimulate the antitumor immune response in various mouse models including but not limited to prostate and malignant glioma (125, 126).

**1.5.2 Clinical translation of VSV:**

Overall, given its excellent safety profile and potent oncolytic and immune-stimulating properties (127, 128) the VSV virus has already entered early-phase clinical trials for solid tumors with limited therapeutic outcomes. In a phase I clinical trial study, VSV-hIFNβ-NIS, an oncolytic VSV engineered to express IFN-β and the sodium iodine symporter (NIS) transgenes was administered in patients with hematological cancers (multiple myeloma, acute myeloid leukemia, or T-cell lymphoma) in 15 patients treated, stable disease was observed. Similar results were observed in stage IV endometrial cancer patients treated with IV VSV-IFNβ-NIS, no shedding was observed in urine or buccal swabs and no VSV lesions were

observed in immunocompromised patients (129, 130). Vesicular stomatitis virus (VSV)-glycoprotein (GP; BI 1831169) which is a chimeric VSV with its neurotropic glycoprotein G replaced by the non-neurotropic GP of the lymphocytic choriomeningitis virus, is currently being investigated in phase I study. VSV-GP (BI 1831169) was used as a monotherapy and in combination with the immune checkpoint inhibitor, ezabenlimab (BI 754091) in patients with advanced or metastatic solid tumors (NCT05155332) and was found to promote substantial antitumor immune response (131).

To further explore the next generation of VSVs, continuing studies to identify the effective therapeutic regimens that could further enhance viral replication, understand biological contributors which correlate with patients' response to therapy, and identify the appropriate combination of OVs with complementary therapies that leverage the immune response are ongoing and a lot of progress has been made in this field.

### 1.6. Limitations of OV therapy

Oncolytic virotherapy (OV therapy) holds immense promise as a potential therapeutic approach to fight cancer by utilizing viruses to selectively target and destroy malignant cells. In recent years, OV therapy has gained significant attention in the realm of cancer treatment due to its potential for specificity and low toxicity. However, like any therapeutic approach, OV therapy faces some limitations including tumor resistance to OV therapy and the antiviral immune response. Despite all the promising therapeutic advantages of OV, a significant challenge has risen in tumor resistance to OV

therapy. Over time, some tumors develop mechanisms to evade the effects of oncolytic viruses, rendering the treatment less effective. In addition to that the natural immune response toward viral infection named antiviral immune response negatively impacts the immunostimulatory properties of OVs. As a result of understanding and addressing these limitations, several therapeutic strategies have been merged to overcome these limitations.

### 1.6.1 Tumor resistance to OV therapy:

Resistance to OV therapy occurs through many mechanisms, including but not limited to genetic and epigenetic changes in the tumor microenvironment or the cancer cells themselves (132). Tumor and tumor microenvironment heterogeneity could also prevent effective cancer therapy and generate poor therapeutic responses to OVs (133, 134, 135, 136). Additionally, the complexity of the tumor microenvironment and its immunosuppressive mechanism are significant obstacles to the resistance in OV therapy that prevents the efficient infection of a tumor (136) and can affect the ability of the immune system to recognize and attack cancer cells. Tumors also develop mechanisms to evade the immune system, including downregulating the expression of antigens or upregulating immune checkpoint molecules (137).

### 1.6.2 Antiviral immune response:

Along with other factors contributing to the resistance to OV therapy, one of the major obstacles to OV therapy is the anti-viral immune response that eradicates the virus before it reaches its immunostimulatory peak effect (138). This can limit the effectiveness of OVs and reduce their ability to replicate and kill cancer cells.

In addition, the presence of pre-existing anti-viral immunity in patients can also reduce the efficacy of OVs (139).

Following viral infection, cell surface receptors and cytoplasmic receptors, including Toll-like receptors (TLRs), melanoma differentiation-associated protein 5 (MDA5; also known as IFIH1), and retinoid acid-inducible receptors (retinoic acid-inducible gene 1 (RIG-1) detect viral particles (140). This interaction initiates type I interferon response by activating myeloid differentiation primary response protein 88 (MYD88) signalling, which in turn activates Janus kinase (JAK)–signal transducer and activator of transcription (STAT) signalling (141). Following that, the expression of genes encoding type I interferons and other interferon-related molecules, in addition to caspases and pro-inflammatory cytokines and chemokines induce cell death. That occurs through caspase-dependent apoptosis in the infected cell through phosphorylation of Protein Kinase R (PKR), cell growth arrest via the cyclin-dependent kinase inhibitor (p21), and RNA silencing through activation of oligoadenylate synthase (OAS) (141). This response also induces innate and adaptive immune responses toward the virus.

### 1.6.3 Therapeutic Strategies to overcome these limitations.

Several strategies have been applied to further improve the oncolytic activity of OVs: genetic engineering is one of the widely used approaches to delete or insert a gene of interest. In addition to that combining existing cancer therapies with OV therapy has been introduced to take advantage of the enhancement of the immune-mediated tumor destruction by these therapies, and the natural immunostimulatory properties of OVs. OVs have been combined with chemotherapy (142), Histone deacetylase (HDAC) inhibitors (143), immune / apoptosis modulators such as

Smac mimetic compounds (SMCs) (144), immune checkpoint inhibitors and adoptive cell therapies (145) to overcome some of the monotherapies' limitations.

ICI therapies have been combined with many immunotherapies including OV therapy to overcome their respective limitations. For example, the combination of T-VEC with Ipilimumab (anti-CTLA4) in patients with advanced unresectable melanoma showed greater antitumor activity in a randomized Phase II study (146). This combination therapy is now in subsequent phase III trials (147, 148 (NCT02263508)). In addition, treatment with oncolytic vesicular stomatitis virus (VSV) expressing IFN-β and a sodium iodide symporter reporter gene (VSV-IFN-β-NIS) with an anti-PDL1 antibody have found to significantly control tumor growth of disseminated acute myeloid leukemia (AML) tumors compared to either treatment alone (149). A similar finding was observed when combining oncolytic vaccinia virus expressing a membrane-bound interleukin (IL)-2 with anti-PD1/PDL1 in a model of colon cancer (150). VV was also tested in combination with both anti-PD-1 and anti-CTLA-4 antibodies and that has been shown to have significant survival advantages (151). There are now multiple ongoing trials that combine checkpoint inhibition and oncolytic virotherapy. Till now, the outcomes of these studies are highly anticipated and provide insight into effective transgene payload. However, there is still a lot to be revealed about the timing and method of delivery, and potential side effects of these combination therapies. All of these are important aspects to design novel combination regimens.

All these preclinical and clinical pieces of evidence have proven that OV therapies can efficiently break apart tumor resistance, induce anti-tumor immune response, improve efficacy in a wide range of tumors and potentiate therapeutic

efficacy with existing therapies. Nevertheless, the clinical translation of OV combination therapies faces several challenges and limitations. One of the challenges in developing OV combination therapies is identifying the most effective combinations and determining which therapies will effectively work in combination. Additionally, the timing and dosing of combination therapies are critical, considering that certain therapies may negatively affect the anti-tumor response of OVs and OVs have different mechanisms of action and target different aspects of the tumor microenvironment.

In addition, OV combination therapies are also associated with potential toxicity, many cancer therapies, such as chemotherapy and radiation, have severe side effects that can limit their use in combination with OVs. Lastly, one of the widely known challenges is the antiviral immune response that limits the effectiveness of the OV.

### 1.7. Viral enhancer as category immunostimulatory enhancer of OVs therapy

The development of new and novel therapeutic regimens has therefore focused on breaking these resistances of tumors and minimizing the antiviral immune response to improve the therapeutic benefits of OVs in the clinic (152). In an effort to improve the clinical therapeutic efficacy of OVs, many pharmacological compounds have been explored and several small molecules have been identified as viral enhancers (152, 153, 154) by which they increase viral infection in tumor cells through the suppression of antiviral response targeting type I IFN production or signaling (152).

As many new viral enhancer drugs have been identified, our group has worked over the last decade to uncover many novel small molecule enhancers of OVs, with the overarching objective to identify effective combination therapy regimens that further improve the clinical efficacy of OVs. More recently, we identified vanadium-based compounds as a unique category of immunostimulatory OV enhancers, effective with RNA-based oncolytic viruses, such as oncolytic vesicular stomatitis virus (VSVΔ51) (155) and NDV (156).

## 1.8. Vanadium compounds and their therapeutic potential

Vanadium is a metal that has been shown to impact several biological and cellular processes, and vanadium oxides have been explored as treatments for a variety of pathological conditions such as diabetes and cancer (157). Vanadate is identified as a phosphatase inhibitor because it is a structural analog to a phosphate with a similar size, charge, and structure (158). As a result, of such a unique feature, vanadate has a high affinity for the active site of tyrosine protein phosphatases (PTPs), resulting in the inhibition of a broad range of PTPs (159, 160).

Indeed, Vanadium compounds have been in clinical development as pharmacological treatments for diabetes (161). Vanadium compounds display insulin-mimetic properties by stimulating the autophosphorylation of the insulin receptor, this involves restoring signal transduction through the insulin receptor and glucose intake via GLUT4 by inhibiting PTP1b based on in vivo studies (162). While many clinical trials have been carried out revealed that vanadium compounds were shown to be safe and tolerated in humans, their utility as antidiabetics did not ultimately pass regulatory scrutiny.

### 1.8.1 Vanadium compounds as anticancer therapy:

Vanadium compounds have been also extensively studied as potential anticancer agents due to their ability to induce apoptosis and inhibit tumor growth in a variety of cancer cell lines and animal models. Numerous studies have been carried out in order to get a deeper insight into the effects of vanadium as potential cancer therapy. In an osteosarcoma cell line, oxidovanadate was found to induce DNA damage and increased the generation of reactive oxygen species, triggering apoptosis (163). It also induces cell death in colonic adenoma and carcinoma in vivo by disrupting cellular metabolism through the generation of ROS (164, 165). Finally, vanadate facilitates IFN alpha-mediated apoptosis, and this is dependent on the generation of ROS and p53 activation (166, 167).

Oxidovanadate was shown to decrease cell proliferation and suppress the development of DMH-induced colonic adenoma and carcinoma (168). Vanadium prevents both the initiation and promotional phases of liver carcinogenesis through growth inhibition of preneoplastic tissues (168). Vanadium exerts anti-cancer activity by disrupting cellular metabolism through the generation of ROS, alteration of cellular organelles such as lysosomes and mitochondria, the spindle protein such as actin and tubulin, cell cycle, and apoptosis as well as cell proliferation (168). Vanadium also has antitumoral effects in malignant melanoma cells through inhibition of cell growth, increasing the number of apoptotic cells in a time and dose-dependent manner, and blocking the cell cycle in G0/G1 phase (164).

### 1.8.2. Vanadium compounds potential impacts on immune response:

Numerous studies have also demonstrated that vanadium compounds have an impact on the immune system. In B cells, vanadium triggers the activation of B cells by a change in cell metabolism, gene expression, and cytoskeleton organization that regulate cellular mechanisms such as survival, apoptosis, proliferation, and differentiation into memory or antibody producing cells. While in T cells, ammonium metavanadate alters the number of mature T cells migrating from the thymus to the spleen and the secretion of IL-2 and IL-6. Vanadium is also found to downregulate interleukin expression including IL-6, IL-10, TNF-α, and IFN-γ (169). In this context, vanadate activates and stimulates T cells by induction of protein-tyrosine phosphorylation (170).

The effect of vanadium compounds on immune cells could be a concentration-dependent effect. For instance, vanadate was found to inhibit the proliferation of CD4+ T cells when given at a concentration higher than 10μM but enhanced antigen-induced IFN-γ secretion by more than a 3-fold increase at lower concentrations (171). In another study, excess dietary Vanadium was shown to induce the proliferation of splenic T cells, coupled with an increase in the percentage of CD4+ and CD8+ T cells and the secretion of IL-2 and IL-6 (172).

### 1.8.3. Vanadium compounds as potential enhancers of OVs therapy

As suggested by preclinical studies, vanadium compounds have potential as components of anticancer therapeutic regimens. They have reached clinical trials as anti-diabetics with well-documented safety profiles. In addition, they have been used recently as OV enhancers. A previous study by our group was the first to explore this effect and showed that vanadium compounds in conjunction with

RNA-based oncolytic viruses such as the oncolytic virus VSVΔ51 (tumor-selective variant of vesicular stomatitis virus) improved viral oncolysis and led to long-term antitumor immunity and prolonged survival (155).

In tumor-bearing mice, combining Vanadate with VSVΔ51 enhanced leukocyte infiltration with significantly increased T cells, including IFN-γ producing CD8+ T cells that contributed to increased tumor control and long-term antitumor immunity. Notably, approximately 80% of DBT tumor-bearing mice (glioma) and 20% of CT26WT (colon) tumor-bearing mice demonstrated complete remission after the combination treatment compared to 40% of DBT tumor-bearing mice (glioma) received VSVΔ51 alone or Vanadate alone controls and all the CT26WT (colon) tumor-bearing treated with monotherapy controls. The combination treatment led to an upregulation in the expression of a number of pro-inflammatory cytokines induced by type II IFN, (155). Remarkably, this effect of vanadate in enhancing the OV activity was found to be associated with a shift from an antiviral type I IFN response into a type II IFN response through the inhibition of STAT2 activation. This led to the upregulation of pro-inflammatory cytokines and chemokines that mediates the generation of a T cell-dependent antitumor response including CXCL9 which plays a key role in leukocyte trafficking (155).

## 1.9. Cytokines and chemokines as targeted transgenes/payloads in immunotherapy

An important part of the immune responses that participate in the therapeutic efficacy of OVs is the secretion of cytokines and chemokines. The secretion of cytokines and chemokines influence the mechanisms through which OVs target cancer cells either through direct oncolysis or through immune response-mediated

effects creating a microenvironment conducive to antitumor immunological activities. To our knowledge, such OV-driven immune responses provide an in-depth understanding of multidimensional implications for OV-induced antitumor activities. Additionally, carefully selected cytokines and chemokines thus hold potential for generating more effective therapeutic strategies and rendering OVs therapies more effective for fighting cancer.

### 1.9.1 Cytokines:

Cytokines are generally small proteins that play a significant role in regulating immune responses by mediating communication between cells in response to various stimuli, including pathogens, antigens, and inflammatory signals. They trigger a signalling cascade through the Janus kinase (JAK) and signal transducers and activators of transcription (STAT) molecules that modulate cellular responses on target cells by binding to specific receptors (173). Cytokines are broadly classified into pro-inflammatory and anti-inflammatory cytokines, depending on their effects on the immune system.

Pro-inflammatory cytokines are secreted by immune cells in response to pathogens and other inflammatory signals. Their roles are to initiate and amplify immune responses by promoting inflammation, activating immune cells, and inducing the expression of other cytokines and chemokines (174). For example, Interferon-gamma (IFN-γ) is a cytokine that is produced by T cells, and NK cells and is involved in the activation of a variety of immune cells (175, 176). IFN-γ has been shown to have antiviral and antitumor effects and is involved in regulating the immune response (177). TNF-α also can activate macrophages and promote their production of reactive oxygen species, which help to kill invading pathogens (178).

In addition, many other cytokines play important roles in shaping the immune response including IL4, IL12, and IL15.

While anti-inflammatory cytokines are secreted by regulatory immune cells and play essential roles in controlling and resolving immune responses. In response to that, their secretion inhibits the production of pro-inflammatory cytokines and suppresses the activation of immune cells and the promotion of tissue repair and regeneration (179). For example, IL-10 can inhibit the production of pro-inflammatory cytokines such as IL-1 and TNF-α and suppress the activation of T cells and macrophages (180).

Following an immune response, the secretion of cytokines also plays important roles in the differentiation and function of different immune cell subsets. For instance, interleukin-2 (IL-2) is a critical cytokine for the proliferation and differentiation of T cells and NK cells and has been shown to have therapeutic potential in the treatment of cancer, as it can enhance the immune response against cancer cells (181). Additionally, IL-2 has been used to enhance the efficacy of cell-based vaccines (182).

#### 1.9.1.2. Cytokines as therapy:

Recently, there has been growing interest in the potential of cytokines as immunotherapy for cancer. Treatment with cytokines including but not limited to interferon-alpha (IFNα), granulocyte-macrophage colony-stimulating factor (GM-CSF), interleukin (IL)-2, IL-12, IL-15, and IL-21 have shown efficacy in multiple murine cancer models as monotherapy in preclinical studies (183). In addition, two cytokines IFNα and IL-2 have reached clinical approval as a monotherapy. IFNα was the first cytokine approved for the treatment of hairy cell leukemia (HCL)

(183) as well as follicular non-Hodgkin lymphoma, melanoma and AIDS-related Kaposi's sarcoma (164). High-dose IL-2 (HDIL-2) was approved for the treatment of metastatic renal cell carcinoma (mRCC) in 1992, and metastatic melanoma in 1998 (183).

Since then, several strategies are being explored, and a lot of efforts have focused on developing novel cytokine therapies by incorporating cytokines in combination with other cancer therapies. In this context, cytokines are being tested in conjunction with anti-PD-1 and anti-PD-L1 monoclonal antibodies, and adoptive T cell therapies including anti-CD19 chimeric antigen receptor (CAR) T cells and tumour-infiltrating T lymphocytes (TILs) (164). However, their therapeutic efficacy has been limited by the associated toxicity, the short half-life of most cytokines and low anti-tumor response (183, 184).

**1.9.1.2. Cytokine-armed OV therapy:**

The expression of cytokines by recombinant viruses has been investigated as another strategy for enhancing cytokines' potential therapeutic efficacy, increasing the immunogenicity of targeted vaccines and for local delivery of cytokines to the tumor microenvironment. Based on many preclinical studies, virus-based cytokine expression therapy has an impact on the immune response as well as tumor growth and survival (185, 186). An example of that is treatment with HSV-amplicon vector to deliver trans IL-2 in tandem with G207 therapy. This treatment significantly controls tumor growth in SCC VII in comparison to G207 alone and control (185, 186). In addition, several cytokine-expressing oncolytic viruses including IL15, IL4, IL-6, IL-18, IL-24, IFN-γ, and GM-CSF have been engineered in a number of OVs and have been effective in pre-clinical models and some of them are now

entering early-stage clinical trials (185, 186). To date, 86 clinical trials have tested or are testing oncolytic viruses expressing cytokines for multiple tumor models anticipating the safety and promising therapeutic outcomes of such a platform (187).

Virus-based cytokine expression therapy is also combined with other more recent cancer therapies, including ICIs (185, 186). For instance, oncolytic vaccinia virus that has a modified IL-2 with a glycosylphosphatidylinositol anchor and rigid peptide linker has been shown to reduce the systemic toxicity of IL12, when combined with the PD-1 and PD-L1 blockade. This virus cured the majority of treated mice, even with a high initial tumor burden (185, 186).

**1.9.1.3. IL12:**

Interleukin-12 (IL-12) emerges as a promising and potent therapeutic payload, holding immense therapeutic potential due to its immunostimulatory properties and promising clinical outcomes. Below, the role of IL12, the potential of IL-12 as a therapeutic payload in immunotherapy (either as monotherapy or armed therapy), ongoing research, and some of the limitations are discussed.

IL12 is a pro-inflammatory type 1 cytokine that is consisted of two subunits, p35 and p40. These subunits are linked by three disulfide bridges to form a p70 heterodimer (188-192). IL12 receptor contains two amino acid chains: IL-12R-β1 and IL-12R-β2 (193) that are expressed either constitutively or in an inducible manner in several types of immune cells (194). In normal response and upon activation through priming and cell-cell interaction signalling, IL12 is secreted mainly by antigen-presenting cells including dendritic cells (DC), monocytes, and macrophages (195). IL12 plays an important role in immune responses and the

activation and proliferation of NK and T cells (195, 196). NK cells and T and B lymphocytes express the IL-12R which is composed of two amino acid chains: IL-12R-β1 and IL-12R-β2 to which secreted IL12 binds (193, 194), triggering JAK-STAT4 signalling pathways (197, 198). This signal enhances the proliferation and cytotoxic activity of both CD8+ T cells and NK cells (199, 200).

Among its diverse functions, IL-12 also plays a significant role as a central mediator in inducing $T_H1$ cell differentiation, increasing activation and cytotoxic capacities of T and NK cells; and inhibiting or reprogramming immunosuppressive cells, namely tumor associated macrophages (TAMs) and myeloid-derived suppressor cells (MDSCs) (201-206). Not surprisingly, since IL12 connects innate and adaptive immunity, it also impacts other immune cells, including B cells, by promoting IgG production (207).

IL-12 is known as a positive mediator of the production of large amounts of IFN-γ which itself is cytostatic/cytotoxic (208, 209), anti-angiogenic (210, 211) and upregulates the expression of MHC I and II on tumor cells (212). IL12 not only mediates the secretion of IFN-γ but also synergizes with the secretion of other cytokines to potentiate the immune response (213, 214). These cytokines are important in inducing CD3+ T cell proliferation, IFN-γ production, and tumor cell death through NK and CD8+ T cell stimulation namely tumor necrosis factor α, IL-2, IL-15, IL-18, and granulocyte–macrophage colony-stimulating factor (GM-CSF) (214).

**1.9.1.3.1. IL12 as monotherapy:**

IL-12 has demonstrated remarkable antitumor effects against a range of malignancies in preclinical studies (215-218). These effects heavily depend on

$CD8^+$ T cells, NK cells, and NK T cells effector and cytotoxic activities in mediating the anti-tumor immune response (216, 219, 220). Since then, light has been shed on the use of IL-12 as a promising therapeutic platform. It has been widely studied as a single agent and, however, high-dose IL12 has also been associated with systemic toxicity and off-target effects.

IL12 has been combined with a number of cancer vaccines in order to maximize antitumor effects. As just a few examples, IL-12 was used in combination with a cancer vaccine comprised of major histocompatibility complex (MHC) class II and CD80-transfected tumor cells (221) and other cell-based vaccines (222), as well as tumor lysate-pulsed DCs (223). These combined therapies, systemically administered, resulted in a high degree of T and NK cell activation, IFN-γ production, resulting in antitumor effects, and significantly inhibited tumor growth. However, as mentioned already, there are several toxic side effects that have been reported related to systemic and high-dose administration of IL-12 (224, 225, 226).

Consequently, one of the limitations of IL12's clinical utility is its toxicity. Indeed, severe toxicities in early clinical trials were reported. For example, 17 patients received rhIL-12, 12 patients were hospitalized, and two patients died (227) due to the impact of frequent systemic injections of IL-12 in large phase 2 studies (228, 229). On the other hand, insufficient and limited delivery of IL-12 to the tumor microenvironment in humans when delivered systemically is a challenge considering that IL-12 like most cytokines, functions locally through paracrine and autocrine mechanisms.

Therefore, and as pointed out by many studies, localized delivery of IL12 is less toxic, and most importantly induces a sustainable anti-tumor immune response (230, 231, 232, 233, 234, 235). Since then, newer therapeutic approaches with IL-12 have been tested focusing on targeted and localized IL12 delivery. Several methods have been identified to maximize the local delivery of IL12 and the associated benefits of tumor-targeted *in situ* vaccination including immunocytokines, by which tumor-reactive monoclonal antibodies are linked to cytokines (236, 237, 238), controlled biodegradable release polymers (239, 240), and oncolytic viruses as gene therapy / immunostimulatory agents for IL12 expression from the tumor (241, 242).

**1.9.1.3.2. OV-armed IL12 therapy:**

The above studies suggest that the local delivery of IL12 circumvents the severe toxicity associated with the systemic delivery of IL12. That is also in line with designing better methods of delivery to achieve a high local concentration of IL-12 and provide further rationale for the anti-tumor mediating immune response, and benefits of an *in situ* vaccine approach. OVs are one of the promising therapeutic platforms that have the potential to combine the distinct advantages of tumor-targeted delivery of transgenes, and/or in situ vaccination.

OVs including but not limited to MG-1, Adenovirus, and HCV have all been previously engineered to express IL-12, a strategy that has been shown to improve anti-tumor immunity in numerous murine carcinoma models by regulating the activation of T cells and NK cells (243, 244). IL-12-expressing OVs have been previously investigated in preclinical studies as a promising cancer therapeutic strategy using Sindbis virus (SINV), Vesicular stomatitis virus (VSV), Semliki

Forest Virus (SFV), Newcastle disease virus (NDV), Herpes simplex virus (HSV), and Adenovirus (245). OV-directed intratumoral IL-12 expression not only induces a significant antitumor effect of these viruses but also increases survival in murine tumor models (246-252). This is a direct impact of IL-12 expressing OVs on immune cells such as cytotoxic and regulatory T cells, NK cells, and DCs in addition to an indirect impact on chemokine induction, such as CXCL9 and IP-10, that together have been shown to interfere with tumor angiogenesis (245, 253). Of note, adenovirus- and HSV-expressing IL-12 therapies are now in human clinical trials (254-257).

Altogether, the therapeutic potential of OVs armed with IL-12 is evident, offering a unique dual-action approach to fight cancer. The oncolytic virus selectively targets and destroys cancer cells, while IL-12 boosts the immune response, enhancing the body's natural ability to recognize and attack cancer cells more effectively. The combination of these two powerful therapeutic approaches creates a synergistic effect, amplifying the anti-tumor response and potentially leading to long-lasting remissions and improved patient outcomes. Moreover, OV-armed IL-12 is also evident in its potential for overcoming systemic toxicity when delivered locally and that also mediates a systemic immune response that enables the treatment of both primary and metastatic tumors, making it a highly promising therapeutic option. However, like any innovative therapy, OV-armed IL-12 faces certain limitations that challenge its translation to the clinic including the toxicity concern especially when combined with OV including the potential for excessive immune activation and off-target effects, and conversely, limitations associated to

insufficient replication of the virus in the tumor owing to various factors such as the antiviral response.

While there is still a lot that needs to be done to unravel the potential of such a therapy, determining the ultimate therapeutic regimen that strikes the right balance between selectively targeting cancer cells and activating immune responses will bring new aspects that will contribute to designing more effective therapeutic platforms. In addition, achieving optimal delivery and distribution of the therapeutic payload within the tumor microenvironment is one of the therapeutic approaches that offer hope for a future where cancer treatment becomes more effective, personalized, and less invasive, leading to improved patients' outcomes.

**1.9.2. Chemokines:**

Chemokines are also generally small proteins known as chemotactic cytokines that mediate immune cell migration (258, 259). They are classified and subdivided according to their structures based on the number and positions of conserved N-terminal cysteine residues into C, CC, CXC, or CXC3C groups (260). They play a role in inducing chemotaxis, promoting differentiation and multiplication of leukocytes, and causing tissue extravasation (258, 259). They bind to seven-transmembrane G protein-coupled receptors (GPCRs) (168, 169) which consist of coupled intracellularly to a heterotrimer of G proteins with α, β, and γ subunits (261)). This interaction creates local chemokine gradients near the site of chemokine production leading to homing of cells to the appropriate area (262). That induces signal transduction through signal transducer and activator of transcription (STAT1) and nuclear factor kappa B (NF-κB) signalling pathway (263). This signal is initiated by exchanging the GDP for GTP by G proteins upon chemokine-

chemokine receptor binding, resulting in the dissociation of the G protein β/γ and α subunits to activate downstream signaling pathway (262).

Chemokines play a critical role in cancer immunity by regulating immune cell biology, especially during tumorigenesis, modulating immune cell activation, recruitment, phenotype, and function. For consideration, the diverse and dynamically regulated expression of chemokine ligands and chemokine receptors provides a wide range of possibilities for response (263, 264). Adding to this complexity, whether these functions and responses generate anti-tumor immunity or pro-tumorigenic immune cell phenotypes is further dependent on the stage of tumorigenesis, the state of immune cell activation, the balance in the immune response between effector and regulatory response, and the dynamic and the relative expression of chemokine receptors on effector and regulatory target cells (264, 265).

**1.9.2.1. Chemokines as a therapy:**

Much research has been conducted on chemokines, leading to substantial advancements in comprehending their involvement in immune cell migration. Despite this progress, chemokines as therapeutic targets have faced challenges over the past decade. Both single small molecules and antibody therapies have been explored with considerable limitations, primarily due to chemokine redundancy, insufficient inhibition of the target, and translational barriers arising from variations in chemokine or chemokine receptor expression and function between animal models and humans (266).

Chemokines can also be employed for virus-encoding therapies. Virally encoded chemokines, chemokines receptors, or chemokines-like proteins have

been previously explored and have been shown to be associated with modulating immune response (267, 268). For this reason, encoding chemokines into oncolytic viruses is a promising though potentially complex approach that could further maximize the immune response and enhance therapeutic potency and/or benefit (268, 270). Taking advantage of OV therapy to modulate the immunostimulatory response by inducing chemokine secretion allows therapeutic developers to produce chemokines and chemokine gradients throughout the tumor flowing from the sites of virus replication.

While the focus to date has mainly been on efforts to attract antitumor immune cells to the tumor, OV encoding chemokines that could further promote immune cell infiltration have also been studied (271-275). Chemokines expressed from oncolytic viruses were shown to improve intratumoral immune cell infiltration and improve efficacy following these therapies (271-275). However, there remain several limitations including a lack of specificity to a singular immune cell type, overcoming a pre-established immunosuppressive tumor microenvironment, and insufficient understanding to choose an appropriate chemokine and oncolytic virus combination, ultimately limiting therapeutic outcome (271-275).

However, the approval of oncolytic Herpes-Simplex-Virus (HSV)-1 expressing GM-CSF by the FDA has at least shown that encoding cytokines and chemokines can lead to improvement in treatment, particularly in the case of metastatic melanoma (257). Arming OVs with transgenes that can alter the immune cell balance toward productive therapeutic immunity holds significant promise. A key advantage of cytokine-expressing oncolytic viruses is the potential to regulate and leverage the balance between an antitumor and an anti-oncolytic virus response by

modulating the types of cells present in the tumor microenvironment along with the immunostimulatory effects of OVs.

#### 1.9.2.2. CXCL9

Chemokines that further induce the recruitment of anti-tumorigenic immune cells and improve their functionality within the TME are attractive therapeutic targets. CXCL9 is one such cytokine that mediates immune cell recruitment. CXCL9 plays a significant role in immune cell infiltration and known as also known as monokine induced by gamma interferon (MIG) (276). Additionally, it is secreted by various cells including mainly monocytes, endothelial cells, fibroblasts, and cancer cells in response to IFN-γ (277). Upon the CXCL-9 expression, it binds to its selective ligand CXCR3, a G protein-coupled receptor (278, 279, 280) which is expressed on the surface of monocytes, T cells, NK cells, dendritic cells, and cancer cells (279, 280).

The expression of CXCR3 is downregulated on naive T cells and is rapidly upregulated by antigen-presenting dendritic cells to facilitate immune response, which (281) leads to Th1 polarization. After polarization, Th1 cells induce CTLs, NK cells, and NKT cell activation through IFN-γ (282). Following Th1 cell activation by DCs, these produce IFN-γ, TNF-α, and IL-2 to enhance anti-tumor immunity by stimulating CTLs, NK cells, NKT cells, and macrophages (283, 284).

##### 1.9.2.2.1 CXCL9 as a therapeutic payload:

Accumulating pre-clinical and clinical evidence has featured the importance of attracting leukocytes to the TME to promote strong anti-tumor responses through CXCL9-based therapy. The use of CXCL9 in immunotherapy has been shown to improve antitumor efficacy by enhancing tumor anti-angiogenesis and apoptosis

and CTL activity in Lewis lung carcinoma (LL/2c) murine models, as well as in the colon carcinoma (CT26) murine model (285). In addition, high CXCL9 expression was also associated with prolonged disease-free survival in 70 breast cancer patients and was an independent predictive factor of disease-free survival (286). CXCL9, CXCL10, CXCL11, and CCL5 were all highly expressed in metastatic melanoma patients and that was an indication of responsiveness to adoptive therapy and IL-2 treatment (287). CXCL9 also plays a significant role in controlling the growth and metastasis of several malignant tumors (288, 289, 290, 291). One report demonstrated that increased CXCL9 transcript or protein levels in colorectal cancer correlated with improved survival (292, 293). Additionally, the production of CXCL9 has been associated with responses to cancer therapy namely Immune checkpoint inhibitors (294), chemotherapy (295), and adoptive cellular therapy (296).

In the context of OV therapeutic platforms, CXCL9 was recently encoded in VSVΔ51 and that has been shown to generate abundant biologically active CXCL9 chemokine with a substantial increase in the CXCL9 chemokine gradient between tumor and blood (297). Even though this also increased intratumoral T cell infiltration, VSVΔ51 encoding CXCL9 provided limited therapeutic benefit (297). Authors claimed that in addition to the number of factors that influence this therapeutic platform's outcome, alternative tumor models might give very different results (297). However, clearly other factors could also be at play, for example tumor resistance via antiviral response mechanisms. In addition, CXCL9 mainly attracts cytotoxic CD8+ T cells and NK cells in comparison with CXCL11 (298) and has a long life in vivo in comparison with CXCL10 (299, 300). In principle,

encoding CXCL9 within an OV should make it an attractive therapeutic approach with promising therapeutic potential, assuming other barriers to OV therapy are addressed.

Based on all the above evidence, the generation of a new OV-based antitumor targeting therapies employing cytokines and chemokines but that also address the inherent barriers to OV therapy could further improve efficacy by recruiting antitumor immune cells to the tumor. The data presented above provide rationale for selecting chemokines and cytokines such as CXCL9 and IL12, or combinations therein, to further enhance immune cell recruitment activity, more specifically CD8+ T cells and NK cells. We consider that VSVΔ51 is a safe and effective OV platform that can be enhanced through the use of vanadium compounds and could provide a good starting point for such therapeutic approaches.

### 1.10. General Rationale and Hypotheses:

The evidence to date supports the possibility that the improved therapeutic efficacy of VSVΔ51 / Vanadium combination therapy could not only depend on enhanced viral spread but also depend on inducing the effector functions of immune cells and mediating robust antigen-specific immune response. To fill the gap in our knowledge of the impact of this combined therapy on the improved immune response and the mechanism of action that regulate these interactions, we pursued our investigations to study the impact of this combination therapy on specific immune cell populations and chemokines/cytokines in established animal models. In addition, we sought to develop new strategies to improve antitumor responses brought about by the combination of Vanadyl Sulfate (VS) and VSVΔ51 encoding

cytokines/chemokines to devise strategies to further drive immunological response and therapeutic benefit.

**I hypothesize that the use of vanadium compounds in conjunction with oncolytic virus-based immunotherapies upregulates certain pro-inflammatory chemokines and cytokines through a cell-type dependent mechanism.**

While promising, and an improvement over VSVΔ51 alone, the efficacy of VSVΔ51 / vanadium combination could be further improved. Given the potential benefit of chemokines and cytokines in stimulating anti-tumor immune response, maximizing the efficiency of cytokine / chemokine expression within the tumor microenvironment within the framework of VSVΔ51 / vanadium combination therapy could be effective.

**Therefore, I hypothesize that anti-cancer activity of the VSVΔ51 / vanadium combination can be further enhanced through complementary immunomodulatory strategies elicited via cytokine / chemokine-armed versions of VSVΔ51.**

More specifically, owing to the likely importance of CD8+ T cells and NK cells in achieving therapeutic efficacy following the combination therapy; **I hypothesize that the inclusion of IL12, CXCL9 or their combination within the VSVΔ51 backbone could further improve the efficacy of vanadium-combined therapy.** To test these hypotheses, I have three main objectives:

1. Characterize the secretion profiles of chemokine and cytokine notably involved in the regulation and recruitment of T cells and the modulation of

the effector function of immune cells, as well the cellular immunological changes upon combination treatment.

2. Evaluate the impact of using cytokine armed VSVΔ51 on vanadium combination therapy efficacy in characterized models, and the relevant immunological changes following the combination treatment with VS+VSVΔ51 expressing IL12.
3. Characterize the therapeutic benefit of including CXCL9 or CXCL9 and IL12 expressed from the VSVΔ51 backbone as part of the vanadium combination therapy.

# Chapter 2: Material and Methods

## 2.1 Drugs

The vanadium-based compound used in this study is Vanadyl sulfate. Vanadyl sulfate at 50mg/kg (VOSO4, Sigma-Aldrich, cat. 204862) dissolved in PBS was used for *in vivo* experiments whereas 100μM was used for *in vitro* experiments.

## 2.2 Cell lines

CT26WT (murine colon carcinoma, Cat.CRL-2638) and Vero cells African green monkey kidney cells, cat. CCL-81) were obtained from the American Type Culture Collection (ATCC). These cells were cultured in HyQ high-glucose Dulbecco's modified Eagle's medium (DMEM; HyClone cat.10-013) supplemented with 1% (v/v) penicillin-streptomycin (Gibco Life Technologies, Waltham, MA), and 10% (v/v) serum composed of 3-parts HyClone newborn calf serum (Thermo Fisher, cat. SH3011803) and 1-part Fetal Bovine Serum (Gibco, cat. 12483020). All cells were incubated at 37C in a 5% CO2 humidified incubator and regularly tested to ensure they were mycoplasma contamination-free.

## 2.3 Viruses

### Rhabdovirus

**VSVΔ51-Fluc:** The Indiana serotype of VSV used throughout this study was propagated in Vero cells and purified on 5-50% Optiprep (Sigma-Aldrich, St. Louis, MO). VSVΔ51 expressing firefly luciferase are recombinant derivatives of VSVΔ51 described previously (155).

**VSVΔ51 encoding/ expressing IL-12:** VSVΔ51 encoding/ expressing IL-12 was generated in the laboratory of Dr. Rebecca Auer using PCR amplified from pORF-

mIL12 [IL12elasti(p35:p40); InvivoGen] (301). Virus was produced and purified on 5-50% Optiprep (Sigma-Aldrich, St. Louis, MO) in our laboratory.

**VSVΔ51 encoding/ expressing CXCL9 and VSVΔ51 encoding/ expressing IL12 and CXCL9** were generated in our lab. Viruses were produced and purified on 5-50% Optiprep (Sigma-Aldrich, St. Louis, MO) in our laboratory.

## 2.4 Cloning, Rescue, and purification of VSVΔ51 encoding/ expressing CXCL9 and VSVΔ51 encoding/ expressing IL12 and CXCL9:

### 2.4.1 Virus Cloning:

All forward and reverse primers were designed with XhoI and Nhel restriction sites, respectively. PCR products were run on a 1% agarose gel, and amplicons of the correct size (murine CXCL9: 381bp, and murine IL12:2076) were cut out and purified using a gel extraction kit (Thermo Fisher Scientific, K0692). PCR products were digested at 37$^{o}$C for 16 hours. Digestions consisted of PCR reaction XhoI, Nhel and cutsmart buffer. Then, from the purified digested backbones and digested fragments, the ligation mixture, which was consisted of desired backbone amount, desired insert amount, 1μL T4 ligase, and 2μL T4 DNA ligase buffer was added and incubated overnight. Followed by transformation using NEB10 bacteria, by inoculating 50μL bacteria with 2μL ligation mixture, incubated on ice for 30 minutes, then heat shocked in 45 $^{0}$C water bath for 30 seconds and immediately placed onto ice for 5 minutes. Under the flame, 900μL of room temperature LB was added to the mix and placed in a 30 $^{0}$C shaker for 1 hour. Onto ampicillin LB plates, 100μL of the mixture was added and spread using a sterilized spreader. Plates were incubated at 30 $^{0}$C incubator for over 24 hours. Colonies of interest were picked

and grown in culture tubes has LB containing ampicillin and placed in a $30^0$C shaker overnight. All positive colonies were sent to sequencing for confirmation.

**2.4.2 Virus Rescue:**

5E5 293T cells were plated per well in 6-well plates. Cells then were infected with 0.05 MOI of vaccinia encoding T7 polymerase. After 1 hour, vaccinia virus was removed and the cells were transfected with 1ug VSV N, 0.25μg VSV L, 1.25μg VSV P, 2μg Construct VSV in with opti-mem and lipofectamine 2000 reagent according to the manufacturer's instructions. The transfection mixtures were added dropwise to the wells and incubated at 37°C. After 24hr, the supernatant was removed at 24 hours and complete media was added to the cells. 24hr after that, the supernatant was collected and filtered through a 0.2μM filer. In freshly plated Vero cells, 1 ml of filtered supernatants was added to the well and incubated in a $37^0$C incubator. After 24-48 hours, supernatants were collected and used for virus purification.

**2.4.3 Virus Purification:**

Three rounds of plaque purification were performed using filtered supernatants from inoculated Vero cells. Briefly, 5E5 cells per well of Vero cells were seeded in 6 well plate, and after 24hrs 1 ml of diluted supernatants was added. After 1 hr, media was removed and replaced with 1ml/well of an agarose overlay (1:1 ratio of 1 % agarose mixed with 2X DMEM containing 20 % FBS). After a 24 hours incubation and once plaques form, colonies were picked and transferred to tube had media and added to new Vero well and mixed by pipetting up and down. Repeating the above steps two times and following the last round, filtered supernatants were used as a virus production seed.

### 2.4.4 Virus Constructs:

**VSV: IL12-T2A-CXCL9**

VSV12-9-F: **XhoI** – **Kozak** – mIL12(p35::p40)-SP

VSV12-9-F: **ATA**CTCGAG**GCCACC**ATGTGTCAATCACGC

**VSV: CXCL9**

VSV9-F: **XhoI** – **Kozak** – mCXCL9-SP

VSV9-F: **ATA**CTCGAG**GCCACC**ATGAAGTCCGCTGTT

VSV common R: NheI – STOP TAA – CXCL9

ATAGCTAGCTTATGTAGTCTTCCTTGAACGACGA

## 2.5 Mouse tumor models

Six-week-old female BALB/c mice obtained from Charles River Laboratories (Senneville, Canada) were implanted with subcutaneous tumors by injecting 3E5 syngeneic CT26WT cells, suspended in 100µl serum-free DMEM. Eleven days post implantation when tumor reached a volume of 100 $mm^3$, mice were treated intratumorally Vanadyl sulfate (dissolved in PBS) at 50mg/kg in 50µl or 50µl of PBS. Four hours later, mice were treated intratumorally with 1E8 plaque forming units (PFU) in 25µl PBS of the indicated viruses as described previously (155). Tumor sizes were measured three times a week using electronic calipers. Tumor volumes were calculated using this equation ($length^2$ X width)/2. All in vivo experiments were performed in accordance with the University of Ottawa Animal Care and Veterinary service guidelines for animal care under the protocol OHRIe-2265-R5 and OHRI-2265-R4 A2.

## 2.6 Blood and serum samples processing

For blood samples, saphenous bleeds were performed in one of the legs and blood was collected in tubes containing Serum-Gel (Sarstedt Inc, Fisher Scientific, Cat. NC9315741) to allow serum separation by centrifugation (14 000 rpm) for 10 mins using Eppendorf centrifuge 5418R. Serum was used for measuring cytokine and chemokines. Serum samples were stored at –80C after collection.

## 2.7 Multiplex assay

Serum from blood samples was collected at day 7 days post implantation as a baseline, and 24 hours to 14 days post treatment. Serum was then added in duplicate for each sample in a 96-well plate, and magnetic microspheres premixed with 32-plex beads were added according to the manufacturer's recommendation (MILLIPLEX MAP Mouse Cytokine/Chemokine Magnetic Bead Panel - Premixed 32 Plex - Immunology Multiplex Assay, Millipore Sigma, Cat. MCYTMAG-70K-PX32) and incubated overnight at $4^0$C. A biotinylated detection antibody was added, followed by streptavidin-PE conjugate antibody incubated for 1 hr at room temperature. Plates were run in the Luminex® analyzer (MAGPIX®), using a CCD-based analysis that captures and detects components with the speed and efficiency of magnetic beads. All measurements were performed using a MAGPIX instrument (Luminex, Ottawa, CA), following the manufacturer's instructions. Data were collected using xPonent software (Luminex, Version 4.2), log transformed, and analyzed as described below in the statistical analysis section.

## 2.8 Peptides for *ex vivo* stimulation

Peptides used for *ex vivo* stimulation were gp70 tumor peptide: H-2Ld SPSYVYHQF (MBL International Corporation, Cat. SPM521) and VSV N virus peptide: H-2Ld MPYLIDFGL (CanPeptide Inc, custom peptide)

## 2.9 Splenocyte processing:

Spleens were processed into single cell suspension by first transferring the spleen into sterile 70μm cell strainers on 50ml conical tubes. Then, spleens were softly minced by pressing against the flat side of a syringe plunger in a circular motion. Cell strainers were washed with 5ml of R 10 media. Tubes containing the cell suspension were topped up with media and spun at 300g for 5 mins. Carefully, supernatants were removed without disturbing the pellet and cells resuspended by gently tapping before adding the ACK (Ammonium-Chloride-Potassium) lysing buffer (Gibco™, Cat# A1049201) for lysing red blood cells in samples for 5 mins. Cells were then washed and resuspended with R 10 media.

## 2.10 Mouse IFN-γ Single-Color ELISPOT (enzyme-linked immune absorbent spot)

Cells from spleens were processed as previously described and then resuspended in CTL media (provided with the ELISPOT kit, Immunospot, Cat# mIFNgp-1M/5) in 2E5 cells/100μl before being added to IFN-γ pre-coated plates (Immunospot, Cat# mIFNgp-1M/5) containing 100μl/well of each stimulant including either gp7 or VSV N peptides at a final concentration of 10μM as well as unstimulated control (equivalent amount of DMSO). PMA ((Phorbol 12-myristate 13-acetate, Sigma-Aldrich, Cat# P8139)/ionomycin (Sigma-Aldric Cat# I9657) for pooled samples

were used as a positive control at 2μg/ml. Plates were then incubated at 37 $^{0}$C for 20 hours. Following that, ELISPOT assays were developed following the manufacturer's protocol. Plates were scanned and spots were counted using CTL S6 ImmunoSpot analyzer.

### 2.11 Migration/ Chemotaxis assay

CT26WT cells were pretreated with 100μM VS or PBS for 4 hours followed by viral infection with VSVΔ51 at MOI 0.01 or mock infection. 24 hours later, cultured supernatants were collected and subsequently used for the assessment of chemokines or for performing chemotaxis assays. Chemotaxis of T cells was assessed using a Trans-well system as described previously (20). Briefly, 700μl of conditioned media from CT26WT cell cultures described above was added to the lower chamber of Trans-well plates with 5-μm pores (Costar, Corning, sigma-Aldrich, Cat. CLS3421-48EA). 5E5 activated CD3+ T cells from naïve spleen were purified by negative selection using EasySep™ mouse isolation T cell kit (Stemcell technologies, Cat. 19851) and then activated with 2μg of anti-CD3/CD28 in a precoated plate (BD Pharmingen™, CD3 Cat. 550275 and CD28 Cat. 553295) supplemented with 2ng/ ml of murine recombinant IL-2 (PeproTech, Cat# 212-12) for 2 days, were added to the upper chamber, and plates were incubated for 24 hours at 37 °C. After 24 hours, cells in the lower chambers were collected, stained with trypan blue and counted with a hemacytometer. Migration percentage was calculated as follows: total number of T cells in bottom chamber/ total number of T cell input) x 100 (301).

## 2.12 Viral growth curves

3E5 of CT26WT Cells were seeded in 24 well plates for overnight confluency. Cells were then inoculated with VSVΔ51-Fluc at an MOI of 0.01 (multi-step growth curve) or 1.0 (single-step growth curve). Cells infected at MOI 1.0 were incubated for 60 minutes, followed by washing and replenishing with fresh medium. Cells were incubated up to 48 hours post infection (hpi), with 200µl of supernatant collected and frozen at -80C at the following timepoints: 0, 4, 8, 12, 24, 32, 48 hpi. Viral titer in collected supernatant was quantified by high-throughput tittering using a standard plaque assay.

## 2.13 Plaque assay

For virus titration using standard plaque assay, Vero cells African green monkey kidney cells, cat. CCL-81) obtained from the American Type Culture Collection (ATCC) were seeded into 12-well plates at a final density of 3E5 cells per well. Infectious supernatants were serially diluted using serum-free DMEM, transferred (500µL/well) onto Vero cells and incubated at 37 °C, 5 % CO2 for 45 minutes, following which media was removed and replaced with 1ml/well of an agarose overlay (1:1 ratio of 1 % agarose mixed with 2X DMEM containing 20 % FBS). After a 24 hours incubation, plaques were fixed with methanol: glacial acetic acid in a 3:1 ratio for a minimum of 1 hour, then stained for 30 minutes with a Coomassie Blue solution (4 g Coomassie Brilliant Blue R (Sigma, Cat. # B0149), 800 ml methanol, 400 ml acetic acid and 2800 ml distilled water) to visualize and count plaques.

## 2.14 IL-12 p70 Enzyme-linked immunosorbent assay (ELISA)

Supernatants from infected CT26WT cells with VSVΔ51 encoded Fluc or IL12 at MOI 0.1 were collected 24 hours post infection. The secretion of IL12 was measured using mouse IL-12 p70 Quantikine ELISA (Mouse IL-12 p70 Quantikine ELISA Kit, R&D system, Cat#M1270) following the manufacturer's instructions. Absorbance values at 450nM were measured on a Multiskan Ascent Microplate Reader (MXT Lab System) and corrected for plate imperfections at 540. Data were analyzed using Prism.

## 2.15 CXCL9 Enzyme-linked immunosorbent assay (ELISA)

CT26WT cells were pretreated with 100μM VS or PBS for 4 hours followed by viral infection with VSVΔ51 at MOI 0.01 or mock infection. 24 hours later, cultured supernatants were collected and the concentration of CXCL9 was measured using mouse MIG/CXCL9 ELISA Kit (ELM-MIG, RayBiotech, Cat# ELM-MIG-2) following the manufacturer's instructions. Absorbance values at 450nM were measured on a Multiskan Ascent Microplate Reader (MXT Lab System) and corrected for plate imperfections at 540. Data were analyzed using Prism.

## 2.16 Tumor dissociation:

At the indicated time points, BALB/c tumor-bearing mice were sacrificed, and tumors were collected dissociated with the gentleMACS Dissociator using Tumor Dissociation Kit-Mouse (Miltenyi Biotec, Auburn, CA) following the manufacturer's instructions. TILs were resuspended in R 10 medium (RPMI supplemented with 10% FBS).

## 2.17 Tumor draining lymph nodes (TdLNs):

At the indicated time points, BALB/c tumor-bearing mice were sacrificed, and lymph node from the tumor implanted side were collected including axillary, inguinal, branchial, superficial cervical lymph nodes. Lymph nodes were processed into single cell suspension by first transferring the spleen into sterile 70μm cell strainers on 50ml conical tubes. Then, lymph nodes were softly minced by pressing against the flat side of a syringe plunger in a circular motion. Cell strainers were washed with 5ml of R 10 media. Tubes containing the cell suspension were topped up with media and spun at 300g for 5 mins. Carefully, supernatants were removed without disturbing the pellet and cells resuspended with 2- 3ml of R 10 media.

## 2.18 Flow cytometry staining:

After processing tissues, cells were stained first with fixable viability dye FVS510 (1:1000, BD Biosciences, NJ, USA, Cat. #564406) for 15 mins at room temperature. Cells were then washed twice with FACS buffer (0.5% BSA/PBS) before incubated with anti-CD16/CD32 (1:100, BD Biosciences, Cat. # 553141) in FACS buffer at 4 C to block unspecific binding of antibody with FC receptors. Cells were then washed twice with FACS buffer. Followed by staining with of multiple antibodies mixture for 30 mins at 4 $^{0}$C as described below.

## 2.19 Immune profiling Staining for flow cytometry analyses:

Cells stained with a combination of anti-CD45-BV786 (1:1000, BD Biosciences, Cat. # 564225), anti- CD3-AlexaFluor 700 (1:50, BD Biosciences, Cat. # 561805), anti-CD8a-PECF94 (1:100, BD Biosciences, Cat. # 562283), and anti- CD4-V450 (1:1000, BD Biosciences, Cat. # 560468), anti-CD25-PE, anti-CD69-BV605, anti-CD49b-FITC, anti-CD279-APC, anti-127- PE-cyanine 7 (BD Biosciences) for 30

mins at 4 $^{0}$C. Another set of cells stained with combination of anti-CD45-BV786, anti-CD11b-APC, anti-CD11c-PE, anti-CD19-FITC, anti-CD86-APC-R700, anti-F4/80-APC-cy7 and anti- IA/IE-BV605for 30 mins. See table 5 and table 6 for more details.

After staining, cells were washed with FACS buffer and fixed in 1% paraformaldehyde. Cells were acquired on Becton Dickinson (BD)flow cytometry (LSRFortessa), and analyses were performed using FlowJo software version (v.)

### 2.20 CD8+ T cell depletion

Mice were injected i.p. with 200µg monoclonal anti-mouse CD8a (Ly2, clone 53-6.8, Leinco Technologies, Inc., Cat# C2848-50 mg) in 200µl PBS per injection on days 3, 7, 11, 17, 24, 31 post tumor implantation as previously described. Cell depletion was confirmed by staining peripheral blood cells with antibodies against CD3 and CD8 T cells as well as CD49b NK cells and CD4 T cells as described below.

### 2.21 NK cells depletion

NK cells were depleted using the commercially available anti-asialo antibody (Cedarlane, Asialo GM1). The antibody vial was resuspended in 2mL of dd$H_2O$, and mice was treated with 10µL anti-asialo antibody in 200µl PBS per injection i.p. on days -3, -1, 1, 4, 8, and 11. Depletions were confirmed by staining peripheral blood cells after 24-48 hrs post each depletion with antibodies against CD49b and NKp40 NK cells as well as CD8 T cells and CD4 T cells as described below.

### 2.22 Blood processing for flow staining

Saphenous bleeds were performed in one of the legs and blood was collected in tubes containing Heparin (Sarstedt Inc, Fisher Scientific, Cat. NC9628695). Blood

was then transferred to heparinized capillary tubes (Fishier Scientific, Cat# 22-260-950). Capillary tubes were spun down for 3 minutes using IEC MB centrifuge, micro hematocrit (L.Pterson) to allow the separation of peripheral blood cells. Tubes were cut above the puffy coat that was transformed into tubes before adding the ACK (Ammonium-Chloride-Potassium) lysing buffer (Gibco™, Cat# A1049201) for lysing red blood cells for 5 mins. Cells were then washed and resuspended with R 10 media.

### 2.23 Flow cytometry staining for depletion experiments:

After processing blood, cells were stained first with fixable viability dye FVS510 (1:1000, BD Biosciences, NJ, USA, Cat. #564406) for 15 mins at room temperature. Cells were then washed with FACS buffer (0.5% BSA/PBS) before being incubated with anti-CD16/CD32 (1:100, BD Biosciences, Cat. # 553141) in FACS buffer at $4^0$C to block non-specific binding of antibodies with FC receptors. Cells were then stained with a combination of anti-CD45-BV786 (1:1000, BD Biosciences, Cat. # 564225), anti- CD3-AlexaFluor 700 (1:50, BD Biosciences, Cat. # 561805), anti-CD8a-PECF94 (1:100, BD Biosciences, Cat. # 562283), anti-CD4-V450 (1:1000, BD Biosciences, Cat. # 560468), anti-CD49b-FITC and anti-NKp46- APC or PE for 30 mins at 4 $^0$C. After staining, cells were washed twice with FACS buffer and spun down at 1500 rpm for 5 minutes. Cells were fixed in 1% paraformaldehyde. Samples were acquired with Becton Dickinson (BD) flow cytometry (BD LSRFortessa™), and analyses were performed using FlowJo software version (v).

## 2.24 RNA extraction from cells:

After treating with 100μM of Vanadyl sulfate for 4hrs and then infecting the cells with the following viruses at either MOI 0.1 or 0.01 or mock uninfected or untreated. Cells were washed twice with cold PBS, and 350μl of RLT (Aurum Total RNA Mini Kit, Cat# 732-6820) was added with 1% β-mercaptoethanol (Sigma-Aldrich, Cat# M6250-100ML) to each sample. RNA extraction was performed by using QiaShredder columns (Qiagen, Hilden, Germany, Cat. # 79656) and RNeasy kits (Qiagen, Cat. # 74106) following the manufacturer's protocol.

## 2.25 Tumour Homogenization and RNA extraction:

Tumour samples were collected into Eppendorf tubes and then the entire tube was flash frozen in liquid nitrogen. Using a sterilized mortar and pestle that were placed in dry ice and continuously poured with liquid nitrogen to keep them extremely cold, the tumour sample was placed into the mortar and gently ground into a fine powder with a pestle. The powder tumours were then collected into collection tubes (Eppendorf safe-lock tubes, 2.0ml Eppendorf Quality, colorless, 500 tubes, cat#. 022363352) that were snap freeze before and after collecting the powder tumours. Glass wool was used to scrap out leftover samples and then wipe down with a Kim wipe between each sample. Following that, 350μl RLT (Aurum Total RNA Mini Kit, Cat# 732-6820) was added with 1% β-mercaptoethanol (Sigma-Aldrich, Cat# M6250-100ML) to each sample with 5mm stainless Steel Bead (QIAGEN, Cat# 69989) and placed in the TissueLyserII by QIAGEN (Cat#. 85300) (2 runs: 30Mhz, 2min). Tubes were then spun down at 14,000 rpm 2 minutes after removing the beads and the supernatants were transferred into QIAshredder (Qiagen,

Cat#79656) and spun down at 14,000 rpm 1 min. RNA extraction was performed RNeasy kits (Qiagen, Cat. # 74106) following the manufacturer's protocol.

### 2.26 Quantitative real-time PCR

RNA extraction was performed using the Qiagen RNeasy kit (Qiagen). RNAs were quantified using a NanoDrop ND-1000 spectrophotometer (Thermo Scientific). RNA was converted to cDNA with RevertAid H Minus First Strand cDNA Synthesis Kit (Thermo Fisher Scientific, Cat. # K1622). Real-time PCR reactions were performed according to the manufacturer's protocol (Thermo Fisher Scientific, Cat. # A25776) on a 7500 Fast Real-Time PCR system (Applied Biosystems). Gene expression relative to HPRT was calculated by the Pfaffl method. Fold-change was determined relative to the Mock control for each gene.

### 2.27 Primers for qPCR

mCXCL9 F: CAGTGTGGAGTTCGAGGAACC

mCXCL9 R: TTTGTTGCAATTGGGGCTTGG

mIL-12 F: ACGAGAGTTGCCTGGCTACTAG

mIL-12 R: CCTCATAGATGCTACCAAGGCAC

VSV M F: ATACTCAGATGTGGCAGCCG

VSV M R: GATCTGCCAATACCGCTGGA)

mHPRT F: TGAAGAGCTACTGTAATGATCAGTCAA

mHPRT R: AGCAAGCTTGCAACCTTAACCA

### 2.28 *Ex vivo* mouse model:

BALB/c mice were implanted with subcutaneous CT26WT cells. Mice were sacrificed after tumors had reached at least 10 mm x 10 mm in size. Tumors were extracted and then cut into 2 mm-thick slices using a metal matrix and razor blades.

Each slice was cored into 2 mm x 2 mm pieces using a punch biopsy. Each tissue core was incubated in 1 mL of Dulbecco's Modified Eagle's Medium (DMEM) supplemented with 10% fetal bovine serum and 30 mM HEPES at 37 °C in a 5% CO2 humidified incubator. Cores were treated for 4 hours with 100μM of Vanadyl sulfate and were infected with indicated viruses at MOI 0.01. After 24hrs supernatants were collected for virus titration using a standard plaque assay.

### 2.29 Statistical analysis

Statistical significance was calculated using Student's t test or one-way or two-way ANOVA tests with Sidak or Dunnett's multiple correction test was applied when groups were split on multiple independent variables and also using Tukey's multiple comparison test. Mantel-Cox log rank test was used to determine significant differences in plots for survival studies. Error bars represent standard error of the mean. Significance is based on a p value $<0.05$. Statistical analyses were performed using Graph-Pad Prism 8.0 (GraphPad software, LLC) and Excel. For multiplex data, the analysis software is milliplex analyst, version 5.1.0.0. VigeneTech Inc using 5 parameter curve fitting (log scale). Data were then transformed to $\log_{10}$ then normalized to the baseline values for each cytokine/ chemokine for each time point to quantify the fold changes. For individual response, data transformed to $\log_{10}$ as plotted in the graphs to be able to see a significant difference. For ELISPOT analysis software is ImmunoSpot version 7.0.20.0, Flow cytometry was performed at the University of Ottawa's Flow Cytometry Core Facility using the BD LSR Fortessa (BD) or BD Celesta (BD) Flow Cytometers. Analysis of flow data was conducted using FlowJo v10 (FlowJo,

LLC, Ashland, OR). For all analyses, *p < 0.05, 872 **p < 0.01, ***p < 0.001, ****p < 0.0001; n.s. = not significant.

# Chapter 3: Results

## 3.1 The impact of VS+VSVΔ51 on the antitumor immune response including the secretion of cytokine and chemokines, antigen specific immune response and T cell infiltration.

This objective focuses on studying the impact of treatment with VS+VSVΔ51 on the antitumor immune response and provides a better understanding of the *in vivo* immunological mechanisms that lead to improved antitumor responses brought about from the combination of VS and VSVΔ51 through evaluating the secretion of cytokines and chemokines at various time points following treatment and the resulting antigen specific immune response. In addition, we study the impact of IL-12 transgene inclusion on VS+VSVΔ51 therapy in the CT26WT tumor model in terms of therapeutic efficacy and the antitumor immune response. **The results and figures presented in objective 3.1 are part of the published manuscript and were rearranged in this thesis (published manuscript in appendix I,** **).**

Aims:

1. Evaluate the secretion of pro-inflammatory cytokines and chemokines following the combined therapy with VS+VSVΔ51.
2. Assess the antigen specific immune response following the treatment.
3. Assess the impact of the combined therapy on T cell infiltration.
4. Study the impact of treatment with VS in combination with VSVΔ51 expressing IL12 on the therapeutic efficacy in the CT26WT tumor model.

5. Evaluate the secretion of pro-inflammatory cytokines and chemokines following the combined therapy with VS+VSVΔ51expressing IL12.

### 3.1.1. VS+VSVΔ51 combination treatment upregulates the secretion of pro-inflammatory chemokines and cytokines *in vivo*.

To explore the immunological mechanisms that lead to improved antitumor responses brought about from the combination of VS+VSVΔ51, we chose to focus on the CT26WT colon cancer model (syngeneic in Balb/C). Subcutaneously implanted CT26WT tumors are inherently resistant to VSVΔ51 and while monotherapy is not curative, improved survival can be observed using a vanadate/VSVΔ51 therapeutic combination in this model, leading to approximately 20% complete remissions (155). Improved virus spread, as measured by VSVΔ51-encoded luciferase transgene-associated luminescence using an in vivo imaging system (IVIS), is also observed in this model (155). To confirm that similar effects were achievable using the body building supplement VS, mice were implanted with the CT26WT cells, and when tumors reached a volume of 100 mm3, three doses delivered intratumorally of VS (50 mg/kg) or PBS, followed by 1E8 plaque forming units (PFU) VSVΔ51 (encoding luciferase) or PBS were administrated over the course of 5 days (Figure 5A). In line with previous studies with vanadate, improved viral replication elicited by VS was confirmed by IVIS imaging one day post the first treatment (Figure 5B). The combination treatment led to 20% survival (Figure 6).

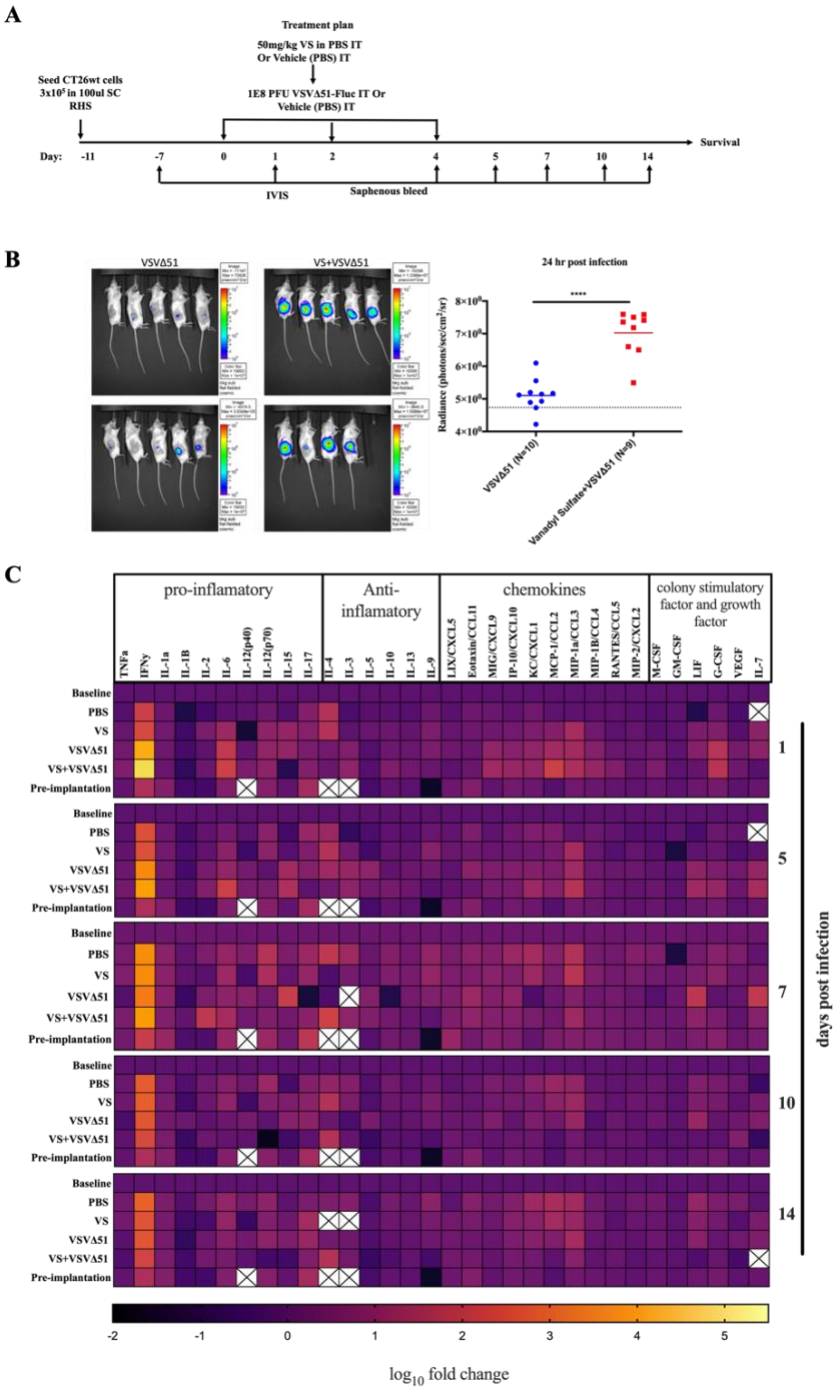


**Figure 5: VS+VSVΔ51 co-treatment upregulates the secretion of pro-inflammatory chemokines and cytokines 1 and 5 days post the treatment.**

**A)** Schematic representation of the treatment schedule: CT26WT-tumor bearing mice received a total of three doses delivered intratumorally of vanadyl sulfate (50mg/kg) and VSVΔ51-fluc (1E8 PFU) or monotreatment injections with PBS, vanadyl sulfate (50mg/kg), or VSVΔ51-fluc (1E8 PFU) alone over 5 days. **(B)** Twenty-four hours post the first treatment; viral replication was monitored by IVIS. Representative bioluminescence image. Scale represented in photons; bar indicates mean. P=0.0007 as compared to mock-treated condition. **(C)** Heatmap represented the $\log_{10}$ fold change per condition of pooled sera for all the treated time points, normalized to day 7 post implantation as a baseline, n= 10 per group.

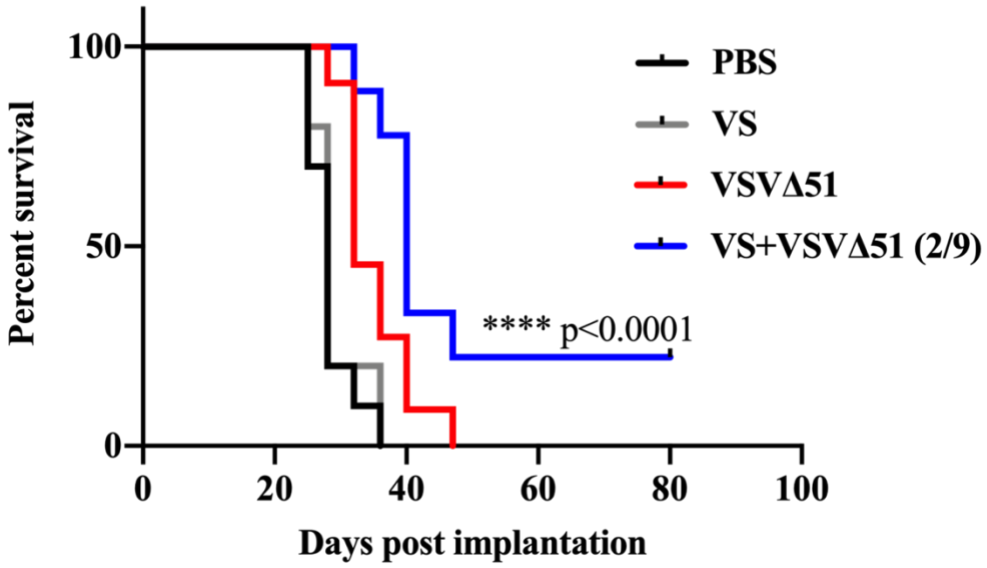


**Figure 6: VS+VSVΔ51 co-treatment improves the therapeutic efficacy in the CT26WT tumor model.**

This figure is part of Figure 5, Survival was monitored over time, the percentage of survival was included for each condition, long rank (Mantel-Cox) test indicated the significant, P<0.0001.

A multiplex assay was subsequently performed using collected sera to evaluate the secretion of a panel of pro-inflammatory chemokines and cytokines in the blood at various time points following the treatment (Figure 5C, Figure 7A, B). Pooled sera were used to map general trends in cytokine profiles over time as that provided an indication of the kinetics and the secretion profile of cytokines and chemokines in the tumor bed and the systemic impact of our treatment since we administered our treatment intratumorally (Figure 5C). Further analyses using sera from individual mice were carried out to confirm trends.

These findings from these analyses revealed that, apart from increasing Interleukin-6 (IL-6) on day 1 (Figure 7A), VS had little impact on overall cytokine secretion. On the other hand, VSVΔ51 alone significantly increased the secretion of proinflammatory cytokines and chemokines including IFN-γ, CXCL9, CXCL10, CCL3, CCL4, and IL15 compared with VS and PBS groups (Figure 7A, B).

Importantly, we observed significant increases in the secretion of a subset of cytokines and chemokines in the group that received the combined therapy as compared to monotherapies. Most notably, we measured a 5-fold increase in IFN-γ secretion 1-day post-infection ((Figure 5C, Figure 7A), p-value=0.0001 compared to PBS and VS, and p-value=0.01 compared to VSVΔ51 alone, Table2).

IL-6, an IFN-γ responsive cytokine, increased most significantly at 5 days post treatment (Figure 5D, Figure 6A). In addition to IL-6, IFN-γ is known to upregulate the secretion of pro-inflammatory cytokines and chemokines.

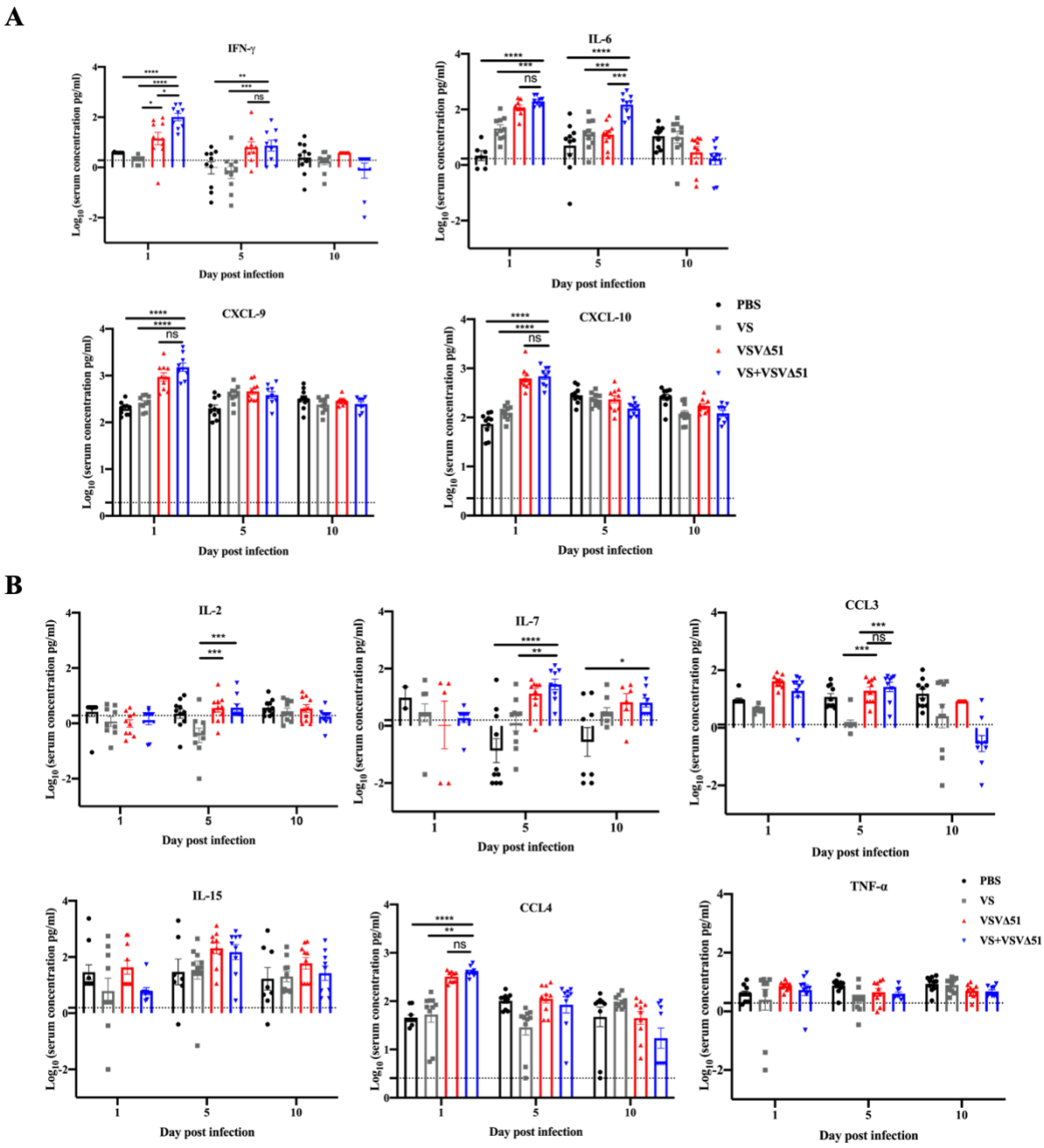


**Figure 7: VS+VSVΔ51 co-treatment induces the secretion of pro-inflammatory chemokines and cytokines 1 and 5 days post the treatment.**

This figure is part of Figure 5, **(A)& (B)** The concentration of Cytokines and chemokines pg/ml for each group for each individual mouse, data transformed into $\log_{10}$. (n=10 per condition), line indicates the detection concentration, Mean±SEM; * P=0.01, ** P=0.003, *** P=0.001, ****P<0.0001, ns= not significant, Two-way ANOVA.

**Table 2: p value for significant comparison between each condition for each tested cytokine and chemokine following treatment at various time points.**
Data were analyzed using two-way ANOVA test, * P=0.01, ** P=0.003, *** P=0.001, ****P<0.0001

| cytokines/ chemokines | day post treatment | PBS vs. VS | PBS vs. VSVΔ51 | PBS vs. VS+VSVΔ51 | VS vs. VSVΔ51 | VS vs. VS+VSVΔ51 | VSVd51 vs. VS+VSVΔ51 |
|---|---|---|---|---|---|---|---|
| IFN-γ | 1 | 0.7394 | 0.1478 | <0.0001 | 0.0111 | <0.0001 | 0.011 |
| | 5 | 0.8883 | 0.0159 | 0.0081 | 0.0017 | 0.0008 | 0.9962 |
| | 10 | 0.9311 | 0.8872 | 0.2183 | 0.5482 | 0.5318 | 0.046 |
| IL-6 | 1 | 0.0034 | <0.0001 | <0.0001 | 0.0157 | 0.0009 | 0.8159 |
| | 5 | 0.3191 | 0.3578 | <0.0001 | 0.9999 | 0.0002 | 0.0002 |
| | 10 | 0.999 | 0.0807 | 0.0073 | 0.1113 | 0.0112 | 0.7809 |
| CXCL10 | 1 | 0.03 | <0.0001 | <0.0001 | <0.0001 | <0.0001 | 0.9455 |
| | 5 | 0.69 | 0.7352 | 0.0106 | 0.9998 | 0.1597 | 0.1373 |
| | 10 | 0.0006 | 0.1538 | 0.0012 | 0.232 | 0.9998 | 0.2888 |
| CXCL9 | 1 | 0.4834 | <0.0001 | <0.0001 | <0.0001 | <0.0001 | 0.1075 |
| | 5 | 0.0068 | 0.0004 | 0.0114 | 0.8439 | 0.9998 | 0.8141 |
| | 10 | 0.4801 | 0.961 | 0.6046 | 0.7807 | 0.9985 | 0.8724 |
| CCL3 | 1 | 0.5511 | 0.0594 | 0.6391 | 0.0014 | 0.0757 | 0.5705 |
| | 5 | 0.0029 | 0.827 | 0.5339 | 0.0001 | <0.0001 | 0.9552 |
| | 10 | 0.013 | 0.727 | <0.0001 | 0.1721 | 0.0019 | <0.0001 |
| CCL4 | 1 | 0.9833 | <0.0001 | <0.0001 | 0.0038 | 0.0016 | 0.2138 |
| | 5 | 0.0327 | 0.9691 | 0.9658 | 0.0263 | 0.2231 | 0.9083 |
| | 10 | 0.4891 | 0.9997 | 0.4514 | 0.1391 | 0.0297 | 0.3638 |
| IL-7 | 1 | 0.8818 | 0.599 | 0.751 | 0.8366 | 0.9728 | 0.9651 |
| | 5 | 0.093 | <0.0001 | <0.0001 | 0.0737 | 0.0094 | 0.8767 |
| | 10 | 0.0739 | 0.0306 | 0.0139 | 0.9039 | 0.882 | >0.9999 |
| IL-15 | 1 | 0.337 | 0.973 | 0.3487 | 0.1551 | >0.9999 | 0.1658 |
| | 5 | 0.9986 | 0.2259 | 0.3963 | 0.2161 | 0.4046 | 0.9875 |
| | 10 | 0.9978 | 0.5626 | 0.9686 | 0.6348 | 0.9913 | 0.8224 |
| IL-2 | 1 | 0.3954 | 0.2134 | 0.5426 | 0.9885 | 0.9953 | 0.9426 |
| | 5 | 0.2294 | 0.8759 | 0.0079 | 0.653 | 0.4987 | 0.0604 |
| | 10 | 0.0131 | 0.98 | 0.0157 | 0.0376 | >0.9999 | 0.0442 |

This includes CXCL-9 and CXCL10, which we have previously shown to be upregulated through vanadate/VSVΔ51 combination treatment in CT26WT cells *in vitro* (155). However, while average levels were highest coinciding with the peak of IFN-γ secretion, there was no statistically significant difference in CXCL9 when comparing VSVΔ51 to VSVΔ51 in combination with VS (p=0.1, Table2).

Our multiplex data also illustrated that the secretion of a number of important cytokines and chemokines followed the same behaviour of IFN-γ secretion in vivo. Indeed, there was also a trend toward an increase in the secretion of interleukin-2 (IL-2) and IL-12, the two cytokine factors that strongly and synergistically affect IFN-γ expression (Figure 5C, Figure 7B).

Next, we observed that pro-inflammatory chemokines involved in immune cell recruitment including CCL2, CCL3, CCL4 and CCL5 showed an increase 1-day post the combined therapy. Levels were particularly sustained for CCL3 and CCL4 after 5 days post-treatment (Figure 5C, Figure 7B). The secretion of IL-4 was also evaluated and found to be up-regulated from 5 to 10 days post-treatment in the group that received the combined therapy compared with all the control groups (figure 5C). The secretion of cytokines involved in mediating T cell and natural killer cell activation, proliferation, and differentiation into effector T cells, as well as those responsible for driving the long-term development of CD8+ T cells, including IL2, IL-7, IL12, and IL-15, were found to be increased after 1 day and 5 days post-treatment in mice treated with the combined therapy with no significant difference in compassion with the VSVΔ51 group (Figure 5C, Figure 7B).

It is important to highlight that VSVΔ51 alone was able to significantly increase the secretion of proinflammatory cytokines and chemokines including IFN- γ, CXCL9, CXCL10, CCL3, CCL4, and IL15 compared with VS and PBS groups with no significant differences compared with VS+ VSVΔ51 group (Figure 5C, Figure 7A, B).

### 3.1.2. Combined VS+VSVΔ51 therapy enhances antigen-specific antitumor immune response.

In conjunction with previous studies (155), the results above support a potential role of activated and IFN-γ producing T-cells in eliciting the response to combined vanadate/VSVΔ51 therapy. I next sought to investigate the impact of VS treatment in combination with VSVΔ51 on viral- and tumor antigen-specific immune responses. I assessed the antigen-specific immune response against peptides for gp70 (the immunodominant antigen in CT26WT tumor model and a common murine tumor-associated antigen that is highly expressed) and VSV N following combined therapy or controls using an IFN-γ ELISPOT assay. Following the same therapeutic regimen, fourteen days post treatment, splenocytes were isolated from mice and then stimulated ex vivo with gp70 or VSV N peptides (Figure 8A). A significant increase in the number of IFN-γ producing splenocytes reacting to the peptide gp70 was detected in the group that received VS+VSVΔ51 when compared with monotherapy alone (Figure 8B). As expected, treatment with VSVΔ51 alone induced an antiviral immune response measured by the reaction against the VSV N peptide in comparison with the combination treatment group (Figure 8B).

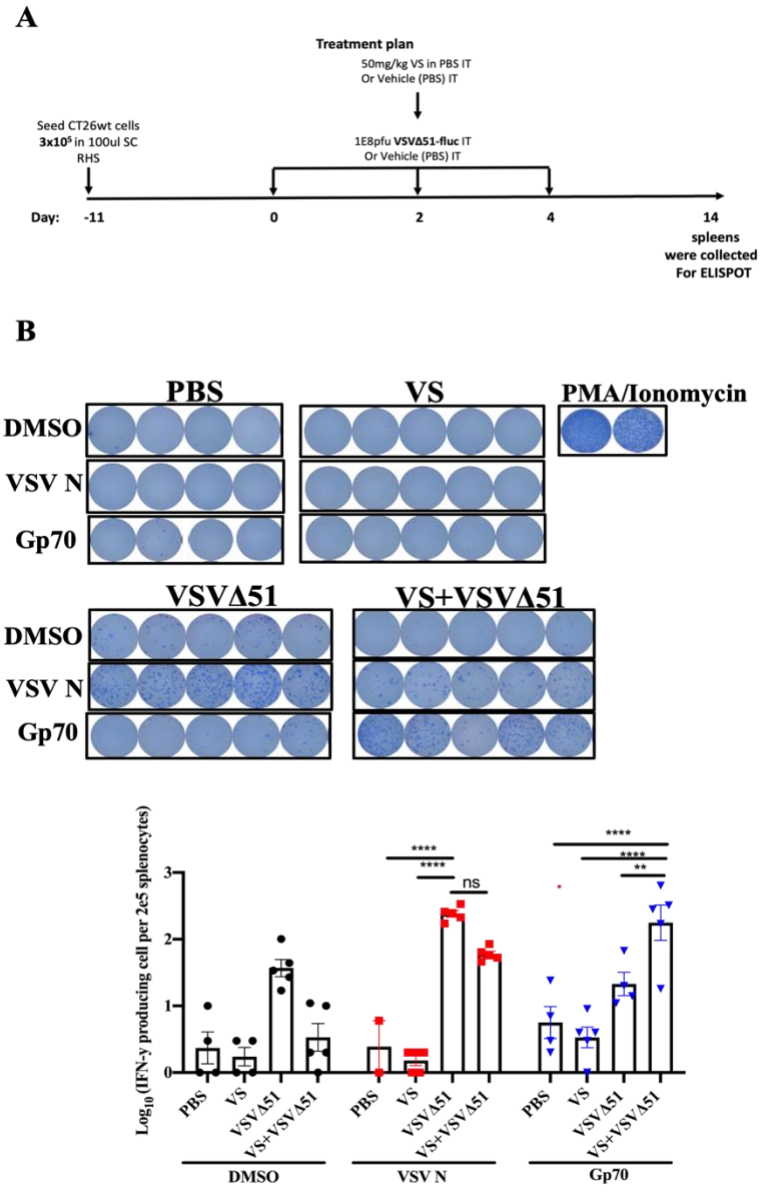


**Figure 8: VS plus VSVΔ51 combination therapy induces antigen specific immune response 14 post treatment.**

**(A)** Schematic representation of the treatment schedule: after 12 days, CT26WT-tumor bearing mice received a total of three doses delivered intratumorally of vanadyl sulfate (50mg/kg) and VSVΔ51-fluc (1E8 PFU) or monotreatment injections with PBS, vanadyl sulfate (50mg/kg), or VSVΔ51-fluc (1E8 PFU) alone over 5 days. Splenocytes from treated mice were processed 14 days post treatment, then co-cultured with either DMSO, VSV N, or gp70 peptides for 20 hours, PMA and ionomycin were used as a positive control. **(B)** Representative wells from an ELISPOT assay, Graph shows quantification of $\log_{10}$ of the number of IFN-γ producing cells per 2E5 splenocytes. N=5 per condition, Mean±SEM; ** P=0.003, ****P<0.0001, ns= not significant, Two-way ANOVA.

However, we did detect a response against the DMSO control in the VSVΔ51 group, suggesting there could be non-specific activation owing to the virus treatment. Altogether, these results suggest that VS/VSVΔ51 combination therapy can improve the tumor antigen-specific T-cell response.

### 3.1.3. T-cell infiltration to the tumor site induces following the combination therapy.

In previous studies, the treatment of cancer cells with vanadate/VSVΔ51 leads to profound changes in gene expression profiles in infected cancer cells and in particular, the up-regulation of multiple cytokines and chemokines associated to response to type II IFN (155). This profile is corroborated from cytokine profiles in Figure 5. However, given that cytokine profiles measured in the blood are representative of systemic responses, it is not possible to discern the specific impact of VS+VSVΔ51 treatment on cancer cells from its potential impact on immune cells; more specifically, mediating T cell infiltration/ recruitment to the tumor site.

Given that has been previously reported that the increased expression of type II IFN response-induced chemo-attractants such as CXCL9 and CXCL10 following vanadate/VSVΔ51 co-treatment, we looked at whether VS+VSVΔ51 co-treatment could promote the recruitment of T-cells in a chemotaxis assay. As illustrated in Figure 9A, cultured CT26WT cells were treated with PBS, VS 100μM, VSVΔ51 (multiplicity of infection (MOI)=0.01) or the combination of VS+VSVΔ51.

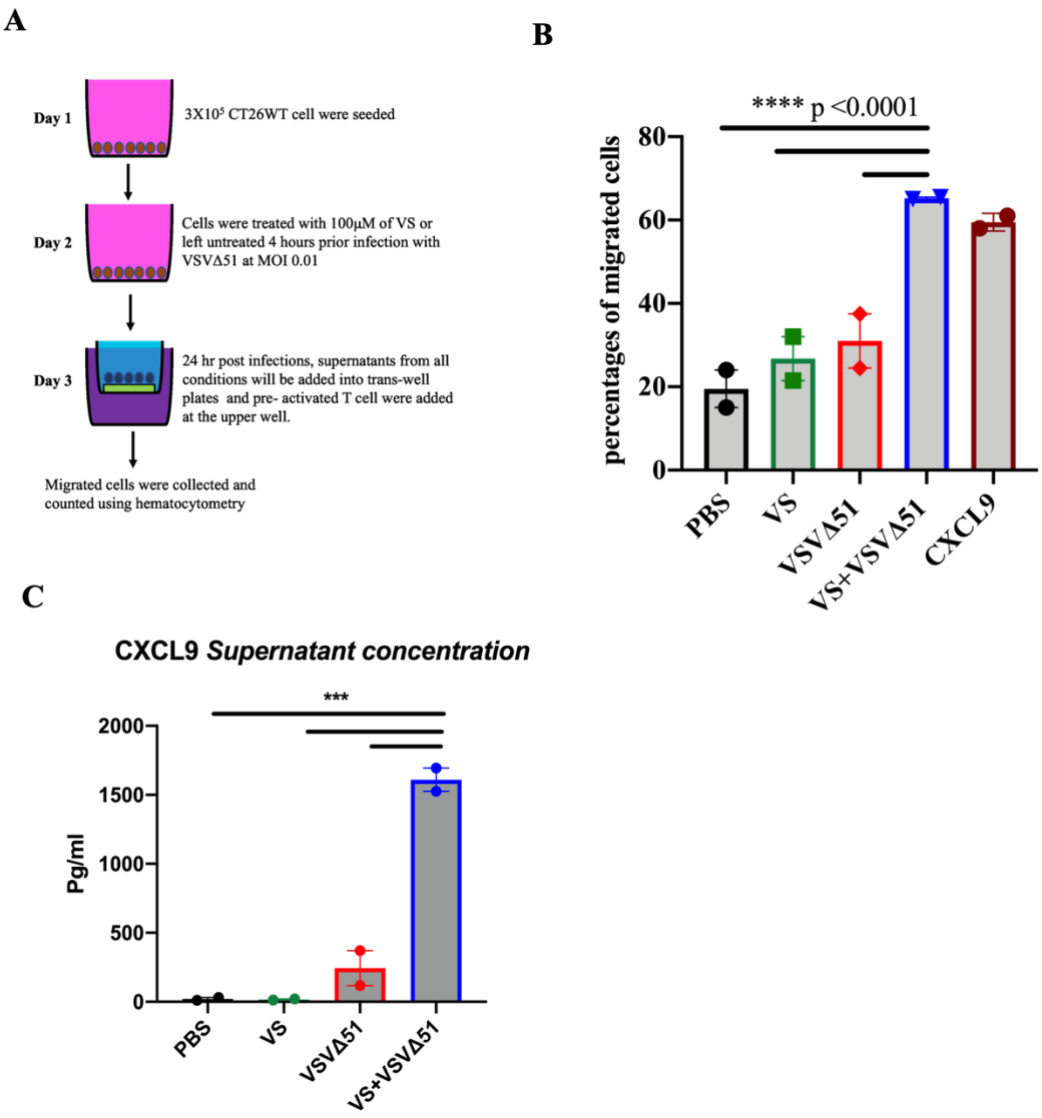


**Figure 9: Vanadyl Sulfate in combination with VSVΔ51 increases the production of T-cell chemoattractant and T-cell migration in vitro.**

***(A)*** Supernatants were collected after treating CT26WT cells with Vanadyl Sulfate at a concentration of 100µM for 4 hours and then subsequently infection with VSVΔ51 at MOI 0.01 or with PBS, Vanadyl Sulfate alone or VSVΔ51 alone for 24 hours. Supernatants were then used for the assessment of chemokines or for performing chemotaxis assays (compared to CXCL9 control). Chemotaxis of T cells was assessed using a Trans-well system. **(B)** Migration percentage was calculated as (total number T cells in bottom chamber/ total number T cell input) x 100, representative data of the average of 2 independent experiments, n=2 per condition. **(C)** The supernatant concentration of CXCL-9, graph shows the pg/ml. Mean±SEM; n=2 per condition, *** P=0.001, Two-way ANOVA.

Supernatants were collected 24h later and added to the lower chamber of Trans-well plates with 5-μm pores. A condition with CXCL9 cytokine (1 μg /ml) was included as a positive control. Mouse T-cells isolated from splenocytes were activated using anti-CD3/CD28 beads and IL-2 and then added to the top chamber. Activated cells were allowed to migrate to the bottom well containing supernatants for a period of 24h post treatment. The results of this chemotaxis assay are shown in Figure 8 and demonstrate that supernatants from VSVΔ51-infected cells co-treated with VS significantly increase the migration of activated T-cells compared to single treatments, to levels exceeding the CXCL9 positive control (Figure 9B).

The CXCL-9 concentration in the supernatants used in the migration assay was measured by ELISA. As shown in Figure 9C, treatment with VS+VSVΔ51 substantially increased the secretion of CXCL-9 compared to single treatments. Altogether, these data support the hypothesis that treatment of cancer cells with vanadium during infection increases their immunogenicity profile and promotes the migration of activated T-cells to the tumor.

### 3.1.4. VS in combination with VSVΔ51 encoding IL-12 further improves therapeutic efficacy.

All the results presented above implicate a role of T-cells in eliciting the enhanced therapeutic effects of VS+VSVΔ51 treatment and that is also associated with up-regulation in the secretion of pro-inflammatory cytokines and chemokines; however, the overall survival is still 20% in the CT26WT tumor model (Figure 6). We, therefore, as an attempt to improve the therapeutic

efficacy of the combined therapy considered whether therapeutic efficacy could be further enhanced by genetically encoding complementary cytokines in VSVΔ51.

As a first candidate and proof of concept, I evaluated the impact of encoding IL-12 within VSVΔ51. IL-12 is produced by dendritic cells (DC) in response to IFN-γ secretion to enhance the activity of CD8+ cytotoxic T-cells (CTL) as well as Natural Killer cells (NK) (302, 303). Further, IL-12 is thought to be a positive regulator of IFN-γ secretion. Many OVs such as Maraba-MG-1, Adenovirus, and HSV-1 have been engineered to express IL-12, leading to improved antitumor effects in numerous murine carcinoma models by promoting both the activation of T cells and NK cells (304, 305).

As a first step, multi-step and single-step viral growth kinetics were determined in CT26WT cells, and the inclusion of IL-12 as transgene had no impact on virus replication kinetics compared with parental virus VSVΔ51encoding firefly luciferase (Figure 10A). In addition, IL12 secretion was confirmed 24 hr following viral infection compared with the parental virus (around 6000pg/ml) (Figure 10B).

To validate the impact of IL-12 on the efficacy of the combination therapy, we performed a similar therapeutic regimen as shown in Figure 5A with VSVΔ51encoding/expressing IL12 (Figure 11A) and then monitored tumor progression and survival following the treatment (Figure 11B). Combination treatment was well-tolerated although we did observe a slight decrease in the body weight of mice treated with VSVΔ51 encoding/expressing IL12 during the week of the treatment followed by quick recovery within the following

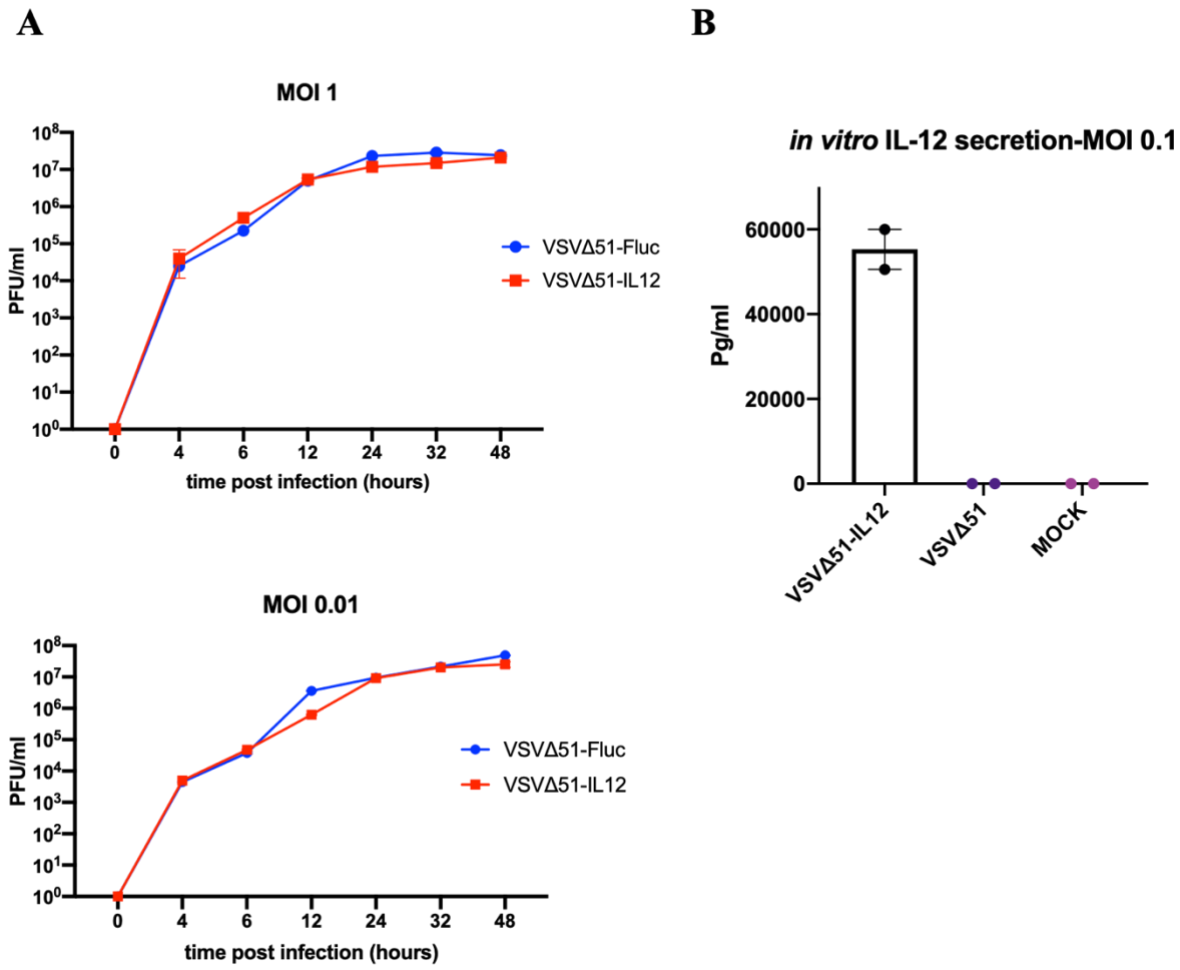


**Figure 10: Replication kinetic of VSVΔ51 encoding IL12 and the secretion of IL12 *in vitro.***

(**A)** Replication kinetic of VSVΔ51 encoding fluc or IL12 was performed in multistep or single-step viral growth curves in CT26WT cells. Cells were incubated up to 48 hours post viral infection, 200µl of supernatant was collected and viral titer in collected supernatant was quantified by high-throughput tittering using a standard plaque assay. Graphs show the plaque performing unit per ml (PFU/ml), n= 3 per each time point. (**B)** CT26WT cells were infected with VSVΔ51 encoding fluc or IL12 at MOI 0.1. 24 hrs post-infection, supernatants were collected and the secretion of IL12 was measured by ELISA. The graph shows the pg/ml. Mean±SEM; n=2 per conditions.

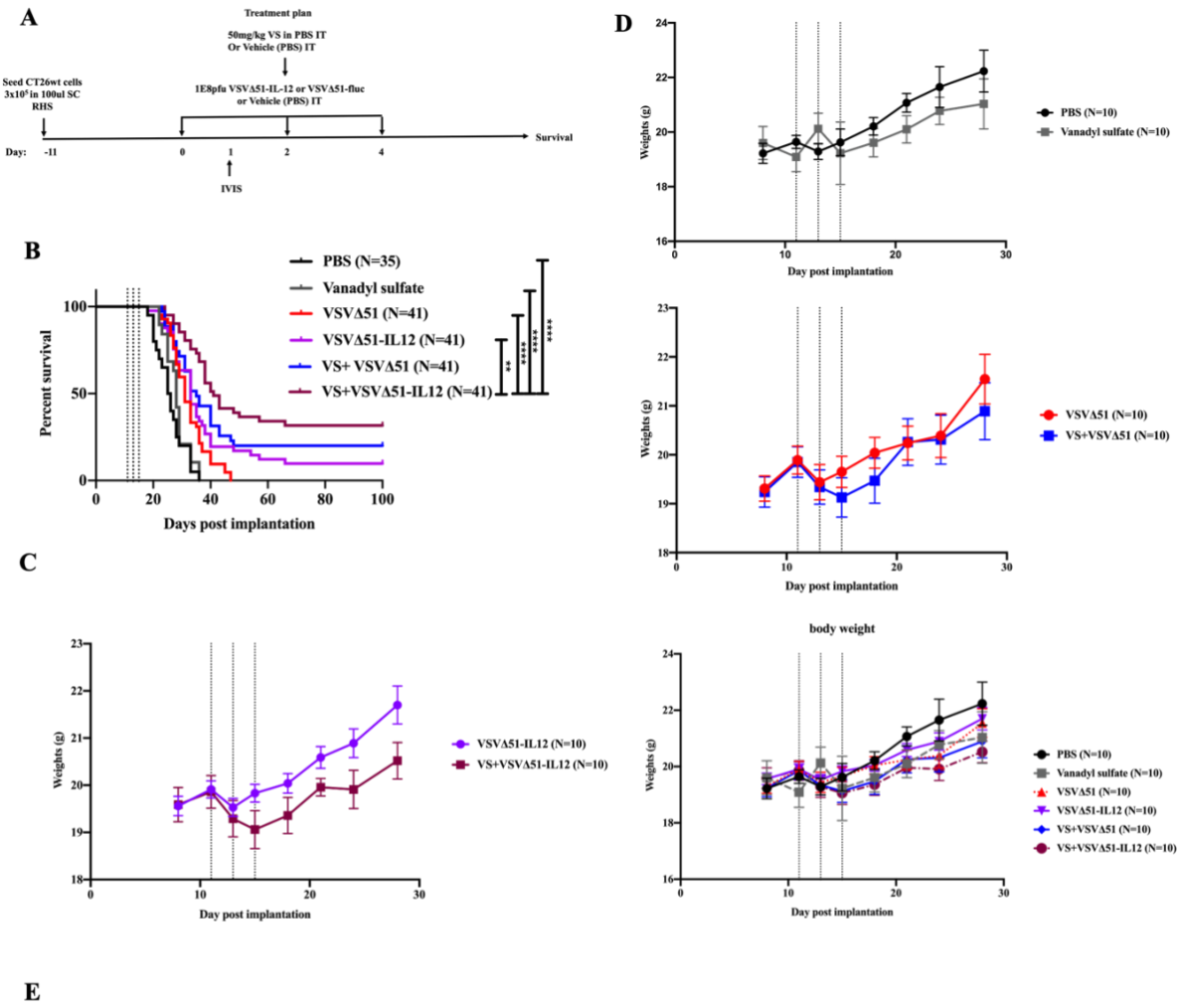


E

| | PBS | Vanadyl Sulfate | VSVΔ51 | VSVΔ51-IL12 | VS+ VSVΔ51 |
|---|---|---|---|---|---|
| PBS | X | ns | 0.0001 | <0.0001 | <0.0001 |
| Vanadyl Sulfate | ns | X | 0.006 | 0.001 | 0.0001 |
| VSVΔ51 | 0.0001 | 0.006 | X | 0.04 | 0.004 |
| VSVΔ51-IL12 | <0.0001 | 0.001 | 0.04 | X | ns |
| VS+VSVΔ51 | <0.0001 | 0.0001 | 0.004 | ns | X |
| VS+VSVΔ51-IL12 | <0.0001 | <0.0001 | <0.0001 | 0.001 | 0.08 |

**Figure 11: Vanadyl Sulfate in combination with VSVΔ51 expressing IL-12 improves the therapeutic efficacy in CT26WT-tumor model.**

**(A)** Schematic representation of the treatment schedule: CT26WT-tumor-bearing mice received a total of three dose delivered intratumorally of vanadyl sulfate (50mg/kg) and VSVΔ51 encoding IL-12 (1E8 PFU) or with PBS, vanadyl sulfate (50mg/kg), or VSVΔ51 encoding IL-12 (1E8 PFU) alone over 5 days. (**B)** Survival was monitored over time, the percentage of survival was included for each condition, long rank (Mantel-Cox) test indicated the significance as shown in table below. Survival data represents an aggregate of 3 independent studies. (**C&D)** Body weight was measured three times a week over the first three weeks of the treatment. Graphs show the average of body weight of each group, Mean±SEM; n=10 per group. **(E)** Table shows the significance values using long rank (Mantel-Cox), * P=0.01, ** P=0.003, *** P=0.001, ****P<0.0001.

week (Figure 11C). Our data demonstrate that approximately 40% of the group receiving VS in combination with VSVΔ51-IL-12 survived compared to 20% in the VS- VSVΔ51 condition, and only 10% in the group receiving the VSVΔ51 expressing IL-12 alone (Figure 11B, D). These mice also showed rejected tumors after re-challenge with CT26WT cells.

The inclusion of IL-12 to VSVΔ51 in combination with VS also further enhanced the antigen specific immune response against the gp70 peptide (Figure 12); however, there was no apparent improvement in comparison with VS+VSVΔ51 treatment (compare Figure 8A and 8B).

Taken together, these data provide compelling evidence that further improvements in therapeutic efficacy can be achieved through genetic complementation by encoding cytokines such as IL-12 that are not otherwise up-regulated by VS/VSVΔ51 co-treatment.

### 3.1.5. VS+VSVΔ51 encoding/ expressing IL-12 combination treatment further upregulates the secretion of pro-inflammatory chemokines and cytokines *in vivo*.

As part of the cytokine profiling by multiplex assay presented in aim 3.1.1 (Figure 13A) two additional groups were included VSVΔ51 expressing IL12 only and VS in combination with VSVΔ51 expressing IL12 to look at the impact of IL-12 inclusion on the cytokine and chemokine secretion in blood following the combination treatment (Figure 13). The multiplex analyses revealed a trend towards increasing systemic IL-12 with VSVΔ51-IL12 and further with VS+VSVΔ51-IL12, which was the only condition showing a

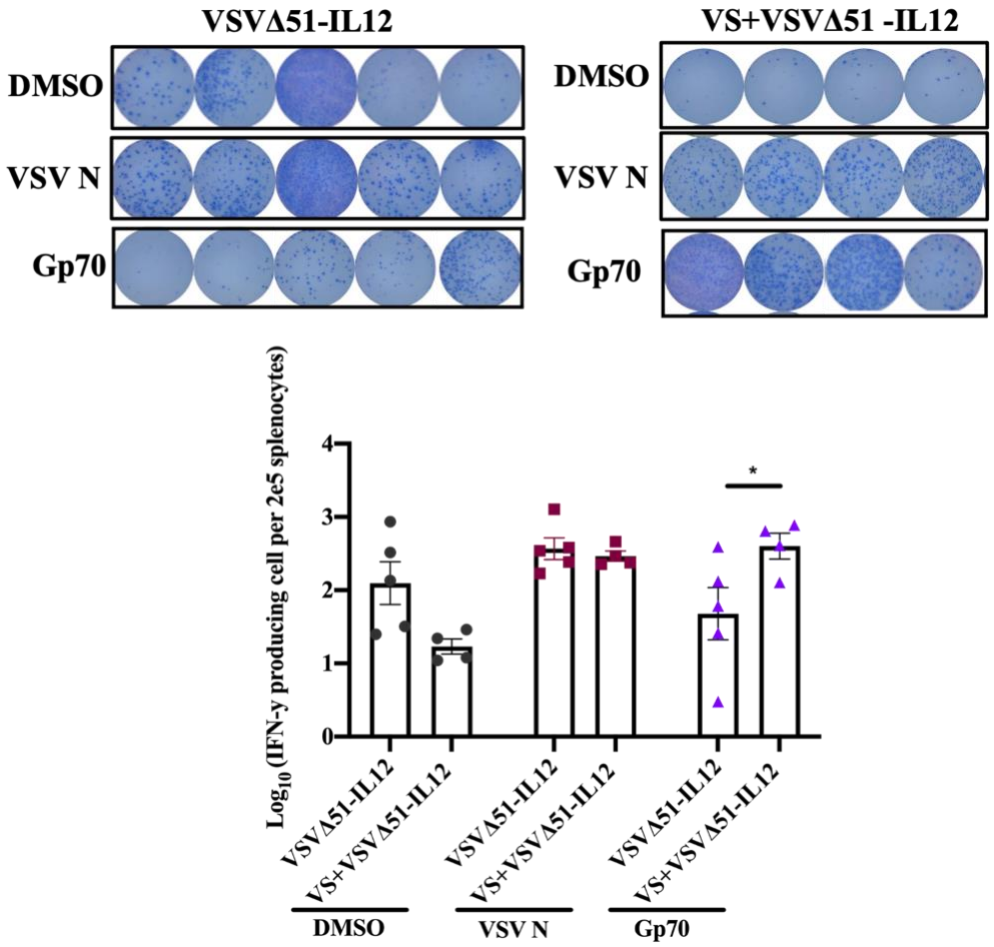


**Figure 12: VS plus VSVΔ51 expressing IL-12 combination therapy further induces antigen specific immune response 14 post treatment.**

As part of Figure 8, two additional groups received three intratumorally vanadyl sulfate (50mg/kg) and VSVΔ51 expressing IL-12 or monotreatment injections over 5 days. representative data from ELISPOT assay and Graph shows quantification of $\log_{10}$ of the number of IFN-γ producing cells per 2E5 splenocytes. N=4-5 per group, Mean±SEM; * P=0.01, Two-way ANOVA.

statistically significant increase in IL-12 relative to PBS (p-value=0.023, Table 3) (Figure 13B, Figure 14A, B). In contrast with results obtained in Figure 5, VS+VSVΔ51-IL12 co-treatment did not elicit a further increase in the levels of IFN-γ compared to VSVΔ51-IL12 (Figure 13B, Figure 14A); however, compared to Figure 7A, it is apparent that when viruses were used alone, IFN-γ reached higher levels on day 1 with VSVΔ51-IL12 compared to VSVΔ51 (more than 200pg/ml vs. around 100pg/ml). On the other hand, and consistent with Figure 1C, levels of IL-6 were significantly higher at day 5 following VS+VSVΔ51-IL12 combination treatment compared to the monotherapies (Figure 13B, Figure 14A).

Additionally, the secretion of CXCL1, CCL2, CCL3, and CCL4 also increased in the group that received VS + VSVΔ51-IL12 after 1 day and continued to be elevated up to 5 days post-treatment with a 2-fold increase in the secretion of CCL2 and an increase in the secretion of CCL3 compared with all the monotherapy groups (Figure 13B), more than 300pg/ml in the serum concentration of CCL4 and more than 50pg/ml in the concentration of the secretion of CCL3 were observed in 5 out 10 mice treated with VS+VSVΔ51 expressing IL12 (Figure 14B).

IL-15 and IL-7 increased to over a fold increase in the combined therapy group on days 10 and 14 post-treatment (Figure 13B, Figure 14B). Similar activity was observed in the secretion of IL-4 on days 10 and 14 post-treatment (Figure 13B).

Taken together, these data prove that encoding cytokines such as IL-12 further induces cytokine and chemokines secretion, and this enhancement could be because of the impact of IL-12 on the immune response and IFN-γ secretion.

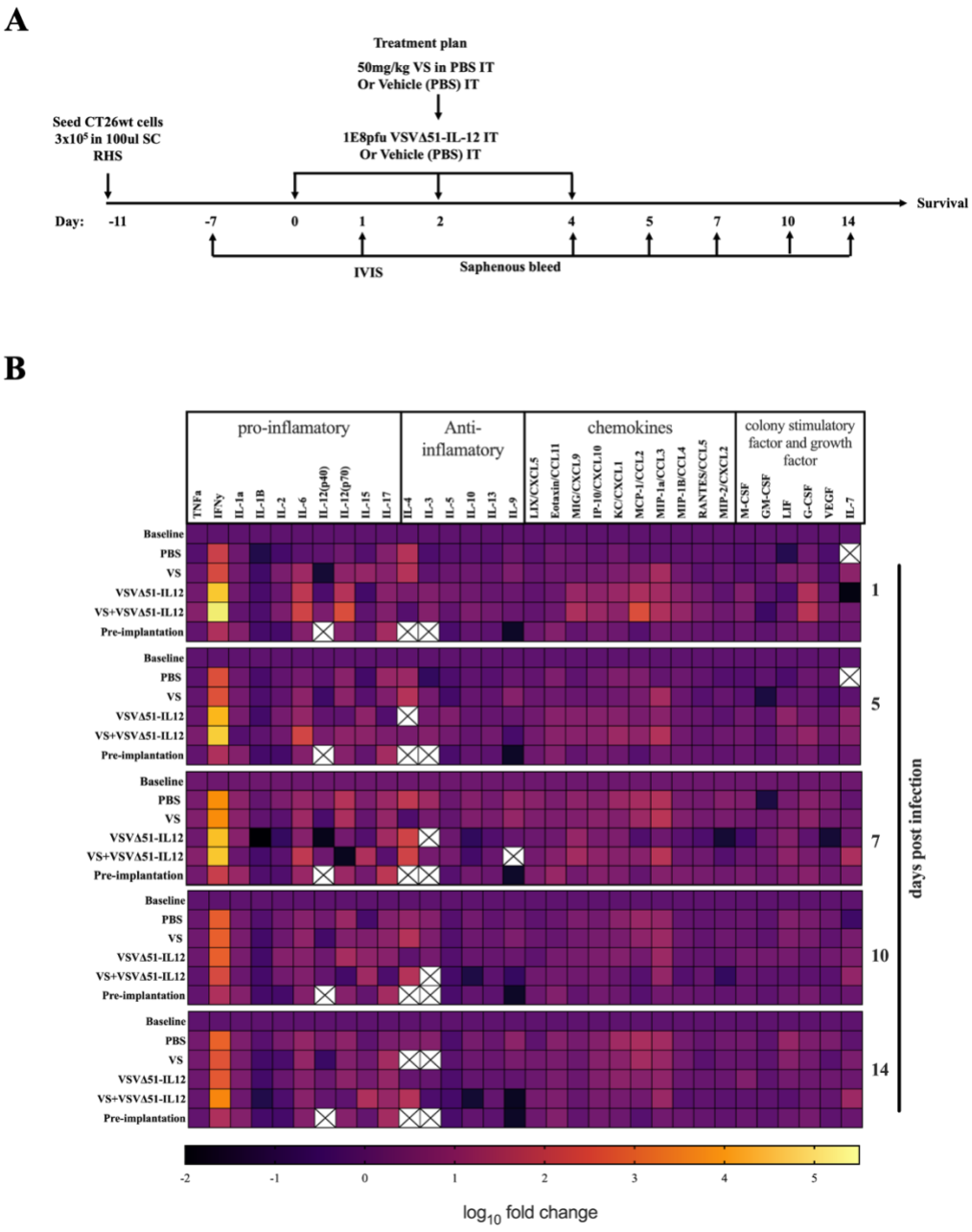


**Figure 13: VS+VSVΔ51 expressing IL-12 co-treatment further induces the upregulation of the secretion of pro-inflammatory chemokines and cytokines 1 day and 5 days post the treatment.**

**(A)** As part of the experiment presented in Figure 5, two additional groups of CT26WT-tumor bearing mice received a total of three doses delivered intratumorally of vanadyl sulfate (50mg/kg) and VSVΔ51 expressing IL-12 (1E8 PFU) or VSVΔ51 expressing IL-12 (1E8 PFU) alone over 5 days were added. **(B)** Heatmap of the $\log_{10}$ fold change per condition of pooled sera, normalized to day 7 post implantation as baseline for all the tested time points, (n=10 per condition).

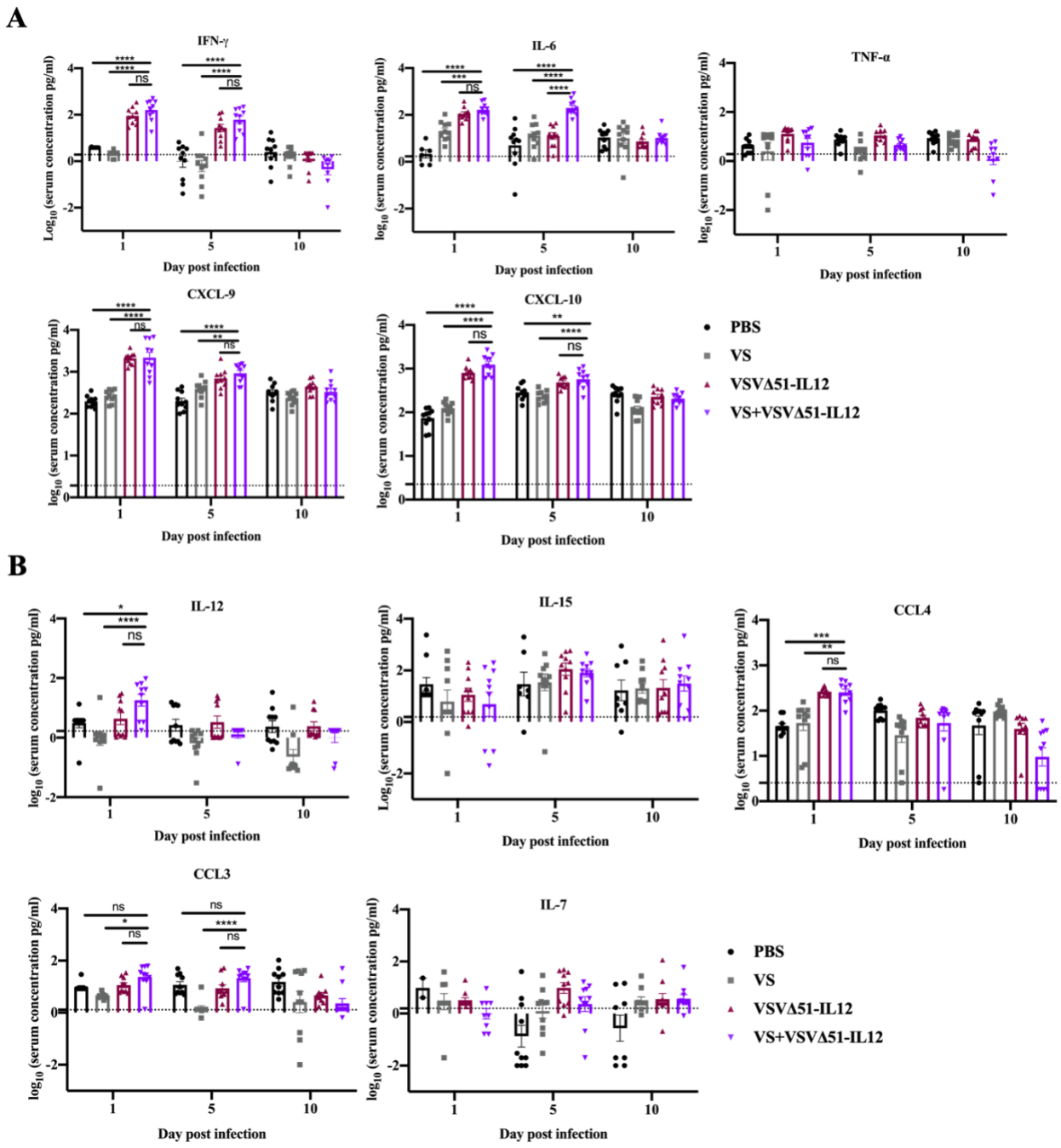


**Figure 14: VS+VSVΔ51 expressing IL-12 co-treatment further induces the secretion of pro-inflammatory chemokines and cytokines 1 day and 5 days post treatment.**

This figure is part of Figure 13, **(A)& (B)** The concentration of cytokines and chemokines pg/ml for each group for each individual mouse (n=10 per condition) was presented in each graph. Data transformed into $Log_{10}$, line indicated the detection concentration, Mean±SEM; * P=0.01, ** P=0.003, *** P=0.001, ****P<0.0001, ns= not significant, Two-way ANOVA.

**Table 3: p value for significant comparison between each condition for each tested cytokine and chemokine following treatment at various time points.**

Data were analyzed using two-way ANOVA test, * P=0.01, ** P=0.003, *** P=0.001, ****P<0.0001

| cytokines/ chemokines | day post treatment | PBS vs. VS | PBS vs. VSVΔ51 -IL12 | PBS vs. VS+VSVΔ51-IL12 | VS vs. VSVΔ51-IL12 | VS vs. VS+VSVΔ51-IL12 | VSVd51 vs. VS+VSVΔ51-IL12 |
|---|---|---|---|---|---|---|---|
| IFN-γ | 1 | 0.6549 | <0.0001 | <0.0001 | <0.0001 | <0.0001 | 0.703 |
| | 5 | 0.8446 | <0.0001 | <0.0001 | <0.0001 | <0.0001 | 0.435 |
| | 10 | 0.9026 | 0.6053 | 0.0128 | 0.946 | 0.0758 | 0.2328 |
| IL-6 | 1 | 0.0007 | <0.0001 | <0.0001 | 0.0046 | 0.0003 | 0.8425 |
| | 5 | 0.216 | 0.2381 | <0.0001 | >0.9999 | <0.0001 | <0.0001 |
| | 10 | 0.9985 | 0.8604 | 0.9996 | 0.9236 | >0.9999 | 0.9025 |
| CXCL10 | 1 | 0.0216 | <0.0001 | <0.0001 | <0.0001 | <0.0001 | 0.088 |
| | 5 | 0.6616 | 0.0213 | 0.0012 | 0.0005 | <0.0001 | 0.8002 |
| | 10 | 0.0003 | 0.8973 | 0.6057 | 0.0038 | 0.0197 | 0.9499 |
| CXCL9 | 1 | 0.5808 | <0.0001 | <0.0001 | <0.0001 | <0.0001 | 0.9991 |
| | 5 | 0.0197 | <0.0001 | <0.0001 | 0.0602 | 0.0013 | 0.5744 |
| | 10 | 0.5777 | 0.473 | 0.9979 | 0.0369 | 0.4648 | 0.5862 |
| CCL3 | 1 | 0.501 | 0.9878 | 0.3473 | 0.3179 | 0.0163 | 0.5417 |
| | 5 | 0.0014 | 0.9424 | 0.7005 | 0.0087 | <0.0001 | 0.3566 |
| | 10 | 0.0073 | 0.1405 | 0.0037 | 0.6737 | 0.9963 | 0.5365 |
| CCL4 | 1 | 0.9864 | 0.0003 | 0.0004 | 0.0011 | 0.0015 | 0.9998 |
| | 5 | 0.0157 | 0.8066 | 0.4117 | 0.1473 | 0.4494 | 0.9142 |
| | 10 | 0.3331 | 0.9732 | 0.0012 | 0.1528 | <0.0001 | 0.0049 |
| IL-7 | 1 | 0.8503 | 0.8842 | 0.4248 | 0.999 | 0.6323 | 0.523 |
| | 5 | 0.0535 | <0.0001 | 0.0071 | 0.086 | 0.8885 | 0.3462 |
| | 10 | 0.0405 | 0.0295 | 0.0254 | 0.9993 | 0.9977 | >0.9999 |
| IL-15 | 1 | 0.4559 | 0.8054 | 0.3253 | 0.9389 | 0.9956 | 0.8505 |
| | 5 | 0.9991 | 0.6589 | 0.8181 | 0.6792 | 0.8481 | 0.9901 |
| | 10 | 0.9985 | 0.9975 | 0.9453 | >0.9999 | 0.9753 | 0.9805 |
| IL-2 | 1 | 0.6319 | 0.9863 | 0.0002 | 0.8394 | 0.0129 | 0.0008 |
| | 5 | 0.041 | 0.8403 | 0.0002 | 0.2422 | 0.4336 | 0.0039 |
| | 10 | 0.9644 | 0.1281 | 0.0055 | 0.3126 | 0.022 | 0.606 |

## 3.2. Cellular immunological changes following treatment with VS+ VSVΔ51 and the impact of IL-12 inclusion on VS+VSVΔ51 therapy in the CT26WT tumor model.

This objective focuses on studying the impact of the combined therapy and the combined therapy with IL12 on the cellular immunological changes following therapy.

**Aims:**

1. Evaluate the impact of combined therapy with VS+ VSVΔ51 on cellular and immunological changes.
2. Evaluate treatment with IL12 combination therapy on cellular immunological changes.
3. Examine the role of T cells in the efficacy following VS+ VSVΔ51 and IL-12 combination therapy.
4. Examine the contribution of NK cells on the therapeutic efficacy of VS+ VSVΔ51 and IL-12 combination therapy.

### 3.2.1. The Relevant Immunological changes 5 days & 10 days following the combined therapy have identified immune profiling.

To identify relevant immunological changes at the cellular level following our combination treatment, immune cells at TILs within the tumor microenvironment (TME) and at tumor draining lymph nodes (TdLNs) were analyzed applying multi-parameter flow cytometry analyses 5 days and 10 days following the combination therapy as indicated in Figure 15 and Figure S1. We designed two multi-parameter panels to

characterize T cells including CD3+, CD4+, and CD8+ T cells and activation markers CD25 and CD69, and the expression of PD1. In addition, NK cells using CD49b and CD69 as markers, B cells (CD19 and CD86 for their activation), Dendritic cells and myeloid cells (CD11b, CD11c, CD86, and the expression of MHC II), and macrophages (CD11b and CD86) were also included (Figure S1).

The effect of the therapy on cellular changes in T cells was assessed at 5 days and 10 days post-treatment using flow cytometry-based analyses. The proportion of CD8+ T cells and activated CD8+ T cells expressing CD25 among all CD45+ leukocytes exhibited a noticeable trend toward an increase in the tumor microenvironment (TME) 5 days after the combined treatment (Figure S3). This trend was consistently observed in both the number of CD8+ T cells and activated T cells expressing CD25 in the TME at both 5 days and 10 days after treatment (Figure 16A).

Furthermore, a significant increase in the number of CD8+ T cells expressing CD25 was detected in the tumor-draining lymph nodes (TdLNs) at 5 days and 10 days post-therapy in the group that received the combined treatment, when compared to the other groups (Figure 16B).

In addition to the changes in CD8+ T cells, the percentage of CD4+ T cells was also found to increase in the group that received the combined therapy. However, some of these increases were not statistically significant when compared with all the control groups.

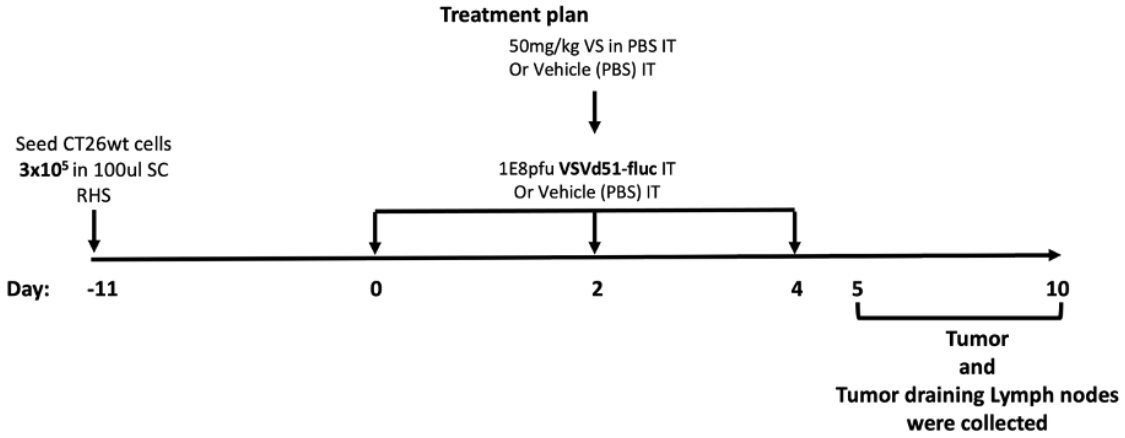


**Figure 15: The impact of VS plus VSVΔ51 combination therapy on immune cells in tumor and tumor draining lymph nodes 5 days and 10 days following treatment.**

**(A)** Schematic representation of the treatment schedule: after 12 days, CT26WT-tumor bearing mice received three intratumorally vanadyl sulfate (50mg/kg) and VSVΔ51 expressing IL-12 (1E8 PFU) or monotherapy over 5 days. Tumor-draining lymph nodes (TdLNs) were collected on day 5 and day 10 post-treatment, and Tumors were dissected and then dissociated by Tumour dissociation kits with the gentleMACS Dissociator to analyze Tumour infiltration leukocytes (TILs). Cells were stained with markers for various subsets of immune cells including activation markers, as described in supplementary figure 1 and 2. (**B)** Relative proportions of various immune cell subsets among all leukocytes of live cells are shown, n=5 per group.

In addition to T cells, various innate and adaptive immune cell types contribute to the efficacy of our treatment, as supported by previous data (155). Therefore, we investigated the impact of the combined treatment of VS+ VSVΔ51 on other immune cell populations, such as dendritic cells, Natural Killer cells (NK), macrophages, and B cells (Figure S3, S4, S5, and S6).

NK cells play a crucial role in the innate immune response, and their activation has been linked to the success of oncolytic virotherapy (243). To assess the impact of our combined therapy, we analyzed the frequency and number of activated NK cells within the tumor microenvironment (TME) and tumor-draining lymph nodes (TdLNs) at 5 days and 10 days after treatment. Our findings revealed that the combined therapy resulted in an increase in the number of activated NK cells (CD49b+ CD69+) compared to other treatments (Figure 16B). While we did not observe significant changes in the number of CD49b+ NK cells and activated NK cells expressing CD49b+CD69+ in the TME, a significant increase in the number of CD49b+ NK cells and activated NK cells expressing both CD49b and CD69 was detected in the TdLNs at 5 days and 10 days following the combined therapy, in comparison to other treatment groups (Figure 16A, B). These results suggest that the combined treatment induces a favourable immune response by enhancing the activation of NK cells in the tumor-draining lymph nodes.

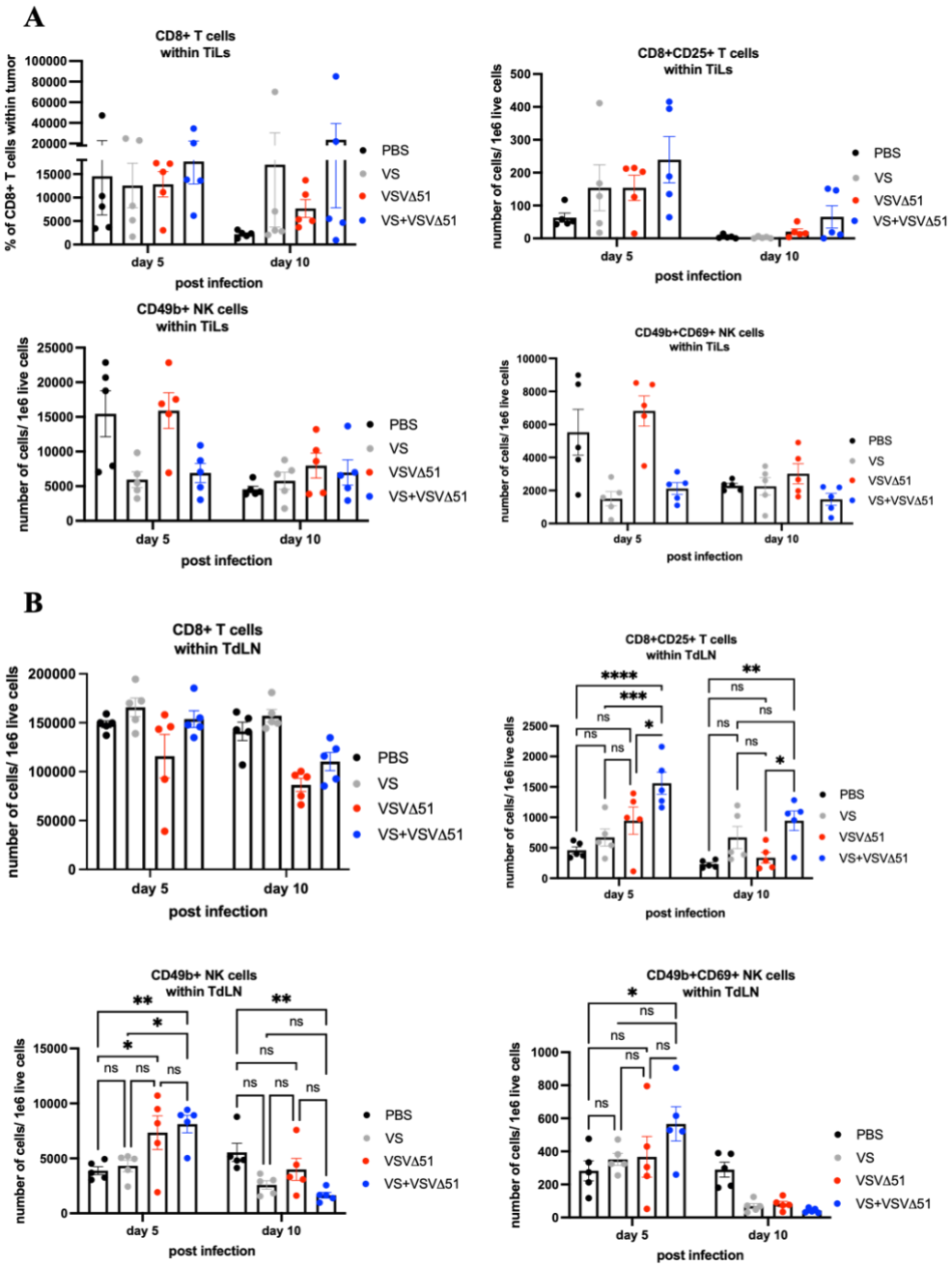


**Figure 16: An increase in the number of activated NK cells and CD8+ T cells was detected following treatment with VS plus VSVΔ51 combination therapy at TdLNs.**

This figure is part of Figure 15**, (A) & (B)** the number of cells per 1e6 live cells including CD8+ T cells and CD8+CD25+ T cells as well as CD49b+ NK and CD49b+CD69+ NK cells at the TILs of TME. N= 5 per group, Mean±SEM; * P=0.01, ** P=0.003, *** P=0.001, ****P<0.0001, ns= not significant, Two-way ANOVA.

We next investigated the relevant cellular changes in various subsets of DCs including CD11c+ cells and CD11b+ cells and their activations following the therapy. The percentage and number of CD11b+ cells and CD11c+ cells in TdLNs and TME were evaluated to further elucidate the role of these cells following the treatment. There was no significant increase in the relative proportion of CD11b+ cells and C11c+ cells detected at the TME and TdLNs (Figure S5, S6). Noticeably, there was an increase in the percentage of CD11b+ cells observed in the PBS control group 10 days post-treatment (Figure S6). The number of CD11b+CD86+ cells was found to be significantly increased at the TME 5 days and 10 days following the combined therapy. Whereas in the TdLNs the number of CD11c+CD86+ cells were found to be significant in the group that received the combined therapy (Figure 17A, B). We also looked at the percentage of macrophages particularly F4/80+ cells, more activated F4/80+ macrophages expressing CD86 were observed at the TME 10 days post the combined therapy (Figure S6). The number of activated F4/80+ macrophages expressing CD86+ was found to be significantly increased 5 days following the combined therapy at TdLNs (Figure 18A, B).

The percentage of activated CD19+ B cells was found to increase following the combined therapy in both TdLNs and TME (Figure 17A, B). This increase was significant when we looked at the number of activated CD19+ B cells expressing CD86 in TME and in the number of CD19+ B cells at the TdLNs 5 days and 10 days following combined therapy compared with their counterparts (Figure 17A, B). These findings suggest

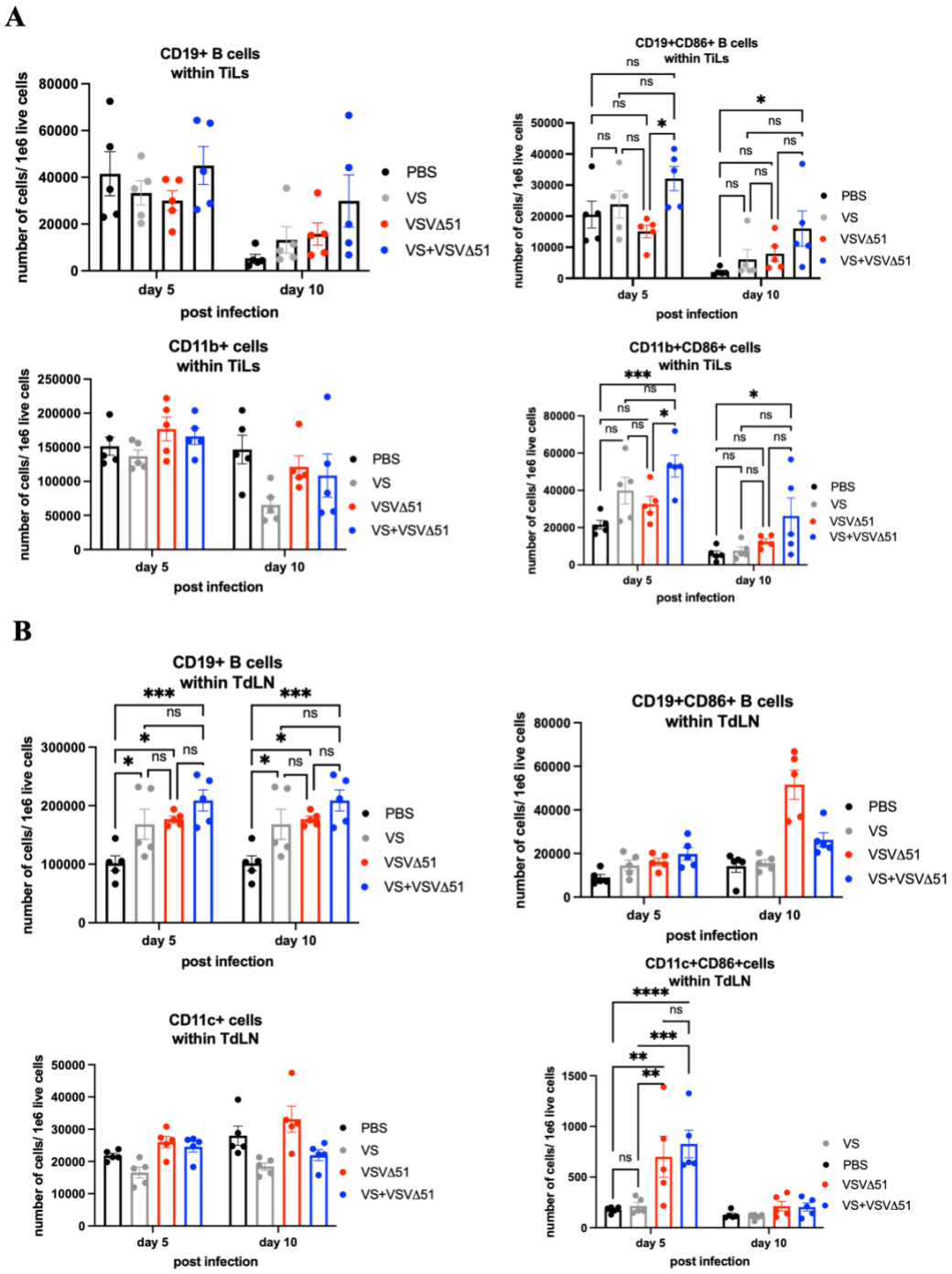


**Figure 17: An increase in the number of activated B cells was observed following treatment with VS plus VSVΔ51 combination therapy.**

This figure part of Figure 15, **(A) & (B)** The number of CD19+ B cells, CD19+CD86+ B cells, CD11b+ cells, and CD11b+CD86+ cells per 1e6 live cells at the TILs of TME or TdLNs. N= 5 per group, Mean±SEM; * P=0.01, ** P=0.003, *** P=0.001, ****P<0.0001, ns=not significant, Two-way ANOVA.

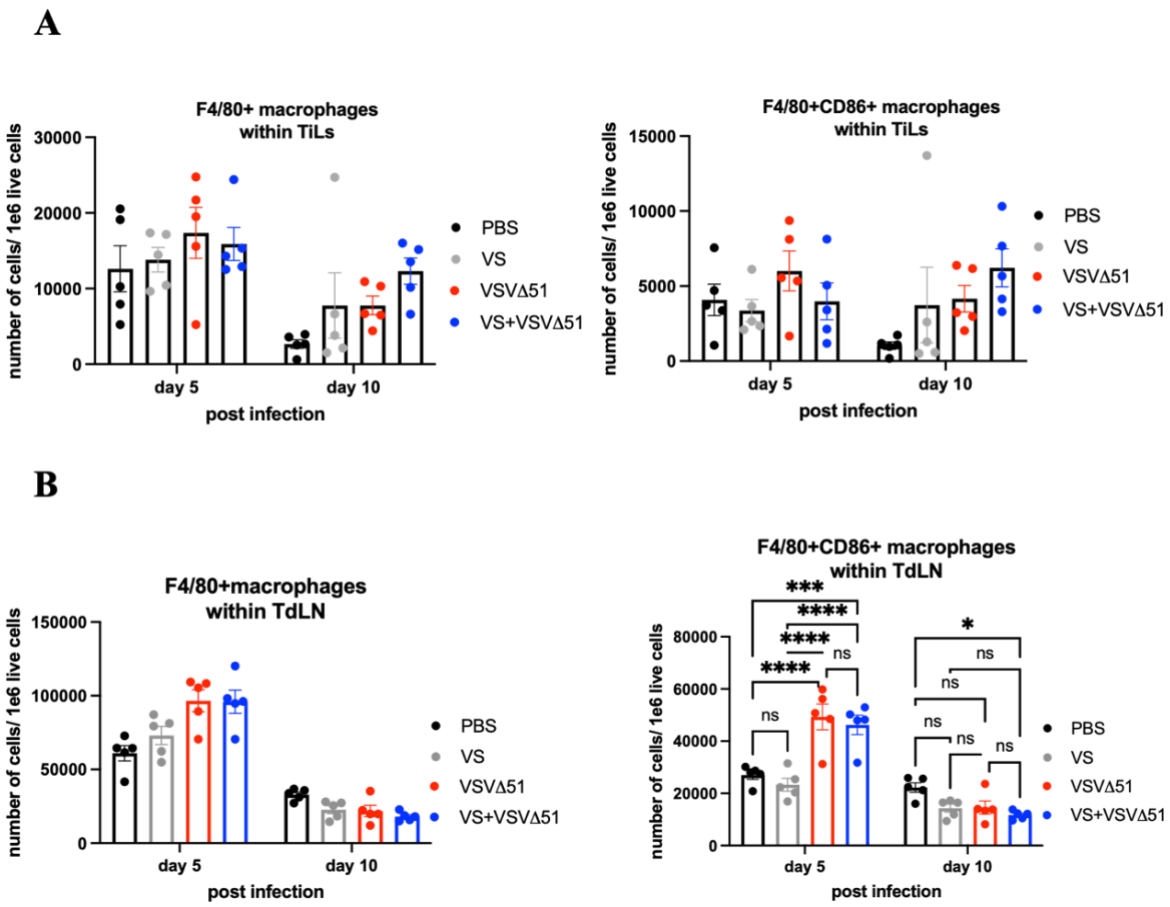


**Figure 18: A significant increase in the number of activated macrophages was observed following treatment with VS plus VSVΔ51 combination therapy at TdLN.**

**This** figure is part of Figure 15, **(A) & (B)** The number of F4/80+ cells and F4/80+CD86+ cells per 1e6 live cells at the TILs of TME or TdLNs. N= 5 per group, Mean±SEM; * P=0.01, ** P=0.003, *** P=0.001, ****P<0.0001, ns=not significant, Two-way ANOVA.

that the combined treatment has a positive impact on B cell activation, which may contribute to the overall antitumor immune response.

It is worth mentioning that no significant changes in the proportion of these cells were observed in TdLNs or the TME in comparison with all the tested groups. However, there were significant increases in the number of these cells following the combined therapy as indicated above especially, CD8+ T cells and NK cells indicating that they significantly contribute to the therapeutic efficacy of the combined therapy along with other immune cells that play a significant role in regulating the immune response including B cells, macrophages and DCs.

### 3.2.2. The impact of IL12 inclusion on the combined therapy on the cellular immunological changes 5 and 10 days following the therapy.

Since the inclusion of IL-12 enhances therapeutic efficacy in our model and further induces the secretion of proinflammatory cytokines and chemokines that play a critical role in immune cell recruitment to the TME, we evaluated the relevant immunological changes at a cellular level 5 and 10 days following the combined therapy in both TME and TdLNs.

Following the same multi-parameter flow cytometry-based analyses described in aim 3.2.1, 5 days following treatment with VS+VSVΔ51 expressing IL-12, a slight increase in the proportions of CD8+ T cells was observed (Figure 19).

Furthermore, we observed a higher percentage of activated CD8+ T cells expressing CD25 and CD4+ T cells in the TME in the group that received the combined therapy compared with other groups (Figure S7).

CD49b+ NK cells and activated CD49b+ NK cells expressing CD69 were found to be increased in the group that received the combined therapy 5 days and 10 days post-treatment at the TME (Figure S7 and S8). The number of activated CD49b+ NK cells expressing CD69 was detected to be increased 5 days following the IL-12 combined therapy in the TdLNs (Figure S7). However, these increases were not statistically significant when compared to the other treatment groups.

Our analyses also revealed that the group that received the combined therapy showed a higher percentage of CD11b+ cells and CD11c+ cells in the TME at 5 days following treatment compared with other treatment groups (Figure S9). Notably, there was a significant increase in the number of CD11b+CD86+ cells in the TME, as well as in the number of CD11c+ and CD11c+CD86+ cells in TdLNs at 5 days following the IL-12 combined therapy compared with other treatment groups (Figure 20A, B). Furthermore, we observed a significant increase in the number of activated macrophages expressing F4/80 and CD86 in the TME at 5 days after the combined therapy (Figure 22A, B). These results suggest that the combined treatment with VS+ VSVΔ51 expressing IL-12 induces a notable increase in the presence of immune cells, particularly CD11b+, CD11c+, and

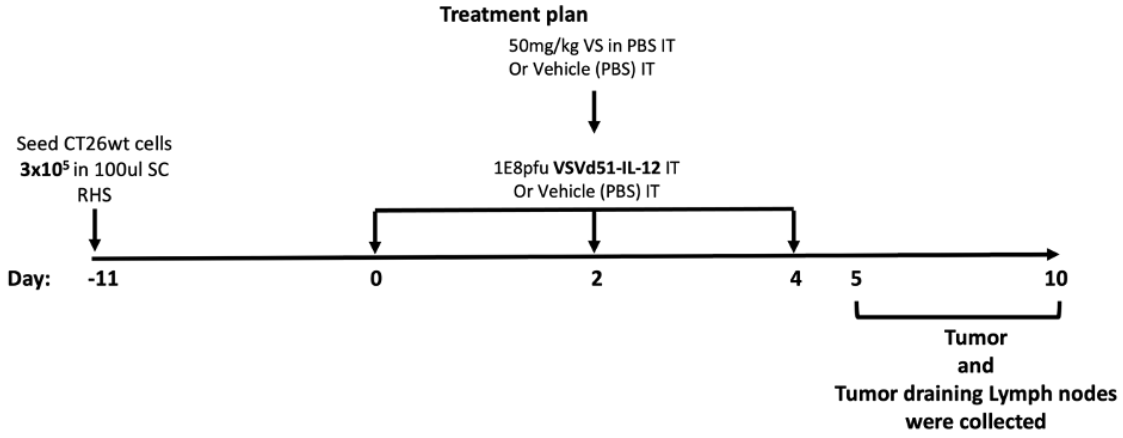


**Figure 19: The impact of VSVΔ51 expressing IL-12 in combination with VS on immune cells in tumor and tumor draining lymph nodes 10 days following treatment.**

**(A)** Experimental outline: after 12 days, CT26WT-tumor bearing mice received either three intratumorally vanadyl sulfate (50mg/kg) and VSVΔ51 expressing IL-12 or monotherapy over 5 days.

Tumor-draining lymph nodes (TdLNs) were collected on day 5 and day 10 post-treatment, and Tumors were dissected as previously described to analyze Tumour infiltration leukocytes (TILs). Cells were stained with markers for various subsets of immune cells as previously described. N= 5 per group.

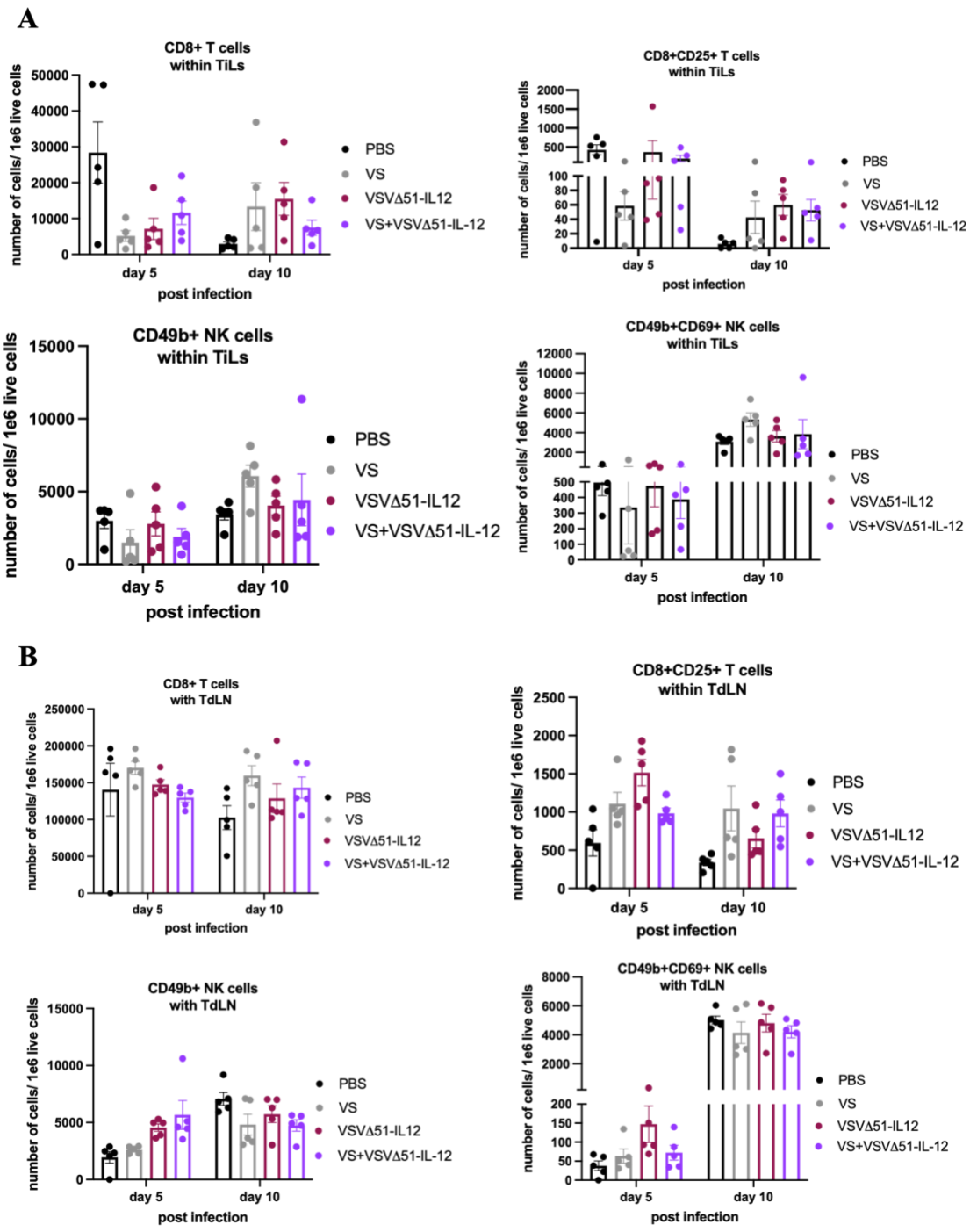


**Figure 20: The impact of treatment with VSVΔ51 expressing IL-12 in combination with VS on T cells and NK cells at TME and TdLNs.**

**This figure is part of Figure 19, (A)&** (**B**) the number of cells per 1e6 live cells including CD8+ T cells and CD8+CD25+ T cells as well as CD49b+ NK and CD49b+CD69+ NK cells at the TILs of TME, n= 5 per group, Mean±SEM, Two-way ANOVA.

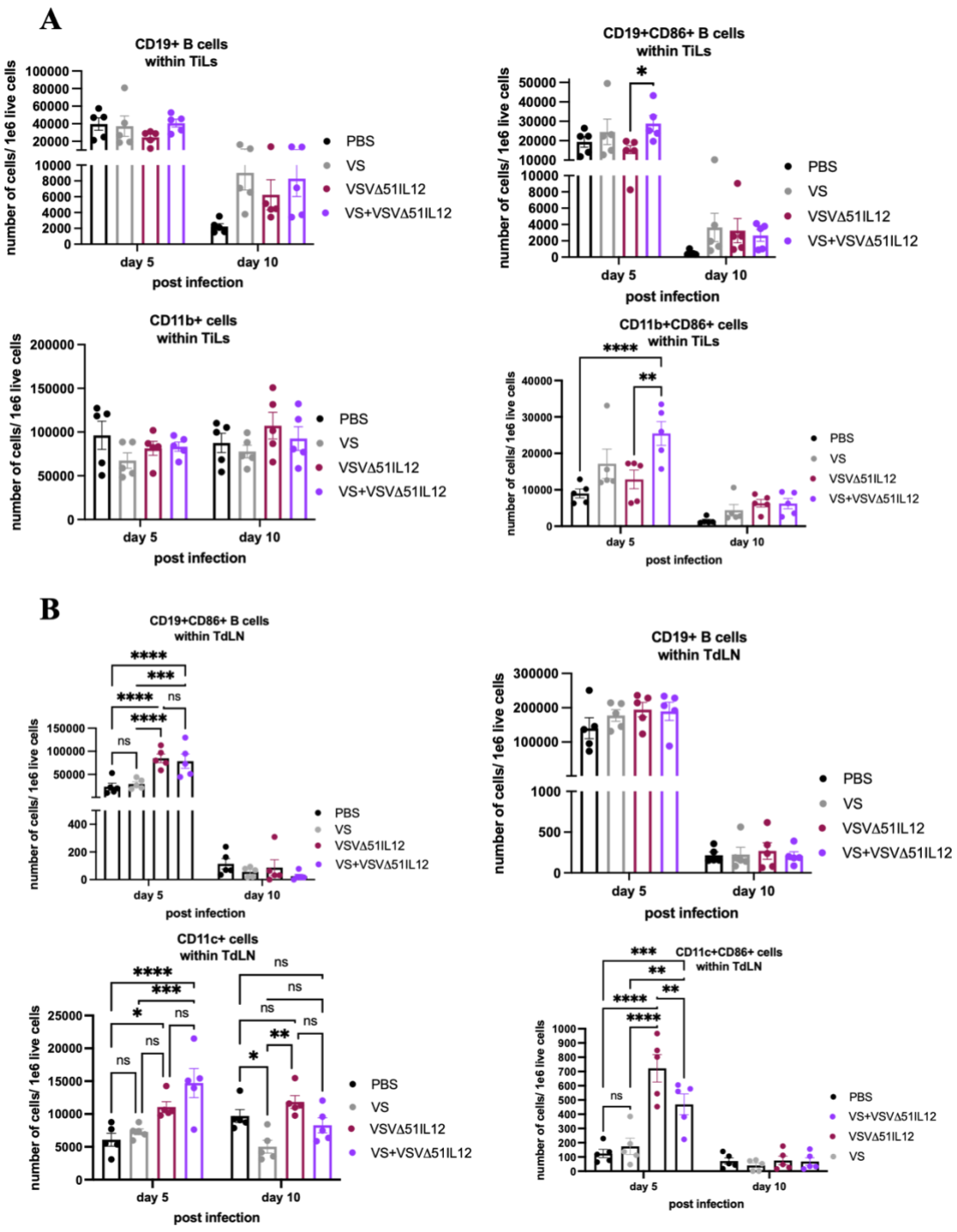


**Figure 21: The impact of treatment with VSVΔ51 expressing IL-12 in combination with VS on B cells and dendritic cells at TME and TdLNs.**

**This figure is part of Figure 19, (A)&(B)** The number of CD19+ B cells, CD19+CD86+ B cells, CD11b+ cells, and CD11b+CD86+ cells per 1e6 live cells at the TILs of TME or TdLNs. N= 5 per group, Mean±SEM; * P=0.01, ** P=0.003, *** P=0.001, ****P<0.0001, ns= not significant, Two-way ANOVA.

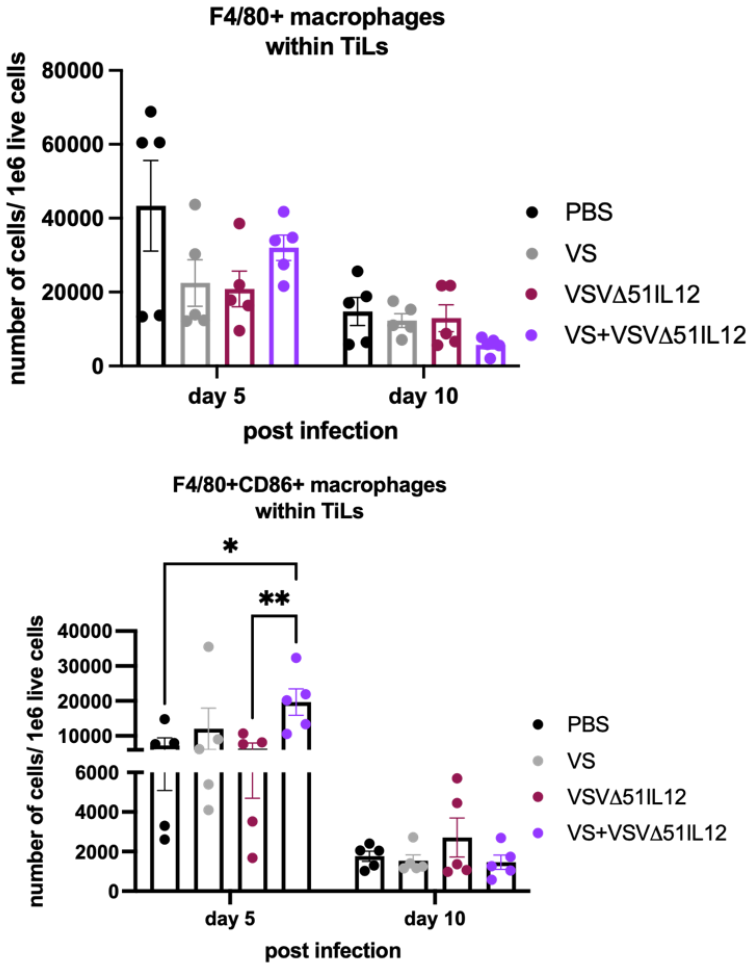


**Figure 22: The impact of treatment with VSVΔ51 expressing IL-12 in combination with VS on macrophages at TME and TdLNs.**

**This figure is part of Figure 19, graphs show t**he number of F4/80+ cells and F4/80+CD86+ cells per 1e6 live cells at the TILs of TME or TdLNs. N= 5 per group, Mean±SEM; * P=0.01, ** P=0.003, *** P=0.001, ****P<0.0001, Two-way ANOVA

activated macrophages, within the TME and TdLNs, which may contribute to the enhanced therapeutic response. This was also associated with an increase in the percentage of activated CD19+B cells expressing CD86 at TdLNs 10 days and at TME 5 days and 10 days post the combined therapy (Figure S9 and S10). The number of activated CD19+ B cells expressing CD86 was significantly increased in TdLNs 5 days post the IL12 combined therapy compared with other groups (Figure 21B).

VS in combination with VSVΔ51 expressing IL-12 generates a sustainable immune response due to the increased number of T cells, NK cells and other immune cells that mediate the antitumor immune response at the TME.

### 3.2.3. CD8+ T cells play a role in the improved therapeutic efficacy of VS+ VSVΔ51.

Complementing previous studies showing increased infiltration of activated T-cells in tumors from combination-treatment responsive animals (155), we observed an increase in the number of tumor antigen-specific T-cells in the spleen and an increase in the percentage and number of T cells, especially CD8+ T cells and NK cells at the TME. Since it was challenging to detect the significant cellular and relevant immunological changes following the combined therapy and to be able to determine which subset of immune cells including T cells and NK cells play a significant role in the therapeutic efficacy of our combination therapy, the cell depletion approach was undertaken using depletion antibodies.

To determine the contribution of CD8+ T cells in the therapeutic efficacy of the treatment with VS+ VSVΔ51, an *in vivo* experiment was performed in the presence or absence of anti-CD8 depleting antibodies. Following the same established *in vivo* therapeutic regimen, the depletion of CD8+ T cells was achieved using an anti-CD8+ antibody as shown in Figure 23A at 200 µg concentration per dose. The CD8+ T cells depletion was confirmed 24-48 hours following i.p. injections on saphenous bleeds by flow cytometry after staining with anti-CD8+ and CD3+ antibodies as well as other extracellular markers (Figure S11 showing the gating strategy) (Figure 23B). Through the flow cytometric examination of the depletion, we observed complete depletion across all the tested time points compared with non-depleted groups (Figure 23B).

While monitoring tumor growth, there was a noticeable delay in the tumor growth following the combination therapy in the depleted groups with no surviving mice in comparison with the non-depleted group that had a 20% survival rate (Figure 24A, B) indicating CD8+ T cells play a role in the achieved therapeutic efficacy following the combined therapy.

We next sought to determine the role of CD8+ T cells and NK cells on the therapeutic efficacy of treatment with VS+VSVΔ51-IL12 since IL12 has major impacts on both T cells and NK cells, as part of our investigation performed above. The impact of CD8+ T cell and NK depletion on the therapeutic efficacy of VS+VSVΔ51-IL12 therapy was studied following the same therapeutic regimen and same time points for depletion presented in (Figure 24A).

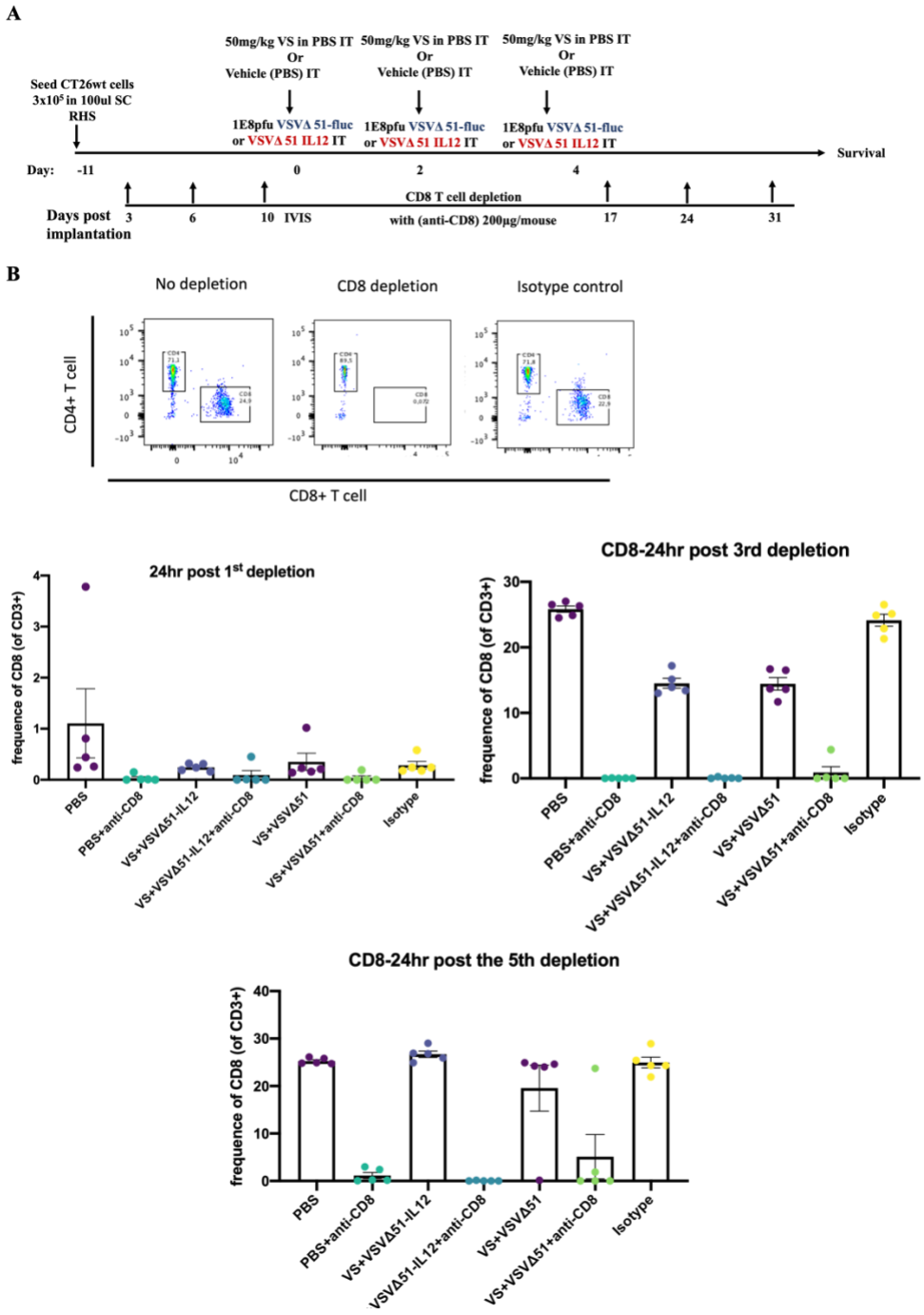


**Figure 23: The depletion of CD8+ T cells was confirmed 24hr post depletion.**

**(A)** Schematic representation of the treatment schedule: CT26WT-tumor-bearing mice were treated with three intratumorally (i.t.) injections of vehicle (PBS) or 50mg/kg of Vanadyl Sulfate for 4 hr and subsequently treated with 1E8 PFU of VSVΔ51 or VSVΔ51 expressing IL-12 or monotherapy over a period of 5 days. CD8+ T cells depletion was performed using 200mg of anti-CD8 antibody administrated i.p., 3 till 30 days post implantations, twice a week the first 14 days and once a week. **(B)** Representative flow cytometry dot plots. The depletion was confirmed on PBMCs by flow cytometry-based analyses using anti-CD3, anti-CD4 and anti-CD8 antibodies, n=5 per group. The percent of PBMCs that are CD3+CD8+, CD3+CD4+.

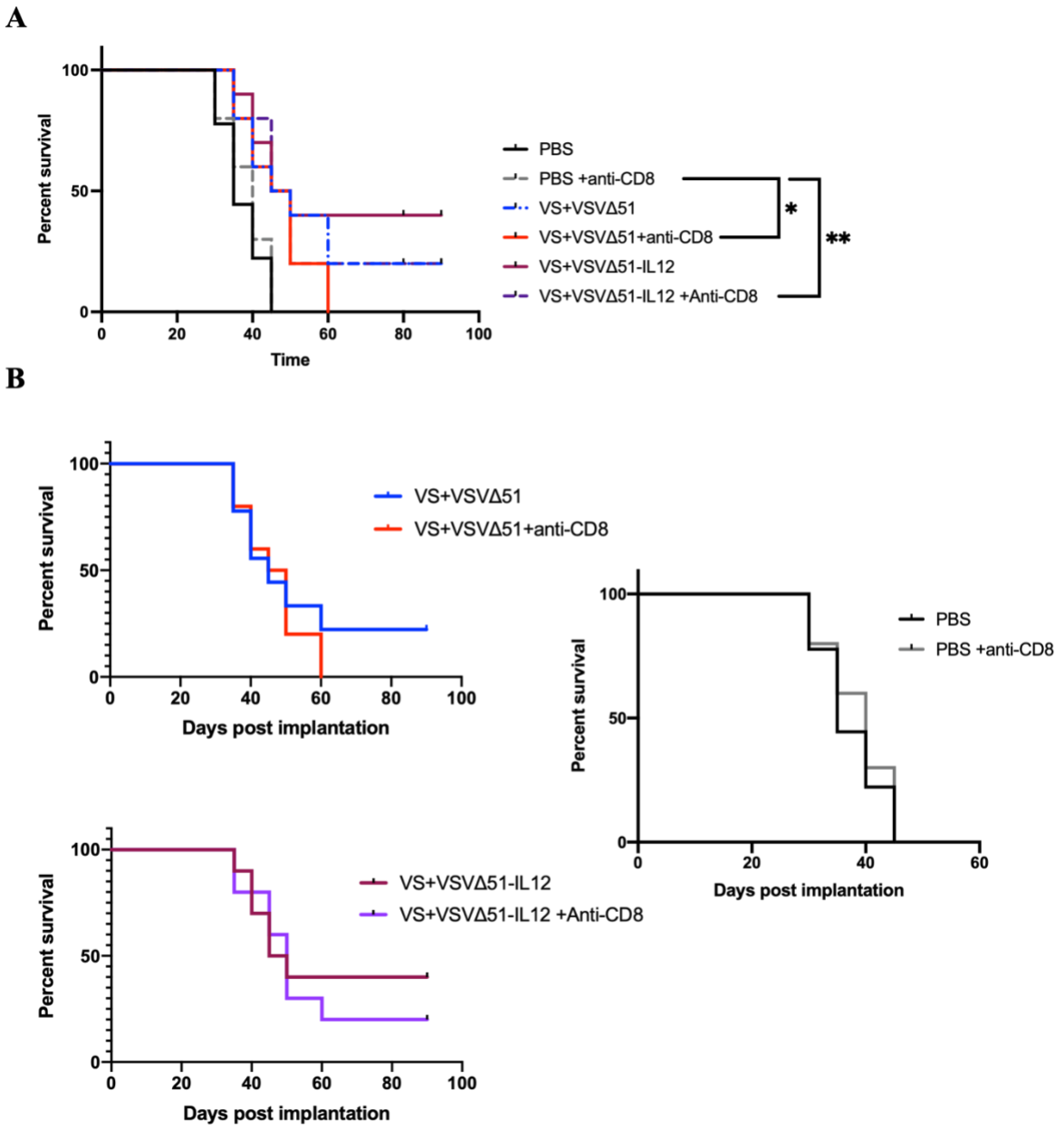


**Figure 24: CD8+ T cells contribute to the therapeutic efficacy of combined therapy.**

**(A&B) Following the treatment schedule presented in Figure 23,** Survival was monitored over time, and the percentage of survival was included for each condition, long rank (Mantel-Cox) test indicated the significance, n= 10 per group.

The depletion of CD8+ T cells was also confirmed by flow cytometry and complete depletion was observed for all the tested time points (Figure 24B). We observed that the therapeutic efficacy following VS+VSVΔ51-IL12 was reduced by 50% from 40% in the non-depleted group to 20% survival in CD8+ T cells depleted groups (Figure 24A, B).

Taken together, the change in the survival rate following CD8+ T cells depletion was observed to be significant when comparing the group that received PBS with the group that received VS+VSVΔ51 (p-value 0.02) and when comparing the group that received PBS with the group that received VS+ VSVΔ51-IL12 (p-value 0.006) (Figure 24). CD8+ T cells could be one of the key mediators of the anti-tumor effect of VS+ VSVΔ51-IL12 combination therapy and our data suggest that other immune cells might also contribute to the therapeutic efficacy of treatment with VS+ VSVΔ51-IL12.

### 3.2.4. NK cells contribute to the therapeutic efficacy of the combined therapy.

To investigate the role of NK on the therapeutic efficacy of the combined therapy, the CT26WT tumor model was established in mice depleted of NK cells using anti-Asialo-GM1 antibody as shown in Figure 25A. The NK depletion was monitored 24-48 hrs following i.p. injections on saphenous bleeds by flow cytometry, a complete depletion of NK cells was observed following the i.p. injections (Figure 25B, Figure S12 shows the gating strategy).

NK depletion reduced therapeutic efficacy in our tumor model by 10% from 20% survival in the non-depleted group following treatment with VS+ VSVΔ51 (Figure 25). This change in the survival rate was not significant when comparing the two groups; however, when comparing survival in VS+ VSVΔ51 NK depleted group with PBS NK depleted groups was found to be significant with a p-value of 0.003 (Figure 25).

Following treatment with VS+ VSVΔ51-IL12, NK depletion had an impact on the therapeutic efficacy of our tumor model and reduced the therapeutic efficacy by half following treatment from 40% survival in the non-depleted group to 20% in the depleted group. This suggested that NK cells contribute to achieving therapeutic efficacy following the combined therapy (Figure 25). This change in the survival rate was not significant when comparing the two groups; however, comparing VS+ VSVΔ51-IL12 NK depleted group with PBS NK depleted group was found to be significant with a p-value of 0.0002 (Figure 25).

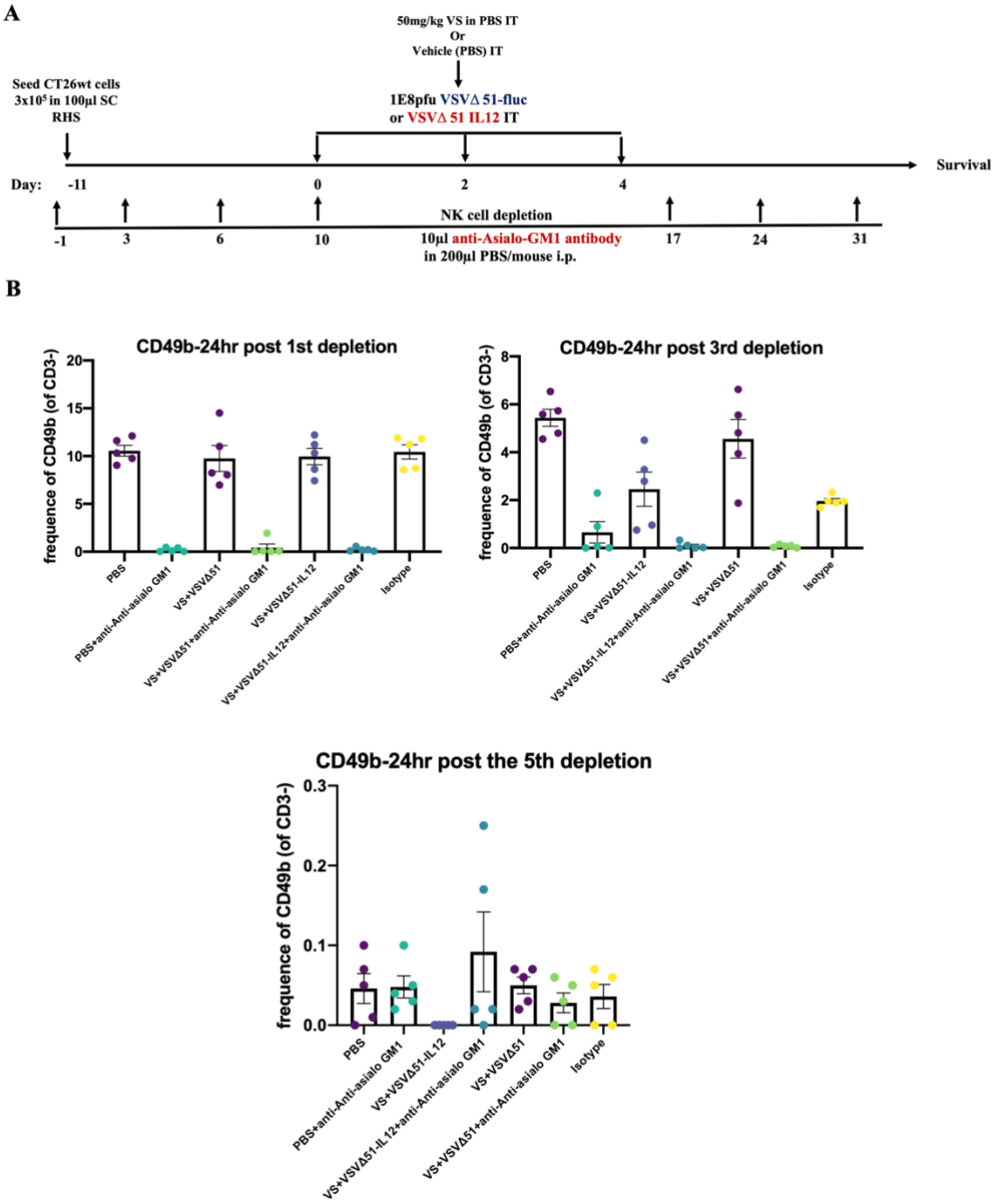


**Figure 25: A complete depletion of NK cells was observed 24hr following the i.p. injections.**

**(A)** following the same established therapeutic regimen for CT26WT tumor models. NK cell depletion was performed using 10 µl of anti-Asialo-GM1 in 200 µl of PBS administrated i.p., -1, 3 till 30 days post implantations, twice a week the first 14 days and once a week. **(B)** The depletion was confirmed on PBMCs by flow cytometry-based analyses using anti-CD3 and anti-CD49b, and anti-NKp46 antibodies, n=5 per group. The percent of PBMCs that are CD3-CD49b+, CD3-NKp46+.

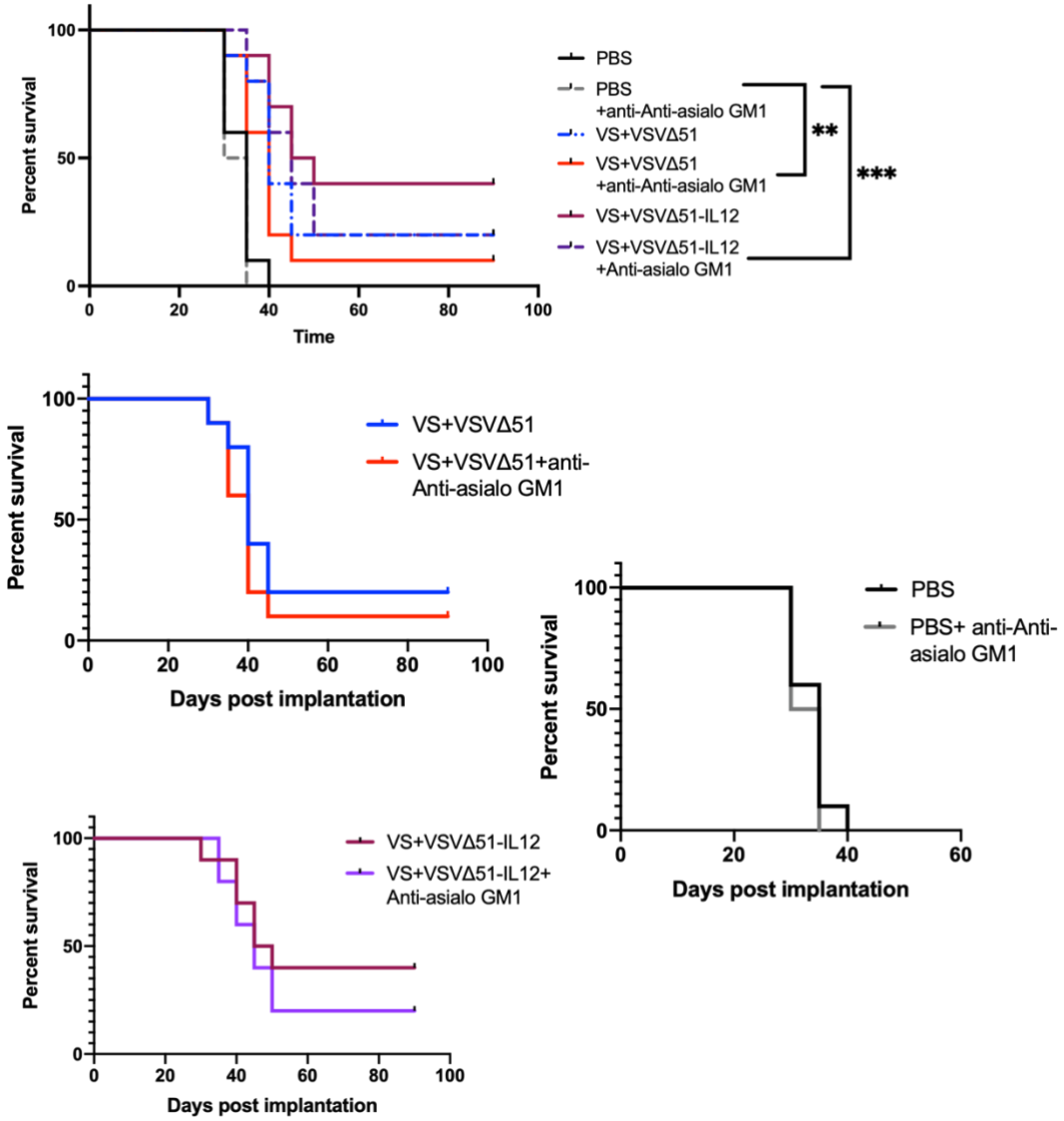


**Figure 26: NK cells contribute to the therapeutic efficacy of the combined therapy.**

**Following the treatment schedule presented in Figure 25,** survival was monitored over time, and the percentage of survival was included for each condition, long rank (Mantel-Cox) test indicated the significance, ** P=0.003, *** P=0.001, n= 10 per group.

## 3.3. Generating multi cytokine armed Vanadyl Sulfate for enhanced oncolytic virus immunotherapy.

There are five aims for this objective:

1. Develop a cloning strategy for generating VSVΔ51 encoding CXCL9 and VSVΔ51 encoding IL12 and CXCL9 and perform subsequent validation.
2. Evaluate the impact of these therapies on the T cells and other immune cell infiltration *in vivo* and *in vitro*.
3. Investigate the impact of these armed combination therapies on improving the therapeutic efficacy of the CT26WT tumor model.
4. Study the impact of these armed therapies on the antigen specific immune response.
5. Characterize the relevant cellular immunological changes 5 days following treatment with these armed combination therapies.

### 3.3.1. The cloning strategy for generating VSVΔ51 encoding CXCL9 and VSVΔ51 encoding IL12 and CXCL9 and validations.

Murine CXCL9 gene (mCXCL9) was engineered in the VSV backbone containing a matrix inactivating mutation (M51R) between the G and L genes (Figure 27A). Additionally, mCXCL9 and mIL12 genes were engineered in the VSV backbone containing a matrix inactivating mutation (M51R) between the G and L genes and a self-cleavage peptide T2A was added in between

these genes. At each gene a secretion peptide was added (Figure 27A). After sequences were confirmed following the PCR amplified system, these viruses were rescued using an established reverse genetic system (306), followed by using three rounds of single-colony purification using a standard plaque assay. Following that, the viruses were successfully produced using high-speed centrifugation and purified on 5-50% Optiprep as previously described.

As a first step of virus validation, multi-step and single-step viral growth kinetics were performed in the CT26WT cell line. CT26WT cells were infected with MOI 1 or MOI 0.1 and supernatants were collected at various time points. Viral replication was assessed by standard plaque assay. CXCL-9 and IL-12 transgenes had no impact on virus replication kinetics compared with parental virus VSVΔ51 encoding fluc or IL12 transgenes (Figure 27B).

CT26WT cells were infected with VSVΔ51 encoding CXCL9, VSVΔ51 encoding IL12-CXCL9, VSVΔ51-fluc or mock infected at an MOI of 0.1 and 24hr post-infection, the gene expression of CXCL-9 and IL-12 was confirmed by qPCR (Figure 28A).

To confirm the secretion of these cytokines and chemokines upon viral infection, supernatants of CT26WT cells were collected 24hr after infection with VSVΔ51 encoding mCXCL9 and VSVΔ51 encoding IL12-mCXCL9, VSVΔ51 encoding fluc, VSVΔ51 encoding IL12 or mock infection at an MOI

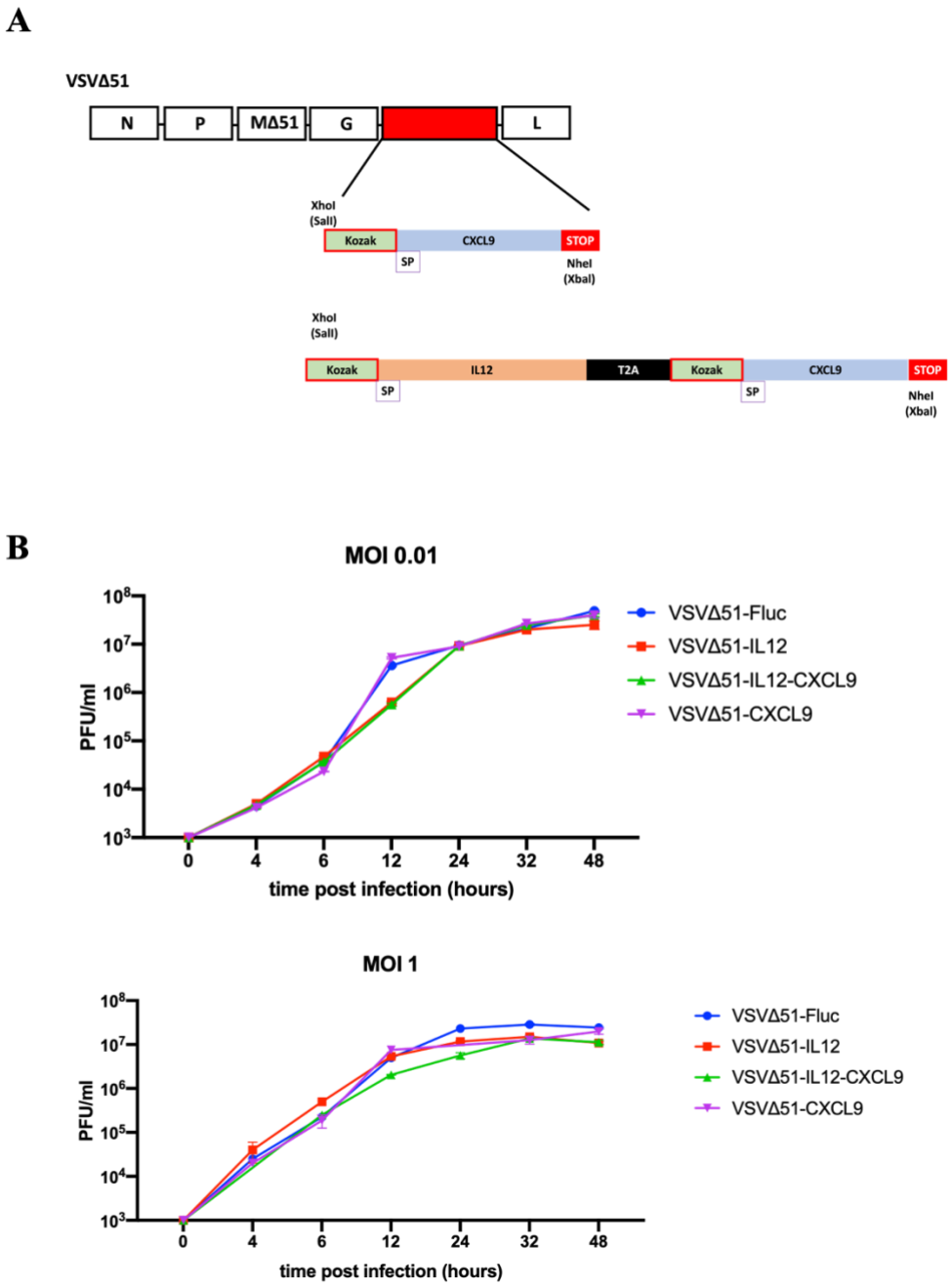


**Figure 27: mCXCL9 and mIL-12-CXCL9 encoding VSVΔ51 did not impact the growth kinetic of the virus.**

**(A)** CXCL9 and CXCL9 and IL12 were cloned in the backbone of VSVΔ51. **(B)** The Replication kinetic of VSVΔ51 encoding fluc, IL12, CXCL9 or IL12 and CXCL9 were performed in single and multistep viral growth curves in CT26WT cells, n= 3 per group.

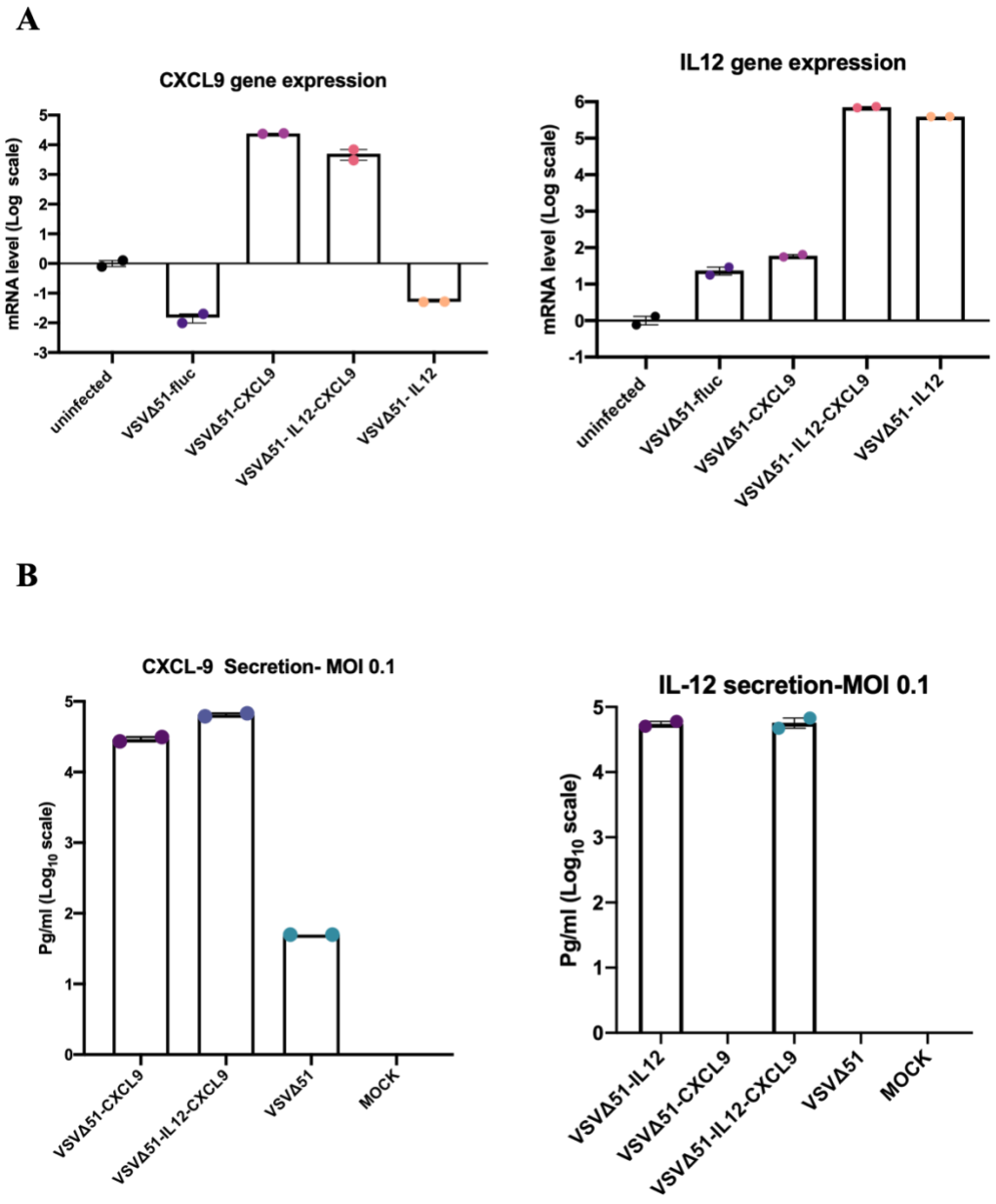


**Figure 28: CXCL9 and IL-12 were found to be expressed at the gene expression level and secreted following treatment with VSVΔ51 encoding CXCL9 or VSVΔ51 encoding IL12 and CXCL9.**

**(A)** The expression of CXCL9 and IL12 was evaluated using qPCR after infecting CT26WT with VSVΔ51 encoding CXCL9, VSVΔ51 encoding IL12 and CXCL9, VSVΔ51 or left untreated for 24hr. **(B)** 24hr post-infection, supernatants were collected and the secretion of IL12 and CXCL9 was measured by ELISA. N= 2 per group, Mean±SEM; Two-way ANOVA, data represent the average of two independent experiments.

of 0.1 and chemokine and cytokines protein concentrations were quantified by enzyme-linked immunosorbent assay (ELISA). mCXCL9 was specifically increased in VSV encoding mCXCL9 infected CT26WT cells and in VSVΔ51 encoding IL12-CXCL9 infected cells (Figure 28B). VSVΔ51-fluc, VSVΔ51 encoding IL12 infection and mock infection did not produce any CXCL9 protein concentration detectable by the ELISA assay. The concentration of IL12 was also quantified by ELISA 24hr post-infection and mIL-12 was found to be secreted following infection with VSVΔ51 encoding IL12-CXCL9 compared with parental viruses (Figure 28B).

We further evaluated the impact of these transgenes on viral growth *ex vivo* using tumor cores obtained from mice implanted with CT26WT cells and observed that the viral growth of VSVΔ51 encoding CXCL9, VSVΔ51 encoding IL12 and VSVΔ51 encoding IL12-CXCL9 was similar to VSVΔ51-fluc *ex vivo* (Figure 29A).

In conclusion, VSVΔ51encoding CXCL9 and VSVΔ51encoding IL12-CXCL9 have similar growth profiles to the control viruses (VSVΔ51-fluc and VSVΔ51 encoding IL12) and both transgenes are secreted where appropriate.

### 3.3.2. The number of CD8+ T cells and NK cells were found to be increased 24hrs following these therapies *in vivo.*

To confirm the biological activity and the chemotactic activity of virally encoded mCXCL9 and mCXCL9-IL12, we used multiple parameter flow cytometry analyses of dissociated tumors to quantify intratumoral T cell

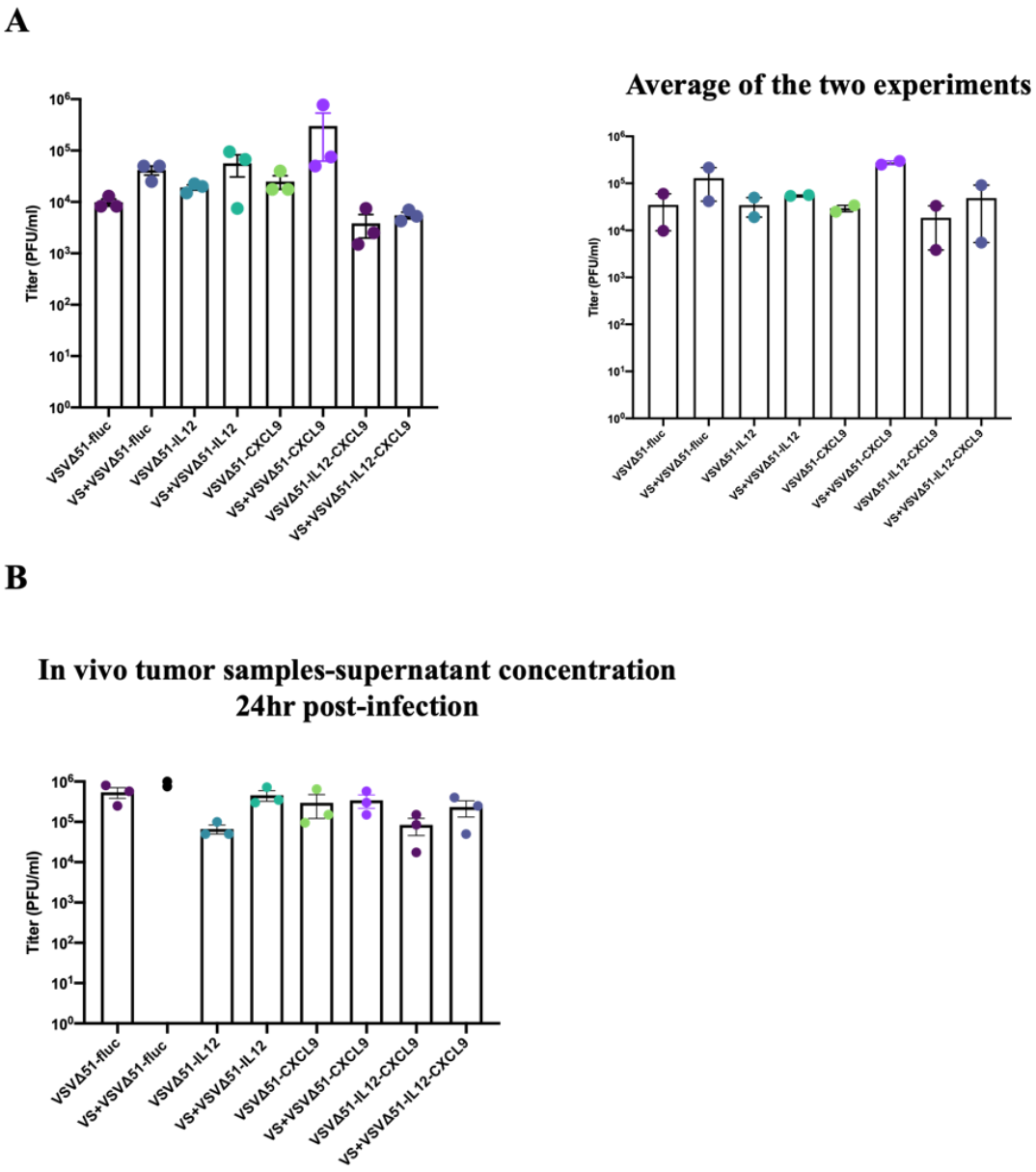


**Figure 29: Viral replication 24hr following ex vivo and in vivo treatment with the combined therapies.**

**(A)** CT26WT tumor cores were pre-treated with 100µM of VS for 4hr and subsequently infected with 1E4PFU of VSVΔ51-fluc, VSVΔ51 encoding IL12, VSVΔ51 encoding CXCL9, or VSVΔ51 encoding IL12-CXCL9, 24hr post infections, supernatants were tittered by plaque assay, n= 3 per group. **(B)** supernatants from *in vivo* treated samples were collected 24hr post-infection and were tittered by plaque assay, n= 3 per group. Mean±SEM; Two-way ANOVA.

infiltration and other immune cells including NK cells 24hr post-infection *in vivo* following the same established therapeutic regiment (Figure 30A). We designed two comprehensive flow panels including extracellular cell surface markers for T cells and NK cells and their activation markers as well as exhaustion markers to be able to characterize the cellular immunological changes 24hrs following the therapy (Figure S12 and Figure S13).

There was a significant increase in the number of CD49b+ NK cells and CD49b+ NK cells expressing CXCR3 in the group that received the VS+ VSVΔ51 encoding CXCL9 compared with other groups at the TME (Figure 30B). In addition, a trend toward an increase in the number of CD3+ expressing CXCR3 and CD8+ T cells expressing CXCR3 was detected in the TME; however, this was not significant when compared with other controls (Figure 30C, Figure 31 A). Furthermore, the number of CD4+ T cells and the number of CD4+CXCR3+ T cells did not show any enhancement following the therapies (Figure 31B).

To quantify the viral replication, the supernatants from *in vivo* tumor samples were collected 24 hr post-infection and tittered using plaque assay. We observed an increase in virus tittering following treatment with combination therapy; however, it was not statistically significant compared with other controls (Figure 29B).

To determine the local production of the virally encoded chemokine in TME, we also measured the supernatant concentration of CXCL9 and IL12 of the tumor samples, 24 hr post-infection.

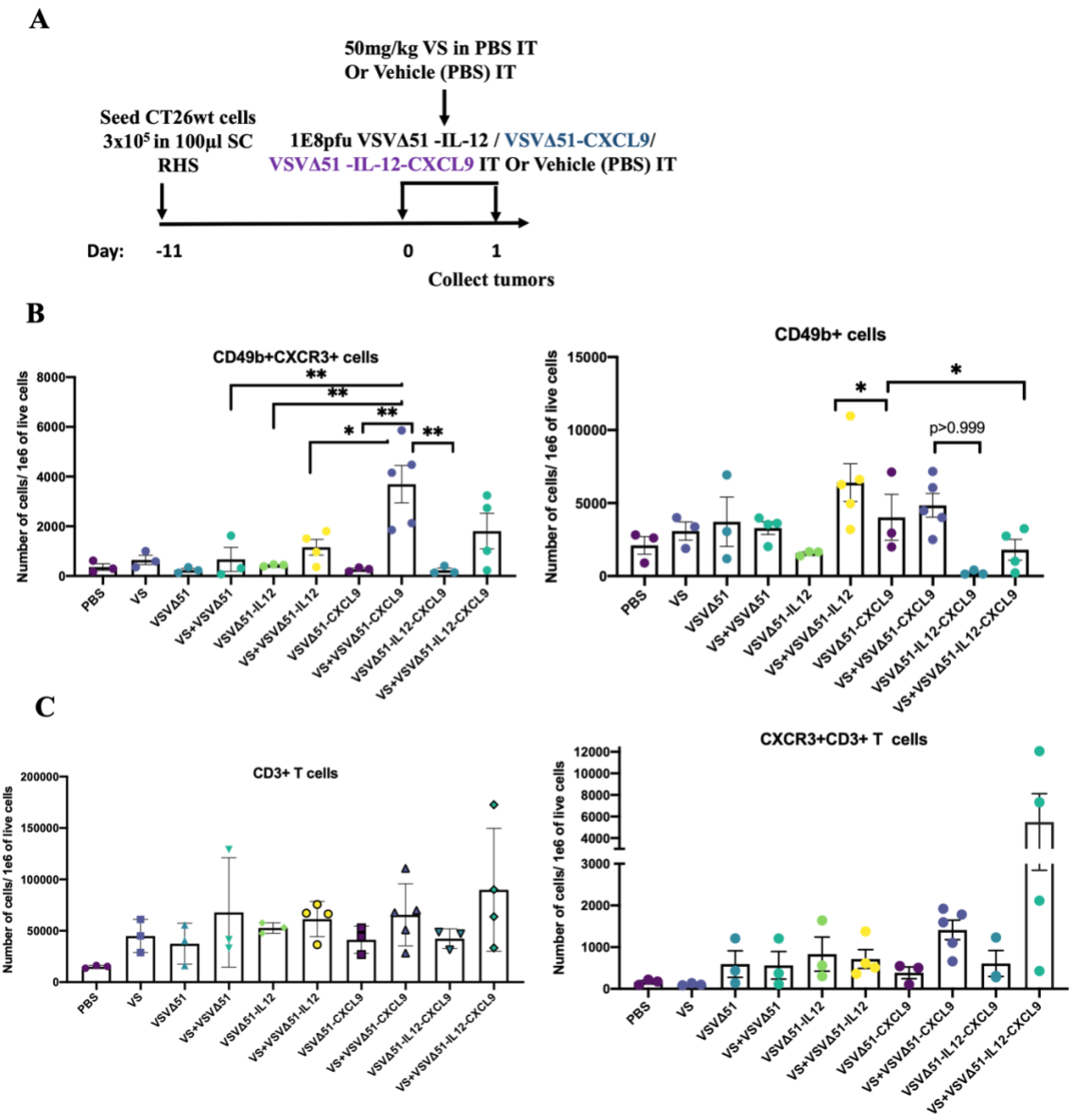


**Figure 30: The biological activity of VSVΔ51 encoding CXCL9 and VSVΔ51 encoding IL12-CXCL9 in vivo 24hr post-infection.**

**(A)** Schematic representation of the treatment schedule: after 12 days, CT26WT-tumor bearing mice received three intratumorally vanadyl sulfate (50mg/kg) and VSVΔ51 encoding IL-12 or VSVΔ51 encoding CXCL9 and VSVΔ51 encoding IL12-CXCL9 (1E8 PFU) or monotherapy. Tumor were collected 24hr post-treatment. Tumors were dissected as previously described. Cells were stained with markers for various subsets of immune cells including CD45, CD3, CD4, CD8, CD49b and CXCR3 including activation markers CD44, and CD69. Relative proportions of various immune cell subsets among all leukocytes of live cells are shown. **(B)** The number of CD49b+ NK cells and CD49b+CXCR3+ NK cells per 1e6 live cells. **(C)** Graphs show the number of CD3+ T cells and CD3+CXCR3+ T cells per 1e6 live cells. N= 3-5 per group, Mean±SEM; * P=0.01, ** P=0.003, *** P=0.001, ****P<0.0001, Two-way ANOVA.

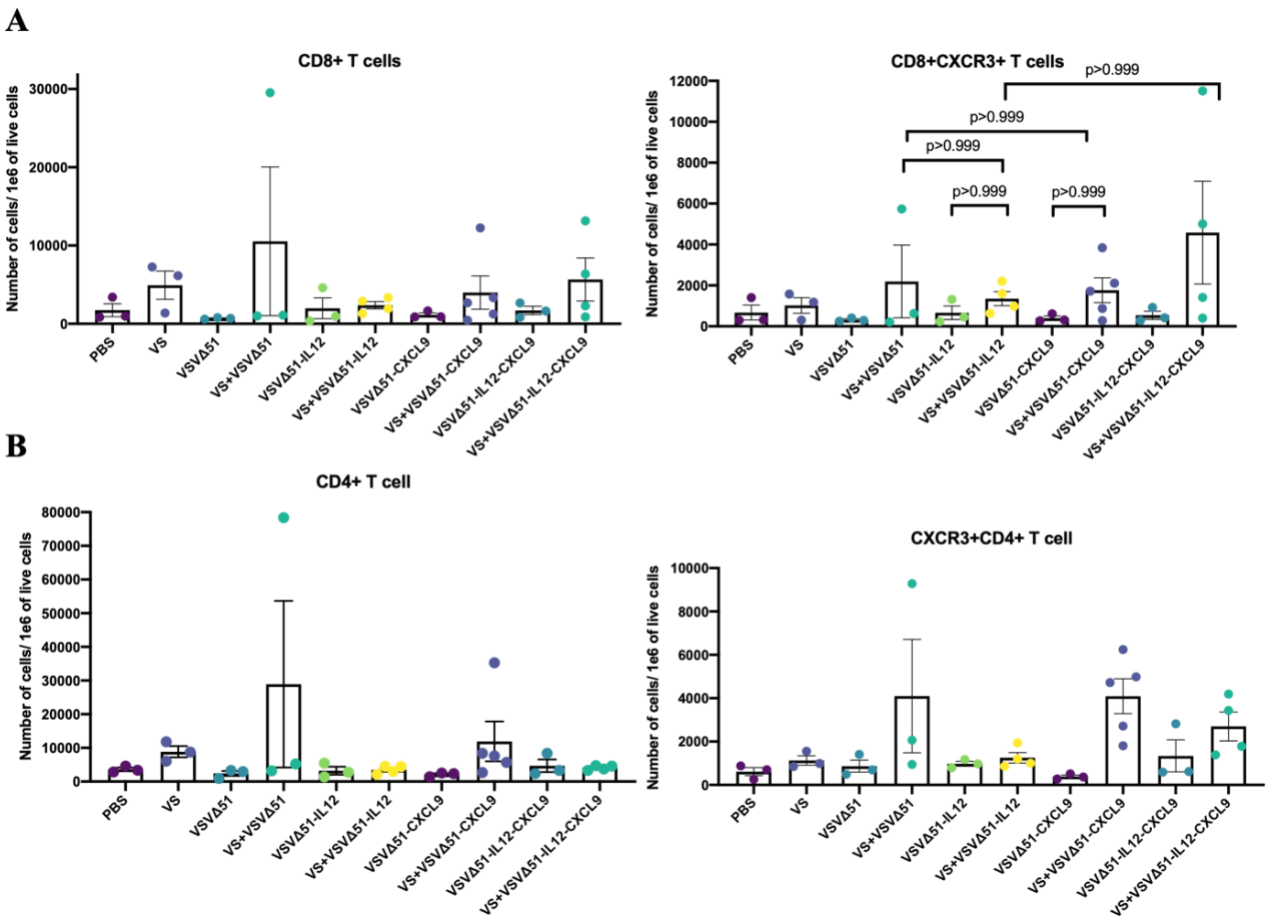


**Figure 31: The number of CD8+ and CD4+ T cells 24hr post-treatment with of VSVΔ51 encoding CXCL9 or VSVΔ51encoding IL12-CXCL-9 in vivo.**

**This figure is part of Figure 30, (A)** Graphs show the number CD8+ T cells and CD8+CXCR3+ T cells per 1e6 live cells. **(B)** Graphs show the number of CD4+ T cells and the number of CD4+CXCR3+ T cells per 1e6 live cells. N= 3-5 per group, Mean±SEM, Two-way ANOVA.

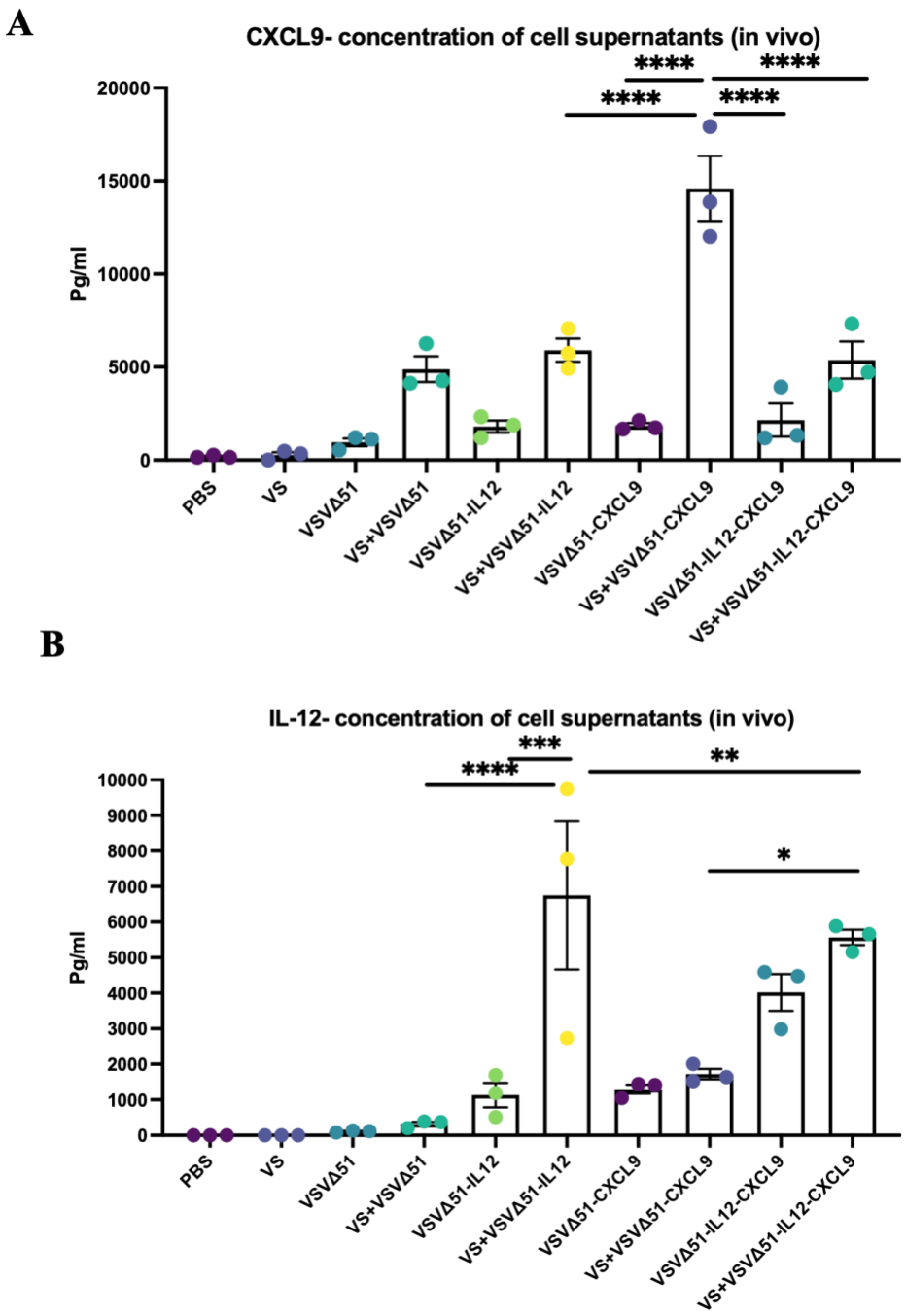


**Figure 32: A significant increase in the CXCL9 concentration in the supernatant of tumor dissociated tissues was detected 24hr post treatment with VS+VSVΔ51 encoding CXCL9.**

**This figure is part of Figure 30,** Supernatants following tumor dissociation were collected, **(A) &(B)** CXCL9 and IL12 tumor concentration measured by ELISA. N= 3 per group, Mean±SEM, * P=0.01, ** P=0.003, *** P=0.001, ****P<0.0001, Two-way ANOVA.

A significant increase in the concentration of CXCL9 was observed in the groups that received the VS+VSVΔ51encoded CXCL9 compared with other groups with more than 15000pg/ml (Figure 32A) and the concentration of IL12 in the group that received VS+VSVΔ51encoded L12 with more than 9000pg/ml as well as the group that received VS+VSVΔ51encoded IL12-CXCL-9 with 5000pg/ml compared with other tested groups (Figure 32B).

Taken together, the virally secreted CXCL9 is biologically active and induces T cells and NK cells recruitment to the TME 24hr post treatment.

### 3.3.3. Cytokine armed combination therapies has impact on the therapeutic efficacy in the CT26wt tumor model.

Measuring the therapeutic impact of the inclusion of CXCL9 encoded VSVΔ51 and CXCL9 and IL12 encoded VSVΔ51on the therapeutic efficacy of our combination therapy is the primary goal of engineering these viruses.

Following the same therapeutic regimen that was performed before, tumor growth was monitored over time following the combination therapies with VS+VSVΔ51 encoding CXCL9, VS+VSVΔ51 encoding IL-12 and CXCL9, and VS+VSVΔ51 encoding IL12 (Figure 33A). The survival rate following treatment with VS+VSVΔ51encoded CXCL9 was 30% compared to control groups (Figure 33B) (p-value 0.0003 compared to PBS, 0.0004 compared to VS, 0.025 compared to VSVΔ51 encoding CXCL9, and 0.09 compared to VSVΔ51 encoding IL12-CXCL9, Figure 33C).

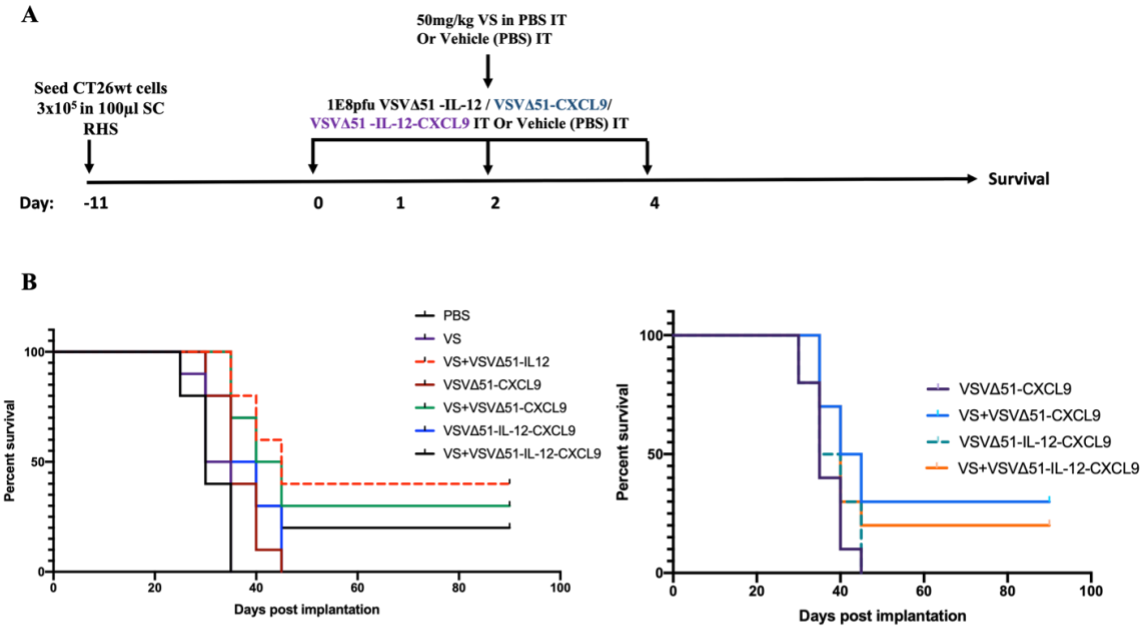


C

| | PBS | Vanadyl Sulfate | VSVΔ51-CXCL9 | VSVΔ51-IL12-CXCL9 | VS+ VSVΔ51-CXCL9 |
|---|---|---|---|---|---|
| PBS | X | ns | 0.0127 | 0.0073 | 0.0003 |
| Vanadyl Sulfate | ns | X | 0.025 | 0.0139 | 0.0004 |
| VSVΔ51-CXCL9 | 0.0127 | 0.025 | X | 0.41 | 0.0250 |
| VSVΔ51-IL12-CXCL9 | 0.0073 | 0.0139 | 0.41 | X | 0.09 |
| VS+VSVΔ51-CXCL9 | 0.0003 | 0.0004 | 0.0250 | 0.09 | X |
| VS+VSVΔ51-IL12-CXCL9 | 0.0003 | 0.0004 | 0.07 | 0.26 | 0.58 |

**Figure 33: Oncolytic activity of VSVΔ51 encoding CXCL9 and VSVΔ51 encoding IL12-CXCL-9 in CT26WT-tumor model.**

**(A)** Schematic representation of the treatment schedule: CT26WT-tumor-bearing mice were treated with three intratumorally (i.t.) injections of vehicle (PBS) or 50mg/kg of Vanadyl Sulfate for 4 hr and subsequently treated with 1E8 PFU of VSVΔ51 encoding CXCL9, VSVΔ51 encoding IL12-CXCL9 or VSVΔ51 encoding IL-12 or monotherapy over a period of 5 days. **(B)** Survival was monitored over time, and the percentage of survival was included for each condition, long rank (Mantel-Cox) test indicated the significance, as indicated in the table. **(C)** Table shows the significance values using long rank (Mantel-Cox), *P=0.01, **P=0.003, ***P=0.001, ****P<0.0001. Survival data represent 2 independent studies, n=10-15 per group.

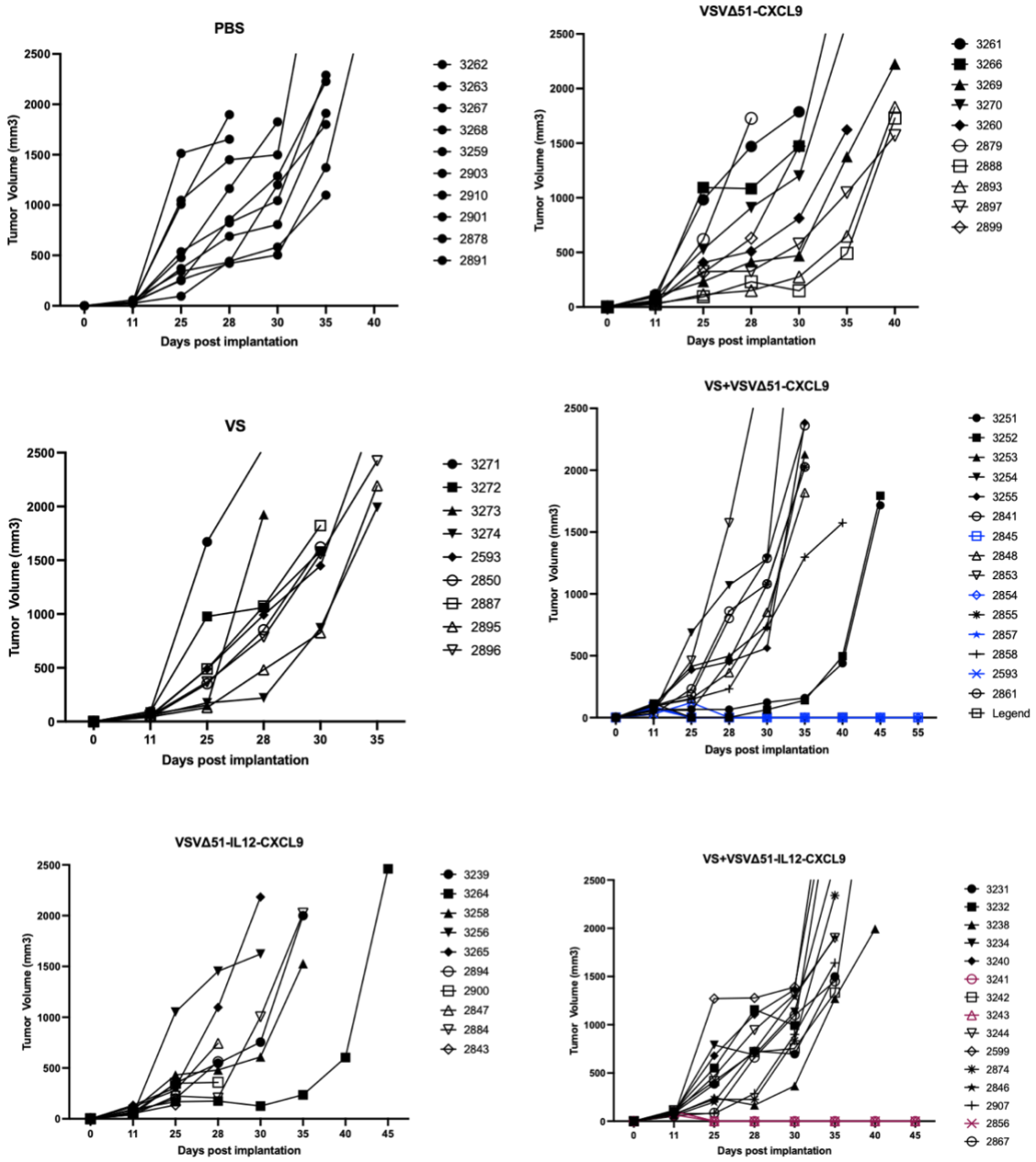


**Figure 34: Tumor volume was monitored following treatment with VSVΔ51 encoding CXCL9 and VSVΔ51 encoding IL12-CXCL-9 in CT26WT-tumor model.**

**This figure is part of Figure 33,** Tumor volume $mm^3$ was measured for each individual mouse, n=10-15. Survival data represent 2 independent studies, n=10-15 per group.

Treatment with VS+VSVΔ51 encoding IL-12-CXCL9 does impact survival by only 20% (Figure 33B) compared to control groups (p-value 0.0003 compared to PBS, 0.0004 compared to VS, and 0.07 compared to VSVΔ51 encoded CXCL9, Figure 33C). As previously observed, treatment with VS+VSVΔ51 encoding IL12 leads to a 40% survival rate compared with all tested groups (Figure 33B).

Noticeably, the addition of these transgenes in the backbone of VSVΔ51 leads to a delay in tumor growth following the combined therapies (Figure 34). Interestingly, VSVΔ51 encoding CXCL9 in combination with VS provided more therapeutic benefit compared with VS+VSVΔ51 encoding both IL12 and CXCL9.

### 3.3.4. NK cells expressing CXCR3 was found to be increased 5 days post armed combination therapies.

To further investigate the impact of the inclusion CXCL9 on immune cell infiltration, we expanded our analyses to characterize the cellular changes at the TME 5 days post-therapy. 5 days post therapy have been chosen as a timepoint to identify the cellular changes after 3 doses of the therapy. Following the same therapeutic regimen (Figure 35A), tumors were collected 5 days post the first treatment followed by tumor dissociation, extracellular staining for anti-CD3, CD8, CD4 and CD49b antibodies as well as activation markers and flow cytometry analyses as previously described in aim 3.3.2.

We did not observe any significant changes in the number of CD4+ and CD8+ T cells expressing CXCR3 (Figure 35 B, C and Figure 37) as well as CD49b+ NK cells expressing CXCR3 (Figure 36).

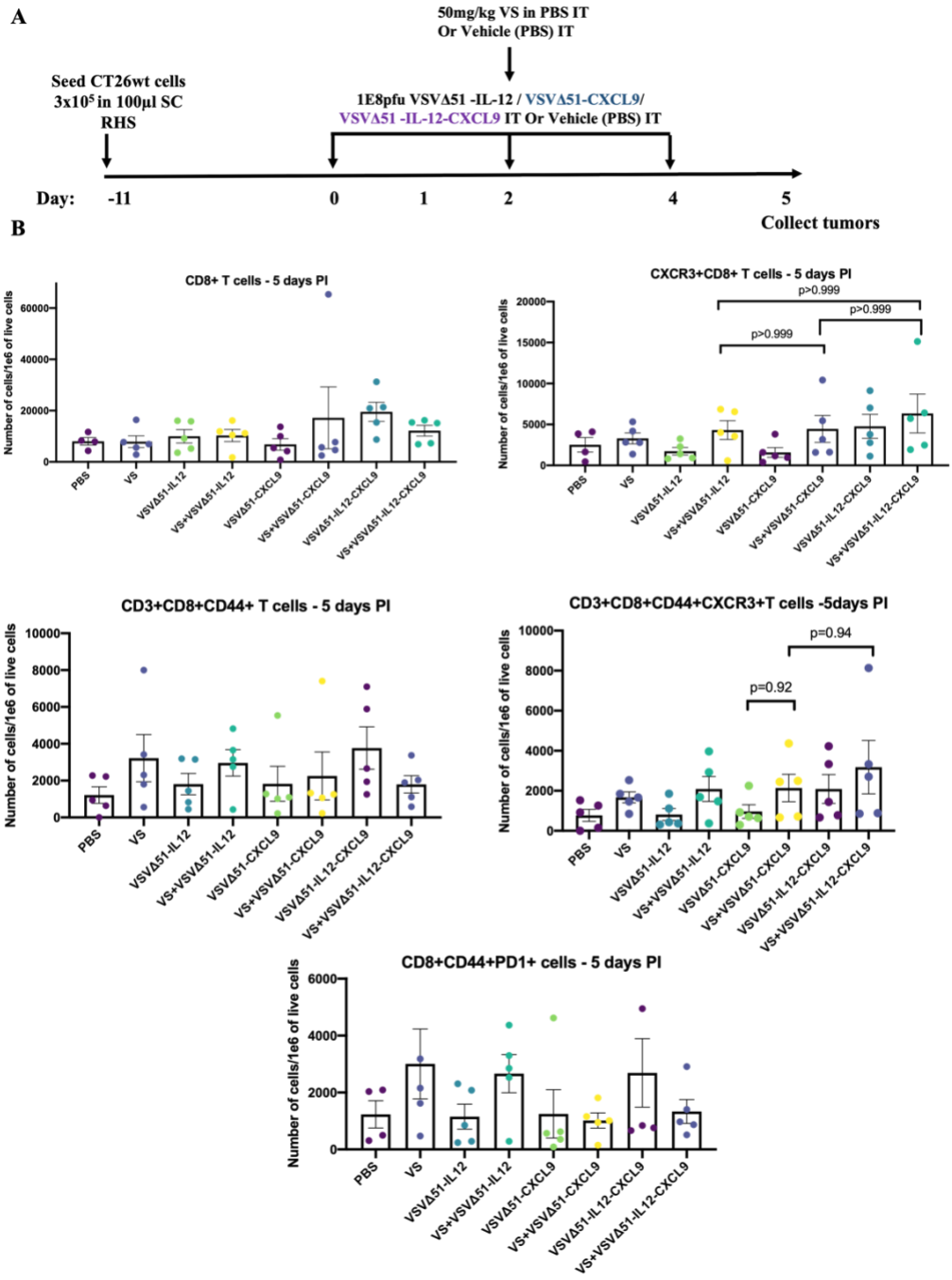


**Figure 35:The impact of treatment with VS in combination with VSVΔ51 encoding CXCL9 and VSVΔ51 encoding IL12-CXCL-9 on the immune response 5 days post treatment.**

**(A)** Schematic representation of the treatment schedule: after 12 days, CT26WT-tumor bearing mice received three intratumorally vanadyl sulfate (50mg/kg) and VSVΔ51 encoding IL-12, VSVΔ51 encoding CXCL9 or VSVΔ51 encoding IL12-CXCL9 (1E8 PFU) or monotherapy. Tumor were collected 5 days post-treatment. Tumors were dissected as previously described. Cells were stained with markers for various subsets of immune cells including CD45, CD3, CD4, CD8, CD49b and CXCR3 including activation markers CD44, and CD69. Relative proportions of various immune cell subsets among all leukocytes of live cells are shown. Graphs show **(B)** The number of CD8+, CD8+CXCR3+, CD8+CD44+, CD8+CD44+CXCR3+ and CD8+CD44+PD1+ T cells per 1e6 live cells. N=5 per group, Mean±SEM, Two-way ANOVA.

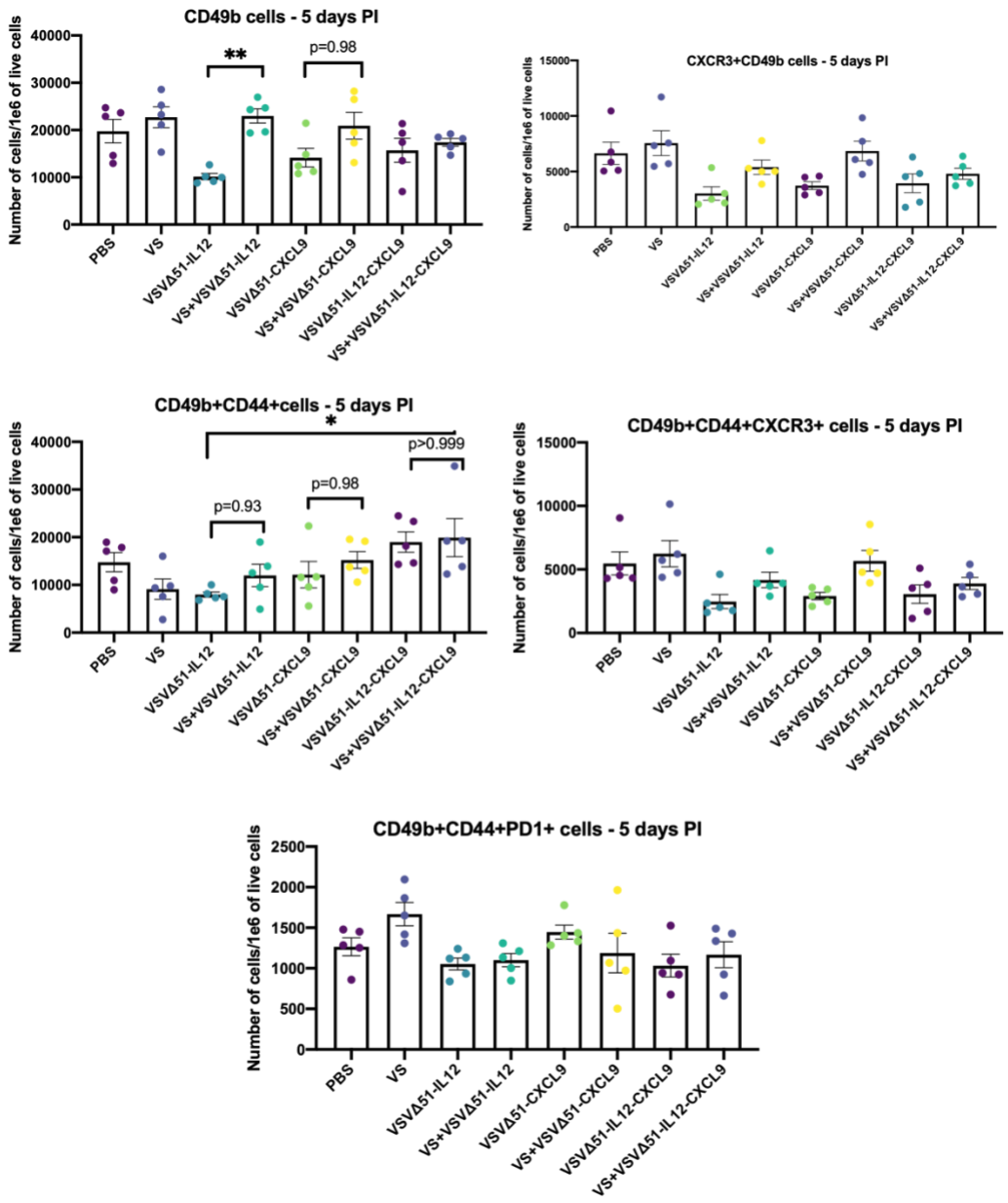


**Figure 36: The number of NK cells 5 days following treatment with VS in combination with VSVΔ51 encoding CXCL9 and VSVΔ51 encoding IL12-CXCL-9.**

This figure is part of Figure 35, graphs show the number of CD49b+, CD49b+CXCR3+, CD49b+CD44+, CD49b+CD44+CXCR3+ and CD49b+CD44+PD1+ NK cells per 1e6 live cells. N=5 per group, Mean±SEM; * P=0.01, ** P=0.003, Two-way ANOVA.

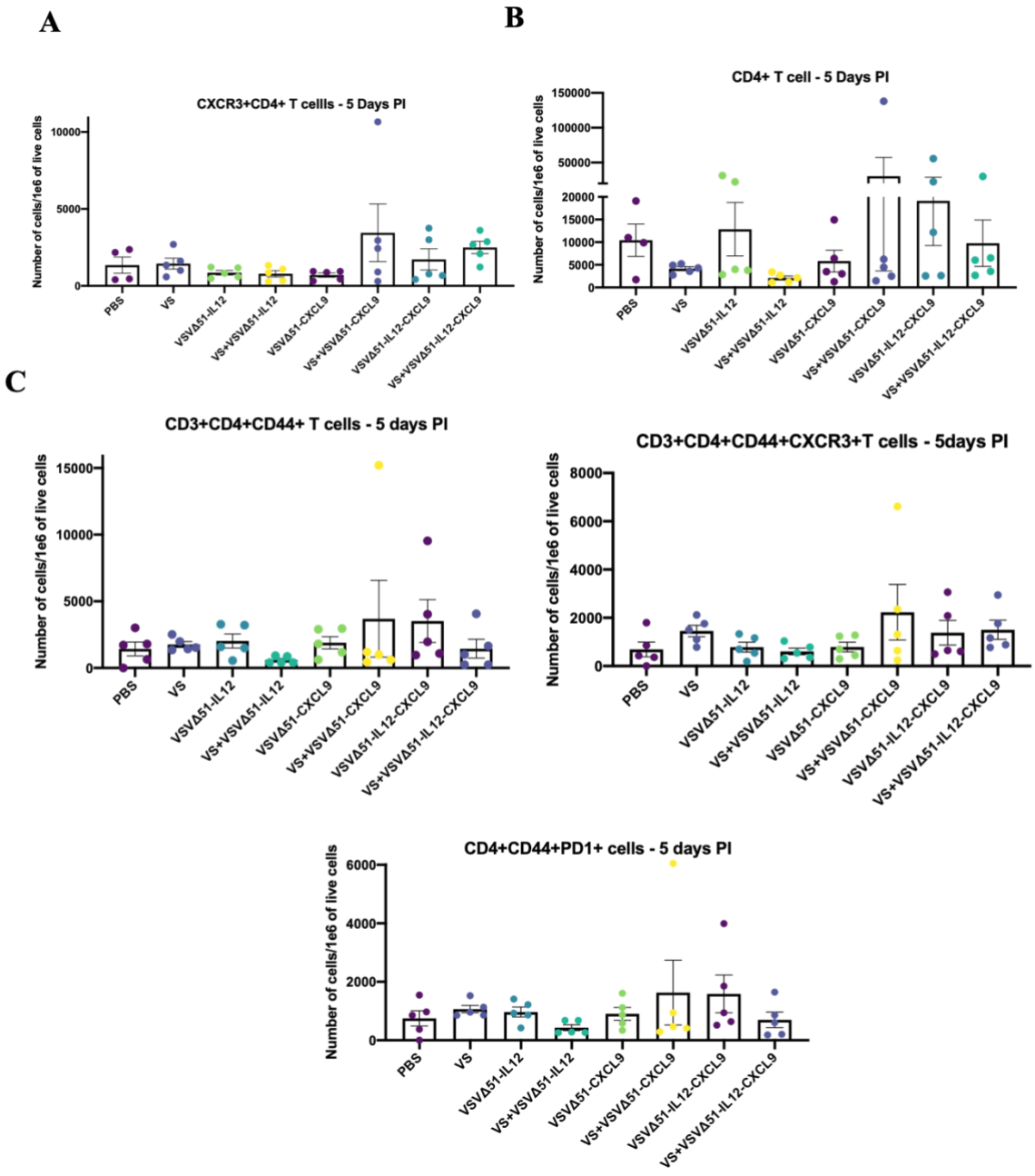


**Figure 37: The number of CD4+CXCR3+ T cells 5 days post treatment.**

From the same experiment presented in Figure 35, CD4+ T cells were also qualified by flow cytometry-based analyses. Graphs show **(A)** the number of CD4+ T cells, **(B)** the number of CD4+CXCR3+ T cells, **& (C)** the number of CD4+CD44+, CD4+CD44+CXCR3+ and CD4+CD44+PD1+ T cells. N=5 per group, Mean±SEM, Two-way ANOVA

We did not observe any significant changes in the number of CD8+CD44+ T cells expressing CXCR3 or CD8+CD44+PD1+ T cells (Figure 35 B). However, there was a trend toward an increase observed in the number of those cells in the group that received VS+VSVΔ51 encoding CXCL9.

There was a significant increase in the number of CD49b+ NK cells in the group that received the VS+VSVΔ51 encoding IL12 and VS+VSVΔ51 encoding CXCL9 compared with other groups (Figure 36). An increase in the number of CXCR3+CD49b+ NK cells and the number of CD49b+CD44+CXCR3+ NK cells was detected in the groups that received the combined therapies (Figure 36).

A significant increase in the CXCL9 concentration in supernatant of tumor dissociated tissues was detected in the group that received VS+VSVΔ51encoding CXCL9 compared with other groups (Figure 38A). The IL12 concentration in supernatant of tumor dissociated tissues was also found to be significantly increased in the group that received VS+VSVΔ51encoding IL-12 and CXCL9 compared with other tested groups (Figure 38B).

In conclusion, treatment with VS+VSVΔ51 encoding CXCL9 increased the number of activated NK cells expressing CXCR3 5 days following the treatment.

### 3.3.5. Cytokine armed combination therapies induced an antigen-specific immune response 14 days post therapy.

We also characterized the antigen-specific immune response to assess if the inclusion of these transgenes could further induce the antigen-specific immune response and based on our previous data, we chose 14 days

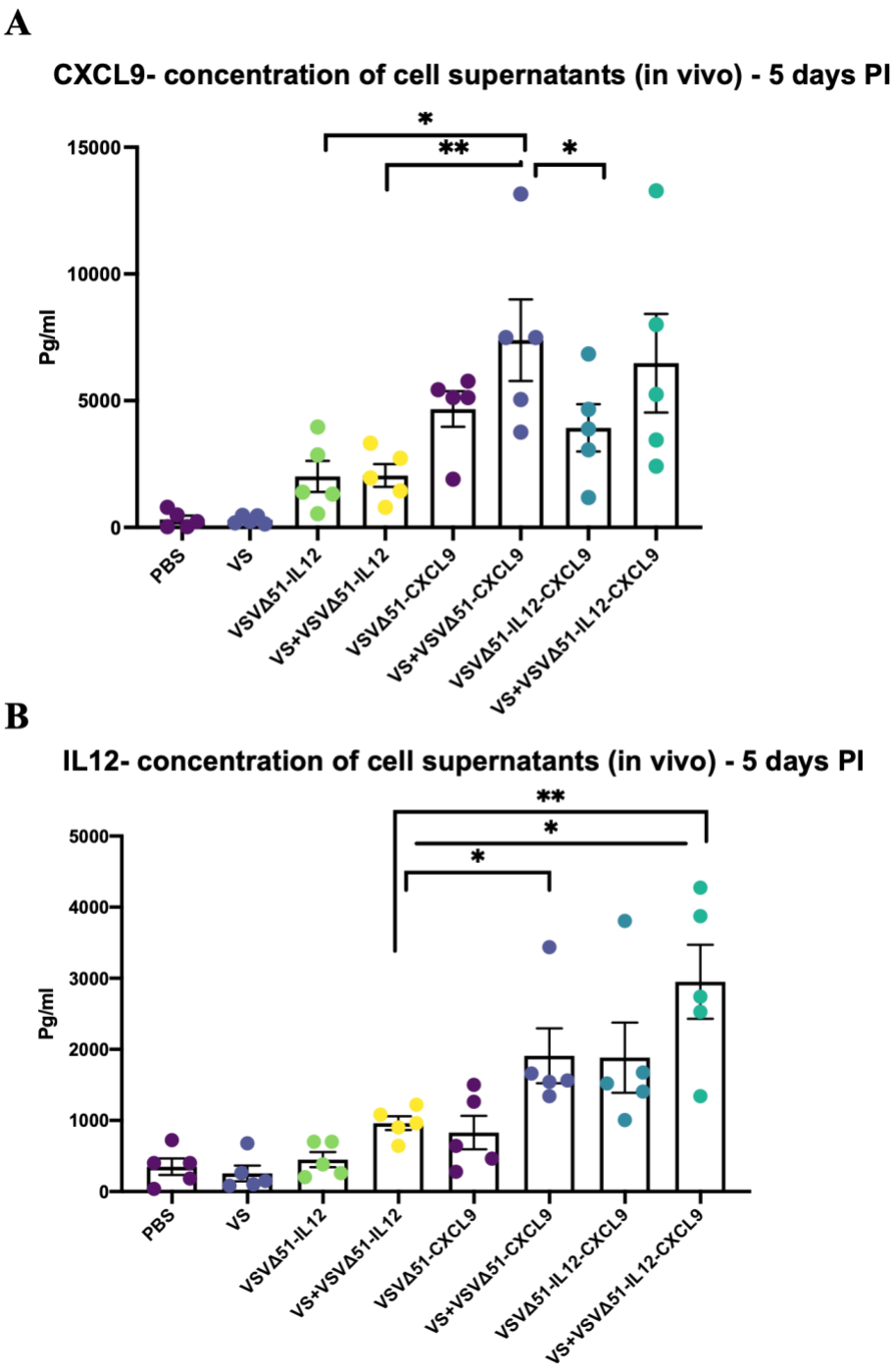


**Figure 38: An increase in the concentration of CXCL9 and IL12 5 days post treatment with VS+VSVΔ51 encoding CXCL9 and VS+VSVΔ51-IL12-CXCL-9.**

**This figure is part of Figure 35, (A)& (B)** CXCL9 and IL12 tumor concentration measured by ELISA. N=5 per group, Mean±SEM, * P=0.01, ** P=0.003, Two-way ANOVA

post-infection as our optimal time point for evaluating the antigen-specific using ELISPOT-based analysis. We assessed the antigen-specific immune response against tumor peptide for gp70 (the immunodominant antigen in CT26WT and a common murine tumor-associated antigen that is highly expressed) and virus peptide VSV N following combined therapy or controls using an IFN-γ ELISPOT assay. Fourteen days post-treatment, splenocytes were isolated from mice and then stimulated *ex vivo* with gp70 or VSV N peptides (Figure 39A). An increase in the number of IFN-γ producing splenocytes reacting to the peptide gp70 was detected in the group that received VS followed by VSVΔ51 encoding CXCL-9 or VSVΔ51 encoding IL12-CXCL9 when compared with monotherapy alone (Figure 39B-C). However, there was no significant increase compared with the virus alone indicating that the inclusion of these transgenes to VSVΔ51 was the main contributing factor increasing the antigen specific anti-tumor immune response.

Furthermore, treatment with VSVΔ51-CXCL9 and VSVΔ51-IL12-CXCL9 as well as VSVΔ51-IL12 alone induced a potent antiviral immune response measured by the reaction against the VSV N peptide (Figure 39C). In contrast with gp70, the response to VSV-N did not increase and trended towards a decrease in the combination treatment indicating that treatments with combined therapies also induce an antiviral immune response.

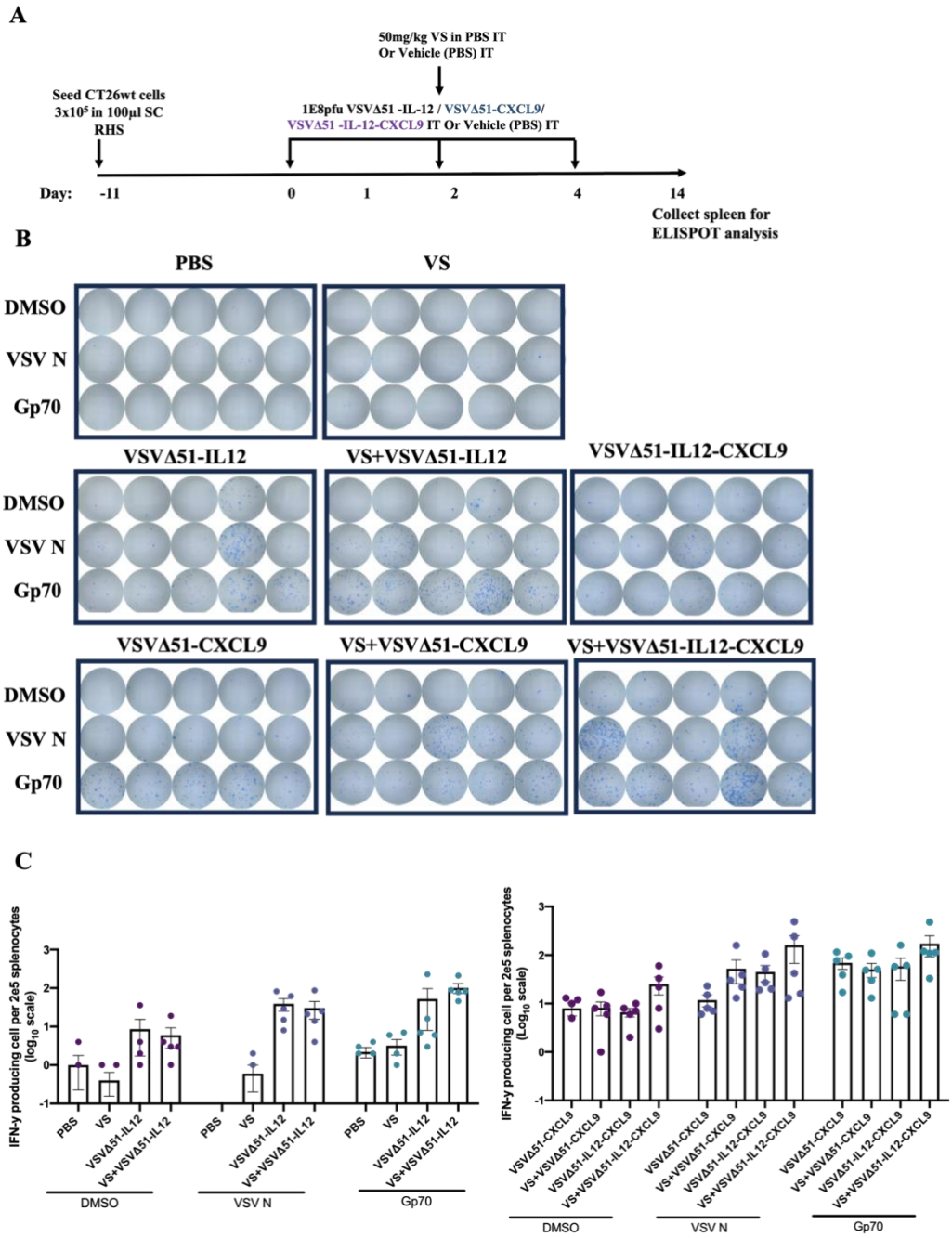


**Figure 39:VS plus VSVΔ51 encoding CXCL9 and VSVΔ51 encoding IL12 and CXCL9 combination therapy induces antigen-specific immune response 14 post-treatment.**

**(A)** Schematic representation of the treatment schedule: after 12 days, CT26WT-tumor bearing mice received three intratumorally vanadyl sulfate (50mg/kg) and VSVΔ51 encoding CXCL9, VSVΔ51 encoding IL-12 CXCL9, or VSVΔ51 encoding IL-12 (1E8 PFU) or monotherapy over 5 days. (**B)** Representative plates from an ELISPOT assay, splenocytes from treated mice were processed 14 days post-treatment, then co-cultured with either VSV N or gp70 peptides for 20 hours. **(C)** The graph shows the quantification of $\log_{10}$ of the number of IFN-γ producing cells per 2E5 splenocytes. N= 5 per group, Mean±SEM, Two-way ANOVA.

# Chapter 4: Discussion

## 4.1 Combined therapy and the improvement of therapeutic efficacy in the CT26WT tumor model.

Oncolytic virus therapy is one of the promising cancer treatments that is considered a targeted therapy because it selectively kills cancer cells while leaving normal cells unharmed. The field of OV therapy has reached a certain level of maturity with clinical and preclinical studies that provide invaluable guidance for approving and accentuating the therapeutic potential of OVs. However, one of the major obstacles limiting the benefits of such a therapy is the antiviral immune response. With a lot of efforts to improve some of the challenges and limitations that compromise the immunostimulatory properties of such a therapy, viral enhancers hold a lot of promise as they not only suppress the antiviral immune response but also enhance viral replication, in some cases to more than 1000-fold (143). In addition, one potential benefit of this approach is the induction of pro-inflammatory cytokines and chemokines following OV therapy, which leads to systemic inflammatory responses and enhancement in antitumor immune responses.

Recently, many vanadium compounds were tested in our laboratory as complementary pharmacological agents in conjunction with oncolytic virus immunotherapy. These include metavanadate, vanadium(V) oxytriethoxyde (VOx), vanadium (IV) oxide sulphate (VS) and bismaltolato oxovanadium (IV) (BMOV). All of these compounds have a similar effect in enhancing VSVΔ51 growth in vitro (155). Throughout this study, we used vanadyl sulfate since in addition to the above reason, its safety profile has been established based on preclinical and clinical studies. It is relatively well tolerated, and it is widely used as a bodybuilding supplement (307). All these properties provide rationale for VS to be tested in humans

alongside OVs. Furthermore, we used VSVΔ51 in this study for several reasons. Among its inherent therapeutic benefits, it is selective to cancer cells and is strongly immunogenic. Importantly, vanadium compounds have been shown to enhance RNA viruses such as VSVΔ51 preferentially (155).

The current project was based on a previous study that showed *in vitro* and *in vivo* efficacy of combined vanadium- VSVΔ51 treatment in multiple cell lines and murine models including but not limited to CT26, B16, DBT, and 4T1 (155). In the current study, we focused on the CT26WT model owing to its particularly high resistance to VSVΔ51 and high level of characterization from previous studies using vanadate. In this model, the combination therapy of VS+ VSVΔ51 enhances therapeutic efficacy compared to monotherapies, leading to long-term survival in only a fraction of mice, leaving room for improvement (155). In addition, the combined therapy generates a sustainable immune response, in particular an enhancement in the number of IFN-γ producing T cells within the tumor microenvironment (155).

Throughout the studies presented here, we looked at the systemic effects of treatment with VS in combination of VSVΔ51.We looked at the relevant immunological changes and the associated enhancement in the immune response by evaluating the secretion of cytokines and chemokines. In addition, we characterized the cellular immunological changes in the tumor microenvironment and tumor draining lymph nodes following the treatment to shed light on the mechanisms driving the efficacy of VS as a viral enhancer in combination with immune-virotherapy contributing to better mechanistic understanding (155& 156).

## 4.2 The cytokine and chemokine profile following the combined therapy and the role of IFN-γ in shaping these responses:

The mechanism that regulates T cell infiltration and functionality within the tumor involves numerous cytokines and chemokines which enable the trafficking and activation of immune cells and as a result, contribute to tumor suppression and can be co-opted to improve therapeutic efficacy. Chemokines and cytokines are key modulators of the immune response and drive a network of interactions to coordinate cellular migration and cell-cell interactions (305, 308). Each one of these cytokines and chemokines also drives several regulatory events that modulate cell recruitment and trafficking (305, 308). Therefore, we characterized the secretion of pro-inflammatory cytokines and chemokines that regulate the immune responses at various time points following the combined therapy to understand the mechanism regulating these interactions.

We show here that the combined therapy of VS in combination with VSV**Δ**51 upregulates the secretion of proinflammatory cytokines and chemokines in blood and that mediates other relevant immunological changes induced by the systemic impact of this combined therapy. The efficacy obtained with VSVΔ51 in enhancing OV therapy was observed to be largely associated with a shift from type I interferon into type II interferon through the activation of STAT1 and the downregulation of STAT2 activation, a mechanism implicating hyperactivation of EGFR (155, 309). This signal "rewiring" is associated with a specific gene expression signature involving the upregulation of pro-inflammatory cytokines (e.g., CCL8, CCL3, IL6, TNF, IFNβ, CCL5) and chemokines (e.g., CXCL9, CXCL10, and CXCL11) (155). While signalling cascade characterization of this phenomenon was carried

out mostly in the 786-0 cell line, the resulting signalling read-out in terms of gene expression profile enhancement was analogous between 786-0 cells and CT26WT (155 Figure S7C).

Our multiplex data reveal that IFN-γ secretion following the combination therapy increased by more than 5-fold (Figure 5); therefore, we believe IFN-γ, in addition to other key important cytokines and chemokines, shape the immune response in a direct way by inducing a robust anti-tumor immune response. IFN-γ secretion induces the secretion of cytokines and chemokines that are important in generating a strong immune response. Of these, the secretion of CXCL9 and CXCL10 was found to be increased by more than 2-fold one day following the combined therapy (Figure 5). It has been reported that CXCL-9 and CXCL10 are released in response to IFN-γ secretion. These chemokines not only stimulate immune cells activation and recruitment including T cell and NK cells, but also induce the production of IFN-γ, TNF-*α*, IL-2 and enhance anti-tumor immunity by mediating the CTLs, NK cells, NKT cells, and macrophage activation (310-313). Recent studies demonstrate that interferon-gamma (IFN-γ) secretion is a critical driver and regulator for intratumoral T cell infiltration via upregulation of its target genes CXCL9/10/11 (314). Consistent with this, we also observed a similar effect of this chemokine on T cell infiltration *in vitro* following the combined therapy, moreover there is a significant increase in the number of migrated T cells and the supernatant concentration of CXCL9 was increased in the group that received the combined therapy (Figure 9). In addition, the number of CD8+ T cells in the tumor microenvironment was found to be significantly increased following the combined therapy and that also has been previously observed (155). CXCL9 synergized with CCL5 and this impact has been shown to correlate with $CD8^+$ T cell infiltration across different cancer types and that was amplified by the secretion of IFN-γ (315, 316).

IFN-γ is produced in response to numerous stimulants from tissue-specific environments and acts as an intermediate factor of complex relationships between distinct immune cells, making it particularly important in providing protection against diseases (317). Considering this effect of IFN-γ on the host immune cells present in the tumor microenvironment with associated antitumor and immunomodulatory properties, 14 days post treatment with the combination therapy, IFN-γ secreting T cells against tumor antigen were found to be significantly increased in the group that received the combined therapy (Figure 8), again indicating that the combined therapy induces a strong antigen-specific anti-tumor immune response.

IL-6 is a cytokine responsive to the secretion of IFN-γ and is also significantly increased following the combined therapy (Figure 5, 7). IL-6 is an NF-kB-regulated cytokine and has a lot of immunostimulatory effects. As previously reported by Fisher *et al.* and others, IL-6 can further increase naïve and central memory T cell trafficking to the tumor as well as promote the recruitment of effector T cells (318, 319, 320). As previously identified by our group the molecular mechanism of vanadate in leading to a shift from type I IFN into type II IFN response is through EGFR pathway activation which leads to simultaneous downregulation of STAT2 and hyperactivation of both STAT1 and NF-kB (309). IL-6 is also known to inhibit T-cell apoptosis and prevent regulatory T-cell differentiation, but also plays an essential role in the differentiation of monocytes to macrophages (308, 319).

Aligning evidence points to the importance of a concerted immune response in driving the efficacy of our vanadium-based combination therapies and the possible role of IFN-γ secretion in shaping such a response. Furthermore, it has been reported that antigen-specific T-cells increase IFN-γ concentrations in tumor tissue, which facilitates tumor clearance (317).

However, IFN-γ also induces the expression of PD-L1 on lymphatic endothelial cells (320). Consequently, high levels of IFN-γ could negatively impact the cytotoxic T-cell activity and migration from the peritumoral space to the TME tumor microenvironment (321). Despite showing an associated improvement in therapeutic efficacy, we have observed an increase in the expression of PDL-1 24hrs following combination therapy (Figure S14). Interestingly, it has been shown that IFN-γ can induce apoptosis in tumor-specific T-cells and that this can compromise antitumor immunity (322, 323). These are altogether factors that could be limiting the benefit of the combination treatment but that could also offer potential strategies to improve efficacy further.

**4.3. The therapeutic potential of IL-12 armed combined therapy.**

As an effort to further improve the therapeutic efficacy of our combined therapy, we used a cytokine armed therapeutic regimen that could further enhance the immune response and further induce the secretion of pro-inflammatory cytokines and chemokines. We chose IL12 due to its well documented direct antitumor properties and for further inducing IFN-γ secretion. We studied the impact of IL12 on the therapeutic efficacy of the combined therapy by using VSVΔ51 expressing/encoding IL12.

We and others (324-327) have noted that IL-12 immunotherapeutic approach would be more effective and less toxic if delivered in the tumor microenvironment directly and through the use of novel delivery technologies. Indeed, as previously demonstrated in several tumor models, the systemic toxicity of IL-12 is limited following oncolytic viruses (OVs) expressing IL12 therapy that is administrated locally in the tumors (328, 329, 330).

We observed that the addition of IL-12 to the backbone of VSV**Δ**51 in combination with VS improves the therapeutic efficacy in our CT26WT tumor model by almost double compared with VS in combination with VSVΔ51. Indeed, the survival in CT26WT tumor model doubles from 20% following treatment with VS+ VSV**Δ**51 to 40% following treatment with VS+VSV**Δ**51 encoding IL12 (Figure 11). We consider that this is achieved through maximizing the amount of IL-12 that is expressed by the virus within the tumor form the effects of VS and propose that is critical for a robust antitumor response when relying on transgene-mediated effects of OVs. Indeed, many OVs encoding IL12 therapies have been tested in various cancer models and expression of IL-12 was associated with the generation of superior anti-tumor immunity (301, 330, 331, 332, 333). In line with this and based on recent investigations multiple i.t. injections of VSV-IL-12 were more effective at eliminating tumors and induced higher long-term survival rates (40 vs. 0%) compared to non-cytokine encoding VSV (334).

**4.4. IL12 in inducing pro-inflammatory cytokines and chemokines:**

The enhancement in anti-cancer efficacy following treatment with IL12 based therapies has been shown to be dependent on T cells, particularly $CD8^+$ T cells. Additionally, IL-12 based therapies are associated with early activation of NK cells and effector T cells, and upregulation of the release of effector anti-tumor cytokines IFN-γ and TNF-α (330) as well as other cytokines and chemokines. Therefore, we characterized the cytokine and chemokine secretion profile following treatment with VS+ VSV**Δ**51 encoding IL12 in the CT26WT model.

Based on the cytokine and chemokine secretion analysis, enhancement in the secretion of pro-inflammatory cytokines and chemokines was observed following the inclusion of IL-12 into our combined therapeutic regimen (Figure 13, 14). One of the benefits of localized IL-12 delivery is the ability to generate a systemic effect that induces the antitumor immunity from a locally initiated immune response (335, 336, 337). Regarding the latter and relevant to our findings, IL-12 armed combined therapy induced the production of large amounts of IFN-γ and large amount of IL12 that is virally secreted. In fact, IFN-γ is secreted by NK cells and T cells in response to IL12 secretion and that augments the proliferation and cytolytic activity of these cells (338, 339). The number of activated NK cell and T cells were found to be increased following the combined therapy in the TME (Figure 20). In addition, IFN-γ secretion stimulates the secretion of IL-12 by APCs which as a result triggers the re-activation of the IFN-γ production cycle; this is known as a positive loop (340, 341, 342, 343). The enhancement in therapeutic efficacity following IL12 armed combined therapy is thus likely due to the generation of sustained immune responses from both NK and T cells in this context.

We observed an enhancement in the secretion of IL-6, CXCL9 and CXCL10 in addition to other cytokines and chemokines (Figure 13). However, only the increase in the secretion of IL-6 was significant in the group that received IL-12 combined therapy indicating that the further enhancement in the secretion of pro-inflammatory cytokines and chemokines could contribute to the enhancement in the therapeutic efficacy following treatment with IL12 combined therapy, which we subsequently explored with CXCL9 co-expression.

## 4.5 The relevant immunological changes at a cellular level following the combined therapy:

We have attempted to characterize the impact of the combined therapy on immune cells in the TME and TdLNs at selected time points. We chose these timepoints based on the cytokine and chemokine profiles where significant changes were observed. Specifically, at day 5 post treatment where an increase in most of the cytokine and chemokine concentrations were observed in the combination treatment, and at day 10 post treatment where a decrease in these cytokines were observed, to identify the relevant immunological changes and correlate cell abundance at TME or TdLNs with the cytokine and chemokines secretion profiles. However, we were not able to detect the statistical significance in most of the observed increases.

Therefore, it must be cautioned that many of the specific cellular changes we observed were both subtle and variable. Being exploratory in nature, our studies were not sufficiently powered to detect more subtle and variable changes. It was further difficult to correlate changes in cellular profiles with chemokine and chemokine profiles. Nevertheless, we believe that as a whole, these data are an indication of the immunological changes occurring following combination therapy and can provide guidance for future study design and generate hypotheses to improve therapeutic efficacy.

## 4.6. CD8+ T cells and NK cells play a critical role in the established therapeutic efficacy following combined therapy.

To better understand the immune mediators of the efficacy observed with VS+VSVΔ51 and treatment with VS+VSVΔ51-IL12 in the CT26WT tumor model, multiple experiments were undertaken to selectively deplete NK or CD8 T cells. Our data support the

possibility that this combined therapy induces the effector functions of CD8+ T cells and mediates the recruitment of T cells and other immune cells. This further supports previous findings describing enhancement in IFN-γ producing CD8+ T cells in mice treated with vanadate and VSVΔ51 compared to the monotherapies and the importance of T cells in mediating the therapeutic efficacy in nude mice (155). Our data also showed an enhancement of the antigen-specific antitumor immune response driven by CD8+ T cells (Figure 8). We, therefore, went further with our analyses to clearly define the role of CD8+ T cells on the therapeutic efficacy of our combined therapy using a cell depletion approach. CD8+ T cells were depleted using anti-CD8 antibody. This depletion was very successful and led to a near-complete ablation of CD8+ T cells in the blood for all the tested time points and a sustained depletion at later time points (Figure 23). CD8+ T cell depletion led to a complete abrogation of the therapeutic efficacy following treatment with VS+VSVΔ51, with no surviving mice in comparison with the non-depleted group that had a 20% survival rate (Figure 24). This finding supports our previous observations in regard to the potential effect of CD8+ T cells in mediating the observed therapeutic efficacy. Additionally, following treatment with VS+VSVΔ51-IL12, CD8+ T cell depletion decreased the therapeutic efficacy by 50% compared to nondepleted mice (Figure 24). The effect of IL12 in mediating superior effector T cell function, potentially via central memory T cell development has been previously demonstrated and it is tempting to speculate that this could be at play in our system (344-347).

We next investigated the impact of NK depletion on the therapeutic efficacy of the combined therapy. The reason for choosing NK cells is that NK cells play a significant role in driving sustainable immune repose and the effects of NK cells on the therapeutic efficacy of OVs such as VSV have been well described. In addition, the immune profile that we conducted

from TIL guided us to further delineate the contribution and the importance of NK in general on the therapeutic efficacy of our therapy. We considered that NK cells contribute to the improved antitumor immune response that we observed. To be able to define the role that NK cells play in the establishment of the immune response that we have observed following the combined therapy, especially with IL12, we used anti-asialo antibodies to deplete NK cells (Figure 25). Following the combined therapy NK cell depletion reduced the survival rate by 50% following treatment with VS+VSVΔ51from 20% in non-depleted group to 10% in NK cell depleted group and following treatment with VS+VSVΔ51-IL12 from 40% in non-depleted group to 20% in NK cell depleted group (Figure 26) indicating that NK cells play a key role in the therapeutic efficacy of our combined therapy, in particular the IL12 combined therapy. In line with these findings, several studies have demonstrated that NK cells are one of the essential contributors to the antitumor effect of IL12 (348-350).

### 4.7.Designing and generating cytokine- armed targeted therapeutic platforms to further improve the therapeutic efficacy of combined therapy.

Various strategies have significantly enhanced the survival of tumor-bearing mice in the CT26WT model through immune checkpoint inhibitors, cytokines-armed OVs therapy, and cell-based vaccines (351, 352, 353, 354).

These strategies have been shown to enhance the anti-tumor immune response through the induction of the adaptive immune system, specifically CD8 T-cells. Based on our CD8+ T cells and NK cells depletion experiments, CD8+ T cells and NK cells both play an important role in the achieved therapeutic efficacy following the combined therapy. Supported by all the evidence presented here and by other studies (352, 355) that point to the importance of recruiting these cells to the TME to generate a sustainable antitumor immune response, we

designed new approaches targeting T cells and NK cells to further improving the efficacy of the combined therapy.

We choose CXCL9 as a potential transgene owing to accumulated evidence in the literature suggesting a role of this cytokine in recruiting immune cells and its association with a better response to cancer therapies (356, 357). CXCL9 mainly attracts only cytotoxic CD8+ T cells compared with CXCL11 (358) and has a long life *in vivo* in comparison with CXCL10 (359, 360). As previously reported, increased CXCL9 transcript or protein levels in colorectal cancer correlated with improved survival (361, 362, 363). This cytokine has been found to be upregulated at a gene expression level and the secretion of CXCL9 is significantly increased following treatment with VS+VSVΔ51 (Figure 22). The impact of the secreted CXCL9 on T cell infiltration following our therapy was also studied using cell chemoattractant assay, the number of migrated cells was found to be significantly increased in the group that received VS+VSVΔ51 (Figure 9). A recent study investigated CXCL9 as a potential therapeutic transgene, which was inserted into the genome of an oncolytic VSV and was the first attempt to assess the migration of CTLs to the tumor site upon infection using this platform (363). An increase in tumor expression of CXCL9 and the expression of $CXCR3^+$ T cell infiltration was observed following this therapy, and as hypothesized by the authors that oncolytic viral activity relatively produced a sufficient chemokine gradient to optimally attract T cells to the TME, without the need for additional chemokine expression (363). However, this therapy did not induce tumor regression after one dose and that could be because the tumor model that was used which was LM2 a mouse mammary adenocarcinoma cell line, and as the authors stated using alternative tumor models might give very different results (363).

All of these factors provided a proof of concept and rationale for selecting this cytokine as a potential candidate to further enhance activity in combination with VS when encoded in the virus either alone or potentially in combination with IL-12. Therefore, VSVΔ51 encoding CXCL9 was engineered to further investigate the impact of including CXCL9 on the therapeutic efficacy in our model. We also successfully engineered VSVΔ51 encoding both IL12 and CXCL9 within the same virus.

### 4.8. The possible therapeutic benefits of cytokine armed combined therapies and the possible role of NK cells.

VSVΔ51 encoding CXCL9 in combination with VS some added therapeutic potential in the CT26WT tumor model, leading to 30% survival compared to VS+VSVΔ51 which leads to 20% survival (Figure 33). There is a trend toward an increase in the number of CD8+ T cells and CD8+ T cells expressing CXCR3 observed at the TME following this combined therapy, although not statistically significant. However, we observed a significant increase in the number of CD49b+ NK cells expressing CXCR3 at the TME 24hrs following treatment with VS+VSVΔ51 encoding CXCL9 (Figure 30). CXCR3 is the receptor/ligand that is expressed on the surface of NK cells and to which CXCL9 binds. It has been previously reported that NK cells are found to be recruited to the tumor site in a CXCR3-dependent manner (364). Supported by other studies, it has been also reported that NK cell accumulation in tumor beds heavily depends on the presence of IFN-γ, CXCL10, and CXCL9 and their expression of CXCR3 (365, 366). In line with this evidence, we believe that NK cells play a critical role in mediating the combined therapy with VSVΔ51 encoding CXCL9.

The increase in the number of NK cells observed following our combined therapy, in addition to the results from our NK depletion experiment (Figure 26, 27) suggest a role for NKs in mediating the effects of our combination therapy. However, the dual nature of NKs as antiviral and antioncogenic effectors. bring forth the possibility that the increase in the number of NK cells following the combined therapy with CXCL9 could also limits the therapeutic efficacy owing to antiviral NK functions (367). Indeed, OVs need at least some extent of selective replication in cancer cells to express transgenes and to elicit strong adaptive immune responses towards the tumor. One of the big challenges for this field is that the virus gets prematurely cleared by the immune system, a function largely mediated by the innate immune response including NK cells (367). In fact, and as reported by several studies, OVs have been shown to induce NK recruitment and activation, which ultimately contribute to the elimination of the virus-infected host cells (368, 369).

However, we did not further assess the role of NK cells in this regard. For this reason, more studies focused on evaluating the role of NK cells are needed. Furthermore, optimizing the timing of NK cell activation and recruitment alongside the timing for OV armed therapy to avoid detrimental OV clearance by NK cells is an aspect that holds significant importance in improving the therapeutic potential of these therapies.

### 4.9. Potentially excessive intratumoral concentration of CXCL9 following treatment with VSVΔ51 encoding CXCL9.

We have observed a high amount of CXCL9 being locally secreted in the TME 24hrs following treatment with VS+VSVΔ51 encoding CXCL9 (Figure 32). Surprisingly, there was not any significant correlation observed when comparing this increase with the number of

infiltrated CD8+ T cells. One of possibility is that excessive levels of intratumoral CXCL9 could negatively affect cell infiltration due to a too heavily accentuated chemokine gradient. Indeed, prolonged local chemokine secretion can in some contexts have a negative impact and has been shown to cause increased chemokine receptor signaling, T cell hypofunction and anergy in some situations (370, 371, 372). In more detail, the intracellular signaling following Chemokine receptor interaction increases intracellular calcium levels via phospholipase C. This increase causes both hypofunction and anergy; as a result, the cells are unable to appropriately migrate to the site of inflammation and/or to function upon antigen recognition.

Another factor likely to influence the therapeutic utility of a virally encoded chemokine is the nature of the virus into which it is engineered, in this case VSVΔ51. We have previously observed that our combined therapy with VSVΔ51 upregulates the expression of CXCL9 and the secretion of CXCL9 at the onset. We hypothesized initially that this could contribute to the therapeutic efficacy of the combined therapy, and this motivated the generation and testing of VSVΔ51 that encoding CXCL9. While some added benefit was achieved, it is possible that more is not better and could in fact negatively impact therapeutic efficacy. Overall, a better understanding of the biology around CXCL9 axis regulation will be needed to overcome these challenges which are likely not unique to CXCL9.

**Future directions:**

While we have made significant progress in characterizing the effects of the combined therapies employing VS + VSVΔ51 on the immune response; and have further generated and characterized improved cytokine-armed derivatives, more questions arose from our work that warrant further study.

We believe that IFN-γ shapes the immune response that we have observed following the combined therapy from the perspective that the secretion of IFN-γ influences the secretion of other cytokines and chemokines. Adding cytokines expressed from withing the virus, exemplified by the combination of VS and VSVΔ51 encoding IL12, can further induce this secretion. One interesting possibility would be to test whether generating cytokine-armed combined therapies that could accentuate the therapeutic benefit of the secreted IFN-γ that is induced by the therapy itself. Some cytokines have been shown to have these IFN-γ-enhancing effects including and not limited to IL18, IL23, IL7, and IL15 (373, 374).

One of the limitations of IFN-γ is that it induces the expression of PDL1 (375), we have observed that the expression of PDL-1 is found to be increased following our combination therapy. Based on this, we believe that combining immune checkpoint inhibitors with our combination therapies could further improve the therapeutic benefits in the CT26WT tumor model. Multiple studies support a correlation between CXCL9, -10, -11/CXCR3 axis and the response to PDL-1/PD-1 therapy (376, 377, 378, 379, 380, 381). A study by Peng et al. demonstrated that anti-PD-1 therapy not only enhances T cell-mediated immune response but also increases the expression of IFN-γ and CXCL10, not CXCL9 and CXCL11 by bone marrow–derived cells (377). In another study a correlation was observed between CXCR3-driven T cells homing to tumor site and anti-PD-1 treatment observed *in vivo* model. In CXCR3 knockout mice, treatment with Anti-PD-1 failed to shrink the tumor and to mediate a strong immune response indicating that anti-PD-1 therapy is not effective without at least a functional CXCL9, -10, -11/CXCR3 axis (376) (381). All of this evidence points to the need for tumour-infiltrating lymphocytes for responding to anti-PD-1 and anti-PDL1 therapies and relatively provides a proof of concept to test ICIs in our system, especially with CXCL9

combined therapy, assuming the expression of CXCL9 can optimized to maximize recruitment of effector cells.

Another study demonstrated that T Cell-Dendritic cell crosstalk involving the cytokines IFN-γ and IL-12 is required for successful Anti-PD-1 Cancer Immunotherapy (382). Based on signatures of IFN-γ signaling, improved patient survival and response to immune checkpoint inhibition in multiple cancer types can be predicted (383, 384, 385). Our combined therapy treatment induces the secretion of IFN-γ and the combined therapy with IL12 further induces the secretion of IFN-γ further indicating that combination with anti-PD1 and PDL1 may provide added therapeutic benefit.

The use of ICIs in combination with other cancer therapies has shown promising therapeutic results and could overcomes tumor resistance mechanisms that currently limit the therapeutic potential of OVs therapy. ICIs have been tested in colorectal tumor models with limited responses on their own (386). ICIs have also been combined with OVs and many studies report better responses (387, 388); however, clinical trials have to date not demonstrated the same benefit and there remain a lot of challenges. One of these challenges is identifying the therapeutic modalities that will most effectively work in combination, including timing and dosing of these combination therapies as well as pairing different mechanisms of action and targeting different aspects of the tumor microenvironment. Therefore, further studies testing different therapeutic regimens including ICIs with the combined therapy are required including additional assessment to evaluate how effective these therapies work together.

Based on our studies, it is clear that CXCL9 secretion has a strong impact on NK cell infiltration; however, further investigations to study the impact of NK cells on the therapeutic

efficacy of the CXCL9 combined therapy will be needed to determine if they contribute to the antiviral response to test the hypothesis that NK over-activation and over-recruitment may in fact ultimately limit therapeutic efficacy.

Additionally, the locally secreted CXCL-9 is retained at least temporarily at the site of production in the tumor may negatively impact infiltration of adaptive immune cells by ultimately impeding their ability to migrate and leading to increasing T cells hypofunction and anergy. This concept of cell hypofunction and anergy needs to be studied following these therapies to confirm whether the excessive CXCL9 release plays a role in negatively impacting the therapeutic efficacy or whether there are other factors contributing to this.

Conversely, the concentration of secreted CXCL9 decreased 5 days after infection, which could be because the virus was cleared in this timeframe. For this and the above reasons and to overcome these possibilities, the expression of these transgenes may need further control using a conditional expression system. As reported recently, the gene expression of GFP and luciferase reporter can be controlled by a guanine-responsive riboswitch engineered into VSV (389, 390). The benefit of such a system is to time CXCL9 expression following initial VSV replication to improve therapeutic outcomes. This conditioned gene expression system and other similar system are powerful tools and can offer new insight into the development of controlled therapeutic platforms.

As we used a condensed therapeutic regimen consisting of three intratumoral injections every other day over the course of 5 days and which is associated with therapeutic benefits in CT26WT tumor model, optimizing the therapeutic regimen by applying the combined therapy without the CXCL9 in the first two treatments and administrate the VSVΔ51 encoded CXCL9 as the last treatment could resolve such a limitation and also should be tested.

We know that CT26WT cells secrete CXCL9 following our combination therapy, and that this secreted CXCL9 is capable of inducing T cells infiltration as shown in the chemoattractant assay *in vitro*. To distinguish the effects of virally released CXCL9 and the released CXCL9 that is mediated by the combined VS + VSVΔ51 therapy itself, we have recently generated a CXCL-9 knockout CT26 cell line for future testing. Studying the impact of such a deletion on therapeutic efficacy or on T cells infiltration will provide some insight, with the caveat that it is possible that there is some redundancy in the function of CXCL9, and CXCL10-11.

## Conclusion:

We conclude that there is a significant increase in the secretion of IFN-γ following the combination therapy using VS+VSVΔ51 and of cytokines and chemokines that are induced by the secretion of IFN-γ including and not limited to IL6, CXCL9, and CXCL10.

Following the VS + VSVΔ51 combined therapy and the VS + VSVΔ51 encoding IL12 combined therapy, both CD8+ T cells and NK cells significantly contribute to the therapeutic efficacy observed. VS + VSVΔ51 encoding IL12 was found to be the most efficient regimen in our system, leading to 40% survival of mice implanted with CT26WT tumors. Combination therapy using VSVΔ51 encoding CXCL9 also showed some therapeutic benefit over VS + VSVΔ51 and this was associated with a significant increase in the number of infiltrated NK cells expressing CXCR3 at the TME 24hrs following the combined therapy. However, this was not observed to be statistically significant for T cells.

Overall, this study has led to advancements in our understanding of the immunological effect of using vanadium compounds as viral enhancers in combination with VSVΔ51.

Overall, the secreted pro-inflammatory cytokines and chemokines that are generated by the combined therapy are enough to induce a sustainable anti-tumor immune response and long-term survival. However, our data points to the importance of a concerted immune response in driving the efficacy of OV therapies and to the knowledge gained will facilitate the development of improved therapeutic regimens employing oncolytic viruses, exemplified by the combination of VS and VSVΔ51-IL12.

## References:


1. Ruddon, R. W. (2007). *Cancer biology* (4th ed.). Oxford University Press.
2. Hanahan, D., & Weinberg, R. A. (2011). Hallmarks of cancer: The next generation. *Cell, 144*(5), 646-674.
3. Hanahan, D., & Weinberg, R. A. (2000). The hallmarks of cancer. *Cell, 100*(1), 57-70.
4. National Cancer Institute. (2023, April 10). Cancer Treatment. https://www.cancer.gov/about-cancer/treatment.
5. Khan, M. S., Tabrez, S., Ansari, I. A., et al. (2020). Drug resistance mechanisms in cancer: A comprehensive review with a focus on molecular targeted therapies. *International Journal of Molecular Sciences, 21*(10), 3450. doi:10.3390/ijms21103450
6. National Cancer Institute. (2023, April 11). Chemotherapy Side Effects. https://www.cancer.gov/about-cancer/treatment/types/chemotherapy/chemo-side-effects.
7. Gajewski, T. F., Schreiber, H., & Fu, Y. X. (2013). Innate and adaptive immune cells in the tumor microenvironment. *Nature Immunology, 14*(10), 1014-1022.
8. Kalluri, R. (2016). The biology and function of fibroblasts in cancer. *Nature Reviews Cancer, 16*(9), 582-598.
9. Li, Y., Patel, S. P., Roszik, J., & Qin, Y. (2018). Hypoxia-driven immunosuppressive metabolites in the tumor microenvironment: New approaches for combinational immunotherapy. *Frontiers in Immunology, 9*, 1591. doi:10.3389/fimmu.2018.01591
10. Najar, M., Raicevic, G., Boufker, H. I., et al. (2016). Mesenchymal stromal cells: Immunomodulatory properties and clinical perspective. *Stem Cells International, 2016*, 1-14.
11. Wang, D., Huang, S., Yuan, X., et al. (2018). The regulation of the Treg/Th17 balance by mesenchymal stem cells in human systemic lupus erythematosus. *Cellular & Molecular Immunology, 15*(5), 1-11.
12. Liotta, L. A., & Kohn, E. C. (2016). The microenvironment of the tumor-host interface. *Nature, 411*(6835), 375-379.
13. Sarkar, A., Lee, C. E., Victor, A. R., et al. (2017). Regulatory T cell memory. *Current Topics in Microbiology and Immunology, 410*, 101-131.
14. Kalluri, R. (2016). The biology and function of fibroblasts in cancer. *Nature Reviews Cancer, 16*(9), 582-598.
15. Kalinski, P. (2012). Regulation of immune responses by prostaglandin E2. *Journal of Immunology, 188*(1), 21-28. doi:10.4049/jimmunol.1101029.
16. Prendergast, G. C., Malachowski, W. P., DuHadaway, J. B., et al. (2018). Discovery of IDO1 Inhibitors: From Bench to Bedside. *Cancer Research, 78*(21), 6717-6725. doi:10.1158/0008-5472.CAN-18-1055.
17. Albini, A., Bruno, A., Bassani, B., et al. (2005). Nitric oxide and cancer: "How where, and why". *Critical Reviews in Oncogenesis, 11*(3-4), 93-108. doi:10.1615/CritRevOncog.v11.i3-4.100.
18. Batlle, E., & Massague, J. (2019). Transforming Growth Factor-beta Signaling in Immunity and Cancer. *Immunity, 50*(4), 924-940. doi:10.1016/j.immuni.2019.03.024.
19. Wang, L., Yi, T., Zhang, W., et al. (2008). IL-10 enhances CTL-mediated tumor rejection by inhibiting highly suppressive CD4+ T cells and promoting CTL

persistence in a murine model of plasmacytoma. *Journal of Immunology, 181*(11), 7178-7186. doi:10.4049/jimmunol.181.11.7178.
20. Kishimoto, T., Akira, S., Narazaki, M., et al. (2020). IL-6 Family of Cytokines and gp130. *Cold Spring Harbor Perspectives in Biology, 10*(8), a028415. doi:10.1101/cshperspect.a028415.
21. Voronov, E., Carmi, Y., & Apte, R. N. (2018). The role IL-1 in tumor-mediated angiogenesis. *Frontiers in Physiology, 9*, 519. doi:10.3389/fphys.2018.00519.
22. Hamilton, J. A. (2008). GM-CSF in inflammation and autoimmunity. *Trends in Immunology, 29*(5), 243-250. doi:10.1016/j.it.2008.02.006.
23. Semenza, G. L. (2014). Oxygen sensing, hypoxia-inducible factors, and disease pathophysiology. *Annual Review of Pathology, 9*, 47-71.
24. Szefel, J., Danielak, A., & Kruszewski, W. J. (2018). Metabolic pathways of L-arginine and therapeutic consequences in tumors. *Advances in Medical Sciences, 64*, 104-110. doi:10.1016/j.advms.2018.08.018.
25. Viganò, S., Alatzoglou, D., Irving, M., Menetrier-Caux, C., Caux, C., Romero, P., et al. (2019). Targeting adenosine in cancer immunotherapy to enhance T-cell function. *Frontiers in Immunology, 10*, 925. doi:10.3389/fimmu.2019.00925.
26. Chen, D. S., & Mellman, I. (2013). Oncology meets immunology: The cancer-immunity cycle. *Immunity, 39*(1), 1-10. doi:10.1016/j.immuni.2013.07.012
27. Topalian, S. L., Hodi, F. S., Brahmer, J. R., Gettinger, S. N., Smith, D. C., McDermott, D. F., ... & Sznol, M. (2012). Safety, activity, and immune correlates of anti-PD-1 antibody in cancer. *New England Journal of Medicine, 366*(26), 2443-2454. doi:10.1056/NEJMoa1200690
28. Yarchoan, M., Hopkins, A., & Jaffee, E. M. (2017). Tumor mutational burden and response rate to PD-1 inhibition. *New England Journal of Medicine, 377*(25), 2500-2501. doi:10.1056/NEJMc1713444
29. Pardoll, D. M. (2012). The blockade of immune checkpoints in cancer immunotherapy. *Nature Reviews Cancer, 12*(4), 252-264. doi:10.1038/nrc3239
30. Dong, H., Strome, S. E., Salomao, D. R., Tamura, H., Hirano, F., Flies, D. B., ... & Chen, L. (2002). Tumor-associated B7-H1 promotes T-cell apoptosis: A potential mechanism of immune evasion. *Nature Medicine, 8*(8), 793-800. doi:10.1038/nm730
31. Chen, D. S., & Mellman, I. (2017). Elements of cancer immunity and the cancer-immune set point. *Nature, 541*(7637), 321-330. doi:10.1038/nature21349
32. Weiss, J. M., Subleski, J. J., Wigginton, J. M., & Wiltrout, R. H. (2011). Immunotherapy of cancer by IL-12-based cytokine combinations. *Expert Opinion on Biological Therapy, 11*(12), 1495-1505. doi:10.1517/14712598.2011.626983
33. Nefedova, Y., Cheng, P., Gilkes, D., Blaskovich, M., Beg, A. A., Sebti, S. M., & Gabrilovich, D. I. (2005). Activation of dendritic cells via inhibition of Jak2/STAT3 signaling. *Journal of Immunology, 175*(7), 4338-4346. doi:10.4049/jimmunol.175.7.4338
34. Xu, L., Yin, W., Sun, R., Wei, H., & Tian, Z. (2018). Tumor necrosis factor-related apoptosis-inducing ligand simultaneously induces apoptosis in tumor and tumor-infiltrating myeloid-derived suppressor cells. *Cancer Research, 78*(9), 2570-2580. doi:10.1158/0008-5472.CAN-17-3637
35. Shankaran, V., Ikeda, H., Bruce, A. T., White, J. M., Swanson, P. E., Old, L. J., & Schreiber, R. D. (2001). IFNγ and lymphocytes prevent primary tumor development

and shape tumor immunogenicity. *Nature, 410*(6832), 1107-1111. doi:10.1038/35074122
36. Schalper, K. A., Brown, J., Carvajal-Hausdorf, D., et al. (2015). Objective measurement and clinical significance of TILs in non-small cell lung cancer. *Journal of the National Cancer Institute, 107*(3), dju435. doi:10.1093/jnci/dju435
37. Bremnes, R. M., Busund, L. T., Kilvær, T. L., et al. (2016). The role of tumor infiltrating lymphocytes in development, progression, and prognosis of non-small cell lung cancer. *Journal of Thoracic Oncology, 11*(6), 789-800. doi:10.1016/j.jtho.2016.01.015
38. García-Martínez, E., Gil, G. L., Benito, A. C., et al. (2014). Tumor-infiltrating immune cell profiles and their change after neoadjuvant chemotherapy predict response and prognosis of breast cancer. *Breast Cancer Research, 16*(6), 488. doi:10.1186/s13058-014-0488-2
39. Kroeger, D. R., Milne, K., & Nelson, B. H. (2016). Tumor infiltrating plasma cells are associated with tertiary lymphoid structures, cytolytic T cell responses, and superior prognosis in ovarian cancer. *Clinical Cancer Research, 22*(12), 3005-3015. doi:10.1158/1078-0432.CCR-15-2767
40. Lee, H. E., Chae, S. W., Lee, Y. J., et al. (2008). Prognostic implications of type and density of tumour-infiltrating lymphocytes in gastric cancer. *British Journal of Cancer, 99*(10), 1704-1711. doi:10.1038/sj.bjc.6604738
41. Li, J., Liao, Y., Ding, T., et al. (2016). Tumor-infiltrating macrophages express interleukin-25 and predict a favorable prognosis in patients with gastric cancer after radical resection. *Oncotarget, 7*(37), 59181-59192. doi:10.18632/oncotarget.11184
42. Pélcher, M., Braun, M., Friedrichs, N., et al. (2010). Foxp3+ cell infiltration and granzyme B+/Foxp3+ cell ratio are associated with outcome in neoadjuvant chemotherapy-treated ovarian carcinoma. *Cancer Immunology, Immunotherapy, 59*(6), 909-919. doi:10.1007/s00262-009-0807-9
43. Schalper, K. A., Velcheti, V., Carvajal, D. E., et al. (2014). In situ tumor PD-L1 mRNA expression is associated with increased TILs and better outcome in breast carcinomas. *Clinical Cancer Research, 20*(10), 2773-2782. doi:10.1158/1078-0432.CCR-13-2702
44. Velcheti, V., Schalper, K. A., Carvajal, D. E., et al. (2014). Programmed death ligand-1 expression in non-small cell lung cancer. *Laboratory Investigation, 94*(1), 107-116. doi:10.1038/labinvest.2013.130
45. Russell, S., & Peng, K. W. (2017). Oncolytic Virotherapy: A contest between apples and oranges. *Molecular Therapy, 25*(5), 1107-1116. doi:10.1016/j.ymthe.2017.03.024
46. Russell, S., & Bell, J. (2012). Oncolytic virotherapy. *Nature Biotechnology, 30*(7), 658-670. doi:10.1038/nbt.2287
47. Maroun, J., Muñoz-Alía, M., Ammayappan, A., Schulze, A., Peng, K. W., & Russell, S. (2017). Designing and building oncolytic viruses. *Future Virology, 12*(4), 193-213. doi:10.2217/fvl-2016-0190
48. Alberts, P., Tilgaļa, A., Rasa, A., et al. (2018). The advent of oncolytic virotherapy in oncology: The Rigvir® story. *European Journal of Pharmacology, 837*, 117-126. doi:10.1016/j.ejphar.2018.08.042
49. Liang, M., & Oncorine, L. M. (2018). Oncorine, the world's first oncolytic virus medicine and its update in China. *Current Cancer Drug Targets, 18*(2), 171-176. doi:10.2174/1568009616666161130101901

50. Andtbacka, R. H., Kaufman, H. L., Collichio, F., et al. (2015). Talimogene laherparepvec improves durable response rate in patients with advanced melanoma. *Journal of Clinical Oncology, 33*(25), 2780-2788. doi:10.1200/JCO.2014.58.3377
51. Zeng, J., Li, X., Sander, M., Zhang, H., Yan, G., & Lin, Y. (2021). Oncolytic viro-immunotherapy: An emerging option in the treatment of gliomas. Frontiers in Immunology, 12, 4108. doi:10.3389/fimmu.2021.721606
52. Rahman, M. M., & McFadden, G. (2021). Oncolytic viruses: Newest frontier for cancer immunotherapy. Cancers (Basel), 13(21), 5452. doi:10.3390/cancers13215452
53. Macedo, N., Miller, D. M., Haq, R., & Kaufman, H. L. (2020). Clinical landscape of oncolytic virus research in 2020. Journal for Immunotherapy of Cancer, 8(2), e001486. doi:10.1136/jitc-2020-001486
54. Slote Morris, Z., Wooding, S., & Grant, J. (2011). The answer is 17 years, what is the question: Understanding time lags in translational research. Journal of the Royal Society of Medicine, 104(12), 510-520. doi:10.1258/jrsm.2011.110180
55. Pasquinucci, G. (1971). Possible effect of measles on leukemia. The Lancet, 1, 136. doi:10.1016/s0140-6736(71)90911-1
56. Gross, S. (1971). Measles and leukaemia. The Lancet, 1, 397-398. doi:10.1016/s0140-6736(71)92005-7
57. Bluming, A. Z., & Ziegler, J. L. (1971). Regression of Burkitt's lymphoma is association with measles infection. The Lancet, 2, 105-106. doi:10.1016/s0140-6736(71)92434-7
58. Hoster, H., Zanes, R., & von Haam, E. (1949). The association of "viral" hepatitis and Hodgkin's disease. Cancer Research, 9, 473-480.
59. Southam, C. M., & Moore, A. E. (1952). Clinical studies of viruses as antineoplastic agents, with particular reference to Egypt 101 virus. Cancer, 5, 1025-1034.
60. Cattaneo, R., Miest, T., Shashkova, E. V., & Barry, M. A. (2008). Reprogrammed viruses as cancer therapeutics: Targeted, armed, and shielded. Nature Reviews Microbiology, 6(7), 529-540. doi:10.1038/nrmicro1912
61. Kaufman, H. L., Kohlhapp, F. J., & Zloza, A. (2015). Oncolytic viruses: A new class of immunotherapy drugs. Nature Reviews Drug Discovery, 14(9), 642-662. doi:10.1038/nrd4663
62. Chiocca, E. A., & Rabkin, S. D. (2014). Oncolytic viruses and their application to cancer immunotherapy. Cancer Immunology Research, 2(4), 295-300. doi:10.1158/2326-6066.CIR-14-0015
63. Bartlett, D. L., Liu, Z., Sathaiah, M., et al. (2013). Oncolytic viruses as therapeutic cancer vaccines. Molecular Cancer, 12, 103. doi:10.1186/1476-4598-12-103
64. Marelli, G., Howells, A., Lemoine, N. R., & Wang, Y. (2018). Oncolytic viral therapy and the immune system: A double-edged sword against cancer. Frontiers in Immunology, 9, 866. doi:10.3389/fimmu.2018.00866
65. Gujar, S., Pol, J. G., Kim, Y., Lee, P. W., & Kroemer, G. (2018). Antitumor benefits of antiviral immunity: An underappreciated aspect of oncolytic virotherapies. Trends in Immunology, 39(3), 209-221. doi:10.1016/j.it.2018.01.003
66. Ghosh, S., Sarkar, S., & Choudhury, J. (2021). Oncolytic viruses as a novel strategy for cancer immunotherapy. Journal of Cancer Research and Clinical Oncology, 147(3), 579-598. doi:10.1007/s00432-020-03494-w

67. Denton, N. L., Chen, C. Y., Scott, T. R., & Cripe, T. P. (2016). Tumor-associated macrophages in oncolytic virotherapy: Friend or foe? Biomedicines, 4(3), E13. doi:10.3390/biomedicines4030013
68. Delwar, Z. M., Kuo, Y., Wen, Y. H., Rennie, P. S., Jia, W. (2018). Oncolytic virotherapy blockade by microglia and macrophages requires STAT1/3. Cancer Research, 78(4), 718-730. doi:10.1158/0008-5472.CAN-17-2214
69. Tan, D. Q., Zhang, L., Ohba, K., et al. (2016). Macrophage response to oncolytic paramyxoviruses potentiates virus-mediated tumor cell killing. European Journal of Immunology, 46(4), 919-928. doi:10.1002/eji.201545677
70. Kleijn, A., Kloezeman, J., Treffers-Westerlaken, E., et al. (2014). The in vivo therapeutic efficacy of the oncolytic adenovirus Delta24-RGD is mediated by tumor-specific immunity. PLOS ONE, 9(5), e97495. doi:10.1371/journal.pone.0097495
71. Gujar, S., & Lee, P. W. (2014). Oncolytic virus-mediated reversal of impaired tumor antigen presentation. Frontiers in Oncology, 4, 77. doi:10.3389/fonc.2014.00077
72. Jiang, H., Clise-Dwyer, K., Ruisaard, K. E., Fan, X., Tian, W., Gumin, J., ... & Lang, F. F. (2014). Delta-24-RGD oncolytic adenovirus elicits anti-glioma immunity in an immunocompetent mouse model. PLOS ONE, 9(1), e97407. doi:10.1371/journal.pone.0097407
73. Milenova, I. E., van der Veen, V. C., van den Dong, W., van Beusechem, V. W., & de Gruijl, T. D. (2019). The in vitro melanoma tumor microenvironment conditions macrophages to an immunosuppressive M2-like phenotype, which is reversible by oncolytic virus ORCA-010 with immune modulators. Cancer Research, 79, 4133.
74. Guillerey, C., Huntington, N. D., & Smyth, M. J. (2016). Targeting natural killer cells in cancer immunotherapy. Nature Immunology, 17(9), 1025-1036. doi:10.1038/ni.3518
75. Yokoyama, W. M. (1995). Natural killer cell receptors specific for major histocompatibility complex class I molecules. Proceedings of the National Academy of Sciences, 92(24), 3081-3085. doi:10.1073/pnas.92.24.3081
76. McDonald, D. R., & Levy, O. (2019). Innate immunity. In R. R. Rich, T. A. Fleisher, W. T. Shearer, H. W. Schroeder, A. J. Frew, & C. M. Weyand (Eds.), Clinical Immunology (pp. 39-53.e1). Content Repository Only.
77. Wang, W., Erbe, A. K., Hank, J. A., Morris, Z. S., & Sondel, P. M. (2015). NK cell-mediated antibody-dependent cellular cytotoxicity in cancer immunotherapy. Frontiers in Immunology, 6, 368. doi:10.3389/fimmu.2015.00368
78. Gerosa, F., Baldani-Guerra, B., Nisii, C., Marchesini, V., Carra, G., & Trinchieri, G. (2002). Reciprocal activating interaction between natural killer cells and dendritic cells. Journal of Experimental Medicine, 195(3), 327-333. doi:10.1084/jem.20010938
79. Liu, C., Lou, Y., Liz√©e, G., Qin, H., Liu, S., Rabinovich, B., ... & Overwijk, W. W. (2008). Plasmacytoid dendritic cells induce NK cell-dependent, tumor antigen-specific T cell cross-priming and tumor regression in mice. Journal of Clinical Investigation, 118(3), 1165-1175. doi:10.1172/JCI33583
80. Annels, N. E., Simpson, G. R., Denyer, M., Arif, M., Coffey, M., Melcher, A., ... & Pandha, H. S. (2020). Oncolytic reovirus-mediated recruitment of early innate immune response reverses immunotherapy-resistance in prostate tumours by inducing a T-cell inflamed microenvironment. Molecular Therapy - Oncolytics, 20, 434-446. doi:10.1016/j.omto.2020.02.005

81. Jennings, V. A., Scott, G. B., Rose, A. M. S., Scott, K. J., Migneco, G., Keller, B., ... & Pandha, H. (2019). Potentiating oncolytic virus-induced immune-mediated tumor cell killing using histone deacetylase inhibition. Molecular Therapy, 27(6), 1139-1152. doi:10.1016/j.ymthe.2019.03.017
82. Alvarez-Breckenridge, C. A., Yu, J., Price, R., Wojton, J., Pradarelli, J., Mao, H., ... & Chiocca, E. A. (2012). NK cells impede glioblastoma virotherapy through NKp30 and NKp46 natural cytotoxicity receptors. Nature Medicine, 18(12), 1827-1834. doi:10.1038/nm.3565
83. Russell, L., Peng, K. W., & Russell, S. J. (2019). Oncolytic viruses: Priming time for cancer immunotherapy. BioDrugs, 33(5), 485-501. doi:10.1007/s40259-019-00368-w
84. Achard, C., Surendran, A., Wedge, M. E., Ungerechts, G., Bell, J., & Ilkow, C. S. (2018). Lighting a fire in the tumor microenvironment using oncolytic immunotherapy. EBioMedicine, 31, 17-24. doi:10.1016/j.ebiom.2018.03.011
85. Albert, M. L., Sauter, B., & Bhardwaj, N. (1998). Dendritic cells acquire antigen from apoptotic cells and induce class I-restricted CTLs. Nature, 392(6671), 86-89. doi:10.1038/32183
86. Benencia, F., Sprague, L., McGinty, J., Pate, M., & Muccioli, M. (2012). Dendritic cells, the tumor microenvironment, and the challenges for an effective antitumor vaccination. Journal of Biomedicine and Biotechnology, 2012, 425476. doi:10.1155/2012/425476
87. Mellman, I., Coukos, G., & Dranoff, G. (2011). Cancer immunotherapy comes of age. Nature, 480(7378), 480-489. doi:10.1038/nature10673
88. Hicken, H. D., V., Shankaran, A. S., Dighe, A. G., Stockert, E., Aguet, M., Old, L. J., & Schreiber, R. D. (1998). Demonstration of an interferon gamma-dependent tumor surveillance system in immunocompetent mice. Proceedings of the National Academy of Sciences, 95(13), 7556-7561. doi:10.1073/pnas.95.13.7556
89. Riond, J., Rodriguez, S., Nicolau, M. L., al Saati, T., & Gairin, J. E. (2009). In vivo major histocompatibility complex class I (MHCI) expression on MHCIlow tumor cells is regulated by Œ≥Œ¥ T and NK cells during the early steps of tumor growth. Cancer Immunity, 9, 10.
90. Timmerman, J. M., & Levy, R. (1999). Dendritic cell vaccines for cancer immunotherapy. Annual Review of Medicine, 50, 507-529. doi:10.1146/annurev.med.50.1.507
91. Koch, F., Stanzl, U., Jennewein, P., Janke, K., Heufler, C., K√§mpgen, E., ... & Schuler, G. (1996). High level IL-12 production by murine dendritic cells: upregulation via MHC class II and CD40 molecules and downregulation by IL-4 and IL-10. Journal of Experimental Medicine, 184(2), 741-746. doi:10.1084/jem.184.2.741
92. Gujar, S. A., Marcato, P., Pan, D., Lee, P. W. (2010). Reovirus virotherapy overrides tumor antigen presentation evasion and promotes protective antitumor immunity. Molecular Cancer Therapeutics, 9(11), 2924-2933. doi:10.1158/1535-7163.MCT-10-0327
93. Liu, S., Zhang, J., Fang, S., Zhang, Q., Zhu, G., Tian, Y., ... & Liu, J. (2021). Macrophage polarization contributes to the efficacy of an oncolytic HSV-1 targeting human uveal melanoma in a murine xenograft model. Experimental Eye Research, 202, 108285. doi:10.1016/j.exer.2020.108285
94. Liu, Y., Cai, J., Liu, W., Lin, Y., Guo, L., Liu, X., ... & Wang, Q. (2020). Intravenous injection of the oncolytic virus M1 awakens antitumor T cells and overcomes resistance

to checkpoint blockade. Cell Death & Disease, 11(10), 1-13. doi:10.1038/s41419-020-03068-0
95. Murphy, K., & Weaver, C. (2017). Janeway's Immunobiology (9th ed.). Garland Science.
96. Voskoboinik, I., Dunstone, M. A., Baran, K., Whisstock, J. C., & Trapani, J. A. (2010). Perforin: Structure, function, and role in human immunopathology. Immunological Reviews, 235(1), 35-54. doi:10.1111/j.0105-2896.2010.00879.x
97. Schroder, K., Hertzog, P. J., Ravasi, T., & Hume, D. A. (2004). Interferon-Œ≥: an overview of signals, mechanisms, and functions. Journal of Leukocyte Biology, 75(2), 163-189. doi:10.1189/jlb.0603252
98. Kaplan, D. H., Shankaran, V., Dighe, A. S., Stockert, E., Aguet, M., Old, L. J., & Schreiber, R. D. (1998). Demonstration of an interferon Œ≥-dependent tumor surveillance system in immunocompetent mice. Proceedings of the National Academy of Sciences, 95(13), 7556-7561. doi:10.1073/pnas.95.13.7556
99. Riond, J., Rodriguez, S., Nicolau, M. L., al Saati, T., & Gairin, J. E. (2009). In vivo major histocompatibility complex class I (MHCI) expression on MHCIlow tumor cells is regulated by Œ≥Œ¥ T and NK cells during the early steps of tumor growth. Cancer Immunity, 9, 10.
100. Liu, M., Guo, S., Hibbert, J. M., Jain, V., Singh, N., Wilson, N. O., & Stiles, J. K. (2011). CXCL10/IP-10 in infectious diseases pathogenesis. Cytokine & Growth Factor Reviews, 22(3), 121-130. doi:10.1016/j.cytogfr.2011.06.001
101. Sharma, P., Wagner, K., Wolchok, J. D., & Allison, J. P. (2011). Novel cancer immunotherapy agents with survival benefit: recent successes and next steps. Nature Reviews Cancer, 11(11), 805-812. doi:10.1038/nrc3153
102. Wang, M., Yin, B., Wang, H. Y., & Wang, R.-F. (2014). Current advances in T-cell-based cancer immunotherapy. Immunotherapy, 6(12), 1265-1278. doi:10.2217/imt.14.95
103. Melero, I., Rouzaut, A., Motz, G. T., & Coukos, G. (2014). T-cell and NK-cell infiltration into solid tumors: A key limiting factor for efficacious cancer immunotherapy. Cancer Discovery, 4(5), 522-526. doi:10.1158/2159-8290.CD-14-0037
104. Dunn, G. P., Old, L. J., & Schreiber, R. D. (2004). The three Es of cancer immunoediting. Annual Review of Immunology, 22, 329-360. doi:10.1146/annurev.immunol.22.012703.104803
105. Liu, T. C., Zhang, T., Fukuhara, H., Kuroda, T., Todo, T., & Kanerva, A. (2014). Oncolytic herpes simplex virus vectors for the treatment of human breast cancer. Journal of Cellular Biochemistry, 115(3), 504-512. doi:10.1002/jcb.24694
106. Jenks, N., Myers, R., Grell, J., Cheema, T., Federico, S., Beliveau, M., ... & Hardcastle, J. (2013). Immune recognition of tumor-associated antigens is not required for eradication of tumors by VSVs expressing defined xenogeneic proteins. Gene Therapy, 20(3), 386-395. doi:10.1038/gt.2012.46
107. Le Boeuf, F., Selman, M., Son, H. H., Bergeron, A., Chen, A., Tsang, J., ... & Diallo, J. S. (2013). Oncolytic vesicular stomatitis virus elicits potent antitumor immune responses when administered intravenously. Journal of Virology, 87(2), 1235-1244. doi:10.1128/JVI.02483-12
108. Knipe, D. M., & Howley, P. M. (Eds.). (2007). Fields Virology. Lippincott Williams & Wilkins.

109. Albertini, A. A. V., Baquero, E., Ferlin, A., & Gaudin, Y. (2012). Molecular and cellular aspects of rhabdovirus entry. Viruses, 4(1), 117-139. doi:10.3390/v4010117
110. Finkelshtein, D., Werman, A., Novick, D., Barak, S., & Rubinstein, M. (2013). LDL receptor and its family members serve as the cellular receptors for vesicular stomatitis virus. Proceedings of the National Academy of Sciences, 110(18), 7306-7311. doi:10.1073/pnas.1305966110
111. Blondel, D., Maarifi, G., Nisole, S., & Chelbi-Alix, M. K. (2015). Resistance to Rhabdoviridae Infection and Subversion of Antiviral Responses. Viruses, 7(7), 3675-3702. doi:10.3390/v7072813
112. Finkelshtein, D., Werman, A., Novick, D., Barak, S., & Rubinstein, M. (2013). LDL receptor and its family members serve as the cellular receptors for vesicular stomatitis virus. Proceedings of the National Academy of Sciences, 110(18), 7306-7311. doi:10.1073/pnas.1305966110
113. Szilagyi, J. F., & Uryvayev, L. (1973). Isolation of an infectious ribonucleoprotein from vesicular stomatitis virus containing an active RNA transcriptase. Journal of Virology, 11(2), 279-286.
114. Ball, L. A., Pringle, C. R., Flanagan, B., Perepelitsa, V. P., & Wertz, G. W. (1999). Phenotypic consequences of rearranging the P, M, and G genes of vesicular stomatitis virus. Journal of Virology, 73(6), 4705-4712.
115. Iverson, L. E., & Rose, J. K. (1981). Localized attenuation and discontinuous synthesis during vesicular stomatitis virus transcription. Cell, 23(2), 477-484.
116. Barr, J. N., Whelan, S. P., & Wert, G. W. (2002). Transcriptional control of the RNA-dependent RNA polymerase of vesicular stomatitis virus. Biochimica et Biophysica Acta (BBA) - Gene Structure and Expression, 1577(3), 337-353. doi:10.1016/S0167-4781(02)00359-0
117. Kiley, M. P., & Wagner, R. R. (1972). Ribonucleic acid species of intracellular nucleocapsids and released virions of vesicular stomatitis virus. Journal of Virology, 10(2), 244-255.
118. Harty, R. N., Paragas, J., Sudol, M., & Palese, P. (1999). A proline-rich motif within the matrix protein of vesicular stomatitis virus and rabies virus interacts with WW domains of cellular proteins: Implications for viral budding. Journal of Virology, 73(4), 2921-2929. doi:10.1128/JVI.73.4.2921-2929.1999
119. Harty, R. N., Paragas, J., Sudol, M., & Palese, P. (1999). A proline-rich motif within the matrix protein of vesicular stomatitis virus and rabies virus interacts with WW domains of cellular proteins: Implications for viral budding. Journal of Virology, 73(4), 2921-2929. doi:10.1128/JVI.73.4.2921-2929.1999
120. Ahmed, M., McKenzie, M. O., Puckett, S., Hojnacki, M., Poliquin, L., & Lyles, D. S. (2003). Ability of the matrix protein of vesicular stomatitis virus to suppress ≈í‚â§ interferon gene expression is genetically correlated with the inhibition of host RNA and protein synthesis. Journal of Virology, 77(9), 4646-4657. doi:10.1128/JVI.77.9.4646-4657.2003
121. Stojdl, D. F., Lichty, B. D., tenOever, B. R., Paterson, J. M., Power, A. T., Knowles, S., ... & Bell, J. C. (2003). VSV strains with defects in their ability to shutdown innate immunity are potent systemic anti-cancer agents. Cancer Cell, 4(4), 263-275. doi:10.1016/S1535-6108(03)00241-1
122. Barr, J. N., Whelan, S. P., & Wert, G. W. (2002). Transcriptional control of the RNA-dependent RNA polymerase of vesicular stomatitis virus. Biochimica et Biophysica

Acta (BBA) - Gene Structure and Expression, 1577(3), 337-353. doi:10.1016/S0167-4781(02)00359-0
123. Lichty, B. D., Power, A. T., Stojdl, D. F., & Bell, J. C. (2004). Vesicular stomatitis virus: Re-inventing the bullet. Trends in Molecular Medicine, 10(5), 210-216. doi:10.1016/j.molmed.2004.03.002
124. Ebert, O., Shinozaki, K., Kournioti, C., Park, M. S., Garc‚àö‚â†a-Sastre, A., & Woo, S. L. (2003). Syncytia induction enhances the oncolytic potential of vesicular stomatitis virus in virotherapy for cancer. Cancer Research, 63(12), 3268-3276.
125. Ahmed, M., et al. (2004). Oncolytic virotherapy for prostate cancer: Efficacy of reovirus as a biological therapeutic. Cancer Research, 64(17), 6087-6093.
126. Zemp, F. J., et al. (2013). Treating brain tumor-initiating cells using a combination of myxoma virus and rapamycin. Neuro-Oncology, 15(7), 904-920.
127. Zhang, L., Steele, M. B., Jenks, N., Grell, J., Suksanpaisan, L., Naik, S., ... & Peng, K. W. (2016). Safety Studies in Tumor and Non-Tumor-Bearing Mice in Support of Clinical Trials Using Oncolytic VSV-IFN‚âí,â§-NIS. Human Gene Therapy Clinical Development, 27(3), 111-122. doi:10.1089/humc.2016.002
128. Barr, J. N., Whelan, S. P., & Wert, G. W. (2002). Transcriptional control of the RNA-dependent RNA polymerase of vesicular stomatitis virus. Biochimica et Biophysica Acta (BBA) - Gene Structure and Expression, 1577(3), 337-353. doi:10.1016/S0167-4781(02)00359-0
129. Hanson, R. P., & Karstad, L. H. (1957). Further studies on enzootic vesicular stomatitis. United States Livestock Sanitary Association Proceedings, 61, 300-307.
130. Patterson, W. C., Mott, L. O., & Jenney, E. W. (1958). Study of vesicular stomatitis in man. Journal of the American Veterinary Medical Association, 133(1), 57-66.
131. Porosnicu, M., Quinson, A. M., Crossley, K., Luecke, S., & Lauer, U. M. (2022). Phase I study of VSV-GP (BI 1831169) as monotherapy or combined with ezabenlimab in advanced and refractory solid tumors. Future Oncology, 18(24), 2627-2638. doi:10.2217/fon-2022-0439
132. Sun, Y. (2016). Tumor microenvironment and cancer therapy resistance. Cancer Letters, 380, 205-215.
133. Liu, Y. P., Suksanpaisan, L., Steele, M. B., Russell, S. J., & Peng, K. W. (2013). Induction of antiviral genes by the tumor microenvironment confers resistance to virotherapy. Scientific Reports, 3, 2375. doi:10.1038/srep02375
134. Liikanen, V., Monsurro, L., Ahtiainen, L., Raki, M., Hakkarainen, T., Diaconu, I., .& Hemminki, A. (2011). Induction of interferon pathways mediates in vivo resistance to oncolytic adenovirus. Molecular Therapy, 19(10), 1858-1866. doi:10.1038/mt.2011.124
135. Vaha-Koskela, M. J., Le Boeuf, F., Lemay, C., De Silva, N., Diallo, J. S., Cox, J., ... & Bell, J. C. (2013). Resistance to two heterologous neurotropic oncolytic viruses, Semliki Forest virus and vaccinia virus, in experimental glioma. Journal of Virology, 87(4), 2363-2366. doi:10.1128/JVI.02753-12
136. Vaha-Koskela, M., & Hinkkanen, A. (2014). Tumor restrictions to oncolytic virus. Biomedicines, 2(3), 163-194. doi:10.3390/biomedicines2030163
137. Pardoll, D. M. (2012). The blockade of immune checkpoints in cancer immunotherapy. Nature Reviews Cancer, 12(4), 252-264.
138. Filley, A. C., & Dey, M. (2017). Immune system, friend or foe of oncolytic virotherapy? Frontiers in Oncology, 7, 106.

139. Rothermel, R. L., Miller, B. A., & Russell, S. J. (2019). Molecular strategies for the treatment of glioma: Encouraging advances and persistent challenges. Neurotherapeutics, 16(2), 387-406. doi:10.1007/s13311-019-00711-x
140. Zamarin, D., Holmgaard, R. B., Subudhi, S. K., Park, J. S., Mansour, M., Palese, P., & Allison, J. P. (2017). Intratumoral modulation of the inducible co-stimulator ICOS by recombinant oncolytic virus promotes systemic anti-tumour immunity. Nature Communications, 8, 14340. doi:10.1038/ncomms14340
141. Barber, G. N. (2001). Host defense, viruses and apoptosis. Cell Death & Differentiation, 8(2), 113-126.
142. Wennier, S. T., Liu, J., & McFadden, G. (2012). Bugs and drugs: oncolytic virotherapy in combination with chemotherapy. Current Pharmaceutical Biotechnology, 13(10), 1817-1833.
143. Diallo, J. S., Le Boeuf, F., Lai, F., Cox, J., Vaha-Koskela, M., Abdelbary, H., ... & Bell, J. C. (2010). A high-throughput pharmacoviral approach identifies novel oncolytic virus sensitizers. Molecular Therapy, 18(6), 1123-1129.
144. Dougan, M., Dougan, S., Slisz, J., Firestone, B., Vanneman, M., Draganov, D., ... & Ploegh, H. L. (2010). IAP inhibitors enhance co-stimulation to promote tumor immunity. Journal of Experimental Medicine, 207(10), 2195-2206.
145. Ajina, A., & Maher, J. (2017). Prospects for combined use of oncolytic viruses and CAR T-cells. Journal for Immunotherapy of Cancer, 5, 90.
146. Chesney, J., Puzanov, I., Collichio, F., et al. (2018). Randomized, open-label phase II study evaluating the efficacy and safety of talimogene laherparepvec in combination with ipilimumab versus ipilimumab alone in patients with advanced, unresectable melanoma. Journal of Clinical Oncology, 36(17), 1658-1667.
147. Ferrucci, P. F., Pala, L., Conforti, F., & Cocorocchio, E. (2021). Talimogene Laherparepvec (T-VEC): An Intralesional Cancer Immunotherapy for Advanced Melanoma. Cancers, 13(6), 1383.
148. ClinicalTrials.gov Identifier: NCT02263508. Retrieved from https://clinicaltrials.gov/ct2/show/NCT02263508
149. Shen, W., Patnaik, M. M., Ruiz, A., Russell, S. J., & Peng, K. W. (2016). Immunovirotherapy with vesicular stomatitis virus and PD-L1 blockade enhances therapeutic outcome in murine acute myeloid leukemia. Blood, 127(11), 1449-1458.
150. Liu, Z., Ge, Y., Wang, H., Ma, C., Feist, M., Ju, S., ... & Hwang, T. H. (2018). Modifying the cancer-immune set point using vaccinia virus expressing re-designed interleukin-2. Nature Communications, 9(1), 4682.
151. Liu, Z., Ravindranathan, R., Kalinski, P., Guo, Z. S., & Bartlett, D. L. (2017). Rational combination of oncolytic vaccinia virus and PD-L1 blockade works synergistically to enhance therapeutic efficacy. Nature Communications, 8, 14754.
152. Forbes, N. E., & Krishnan, R. (2014). Pharmacological modulation of anti-tumor immunity induced by oncolytic viruses. Frontiers in Oncology, 4, 191.
153. Kim, M., Nitschke, M., Sennino, B., Murer, P., Schriver, B. J., Bell, A. M., ... & Jemison, W. (2017). Amplification of oncolytic vaccinia virus widespread tumor cell killing by sunitinib through multiple mechanisms. Cancer Research, 77(15 Supplement), 4490. doi:10.1158/1538-7445.AM2017-4490
154. Garza-Morales, R., Yaddanapudi, K., Perez-Hernandez, R., Riedinger, E., McMasters, K. M., Shirwan, H., & Yolcu, E. S. (2017). Temozolomide renders murine

cancer cells susceptible to oncolytic adenovirus replication and oncolysis. Cancer Biology & Therapy, 0(0), 1-12. doi:10.1080/15384047.2017.1338236
155. Selman, M., Rousso, C., Bergeron, A., Son, H. H., Krishnan, R., El-Sayes, N. A., & Diallo, J. S. (2018). Multi-modal potentiation of oncolytic virotherapy by vanadium compounds. Molecular Therapy, 26(1), 56-69. doi:10.1016/j.ymthe.2017.10.014
156. McAusland, T., van Vloten, J., Santry, L., Guilleman, M., Rghei, A., Ferreira, E., ... & Bastin, D. (2021). Combining vanadyl sulfate with Newcastle disease virus potentiates rapid innate immune-mediated regression with curative potential in murine cancer models. Molecular Therapy - Oncolytics, 20, 306-324. doi:10.1016/j.omto.2021.01.009
157. Pessoa, J. C., Etcheverry, S., & Gambino, D. (2015). Vanadium compounds in medicine. Coordination Chemistry Reviews, 301-302, 24-48.
158. Rehder, D. (2013). Vanadium compounds as potential therapeutic agents. In Interrelations between Essential Metal Ions and Human Diseases (pp. 139-169). Springer.
159. Crans, D. C., Smee, J. J., Gaidamauskas, E., Yang, L. (2004). The chemistry and biochemistry of vanadium and the biological activities exerted by vanadium compounds. Chemical Reviews, 104(2), 849-902.
160. Irving, E., & Stoker, A. W. (2017). Vanadium Compounds as PTP Inhibitors. Molecules, 22(12), 2269.
161. Scior, T., Guevara-Garcia, J. A., Do, Q. T., Bernard, P., & Laufer, S. (2016). Why antidiabetic vanadium complexes are not in the pipeline of "Big Pharma" drug research? A critical review. Current Medicinal Chemistry, 23(27), 2874-2891. doi:10.2174/0929867323666160510151937
162. Thompson, K. H., Lichter, J., LeBel, C., Scaife, M. C., McNeill, J. H., & Orvig, C. (2009). Vanadium treatment of type 2 diabetes: A view to the future. Journal of Inorganic Biochemistry, 103(4), 554-558. doi:10.1016/j.jinorgbio.2008.12.003
163. Petanidis, S., Kioseoglou, E., Domvri, K., Zarogoulidis, P., Carthy, J. M., Anestakis, D., & Salifoglou, A. (2016). In vitro and ex vivo vanadium antitumor activity in (TGF-B)-induced EMT. Synergistic activity with carboplatin and correlation with tumor metastasis in cancer patients. International Journal of Biochemistry and Cell Biology, 74, 121-134. doi:10.1016/j.biocel.2016.02.015
164. Rozzo, C., Sanna, D., Garribba, E., Serra, M., Cantara, A., Palmieri, G., & Pisano, M. (2017). Antitumoral effect of vanadium compounds in malignant melanoma cell lines. Journal of Inorganic Biochemistry, 174(May), 14-24. doi:10.1016/j.jinorgbio.2017.05.010
165. Leon, I. E., Butenko, N., Di Virgilio, A. L., Muglia, C. I., Baran, E. J., Cavaco, I., & Etcheverry, S. B. (2014). Vanadium and cancer treatment: Antitumoral mechanisms of three oxidovanadium(IV) complexes on a human osteosarcoma cell line. Journal of Inorganic Biochemistry, 134, 106-117.
166. Gamero, A. M., & Larner, A. C. (2001). Vanadate Facilitates Interferon ,âà√≠¬¨±-mediated Apoptosis That Is Dependent on the Jak/Stat Pathway. Journal of Biological Chemistry, 276(17), 13547-13553. doi:10.1074/jbc.M007948200
167. Huang, C., Zhang, Z., Ding, M., Li, J., Ye, J., Leonard, S. S., & Shi, X. (2000). Vanadate induces p53 transactivation through hydrogen peroxide and causes apoptosis. Journal of Biological Chemistry, 275(42), 32516-32522. doi:10.1074/jbc.M005366200

168. Kioseoglou, E., Petanidis, S., Gabriel, C., & Salifoglou, A. (2015). The chemistry and biology of vanadium compounds in cancer therapeutics. Coordination Chemistry Reviews, 301-302, 87-105. doi:10.1016/j.ccr.2015.03.010
169. Tsave, O., Petanidis, S., Kioseoglou, E., Yavropoulou, M. P., Yovos, J. G., Anestakis, D., & Salifoglou, A. (2016). Role of vanadium in cellular and molecular immunology: Association with immune-related inflammation and pharmacotoxicology mechanisms. Oxidative Medicine and Cellular Longevity, 2016, 1-10. doi:10.1155/2016/4013639
170. O'Shea, J. J., McVicar, D. W., Bailey, T. L., Burns, C., & Smyth, M. J. (1992). Activation of human peripheral blood T lymphocytes by pharmacological induction of protein-tyrosine phosphorylation. Proceedings of the National Academy of Sciences, 89(21), 10306-10310. doi:10.1073/pnas.89.21.10306
171. Shen, X., Lee, K., & Ko, R. (2001). Effects of heavy metal ions on resting and antigen-activated-CD4+ T cells. Toxicology, 169, 67-80.
172. Cui, W., Cui, H., Peng, X., Fang, J., Zuo, Z., Liu, X., & Wu, B. (2011). Excess dietary vanadium induces changes in subsets and proliferation of splenic T cells in broilers. Biological Trace Element Research, 143(2), 932-938. doi:10.1007/s12011-010-8890-z
173. Dinarello, C. A. (2000). Proinflammatory cytokines. Chest, 118(1), 503-508. doi:10.1378/chest.118.1.503
174. Medzhitov, R. (2008). Origin and physiological roles of inflammation. Nature, 454(7203), 428-435. doi:10.1038/nature07201
175. Hu, X., & Ivashkiv, L. B. (2009). Cross-regulation of signaling pathways by interferon-gamma: Implications for immune responses and autoimmune diseases. Immunity, 31(4), 539-550. doi:10.1016/j.immuni.2009.09.002
176. Schroder, K., Hertzog, P. J., Ravasi, T., & Hume, D. A. (2004). Interferon-gamma: An overview of signals, mechanisms, and functions. Journal of Leukocyte Biology, 75(2), 163-189. doi:10.1189/jlb.0603252
177. Billiau, A., & Matthys, P. (2009). Interferon-gamma: A historical perspective. Cytokine & Growth Factor Reviews, 20(2), 97-113. doi:10.1016/j.cytogfr.2009.01.009
178. Tracey, K. J. (2002). The inflammatory reflex. Nature, 420(6917), 853-859. doi:10.1038/nature01321
179. Ouyang, W., Rutz, S., Crellin, N. K., Valdez, P. A., & Hymowitz, S. G. (2011). Regulation and functions of the IL-10 family of cytokines in inflammation and disease. Annual Review of Immunology, 29, 71-109. doi:10.1146/annurev-immunol-031210-101312
180. Moore, K. W., de Waal Malefyt, R., Coffman, R. L., & O'Garra, A. (2001). Interleukin-10 and the interleukin-10 receptor. Annual Review of Immunology, 19, 683-765. doi:10.1146/annurev.immunol.19.1.683
181. Atkins, M. B., Lotze, M. T., Dutcher, J. P., Fisher, R. I., Weiss, G., Margolin, K., ... & Mier, J. (1999). High-dose recombinant interleukin 2 therapy for patients with metastatic melanoma: Analysis of 270 patients treated between 1985 and 1993. Journal of Clinical Oncology, 17(5), 2105-2116.
182. Sadoff, J. C., Jaffe, H. A., Sannella, E. C., et al. (1995). Safety and immunogenicity of recombinant bacille Calmette-Gu,àö¬©rin vaccines for human immunodeficiency virus type 1 and Mycobacterium tuberculosis. Journal of Infectious Diseases, 171(3), 641-644.

183. Conlon, K. C., Miljkovic, M. D., & Waldmann, T. A. (2019). Cytokines in the treatment of cancer. Journal of Interferon & Cytokine Research, 39(1), 6-21. doi:10.1089/jir.2018.0019
184. Berraondo, P., Sanmamed, M. F., Ochoa, M. C., & Melero, I. (2019). Cytokines in clinical cancer immunotherapy. British Journal of Cancer, 120(1), 6-15. doi:10.1038/s41416-018-0328-y
185. Pearl, T. M., Markert, J. M., Cassady, K. A., & Ghonime, M. G. (2019). Oncolytic virus-based cytokine expression to improve immune activity in brain and solid tumors. Molecular Therapy Oncolytics, 13, 14-21. doi:10.1016/j.omto.2019.03.001
186. de Graaf, J. F., de Vor, L., Fouchier, R. A. M., & van den Hoogen, B. G. (2018). Armed oncolytic viruses: A kick-start for anti-tumor immunity. Cytokine & Growth Factor Reviews, 41, 28-39. doi:10.1016/j.cytogfr.2018.03.006
187. Andtbacka, R. H. I. (2015). Talimogene laherparepvec improves durable response rate in patients with advanced melanoma. Journal of Clinical Oncology, 33(25), 2780-2788.
188. Gubler, U., Chua, A. O., Schoenhaut, D. S., Dwyer, C. M., McComas, W., Motyka, R., ... & Gray, P. W. (1991). Coexpression of two distinct genes is required to generate secreted bioactive cytotoxic lymphocyte maturation factor. Proceedings of the National Academy of Sciences, 88(10), 4143-4147.
189. Kobayashi, M., Fitz, L., Ryan, M., Hewick, R. M., Clark, S. C., Chan, S., ... & Cerretti, D. P. (1989). Identification and purification of natural killer cell stimulatory factor (NKSF), a cytokine with multiple biologic effects on human lymphocytes. Journal of Experimental Medicine, 170(3), 827-845.
190. Wolf, S. F., Temple, P. A., Kobayashi, M., Young, D., Dicig, M., Lowe, L., ... & Gillis, S. (1991). Cloning of cDNA for natural killer cell stimulatory factor, a heterodimeric cytokine with multiple biologic effects on T and natural killer cells. Journal of Immunology, 146(10), 3074-3081.
191. Schoenhaut DS, Chua AO, Wolitzky AG, Quinn PM, Dwyer CM, McComas W, et al. (1992). Cloning and expression of murine IL-12. Journal of Immunology, 148(11), 3433-3440.
192. Trinchieri, G. (2003). Interleukin-12 and the regulation of innate resistance and adaptive immunity. Nature Reviews Immunology, 3, 133-146. doi:10.1038/nri1001
193. Lasek, W., Zago,âà¬∫d,âà¬∫on, R., & Jakobisiak, M. (2014). Interleukin 12: Still a promising candidate for tumor immunotherapy?. Cancer Immunology, Immunotherapy, 63(5), 419-435. doi:10.1007/s00262-014-1523-1
194. Pistoia, V., Cocco, C., & Airoldi, I. (2009). Interleukin-12 receptor ≈í,â§2: From cytokine receptor to gatekeeper gene in human B-cell malignancies. Journal of Clinical Oncology, 27(28), 4809-4816. doi:10.1200/JCO.2008.21.3579
195. Gately, M. K., Renzetti, L. M., Magram, J., Stern, A. S., Adorini, L., Gubler, U., & Presky, D. H. (1998). The interleukin-12/interleukin-12-receptor system: Role in normal and pathologic immune responses. Annual Review of Immunology, 16, 495-521. doi:10.1146/annurev.immunol.16.1.495
196. Germann, T., Gately, M. K., Schoenhaut, D. S., Lohoff, M., Mattner, F., Fischer, S., & Presky, D. H. (1993). Interleukin-12/T cell stimulating factor, a cytokine with multiple effects on T helper type 1 (Th1) but not on Th2 cells. European Journal of Immunology, 23(7), 1762-1770.

197. Bacon, C. M., McVicar, D. W., Ortaldo, J. R., Rees, R. C., O'Shea, J. J., & Johnston, J. A. (1995). Interleukin 12 (IL-12) induces tyrosine phosphorylation of JAK2 and TYK2: Differential use of Janus family tyrosine kinases by IL-2 and IL-12. Journal of Experimental Medicine, 181(2), 399-404.
198. Bacon, C. M., Petricoin III, E. F., Ortaldo, J. R., Rees, R. C., Larner, A. C., Johnston, J. A., ... & O'Shea, J. J. (1995). Interleukin 12 induces tyrosine phosphorylation and activation of STAT4 in human lymphocytes. Proceedings of the National Academy of Sciences USA, 92(16), 7307-7311.
199. Trinchieri, G. (1995). Interleukin-12: A proinflammatory cytokine with immunoregulatory functions that bridge innate resistance and antigen-specific adaptive immunity. Annual Review of Immunology, 13, 251-276. doi:10.1146/annurev.iy.13.040195.001343
200. Briukhovetska, D., D‚àö‚àÇrr, J., Endres, S., Libby, P., Dinarello, C. A., & Libby, P. (2021). Interleukins in cancer: From biology to therapy. *Nature Reviews Cancer, 1-19. doi:10.1038/s41568-021-00363-z
201. Watkins, S. K., Egilmez, N. K., Suttles, J., & Stout, R. D. (2007). IL-12 rapidly alters the functional profile of tumor-associated and tumor-infiltrating macrophages in vitro and in vivo. Journal of Immunology, 178(3), 1357-1362. doi:10.4049/jimmunol.178.3.1357
202. Steding, C. E., Wu, S. T., Zhang, Y., Jeng, M. H., Elzey, B. D., & Kao, C. (2011). The role of interleukin-12 on modulating myeloid-derived suppressor cells, increasing overall survival and reducing metastasis. Immunology, 133(2), 221-238. doi:10.1111/j.1365-2567.2011.03429.x
203. Bashyam, H. (2007). Interleukin-12: A master regulator. Journal of Experimental Medicine, 204(10), 969. doi:10.1084/jem.2045fta
204. Smith, S. G., Baltz, J. L., Koppolu, B. P., Ravindranathan, S., Nguyen, K., & Zaharoff, D. A. (2017). Immunological mechanisms of intravesical chitosan/interleukin-12 immunotherapy against murine bladder cancer. OncoImmunology, 6(12), e1259050. doi:10.1080/2162402X.2016.1259050
205. Zhao, J., Zhao, J., & Perlman, S. (2012). Differential effects of IL-12 on Tregs and non-Treg T cells: Roles of IFN-‚àí,â•, IL-2, and IL-2R. PLOS ONE, 7(9), e46241. doi:10.1371/journal.pone.0046241
206. Kerkar, S. P., Goldszmid, R. S., Muranski, P., Chinnasamy, D., Yu, Z., Reger, R. N., ... & Rosenberg, S. A. (2011). IL-12 triggers a programmatic change in dysfunctional myeloid-derived cells within mouse tumors. Journal of Clinical Investigation, 121(12), 4746-4757. doi:10.1172/JCI58814
207. Trinchieri, G. (2003). Interleukin-12 and the regulation of innate resistance and adaptive immunity. Nature Reviews Immunology, 3, 133-146. doi:10.1038/nri1001
208. Buszello, H. (1995). Antiproliferative effects of four different cytokines on renal carcinoma cell lines. Anticancer Research, 15(4), 735-738.
209. Wall, L., Burke, F., Barton, C., Smyth, J., & Balkwill, F. (2003). IFN-‚àí,â• induces apoptosis in ovarian cancer cells in vivo and in vitro. Clinical Cancer Research, 9(7), 2487-2496.
210. Voest, E. E., Kenyon, B. M., O'Reilly, M. S., Truitt, G., D'Amato, R. J., & Folkman, J. (1995). Inhibition of angiogenesis in vivo by interleukin 12. Journal of the National Cancer Institute, 87(8), 581-586. doi:10.1093/jnci/87.8.581

211. Saiki, I., Sato, K., Yoo, Y. C., Murata, J., Yoneda, J., Kiso, M., ... & Azuma, I. (1992). Inhibition of tumor-induced angiogenesis by the administration of recombinant interferon-gamma followed by a synthetic lipid-A subunit analogue (GLA-60). International Journal of Cancer, 51(4), 641-645. doi:10.1002/ijc.2910510422
212. Boehm, U., Klamp, T., Groot, M., & Howard, J. C. (1997). Cellular responses to interferon-gamma. Annual Review of Immunology, 15, 749-795. doi:10.1146/annurev.immunol.15.1.749
213. Lasek, W., Zago,âà¬∫d,âà¬∫on, R., & Jakobisiak, M. (2014). Interleukin 12: Still a promising candidate for tumor immunotherapy?. Cancer Immunology, Immunotherapy, 63(5), 419-435. doi:10.1007/s00262-014-1523-1
214. Weiss, J. M., Subleski, J. J., Wigginton, J. M., & Wiltrout, R. H. (2007). Immunotherapy of cancer by IL-12-based cytokine combinations. Expert Opinion on Biological Therapy, 7(11), 1705-1721. doi:10.1517/14712598.7.11.1705
215. Colombo, M. P., & Trinchieri, G. (2002). Interleukin-12 in anti-tumor immunity and immunotherapy. Cytokine & Growth Factor Reviews, 13(2), 155-168. doi:10.1016/S1359-6101(01)00032-6
216. Zaharoff, D. A., Hance, K. W., Rogers, C. J., Schlom, J., & Greiner, J. W. (2010). Intratumoral immunotherapy of established solid tumors with chitosan/IL-12. Journal of Immunotherapy, 33(7), 697-705. doi:10.1097/CJI.0b013e3181eb826d
217. Noguchi, Y., Jungbluth, A., Richards, E. C., & Old, L. J. (1996). Effect of interleukin 12 on tumor induction by 3-methylcholanthrene. Proceedings of the National Academy of Sciences USA, 93(21), 11798-11801. doi:10.1073/pnas.93.21.11798
218. Vizler, C., Rosato, A., Calderazzo, F., Quintieri, L., Fruscella, P., Wainstok de Calmanovici, R., ... & Romani, L. (1998). Therapeutic effect of interleukin 12 on mouse haemangiosarcomas is not associated with an increased anti-tumour cytotoxic T-lymphocyte activity. British Journal of Cancer, 77(4), 656-662. doi:10.1038/bjc.1998.105
219. Smyth, M. J., Taniguchi, M., & Street, S. E. (2000). The anti-tumor activity of IL-12: Mechanisms of innate immunity that are model and dose dependent. Journal of Immunology, 165(5), 2665-2670. doi:10.4049/jimmunol.165.5.2665
220. Brunda, M. J., Luistro, L., Warrier, R. R., Wright, R. B., Hubbard, B. R., Murphy, M., ... & Stern, A. S. (1993). Antitumor and antimetastatic activity of interleukin 12 against murine tumors. Journal of Experimental Medicine, 178(4), 1223-1230. doi:10.1084/jem.178.4.1223
221. Pulaski BA, Clements VK, Pipeling MR, Ostrand-Rosenberg S. (2000). Immunotherapy with vaccines combining MHC class II/CD80+ tumor cells with interleukin-12 reduces established metastatic disease and stimulates immune effectors and monokine induced by interferon gamma. Cancer Immunology, Immunotherapy, 49(1), 34-45. doi:10.1007/s002620050024
222. Zapa,âà√áa ,âà√Ö, Wolny R, Wachowska M, Jak,àö,â•bisiak M, Lasek W. (2013). Synergistic antitumor effect of JAWSII dendritic cells and interleukin 12 in a melanoma mouse model. Oncology Reports, 29(3), 1208-1214. doi:10.3892/or.2012.2193
223. Atsumi T, Takehara T, Kanto T, Miyagi T, Kuzushita N et al. (2001). Administration of interleukin-12 enhances the therapeutic efficacy of dendritic cell-based tumor vaccines in mouse hepatocellular carcinoma. Cancer Research, 61(20), 7563-7567.

224. Car BD, Eng VM, Lipman JM, Anderson TD. (1999). The toxicology of interleukin-12: a review. Toxicologic Pathology, 27(1), 58-63. doi:10.1177/019262339902700112
225. Bortolanza S, Bunuales M, Otano I, Gonzalez-Aseguinolaza G, Ortiz-de-Solorzano C et al. (2009). Treatment of pancreatic cancer with an oncolytic adenovirus expressing interleukin-12 in Syrian hamsters. Molecular Therapy, 17(4), 614-622. doi:10.1038/mt.2009.9
226. Motzer RJ, Rakhit A, Schwartz LH, Olencki T, Malone TM et al. (1998). Phase I trial of subcutaneous recombinant human interleukin-12 in patients with advanced renal cell carcinoma. Clinical Cancer Research, 4(5), 1183-1191.
227. Leonard JP, Sherman ML, Fisher GL, Buchanan LJ, Larsen G, Atkins MB, et al. (1997). Effects of single-dose interleukin-12 exposure on interleukin-12-associated toxicity and interferon-gamma production. Blood, 90(7), 2541-2548.
228. Hurteau JA, Blessing JA, DeCesare SL, Creasman WT. (2001). Evaluation of recombinant human interleukin-12 in patients with recurrent or refractory ovarian cancer: a gynecologic oncology group study. Gynecologic Oncology, 82(1), 7-10. doi:10.1006/gyno.2001.6255
229. Motzer RJ, Rakhit A, Thompson JA, Nemunaitis J, Murphy BA, Ellerhorst J, et al. (2001). Randomized multicenter phase II trial of subcutaneous recombinant human interleukin-12 versus interferon-alpha 2a for patients with advanced renal cell carcinoma. Journal of Interferon & Cytokine Research, 21(4), 257-263. doi:10.1089/107999001750169934
230. Mills BN, Connolly KA, Ye J, Murphy JD, Uccello TP et al. (2019). Stereotactic body radiation and interleukin-12 combination therapy eradicates pancreatic tumors by repolarizing the immune microenvironment. Cell Reports, 29(2), 406-421. doi:10.1016/j.celrep.2019.08.095
231. Deplanque G, Shabafrouz K, Obeid M. (2017). Can local radiotherapy and IL-12 synergize to overcome the immunosuppressive tumor microenvironment and allow "in situ tumor vaccination"? Cancer Immunology, Immunotherapy, 66(7), 833-840. doi:10.1007/s00262-017-2000-4
232. Wu CJ, Tsai YT, Lee IJ, Wu PY, Lu LS et al. (2018). Combination of radiation and interleukin 12 eradicates large orthotopic hepatocellular carcinoma through immunomodulation of tumor microenvironment. OncoImmunology, 7(10), e1488562. doi:10.1080/2162402X.2018.1488562
233. Marabelle A, Kohrt H, Caux C, Levy R. (2014). Intratumoral immunization: a new paradigm for cancer therapy. Clinical Cancer Research, 20(7), 1747-1756. doi:10.1158/1078-0432.CCR-13-2116
234. Baniel CC, Heinze CM, Hoefges A, Sumiec EG, Hank JA et al. (2020). In situ vaccine plus checkpoint blockade induces memory humoral response. Frontiers in Immunology, 11, 1610. doi:10.3389/fimmu.2020.01610
235. Sagiv-Barfi I, Czerwinski DK, Levy S, Alam IS, Mayer AT et al. (2018). Eradication of spontaneous malignancy by local immunotherapy. Science Translational Medicine, 10(426), eaan4488. doi:10.1126/scitranslmed.aan4488
236. Sondel PM, Gillies SD. (2012). Current and potential uses of immunocytokines as cancer immunotherapy. Antibodies, 1(2), 149-171. doi:10.3390/antib1020149
237. Puca E, Probst P, Stringhini M, Murer P, Pellegrini G et al. (2020). The antibody-based delivery of interleukin-12 to solid tumors boosts NK and CD8+ T cell activity

and synergizes with immune checkpoint inhibitors. International Journal of Cancer, 146(9), 2518-2530. doi:10.1002/ijc.32603
238. Halin C, Rondini S, Nilsson F, Berndt A, Kosmehl H et al. (2002). Enhancement of the antitumor activity of interleukin-12 by targeted delivery to neovasculature. Nature Biotechnology, 20(3), 264-269. doi:10.1038/nbt0302-264
239. Egilmez NK, Jong YS, Sabel MS, Jacob JS, Mathiowitz E et al. (2000). In situ tumor vaccination with interleukin-12-encapsulated biodegradable microspheres: induction of tumor regression and potent antitumor immunity. Cancer Research, 60(14), 3832-3837.
240. Zaharoff DA, Hance KW, Rogers CJ, Schlom J, Greiner J. (2010). Intratumoral immunotherapy of established solid tumors with chitosan/IL-12. Journal of Immunotherapy, 33(7), 697-705. doi:10.1097/CJI.0b013e3181eb826d
241. Kim KJ, Moon D, Kong SJ, Lee YS, Yoo Y et al. (2021). Antitumor effects of IL-12 and GM-CSF co-expressed in an engineered oncolytic HSV-1. Gene Therapy, 28(3-4), 186-198. doi:10.1038/s41434-020-00205-x
242. Nakao S, Arai Y, Tasaki M, Yamashita M, Murakami R et al. (2020). Intratumoral expression of IL-7 and IL-12 using an oncolytic virus increases systemic sensitivity to immune checkpoint blockade. Science Translational Medicine, 12(569), eaax7992. doi:10.1126/scitranslmed.aax7992
243. Lemay CG, Rintoul JL, Kus A, Paterson JM, Garcia V, Falls TJ, Auer RC. (2012). Harnessing oncolytic virus-mediated antitumor immunity in an infected cell vaccine. Molecular Therapy, 20(9), 1791-1799.
244. Thomas ED, Meza-Perez S, Bevis KS, Randall TD, Gillespie GY, Langford C, Alvarez RD. (2016). IL-12 expressing oncolytic herpes simplex virus promotes anti-tumor activity and immunologic control of metastatic ovarian cancer in mice. Journal of Ovarian Research, 9(1), 1-11.
245. Alkayyal AA, Mahmoud AB, Auer RC. (2016). Interleukin-12-expressing oncolytic virus: A promising strategy for cancer immunotherapy. Journal of Taibah University Medical Sciences, 11(3), 187-193.
246. Addison CL, Bramson JL, Hitt MM, Muller WJ, Gauldie J, Graham FL. (1998). Intratumoral coinjection of adenoviral vectors expressing IL-2 and IL-12 results in enhanced frequency of regression of injected and untreated distal tumors. Gene Therapy, 5(10), 1400-1409.
247. Huang JH, Zhang SN, Choi KJ, Choi IK, Kim JH, Lee MG, Kim H, Yun CO. (2010). Therapeutic and tumor-specific immunity induced by combination of dendritic cells and oncolytic adenovirus expressing IL-12 and 4-1BBL. Molecular Therapy, 18(2), 264-274.
248. Nasu Y, Bangma CH, Hull GW, Lee HM, Hu J, Wang J, McCurdy MA, Shimura S, Yang G, Timme TL et al. (1999). Adenovirus-mediated interleukin-12 gene therapy for prostate cancer: suppression of orthotopic tumor growth and pre-established lung metastases in an orthotopic model. Gene Therapy, 6(3), 338-349.
249. Ren G, Tian G, Liu Y, He J, Gao X, Yu Y, Liu X, Zhang X, Sun T, Liu S et al. (2015). Recombinant Newcastle Disease Virus Encoding IL-12 and/or IL-2 as Potential Candidate for Hepatoma Carcinoma Therapy. Technology in Cancer Research & Treatment, 14(5), 477-487.

250. Rodriguez-Madoz JR, Prieto J, Smerdou C. (2005). Semliki forest virus vectors engineered to express higher IL-12 levels induce efficient elimination of murine colon adenocarcinomas. Molecular Therapy, 12(1), 153-163.
251. Shin EJ, Wanna GB, Choi B, Aguila D 3rd, Ebert O, Genden EM, Woo SL. (2007). Interleukin-12 expression enhances vesicular stomatitis virus oncolytic therapy in murine squamous cell carcinoma. The Laryngoscope, 117(2), 210-214.
252. Cheema TA, Wakimoto H, Fecci PE, Ning J, Kuroda T, Jeyaretna DS, Martuza RL, Rabkin SD. (2013). Multifaceted oncolytic virus therapy for glioblastoma in an immunocompetent cancer stem cell model. Proceedings of the National Academy of Sciences of the United States of America, 110(29), 12006-12011.
253. Wong RJ, Chan MK, Yu Z, Ghossein RA, Ngai I, Adusumilli PS, Stiles BM, Shah JP, Singh B, Fong Y. (2004). Angiogenesis inhibition by an oncolytic herpes virus expressing interleukin 12. Clinical Cancer Research, 10(13), 4509-4516.
254. Bauer DF et al. (2016). Effect of HSV-IL12 Loaded Tumor Cell-Based Vaccination in a Mouse Model of High-Grade Neuroblastoma. *Journal of Immunology Research, 1-10.
255. Lasek W, Zago,âà¬∫d,âà¬∫on R, Jakobisiak M. (2014). Interleukin 12: still a promising candidate for tumor immunotherapy? Cancer Immunology, Immunotherapy, 63, 419-435.
256. Genetically Engineered HSV-1 Phase 1 Study for the Treatment of Recurrent Malignant Glioma - Full Text View - ClinicalTrials.gov. Available at: https://clinicaltrials.gov/ct2/show/NCT02062827?term=Interleukin-12&cond=HSV&rank=1. Accessed: June 3, 2018.
257. Safety Study of Adenovirus Vector Engineered to Express hIL-12 in Combination With Activator Ligand to Treat Melanoma - Full Text View - ClinicalTrials.gov. Available at: https://clinicaltrials.gov/ct2/show/NCT01397708. Accessed: June 3, 2018.
258. Franciszkiewicz K, Boissonnas A, Boutet M, Combadiere C, Mami-Chouaib F. (2012). Role of chemokines and chemokine receptors in shaping the effector phase of the antitumor immune response. Cancer Research, 72, 6325-6332. doi:10.1146/annurev-immunol-032713-120145
259. Garris CS, Arlauckas SP, Kohler RH, Trefny MP, Garren S, Piot C, Engblom C, Pfirschke C, Siwicki M, Gungabeesoon J, et al. (2018). Successful anti-PD-1 cancer immunotherapy requires T cell-dendritic cell crosstalk involving the cytokines IFN-≈í,â• and IL-12. Immunity, 49(6), 1148-1161.e7. doi:10.1016/j.immuni.2018.09.024
260. Legler, D.F., Thelen, M. (2018). New insights in chemokine signaling. F1000Research, 7, 95.
261. Griffith, J.W., Sokol, C.L., Luster, A.D. (2014). Chemokines and chemokine receptors: positioning cells for host defense and immunity. Annual Review of Immunology, 32, 659-702.
262. Hiroi, M., & Ohmori, Y. (2003). The transcriptional coactivator CREB-binding protein cooperates with STAT1 and NF-kappa B for synergistic transcriptional activation of the CXC ligand 9/monokine induced by interferon-gamma gene. Journal of Biological Chemistry, 278(1), 651-660.
263. Mukaida N, Sasaki S, Baba T. (2014). Chemokines in cancer development and progression and their potential as targeting molecules for cancer treatment. Mediators of Inflammation, 2014, 170381.

264. Balkwill F. (2004). Cancer and the chemokine network. Nature Reviews Cancer, 4, 540-550.
265. Nagarsheth N, Wicha MS, Zou W. (2017). Chemokines in the cancer microenvironment and their relevance in cancer immunotherapy. Nature Reviews Immunology, 17, 559-572.
266. Solari, R., Pease, J.E., Begg, M. (2015). Chemokine receptors as therapeutic targets: Why aren't there more drugs? European Journal of Pharmacology, 746, 363-367.
267. Holst, P.J., Lu√É√†ttichau, H.R., Schwartz, T.W., Rosenkilde, M.M. (2003). Virally encoded chemokines and chemokine receptors in the role of viral infections. Contributions to Microbiology, 10, 232-252.
268. Lu√É√†ttichau, H.R. (2010). The cytomegalovirus UL146 gene product vCXCL1 targets both CXCR1 and CXCR2 as an agonist. Journal of Biological Chemistry, 285(12), 9137-9146.
269. Wu, L., Huang, T.G., Meseck, M., Altomonte, J., Ebert, O., Shinozaki, K., Garc‚àö‚â†¬¨®a-Sastre, A., Fallon, J., Mandeli, J., Woo, S.L. (2008). rVSV(M,Äö√†√ú51)-M3 is an effective and safe oncolytic virus for cancer therapy. Human Gene Therapy, 19(6), 635-647.
270. Altomonte, J., Wu, L., Chen, L., Meseck, M., Ebert, O., Garc‚àö‚â†¬¨®a-Sastre, A., Fallon, J., Woo, S.L. (2008). Exponential enhancement of oncolytic vesicular stomatitis virus potency by vector-mediated suppression of inflammatory responses in vivo. Molecular Therapy, 16(1), 146-153.
271. Li J, O'Malley M, Urban J, Sampath P, Guo ZS, Kalinski P, Thorne SH, Bartlett DL. (2011). Chemokine expression from oncolytic vaccinia virus enhances vaccine therapies of cancer. Molecular Therapy, 19(4), 650-657.
272. Lapteva N, Aldrich M, Weksberg D, Rollins L, Goltsova T, Chen S, Huang X. (2014). Targeting the Intratumoral Dendritic Cells by the Oncolytic Adenoviral Vaccine Expressing RANTES Elicits Potent Antitumor Immunity. Journal of Immunotherapy, 32(2), 145-156.
273. Li J, O'Malley M, Sampath P, Kalinski P, Bartlett DL, Thorne SH. (2012). Expression of CCL19 from oncolytic vaccinia enhances immunotherapeutic potential while maintaining oncolytic activity. Neoplasia, 14(12), 1115-1121.
274. Francis L, Guo ZS, Liu Z, Ravindranathan R, Urban JA, Sathaiah M, Magge D, Kalinski P, Bartlett DL. (2016). Modulation of chemokines in the tumor microenvironment enhances oncolytic virotherapy for colorectal cancer. Oncotarget, 7(16), 22174-22185.
275. Liu Z, Ravindranathan R, Li J, Kalinski P, Guo ZS, Bartlett DL. (2016). CXCL11-Armed oncolytic poxvirus elicits potent antitumor immunity and shows enhanced therapeutic efficacy. OncoImmunology, 5(3), e1091554.
276. Farber JM. (1997). Mig and IP-10: CXC chemokines that target lymphocytes. Journal of Leukocyte Biology, 61(3), 246-257.
277. Ohmori Y, Schreiber RD, Hamilton TA. (1997). Synergy between interferon-gamma and tumor necrosis factor-alpha in transcriptional activation is mediated by cooperation between signal transducer and activator of transcription 1 and nuclear factor kappaB. Journal of Biological Chemistry, 272(23), 14899-14907.
278. Billottet C, Quemener C, Bikfalvi A. (2013). CXCR3, a double-edged sword in tumor progression and angiogenesis. Biochimica et Biophysica Acta, 1836(2), 287-295.

279. Muehlinghaus G, Cigliano L, Huehn S, Peddinghaus A, Leyendeckers H, Hauser AE, et al. (2005). Regulation of CXCR3 and CXCR4 expression during terminal differentiation of memory B cells into plasma cells. Blood, 105(9), 3965-3971.
280. Nakajima C, Mukai T, Yamaguchi N, Morimoto Y, Park WR, Iwasaki M, et al. (2002). Induction of the chemokine receptor CXCR3 on TCR-stimulated T cells: dependence on the release from persistent TCR-triggering and requirement for IFN-gamma stimulation. European Journal of Immunology, 32(6), 1792-1801.
281. Kim CH, Rott L, Kunkel EJ, Genovese MC, Andrew DP, Wu LJ, et al. (2001). Rules of chemokine receptor association with T cell polarization in vivo. Journal of Clinical Investigation, 108, 1331-1339.
282. Schoenborn JR, Wilson CB. (2007). Regulation of interferon-gamma during innate and adaptive immune responses. Advances in Immunology, 96, 41-101.
283. Mosser DM, Edwards JP. (2008). Exploring the full spectrum of macrophage activation. Nature Reviews Immunology, 8, 958-969.
284. Schoenborn JR, Wilson CB. (2007). Regulation of interferon-gamma during innate and adaptive immune responses. Advances in Immunology, 96, 41-101.
285. Zhang R, Tian L, Chen LJ, Xiao F, Hou JM, Zhao X, et al. (2006). Combination of MIG (CXCL9) chemokine gene therapy with low-dose cisplatin improves therapeutic efficacy against murine carcinoma. Gene Therapy, 13(15), 1263-1271.
286. Specht K, Harbeck N, Smida J, Annecke K, Reich U, Naehrig J, et al. (2009). Expression profiling identifies genes that predict recurrence of breast cancer after adjuvant CMF-based chemotherapy. Breast Cancer Research and Treatment, 118(1), 45-56.
287. Bedognetti D, Spivey TL, Zhao Y, Uccellini L, Tomei S, Dudley ME, et al. (2013). CXCR3/CCR5 pathways in metastatic melanoma patients treated with adoptive therapy and interleukin-2. British Journal of Cancer, 109(8), 2412-2423.
288. Li S, Xia X, Mellieon FM, Liu J, Steele S. (2004). Candidate genes associated with tumor regression mediated by intratumoral IL-12 electroporation gene therapy. Molecular Therapy, 9(3), 347-354.
289. Gustafsson K, Junevik K, Werlenius O, Holmgren S, Karlsson-Parra A, Andersson PO. (2011). Tumour-loaded alpha-type 1-polarized dendritic cells from patients with chronic lymphocytic leukaemia produce a superior NK-, NKT- and CD8+ T cell-attracting chemokine profile. Scandinavian Journal of Immunology, 74(4), 318-326.
290. Reckamp KL, Figlin RA, Moldawer N, Pantuck AJ, Belldegrun AS, Burdick MD, et al. (2007). Expression of CXCR3 on mononuclear cells and CXCR3 ligands in patients with metastatic renal cell carcinoma in response to systemic IL-2 therapy. Journal of Immunotherapy, 30(4), 417-424.
291. Soong RS, Song L, Trieu J, Knoff J, He L, Tsai YC, et al. (2014). Toll-like receptor agonist imiquimod facilitates antigen-specific CD8+ T-cell accumulation in the genital tract leading to tumor control through IFN-gamma. Clinical Cancer Research, 20(21), 5456-5467.
292. Wu Z, Huang X, Han X, Li Z, Zhu Q, Yan J, et al. (2016). The chemokine CXCL9 expression is associated with better prognosis for colorectal carcinoma patients. Biomedicine & Pharmacotherapy, 78, 8-13.
293. Mlecnik B, Tosolini M, Charoentong P, Kirilovsky A, Bindea G, Berger A, et al. (2010). Biomolecular network reconstruction identifies T-cell homing factors associated with survival in colorectal cancer. Gastroenterology, 138(4), 1429-1440.

294. House IG, Savas P, Lai J, Chen AXY, Oliver AJ, Teo ZL, et al. (2020). Macrophage-Derived CXCL9 and CXCL10 Are Required for Antitumor Immune Responses Following Immune Checkpoint Blockade. Clinical Cancer Research, 26(2), 487-504.
295. Specht K, Harbeck N, Smida J, Annecke K, Reich U, Naehrig J, et al. (2009). Expression profiling identifies genes that predict recurrence of breast cancer after adjuvant CMF-based chemotherapy. Breast Cancer Research and Treatment, 118(1), 45-56.
296. Weng Y, Siciliano SJ, Waldburger KE, Sirotina-Meisher A, Staruch MJ, Daugherty BL, et al. (1998). Binding and functional properties of recombinant and endogenous CXCR3 chemokine receptors. Journal of Biological Chemistry, 273(33), 18288-18291.
297. Eckert EC, Nace RA, Tonne JM, Evgin L, Vile RG, Russell SJ. (2019). Generation of a Tumor-Specific Chemokine Gradient Using Oncolytic Vesicular Stomatitis Virus Encoding CXCL9. Molecular Therapy - Oncolytics, 16, 63-74.
298. Karin N, Wildbaum G. (2015). The role of chemokines in adjusting the balance between CD4+ effector T cell subsets and FOXp3-negative regulatory T cells. International Immunopharmacology, 28(2), 829-835.
299. Barreira da Silva R, Laird ME, Yatim N, Fiette L, Ingersoll MA, Albert ML. (2015). Dipeptidylpeptidase 4 inhibition enhances lymphocyte trafficking, improving both naturally occurring tumor immunity and immunotherapy. Nature Immunology, 16(8), 850-858.
300. Nishina S, Yamauchi A, Kawaguchi T, Kaku K, Goto M, Sasaki K, et al. (2018). Dipeptidyl Peptidase 4 Inhibitors Reduce Hepatocellular Carcinoma by Activating Lymphocyte Chemotaxis in Mice. Cellular and Molecular Gastroenterology and Hepatology, 7(1), 115-134.
301. Alkayyal AA, Tai LH, Kennedy MA, de Souza CT, Zhang J, Lefebvre C, et al. (2017). NK-cell recruitment is necessary for eradication of peritoneal carcinomatosis with an IL12-expressing Maraba virus cellular vaccine. Cancer Immunology Research, 5(3), 211-221.
302. De Graaf JF, De Vor L, Fouchier RAM, Van Den Hoogen BG. (2018). Armed oncolytic viruses: A kick-start for antitumor immunity. Cytokine and Growth Factor Reviews, 41, 28-39.
303. Yu J, Wei M, Becknell B, Trotta R, Liu S, Boyd Z, et al. (2006). Pro- and antiinflammatory cytokine signaling: reciprocal antagonism regulates interferon-gamma production by human natural killer cells. Immunity, 24(5), 575-590.
304. Thomas ED, Meza-Perez S, Bevis KS, Randall TD, Gillespie GY, Langford C, et al. (2016). IL-12 Expressing oncolytic herpes simplex virus promotes antitumor activity and immunologic control of metastatic ovarian cancer in mice. Journal of Ovarian Research, 9(1), 1-11.
305. Turner MD, Nedjai B, Hurst T, Pennington DJ. (2014). Cytokines and chemokines: At the crossroads of cell signalling and inflammatory disease. Biochimica et Biophysica Acta, 1843(11), 2563-2582.
306. Yang, F., Tan, J., Fang, Y., Chen, G., Zhang, Y., Hu, Q., Han, W., Liu, Y., Fu, B., Jing, Z., & Li, W. (2022). The Multiplicity of Infection of Recombinant Vaccinia Virus Expressing the T7 RNA Polymerase Determines the Rescue Efficiency of Vesicular Stomatitis Virus. Frontiers in microbiology, 13, 846426. https://doi.org/10.3389/fmicb.2022.846426

307. ≈öcibior, A., Pietrzyk, ≈Å., Plewa, Z., & Skiba, A. (2020). Vanadium: Risks and possible benefits in the light of a comprehensive overview of its pharmacotoxicological mechanisms and multi-applications with a summary of further research trends. Journal of Trace Elements in Medicine and Biology, 61, 126508.
308. Ding, Q., Lu, P., Xia, Y., Ding, S., Fan, Y., Li, X., & Liu, M. (2016). CXCL9: evidence and contradictions for its role in tumor progression. Cancer Medicine, 5(11), 3246-3259.
309. Wong B, Bergeron A, Alluqmani N, Maznyi G, Chen A, Arulanandam R, et al. (2022). Dependency of EGFR activation in vanadium-based sensitization to oncolytic virotherapy. Molecular Therapy - Oncolytics, 25, 146-159.
310. Guirnalda P. Wood L. Goenka R. Crespo J. Paterson Y. (2013). Interferon-≈í,â•-induced intratumoral expression of CXCL9 alters the local distribution of T cells following immunotherapy with Listeria monocytogenes. OncoImmunology, 2(3).
311. Schroder, K., Hertzog, P. J., Ravasi, T., & Hume, D. A. (2004). IFN Gamma. In Journal of Leukocyte Biology (Vol. 75).
312. Schoenborn, J. R., & Wilson, C. B. (2007). Regulation of interferon-gamma during innate and adaptive immune responses. Advances in Immunology, 96, 41-101.
313. Mosser, D. M., & Edwards, J. P. (2008). Exploring the full spectrum of macrophage activation. Nature Reviews Immunology, 8(12), 958-969.
314. Kistner L., Doll D., Holtorf A., Nitsche U., Janssen K. (2017). Interferon-inducible CXC-chemokines are crucial immune modulators and survival predictors in colorectal cancer. Oncotarget, 8, 89998-90012.
315. Kohli, K., Pillarisetty, V.G., & Kim, T.S. (2022). Key chemokines direct migration of immune cells in solid tumors. Cancer Gene Therapy, 29, 10-21.
316. Dangaj, D., Bruand, M., Grimm, A. J., Ronet, C., Barras, D., Duttagupta, P. A., ... & Coukos, G. (2019). Cooperation between Constitutive and Inducible Chemokines Enables T Cell Engraftment and Immune Attack in Solid Tumors. Cancer Cell, 35(6), 885-900.e10.
317. Jorgovanovic, D., Song, M., Wang, L., et al. (2020). Roles of IFN-≈í,â• in tumor progression and regression: a review. Biomarker Research, 8(1), 49.
318. Vlaykova, T., Talve, L., Hahka-Kemppinen, M., Hernberg, M., Muhonen, T., Collan, Y., ... Pyrh√∂nen, S. (2002). Immunohistochemically detectable bcl-2 expression in metastatic melanoma: association with survival and treatment response. Oncology, 62(3), 259-268. http://dx.doi.org/10.1159/000059574
319. Fisher, D. T., Chen, Q., Skitzki, J. J., Muhitch, J. B., Zhou, L., Appenheimer, M. M., ... Gollnick, S. O. (2011). IL-6 trans-signaling licenses mouse and human tumor microvascular gateways for trafficking of cytotoxic T cells. Journal of Clinical Investigation, 121(10), 3846-3859. http://dx.doi.org/10.1172/JCI44952
320. Kimura, A., Naka, T., & Kishimoto, T. (2007). IL-6-dependent and -independent pathways in the development of interleukin 17-producing T helper cells. Proceedings of the National Academy of Sciences of the United States of America, 104(29), 12099-12104. http://dx.doi.org/10.1073/pnas.0705268104
321. Lane, R. S., Femel, J., Breazeale, A. P., Loo, C. P., Thibault, G., Kaempf, A., ... & Lund, A. W. (2018). IFN-≈í,â•-activated dermal lymphatic vessels inhibit cytotoxic T cells in melanoma and inflamed skin. The Journal of Experimental Medicine, 215(12), 3057-3074.

322. Russell, L., Peng, K. W., Russell, S. J., & Diaz, R. M. (2019). Oncolytic Viruses: Priming Time for Cancer Immunotherapy. BioDrugs, 33(5), 485-501.
323. Pai, C. S., Huang, J. T., Lu, X., Simons, D. M., Park, C., Chang, A., ... & Fong, L. (2019). Clonal Deletion of Tumor-Specific T Cells by Interferon-≈í,â• Confers Therapeutic Resistance to Combination Immune Checkpoint Blockade. Immunity, 50(2), 477-492.e8.
324. Bramson JL, Hitt M, Addison CL, Muller WJ, Gauldie J, Graham FL. (1996). Direct intratumoral injection of an adenovirus expressing interleukin-12 induces regression and long-lasting immunity that is associated with highly localized expression of interleukin-12. Human Gene Therapy, 7(16), 1995-2002.
325. Osada T, Berglund P, Morse MA, Hubby B, Lewis W, Niedzwiecki D, et al. (2012). Co-delivery of antigen and IL-12 by Venezuelan equine encephalitis virus replicon particles enhances antigen-specific immune responses and antitumor effects. Cancer Immunology, Immunotherapy, 61(12), 1941-1951.
326. Lyerly HK, Osada T, Hartman ZC. (2019). Right time and place for IL12: targeted delivery stimulates immune therapy. Clinical Cancer Research, 25(1), 9-11.
327. Tugues S, Burkhard SH, Ohs I, Vrohlings M, Nussbaum K, Vom Berg J, ... & Becher B. (2015). New insights into IL-12-mediated tumor suppression. Cell Death & Differentiation, 22(2), 237-246.
328. Poutou J., Bunuales M., Gonzalez-Aparicio M., Garcia-Aragoncillo E., Quetglas J.I., Casado R., Bravo-Perez C., Alzuguren P., Hernandez-Alcoceba R. (2015). Safety and antitumor effect of oncolytic and helper-dependent adenoviruses expressing interleukin-12 variants in a hamster pancreatic cancer model. Gene Therapy, 22(9), 696-706.
329. Saha D., Martuza R.L., Rabkin S.D. (2017). Macrophage Polarization Contributes to Glioblastoma Eradication by Combination Immunovirotherapy and Immune Checkpoint Blockade. Cancer Cell, 32(2), 253-267.e255.
330. Veinalde R., Grossardt C., Hartmann L., Bourgeois-Daigneault M.C., Bell J.C., Jager D., von Kalle C., Ungerechts G., Engeland C.E. (2017). Oncolytic measles virus encoding interleukin-12 mediates potent antitumor effects through T cell activation. OncoImmunology, 6(3), e1285992.
331. Freytag S.O., Barton K.N., Zhang Y. (2013). Efficacy of oncolytic adenovirus expressing suicide genes and interleukin-12 in preclinical model of prostate cancer. Gene Therapy, 20(11), 1131-1139.
332. Choi I.K., Lee J.S., Zhang S.N., Park J., Sonn C.H., Lee K.M., Yun C.O. (2011). Oncolytic adenovirus co-expressing IL-12 and IL-18 improves tumor-specific immunity via differentiation of T cells expressing IL-12Rbeta2 or IL-18Ralpha. Gene Therapy, 18(9), 898-909.
333. El-Shemi A.G., Ashshi A.M., Na Y., Li Y., Basalamah M., Al-Allaf F.A., Oh E., Jung B.K., Yun C.O. (2016). Combined therapy with oncolytic adenoviruses encoding TRAIL and IL-12 genes markedly suppressed human hepatocellular carcinoma both in vitro and in an orthotopic transplanted mouse model. Journal of Experimental & Clinical Cancer Research, 35(1), 74.
334. Shin, E. J., Wanna, G. B., Choi, B., Aguila, D., 3rd, Ebert, O., Genden, E. M., & Woo, S. L. (2007). Interleukin-12 expression enhances vesicular stomatitis virus oncolytic therapy in murine squamous cell carcinoma. The Laryngoscope, 117(2), 210-214.

335. Sangro B, Melero I, Qian C, Prieto J. (2005). Gene therapy of cancer based on interleukin 12. Current Gene Therapy, 5(6), 573-581.
336. Vo JL, Yang L, Kurtz SL, Smith SG, Koppolu BP, Ravindranathan S, et al. (2014). Neoadjuvant immunotherapy with chitosan and interleukin-12 to control breast cancer metastasis. OncoImmunology, 3(9), e968001.
337. Smith SG, Koppolu BP, Ravindranathan S, Kurtz SL, Yang L, Katz MD, et al. (2015). Intravesical chitosan/interleukin-12 immunotherapy induces tumor-specific systemic immunity against murine bladder cancer. Cancer Immunology, Immunotherapy, 64(6), 689-696.
338. Gately MK, et al. (1998). The interleukin-12/interleukin-12 receptor system: role in normal and pathologic immune responses. Annual Review of Immunology, 16, 495-521.
339. Tugues, S. et al. (2015). New insights into IL-12-mediated tumor suppression. Cell Death & Differentiation, 22(2), 237-246.
340. Buszello H. (1995). Antiproliferative effects of four different cytokines on renal carcinoma cell lines. Anticancer Research, 15(3), 735-738.
341. Wall, L., Burke, F., Barton, C., Smyth, J., & Balkwill, F. (2003). IFN-gamma induces apoptosis in ovarian cancer cells in vivo and in vitro. Clinical Cancer Research, 9(7), 2487-2496.
342. Garris, C. S. et al. (2018). Successful Anti-PD-1 Cancer Immunotherapy Requires T Cell-Dendritic Cell Crosstalk Involving the Cytokines IFN-≈í,â• and IL-12. *Immunity, doi:10.1016/j.immuni.2018.09.024.
343. Ruffell, B. et al. (2014). Macrophage IL-10 Blocks CD8+ T Cell-Dependent Responses to Chemotherapy by Suppressing IL-12 Expression in Intratumoral Dendritic Cells. Cancer Cell, 26, 623-637.
344. Pearce EL, Shen H. (2007). Generation of CD8 T Cell Memory Is Regulated by IL-12. Journal of Immunology, 179(4), 2074-2081.
345. Ye Z, Xu S, Moyana T, Yang J, Xiang J. (2008). Defect of CD8+ Memory T Cells Developed in Absence of IL-12 Priming for Secondary Expansion. Cellular and Molecular Immunology, 5(2), 147-152.
346. Chowdhury FZ, Ramos HJ, Davis LS, Forman J, Farrar JD. (2011). IL-12 selectively programs effector pathways that are stably expressed in human CD8+ effector memory T cells in vivo. Blood, 118(14), 3890-3900.
347. Leleux JA, Albershardt TC, Reeves R, James R, Krull J, Parsons AJ, et al. (2021). Intratumoral expression of IL-12 from lentiviral or RNA vectors acts synergistically with TLR4 agonist (GLA) to generate anti-tumor immunological memory. PLOS ONE, 16(12), e0259301.
348. Yue, T., Zheng, X., Dou, Y., (2016). Interleukin 12 shows a better curative effect on lung cancer than paclitaxel and cisplatin doublet chemotherapy. BMC Cancer, 16, 665.
349. Se-Ho Park, Tim Kyin, Albert Bendelac, Claude Carnaud; (2003). The Contribution of NKT Cells, NK Cells, and Other ,âà√≠,Äö√¢o-Chain-Dependent Non-T Non-B Cells to IL-12-Mediated Rejection of Tumors. Journal of Immunology, 170(3), 1197-1201.
350. Sato, Y., Fu, Y., Liu, H. et al. Tumor-immune profiling of CT-26 and Colon 26 syngeneic mouse models reveals mechanism of anti-PD-1 response. BMC Cancer 21, 1222 (2021). https://doi.org/10.1186/s12885-021-08974-3

351. Ciardiello, D., Vitiello, P. P., Cardone, C., Martini, G., Troiani, T., Martinelli, E., & Ciardiello, F. (2019). Immunotherapy of colorectal cancer: Challenges for therapeutic efficacy. Cancer treatment reviews, 76, 22-32. https://doi.org/10.1016/j.ctrv.2019.04.003
352. Rodr,àö,â†guez-Calvillo, M., Duarte, M., Tirapu, I., Berraondo, P., Mazzolini, G., Qian, C., Prieto, J., & Melero, I. (2002). Upregulation of natural killer cells functions underlies the efficacy of intratumorally injected dendritic cells engineered to produce interleukin-12. Experimental Hematology, 30(3), 195-204.
353. Cui J, Shin T, Kawano T, et al. (1997). Requirement for V14 NKT cells in IL-12-mediated rejection of tumors. Science, 278(5339), 1623.
354. Raskov, H., Orhan, A., Christensen, J.P. et al. (2021). Cytotoxic CD8+ T cells in cancer and cancer immunotherapy. British Journal of Cancer, 124(2), 359-367.
355. Smyth, M. J., Hayakawa, Y., Takeda, K., & Yagita, H. (2002). New aspects of natural-killer-cell surveillance and therapy of cancer. Nature Reviews Cancer, 2(11), 850-861.
356. Ding, Q., Lu, P., Xia, Y., Ding, S., Fan, Y., Li, X., Han, P., Liu, J., Tian, D., & Liu, M. (2016). CXCL9: evidence and contradictions for its role in tumor progression. Cancer Medicine, 5(11), 3246-3259.
357. Seitz S, Dreyer TF, Stange C, et al. (2022). CXCL9 inhibits tumour growth and drives anti-PD-L1 therapy in ovarian cancer. British Journal of Cancer, 126(10), 1470-1480.
358. Karin, N., & Wildbaum, G. (2015). The role of chemokines in adjusting the balance between CD4+ effector T cell subsets and FOXp3-negative regulatory T cells. International Immunopharmacology, 28(2), 829-835.
359. Barreira da Silva, R., Laird, M. E., Yatim, N., Fiette, L., Ingersoll, M. A., & Albert, M. L. (2015). Dipeptidylpeptidase 4 inhibition enhances lymphocyte trafficking, improving both naturally occurring tumor immunity and immunotherapy. Nature Immunology, 16(8), 850-858.
360. Nishina, S., Yamauchi, A., Kawaguchi, T., Kaku, K., Goto, M., Sasaki, K., Hara, Y., Tomiyama, Y., Kuribayashi, F., Torimura, T., & Hino, K. (2018). Dipeptidyl Peptidase 4 Inhibitors Reduce Hepatocellular Carcinoma by Activating Lymphocyte Chemotaxis in Mice. Cellular and Molecular Gastroenterology and Hepatology, 7(1), 115-134.
361. Wu, Z., Huang, X., Han, X., Li, Z., Zhu, Q., Yan, J., Yu, S., Jin, Z., Wang, Z., Zheng, Q., & Wang, Y. (2016). The chemokine CXCL9 expression is associated with better prognosis for colorectal carcinoma patients. *Biomedicine & Pharmacotherapy, 78, 8-13.
362. Mlecnik, B., Tosolini, M., Charoentong, P., Kirilovsky, A., Bindea, G., Berger, A., Camus, M., Gillard, M., Bruneval, P., Fridman, W. H., Pag,àö¬Æs, F., Trajanoski, Z., & Galon, J. (2010). Biomolecular network reconstruction identifies T-cell homing factors associated with survival in colorectal cancer. Gastroenterology, 138(4), 1429-1440.
363. Eckert E.C., Nace R.A., Tonne J.M., Evgin L., Vile R.G., Russell S.J. (2019). Generation of a Tumor-Specific Chemokine Gradient Using Oncolytic Vesicular Stomatitis Virus Encoding CXCL9. Molecular Therapy - Oncolytics, 16, 63-74.
364. Martin-Fontecha A, Thomsen LL, Brett S, Gerard C, Lipp M, Lanzavecchia A, et al. (2004). Induced recruitment of NK cells to lymph nodes provides IFN-gamma for T(H)1 priming. Nature Immunology, 5(12), 1260-1265.

365. Walser TC, Rifat S, Ma X, et al. (2006). Antagonism of CXCR3 inhibits lung metastasis in a murine model of metastatic breast cancer. Cancer Research, 66(15), 7701-7707.
366. Wendel M, Galani IE, Suri-Payer E, Cerwenka A. (2008). Natural killer cell accumulation in tumors is dependent on IFN-gamma and CXCR3 ligands. Cancer Research, 68(20), 8437-8445.
367. Leung EYL, Ennis DP, Kennedy PR, Hansell C, Dowson S, Farquharson M, et al. (2020). NK cells augment oncolytic adenovirus cytotoxicity in ovarian cancer. Molecular Therapy - Oncolytics, 16, 289-301.
368. Sivori, S., Della Chiesa, M., Carlomagno, S., Quatrini, L., Munari, E., Vacca, P., Tumino, N., Mariotti, F.R., Mingari, M.C., Pende, D., et al. (2020). Inhibitory Receptors and Checkpoints in Human NK Cells, Implications for the Immunotherapy of Cancer. Frontiers in Immunology, 11, 2156.
369. Brandstadter, J.D., Yang, Y. (2011). Natural Killer cell responses to viral infection. Journal of Innate Immunology, 3(3), 274-279.
370. Heissmeyer, V., Macian, F., Im, S.H., Varma, R., Feske, S., Venuprasad, K., Gu, H., Liu, Y.C., Dustin, M.L., and Rao, A. (2004). Calcineurin imposes T cell unresponsiveness through targeted proteolysis of signaling proteins. Nature Immunology, 5(3), 255-265.
371. Adachi, Y., Hattori, M., and Yoshida, T. (2010). Regulation of T cell activation and anergy by the intensity of the Ca(2)+ signal in cooperation with other signals. Bioscience, Biotechnology, and Biochemistry, 74(9), 1788-1793.
372. Fracchia, K. M., Pai, C. Y., & Walsh, C. M. (2013). Modulation of T Cell Metabolism and Function through Calcium Signaling. Frontiers in Immunology, 4, 324.
373. Hamza T, Barnett JB, Li B. (2010). Interleukin 12 a key immunoregulatory cytokine in infection applications. International Journal of Molecular Sciences, 11(3), 789-806.
374. Pien GC, Satoskar AR, Takeda K, Akira S, Biron CA. (2000). Cutting edge: Selective IL-18 requirements for induction of compartmental IFN-gamma responses during viral infection. Journal of Immunology, 165(9), 4787-4791.
375. Lane, R. S., Femel, J., Breazeale, A. P., Loo, C. P., Thibault, G., Kaempf, A., Mori, M., Tsujikawa, T., Chang, Y. H., & Lund, A. W. (2018). IFN,âà√≠,Äö√¢o-activated dermal lymphatic vessels inhibit cytotoxic T cells in melanoma and inflamed skin. The Journal of Experimental Medicine, 215(12), 3057-3074.
376. Chheda ZS, Sharma RK, Jala VR, Luster AD, Haribabu B. (2016). Chemoattractant Receptors BLT1 and CXCR3 Regulate Antitumor Immunity by Facilitating CD8+ T Cell Migration into Tumors. Journal of Immunology, 197, 2016-2026.
377. Peng W, Liu C, Xu C, Lou Y, Chen J, Yang Y, et al. (2012). PD-1 blockade enhances T-cell migration to tumors by elevating IFN-gamma inducible chemokines. Cancer Research, 72, 5209-5218.
378. Curran MA, Montalvo W, Yagita H, Allison JP. (2010). PD-1 and CTLA-4 combination blockade expands infiltrating T cells and reduces regulatory T and myeloid cells within B16 melanoma tumors. Proceedings of the National Academy of Sciences of the United States of America, 107(9), 4275-4280.
379. Ji RR, Chasalow SD, Wang L, Hamid O, Schmidt H, Cogswell J, et al. (2012). An immune-active tumor microenvironment favors clinical response to ipilimumab. Cancer Immunology, Immunotherapy, 61(10), 1019-1031.

380. Dangaj D, Bruand M, Grimm AJ, et al. (2019). Cooperation between constitutive and inducible chemokines enables T cell engraftment and immune attack in solid tumors. Cancer Cell, 35(6), 885-900.e10.
381. Chow MT, Ozga AJ, Servis RL, et al. (2019). Intratumoral activity of the CXCR3 chemokine system is required for the efficacy of anti-PD-1 therapy. Immunity, 50(6), 1498-1512.e5.
382. Garris, C. S., Arlauckas, S. P., Kohler, R. H., Trefny, M. P., Garren, S., Piot, C., Engblom, C., Pfirschke, C., Siwicki, M., Gungabeesoon, J., Freeman, G. J., Warren, S. E., Ong, S., Browning, E., Twitty, C. G., Pierce, R. H., Le, M. H., Algazi, A. P., Daud, A. I., Pai, S. I., ,Äö√Ñ Pittet, M. J. (2018). Successful Anti-PD-1 Cancer Immunotherapy Requires T Cell-Dendritic Cell Crosstalk Involving the Cytokines IFN-,âà√≠,Äö√¢o and IL-12. Immunity, 49(6), 1148-1161.e7.
383. Ayers, M., Lunceford, J. K., Nebozhyn, M., Murphy, E., Loboda, A., Kaufman, D. R., Albright, A., Cheng, J. D., Kang, S. P., Shankaran, V., Piha-Paul, S. A., Yearley, J. H., Seiwert, T. Y., Ribas, A., McClanahan, T. K., and the IMvigor210 Study Group. (2017). IFN-,âà√≠,Äö√¢o-related mRNA profile predicts clinical response to PD-1 blockade. Journal of Clinical Investigation, 127(8), 2930-2940.
384. Cursons, J., Souza-Fonseca-Guimaraes, F., Foroutan, M., Anderson, A., Hollande, F., Hediyeh-Zadeh, S., Behren, A., Huntington, N., and Davis, M. J. (2019). A gene signature predicting natural killer cell infiltration and improved survival in melanoma patients. Cancer Immunology Research, 7(8), 1162-1174.
385. Lee, H., Bao, X., Miller, A., Zhang, C., Wu, Y., Zheng, J., Xu, Y., Huang, Z., Lu, H., Rabinovich, B., Liu, X., Bremner, R., Li, S., Shen, L., Xi, L., Lei, Y., Markovic, S. N., Zarour, H. M., ... Luo, Y. (2019). Integrated molecular and immunophenotypic analysis of NK cells in anti-PD-1 treated metastatic melanoma patients. OncoImmunology, 8(7), e1605438.
386. Shiravand, Y., Khodadadi, F., Kashani, S. M. A., Hosseini-Fard, S. R., Hosseini, S., Sadeghirad, H., Ladwa, R., O'Byrne, K., & Kulasinghe, A. (2022). Immune Checkpoint Inhibitors in Colorectal Cancer: Challenges and Future Prospects. Biomedicines, 9(9), 1075.
387. Cursons, J., Gopalakrishnan, S., Lomax, A. J., Cortez, M. A., Correia, C., Harding, A., et al. (2021). Identifying immunotherapy-responsive tumours and immune cell-rich tissues with organoid models. Nature, 591(7848), 234-239.
388. Robert, C. (2020). A decade of immune-checkpoint inhibitors in cancer therapy. Nature Communications, 11(1), 3801.
389. Takahashi, K., Yokobayashi, Y. (2019). Reversible Gene Regulation in Mammalian Cells Using Riboswitch-Engineered Vesicular Stomatitis Virus Vector. ACS Synthetic Biology, 8(9), 1976-1982.
390. Strobel, B., Duchs, M. J., Blazevic, D., Rechtsteiner, P., Braun, C., Baum-Kroker, K. S., Schmid, B., Ciossek, T., Gottschling, D., Hartig, J. S., & Kreuz, S. (2020). A Small-Molecule-Responsive Riboswitch Enables Conditional Induction of Viral Vector-Mediated Gene Expression in Mice. ACS Synthetic Biology, 9(6), 1292-1305.

# Supplementary Figures and Tables

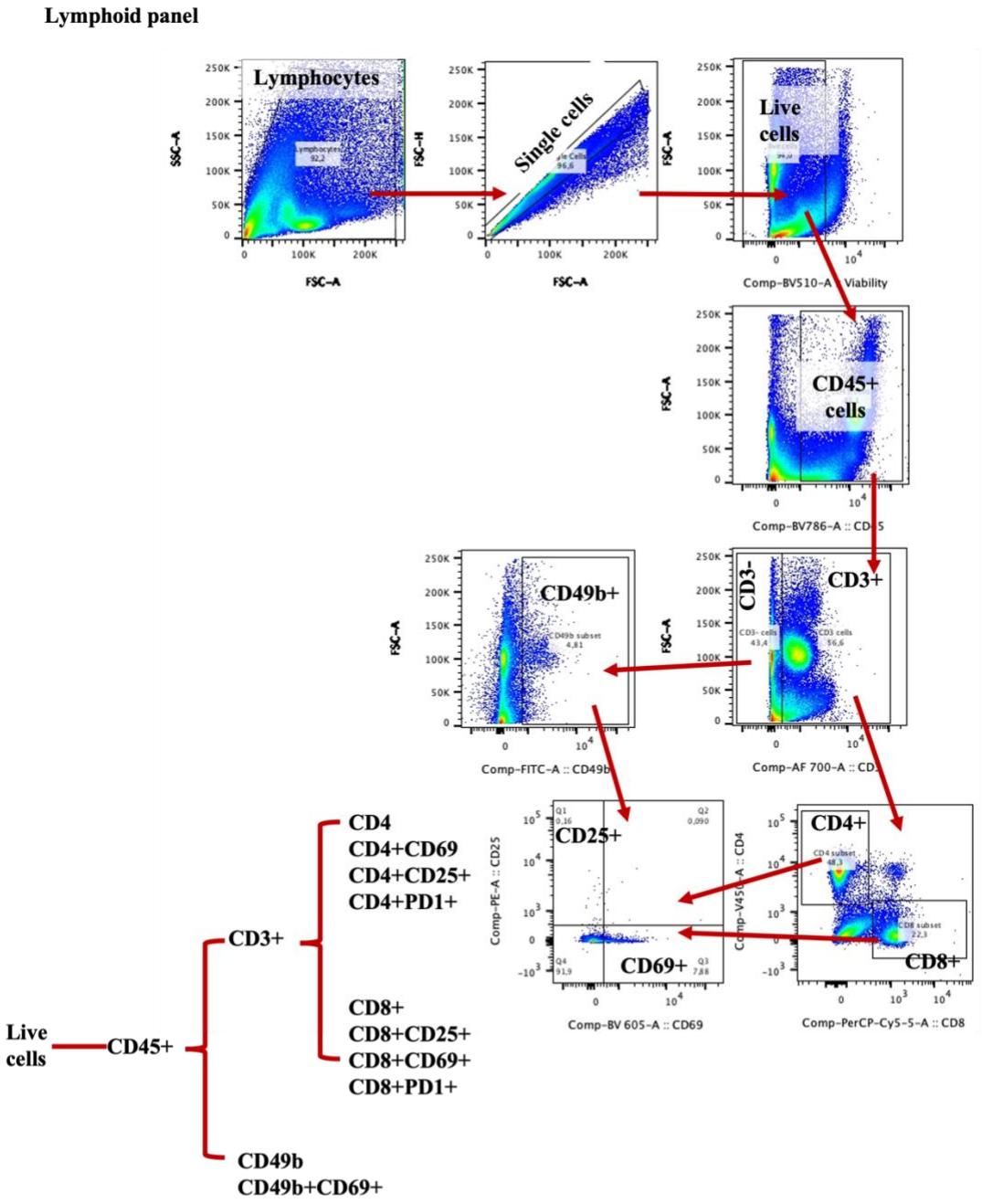


**Figure S1: flow cytometry gating strategy for lymphoid panel.**
Lymphoid panel for T cell and NK cells analyses, T cells were gated based on CD3+ cells that are CD45+ live cells, then CD8+ T cells and CD4+ T cells were gated from CD3+ T cells. NK cells were gated from $CD3^{negative}$ cells and CD49b+ cells.

**Antigen precenting cell panel**

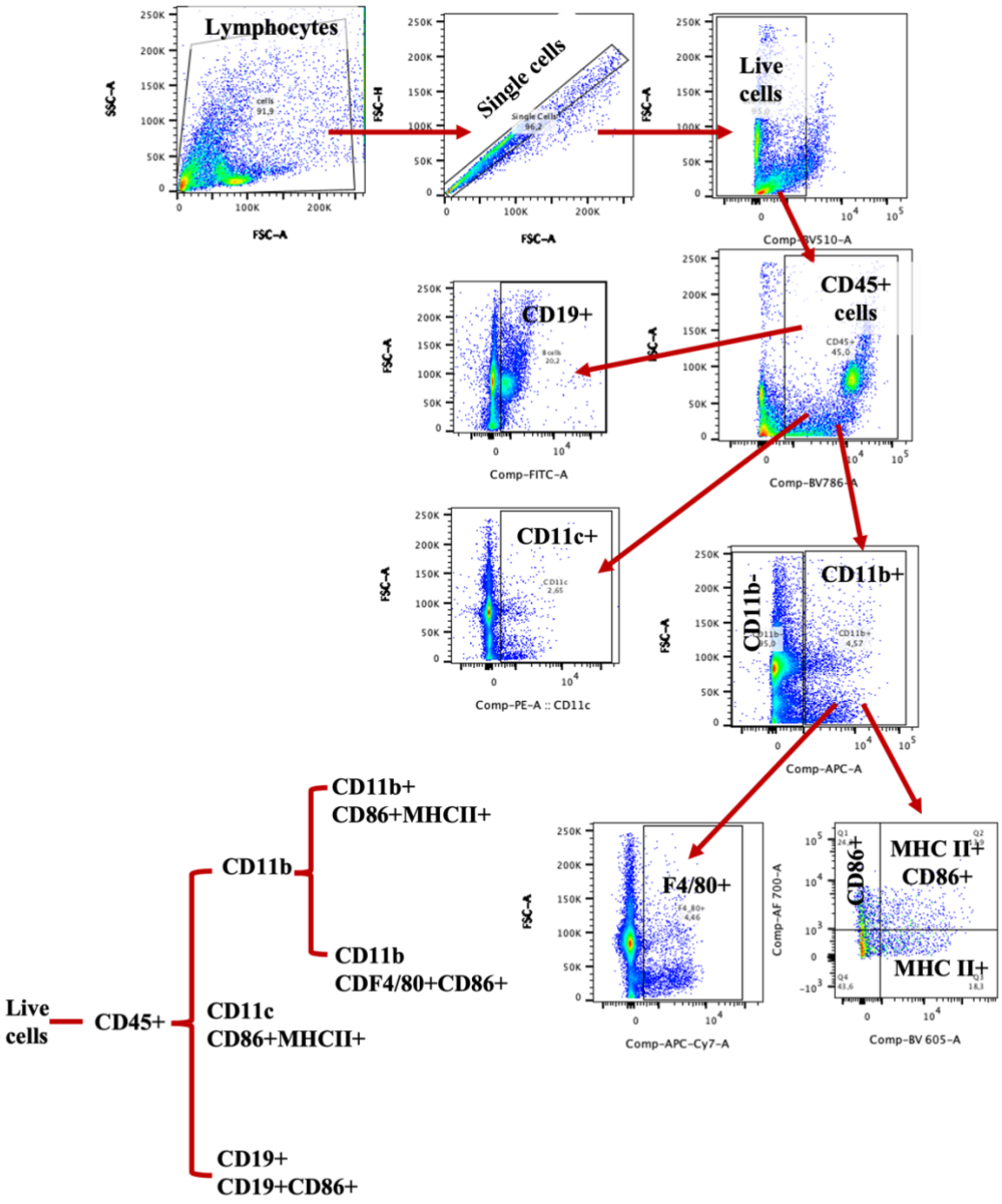


**Figure S 2: flow cytometry gating strategy for antigen presenting cell panel.**
Antigen presenting cell panel, CD11b+, CD11c+, and CD19 cells were gated from CD45+ live cells. F4/80+ macrophages were gated from CD11b+ cells.

**Table 4: T cells and NK cells flow panel.**

| | Fluorochrome | Marker | Dilution |
|---|---|---|---|
| Viability | FV510 | Dead cell Stain | 1:1000 |
| CD45 | BV786 | Leukocyte marker | 1:1000 |
| CD3 | AF700 | T cell marker | 1:50 |
| CD4 | V450 | T cell marker | 1:1000 |
| CD8a | PercPcy5.5 | T cell marker | 1:100 |
| CD25 | PE | Activation marker | 1:100 |
| CD69 | BV605 | Activation marker | 1:100 |
| PD1 | APC-cy7 | Immunochekpoint | 1:50 |
| CD127 | PE-Cy7 | Tregulatory marker | 1:100 |
| CD49b | FITC | NK cells | 1:200 |

**Table 5: myeloid and antigen presenting flow panel.**

| | Fluorochrome | Marker | Dilution |
|---|---|---|---|
| Viability | FV510 | Dead cell stain | 1:1000 |
| CD45 | BV786 | Leukocyte marker | 1:1000 |
| CD11b | APC | Pan-myeloid marker | 1:100 |
| CD11c | PE | Granulocytes mainly DC | 1:100 |
| F4/80 | APC-cy7 | Macrophage marker | 1:50 |
| CD86 | ACPR700 | Co-stimulatory molecule | 1:100 |
| IA/IE | BV605 | MHC-II | 1:100 |
| CD19 | FITC | B cells marker | 1:200 |

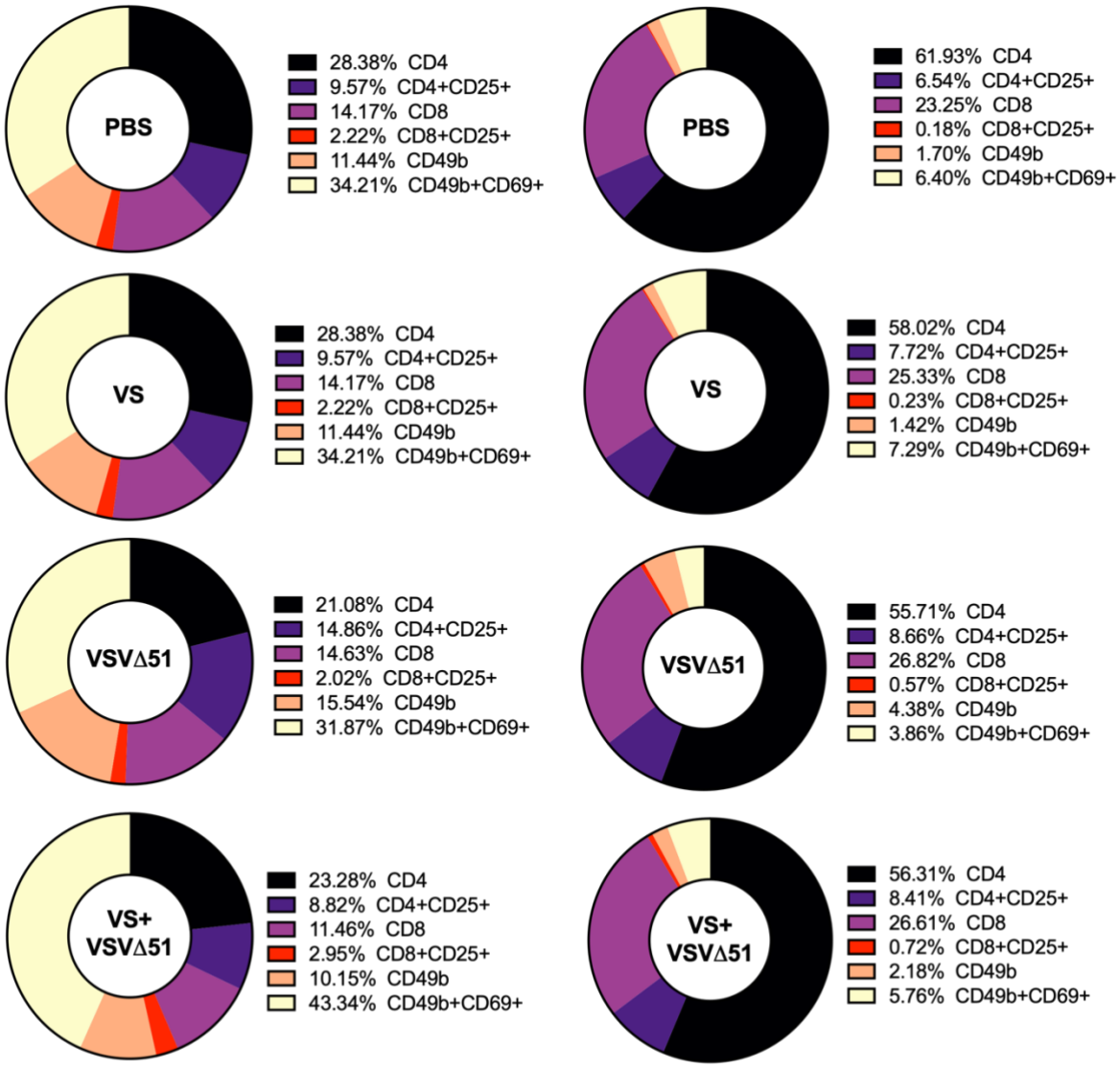


**Figure S3: VS plus VSVΔ51 combination therapy generates identified cellular immunological changes 5 days following treatment.**
**This figure is part of Figure 15, r**elative proportions of various immune cell subsets among all leukocytes of live cells are shown.

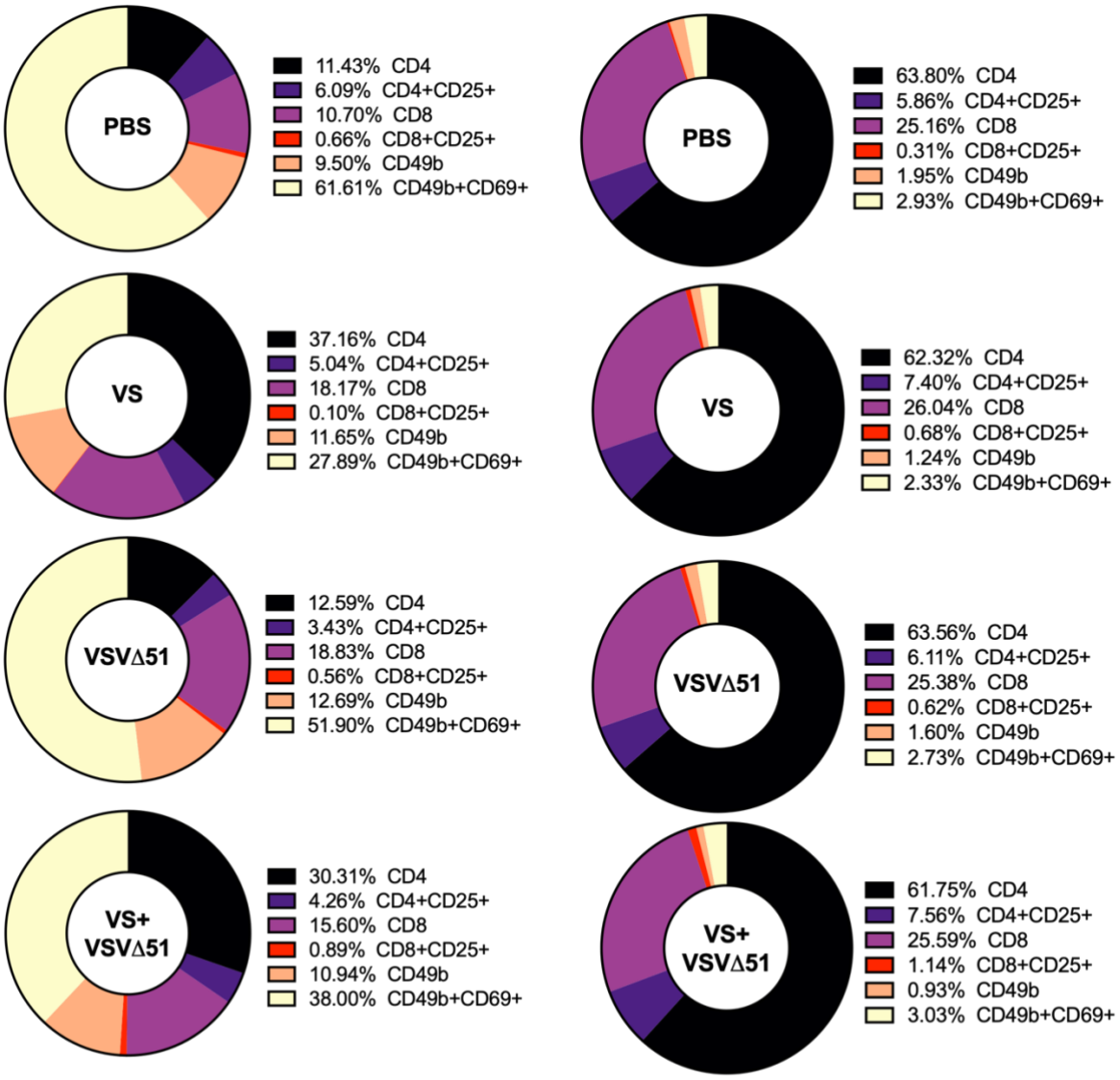


**Figure S4: VS plus VSVΔ51 combination therapy generates identified cellular immunological changes 10 days following treatment.**
**This figure is part of figure15,** relative proportions of various immune cell subsets among all leukocytes of live cells are shown.

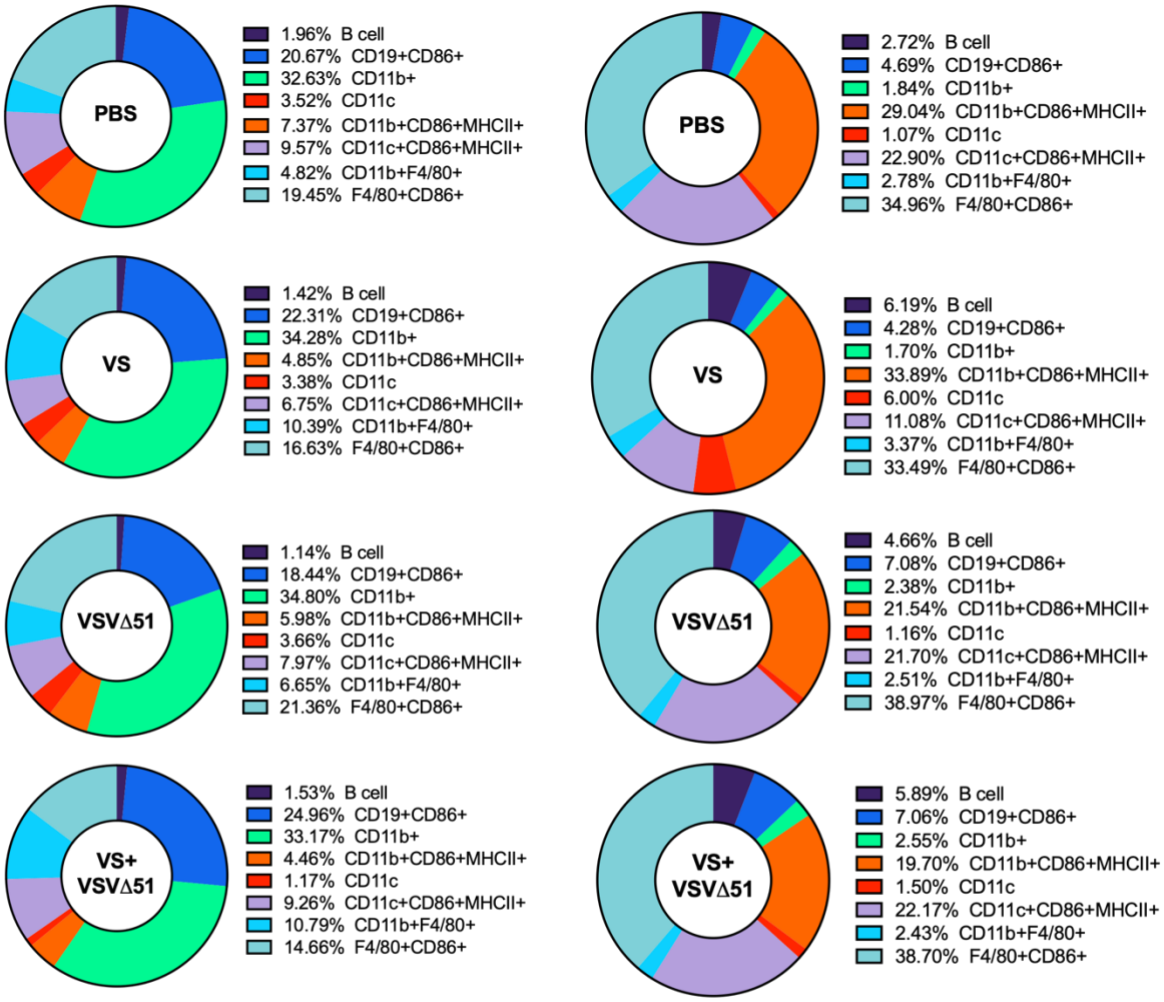


**Figure S5: The impact of VS plus VSVΔ51 combination therapy on dendritic cells and macrophages 5 days following treatment.**
**This figure is part of Figure 15,** relative proportions of various immune cell subsets among all leukocytes of live cells are shown.

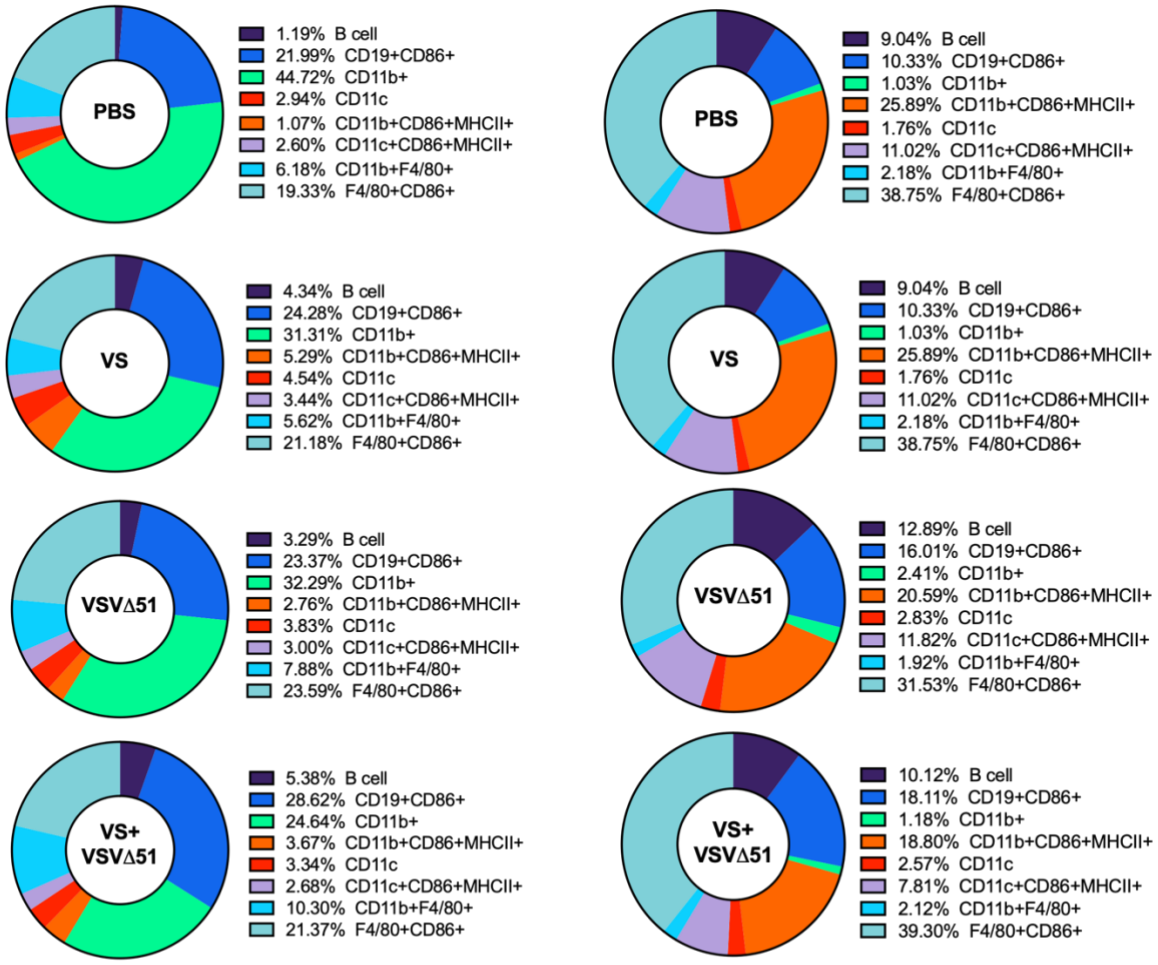


**<u>Figure S6:</u> The impact of VS plus VSVΔ51 combination therapy on dendritic cells and macrophages 10 days following treatment.**
**This figure is part of Figure 15,** relative proportions of various immune cell subsets among all leukocytes of live cells are shown.

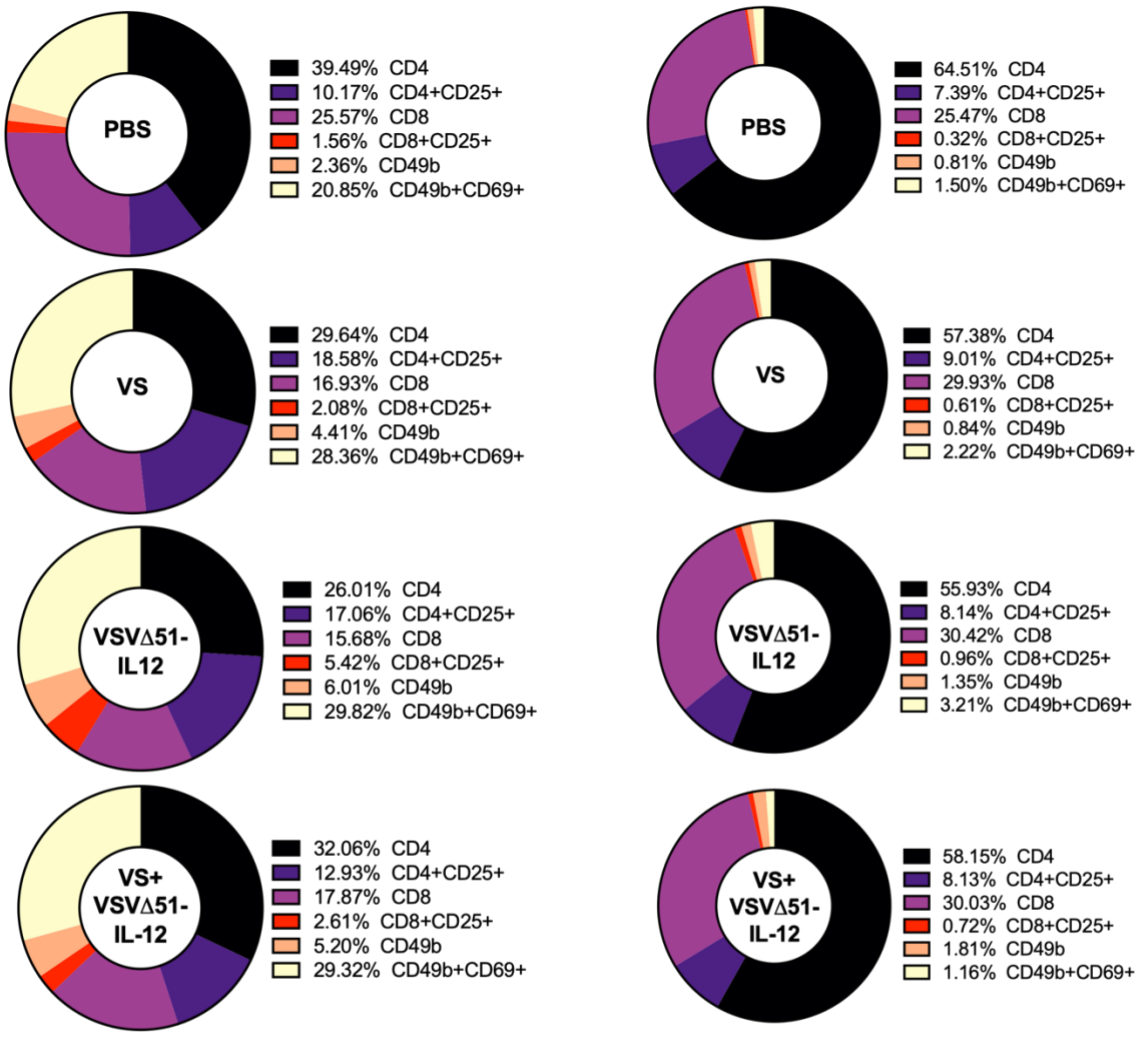


**Figure S7: VSVΔ51 expressing IL-12 in combination with VS enhances the percentage of activated T cells, macrophages, and NK cells at TME and TdLNs 5 days post treatment.**
**This figure is part of Figure 19,** Relative proportions of various immune cell subsets among all leukocytes of live cells are shown.

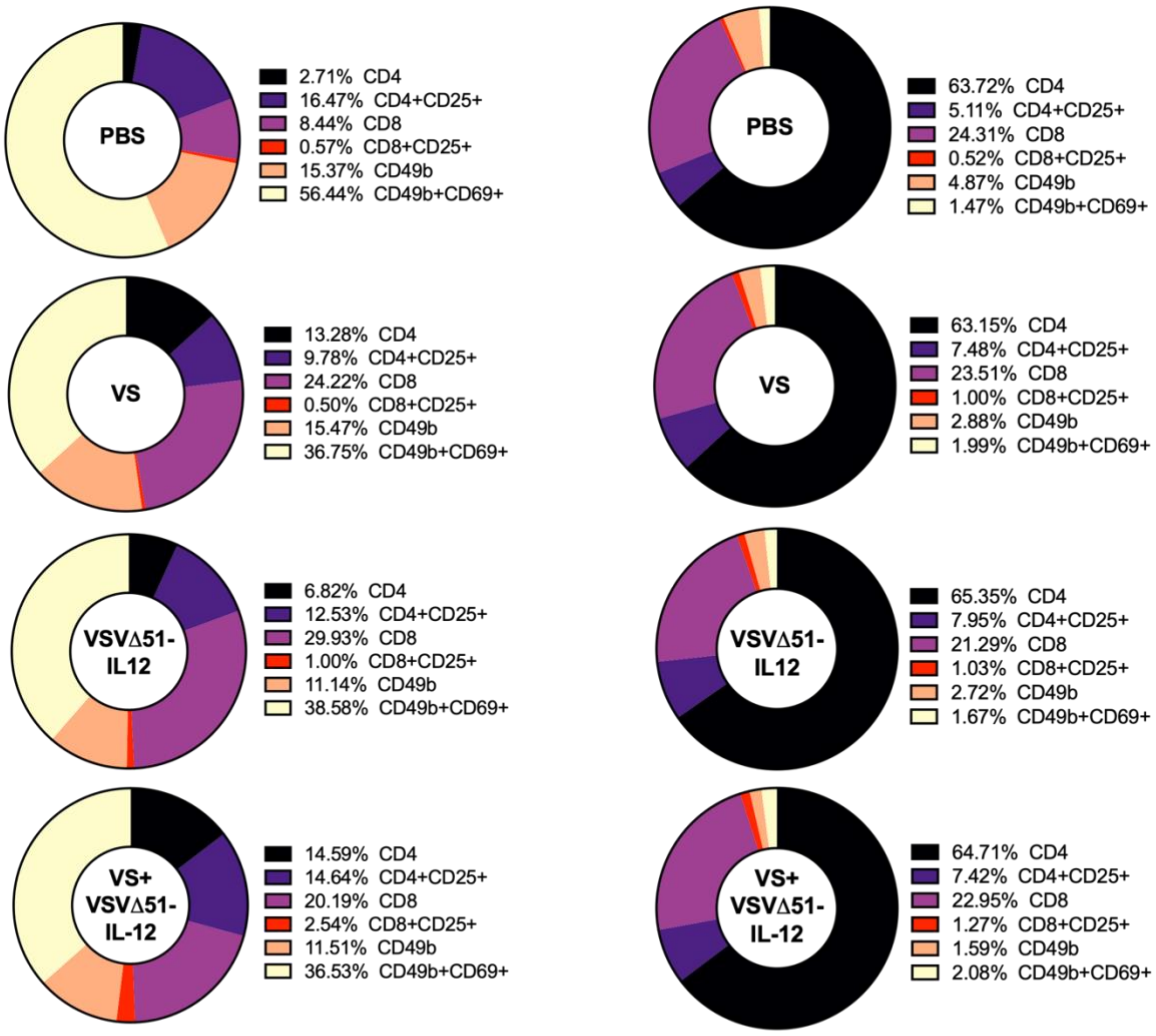


**Figure S8: VSVΔ51 expressing IL-12 in combination with VS enhances the percentage of activated T cells, macrophages, and NK cells at TME and TdLNs 10 days post treatment.**
**This figure is part of Figure 19,** Relative proportions of various immune cell subsets among all leukocytes of live cells are shown.

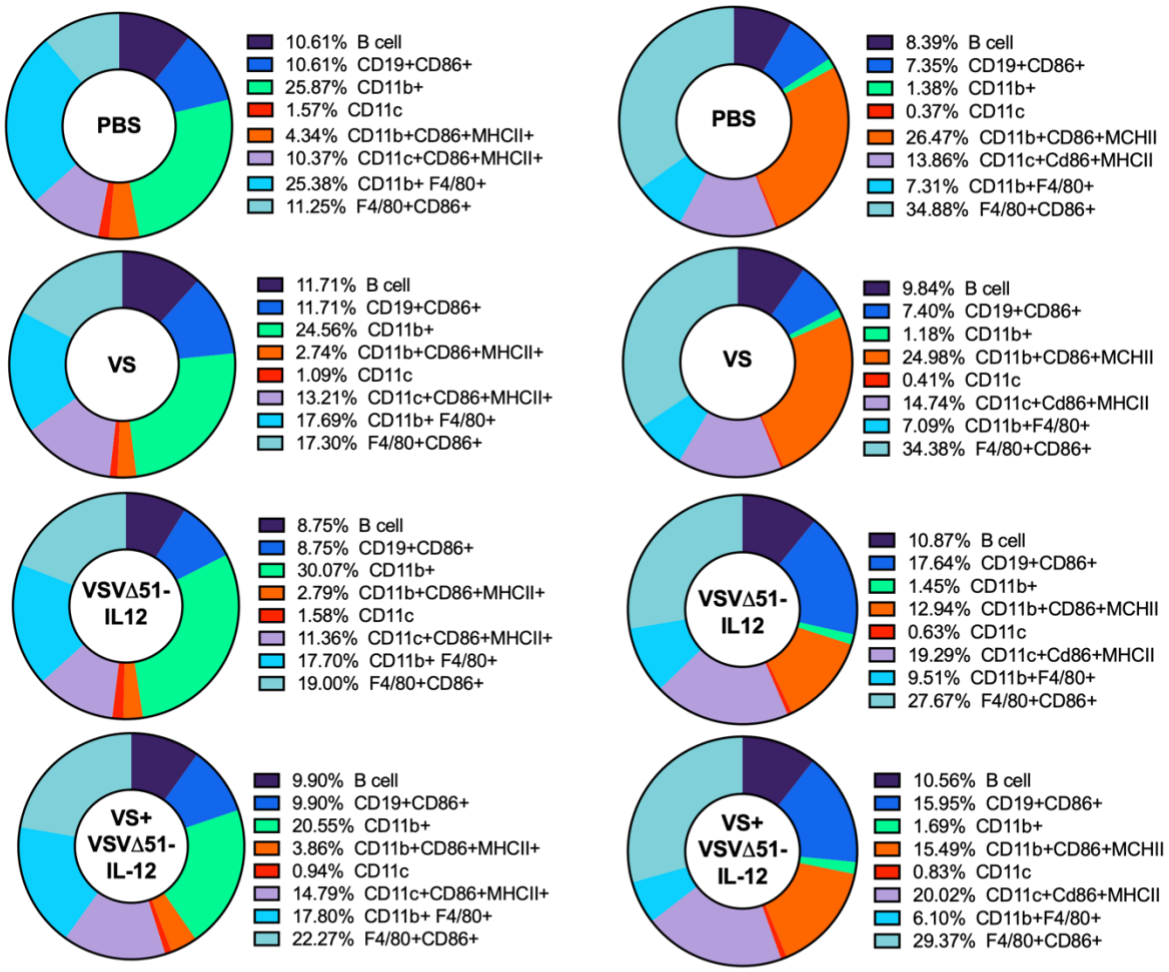


**Tumor infiltrating leukocytes** **Tumor draining Lymph nodes**

**<u>Figure S9:</u> The impact of VSVΔ51 expressing IL-12 in combination with VS on the percentage of B cells, macrophages, and dendritic cells at TME and TdLNs 5 days post treatment.**

**This figure is part of Figure 19,** Relative proportions of various immune cell subsets among all leukocytes of live cells are shown.

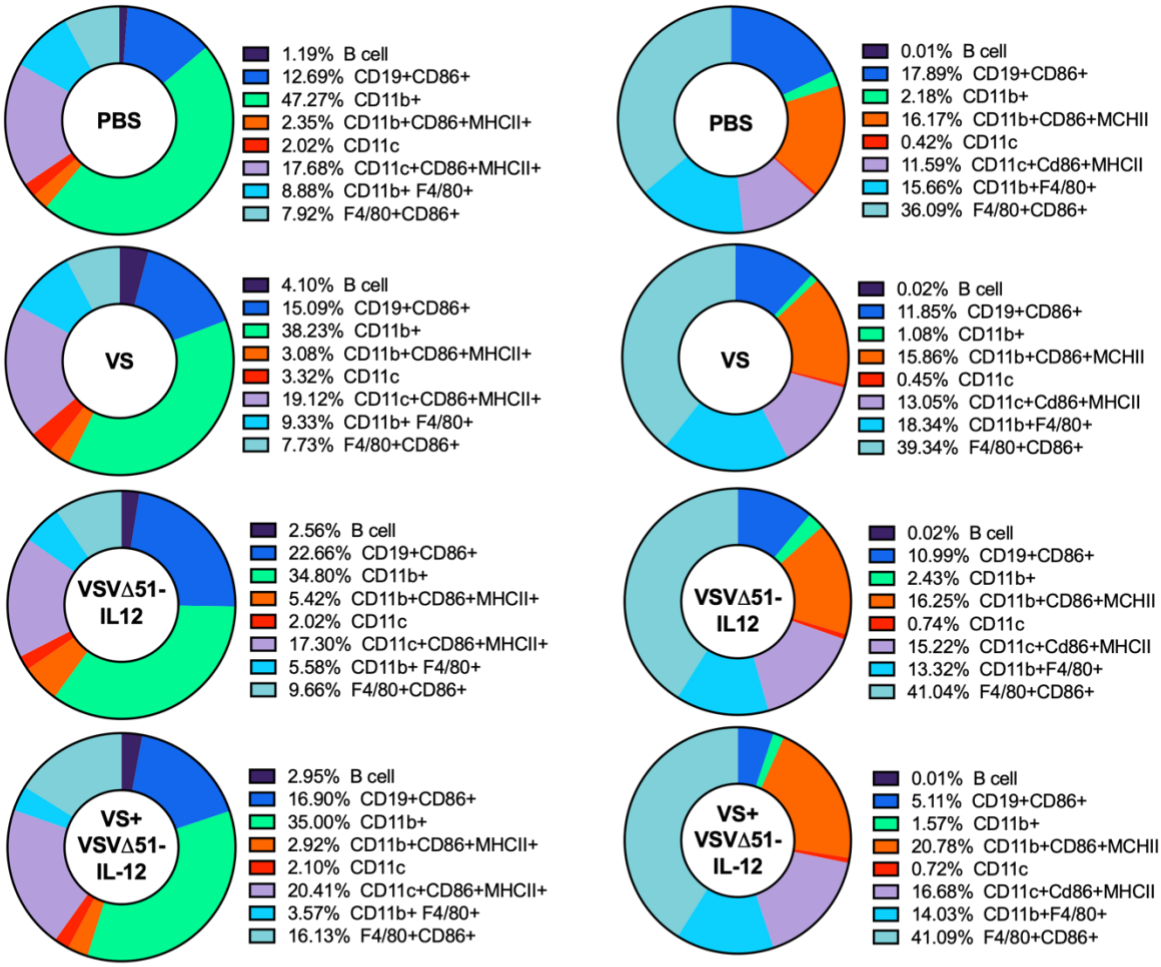


**Tumor infiltrating leukocytes** **Tumor draining Lymph nodes**

**Figure S10: The impact of VSVΔ51 expressing IL-12 in combination with VS on the percentage of B cells, macrophages, and dendritic cells at TME and TdLNs 10 days post treatment.**

**This figure is part of Figure 19,** Relative proportions of various immune cell subsets among all leukocytes of live cells are shown.

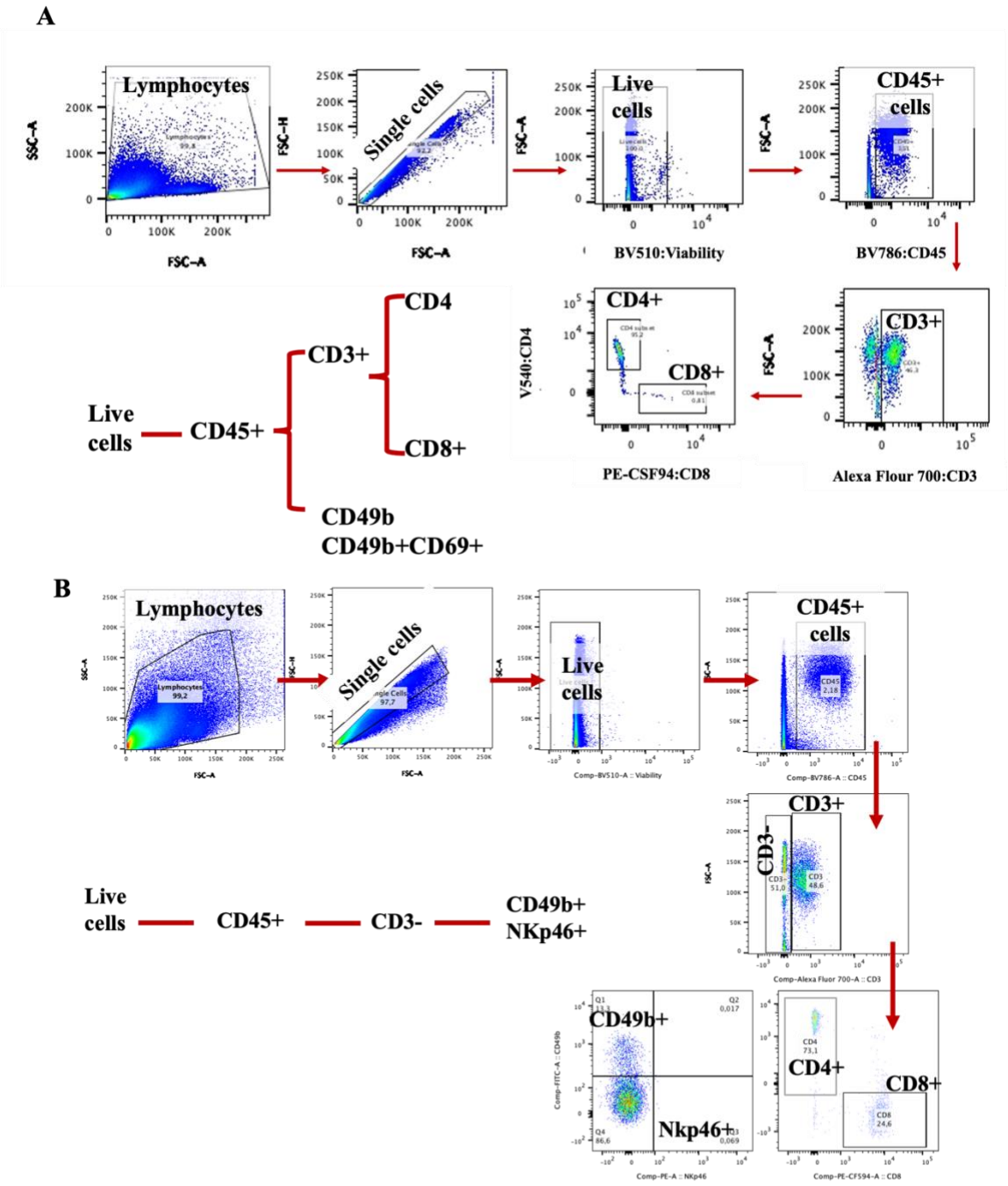


**Figure S11: flow cytometry gating strategy for CD8+ T cell depletion and NK cell depletion experiments.**

Peripheral blood cells were stained with viability dye followed by Fc blocking. **A.** Cells were then stained with anti-CD45, anti-CD3, anti-CD8 and anti-CD4 antibodies. Cells were gated from CD45+ cells of single viable cells to include only the leukocytes. Then, T cells were gated from CD3+ subset and CD4+ cells or CD8+ cells. **B.** Cells were stained with anti-CD45, anti-CD3, anti-CD49b and anti-NKp46 antibodies. Cells were gated from CD45+ cells of single viable cells to include only the leukocytes. Then, NK cells were gated from CD3- subset and then CD49b+NKp46+.

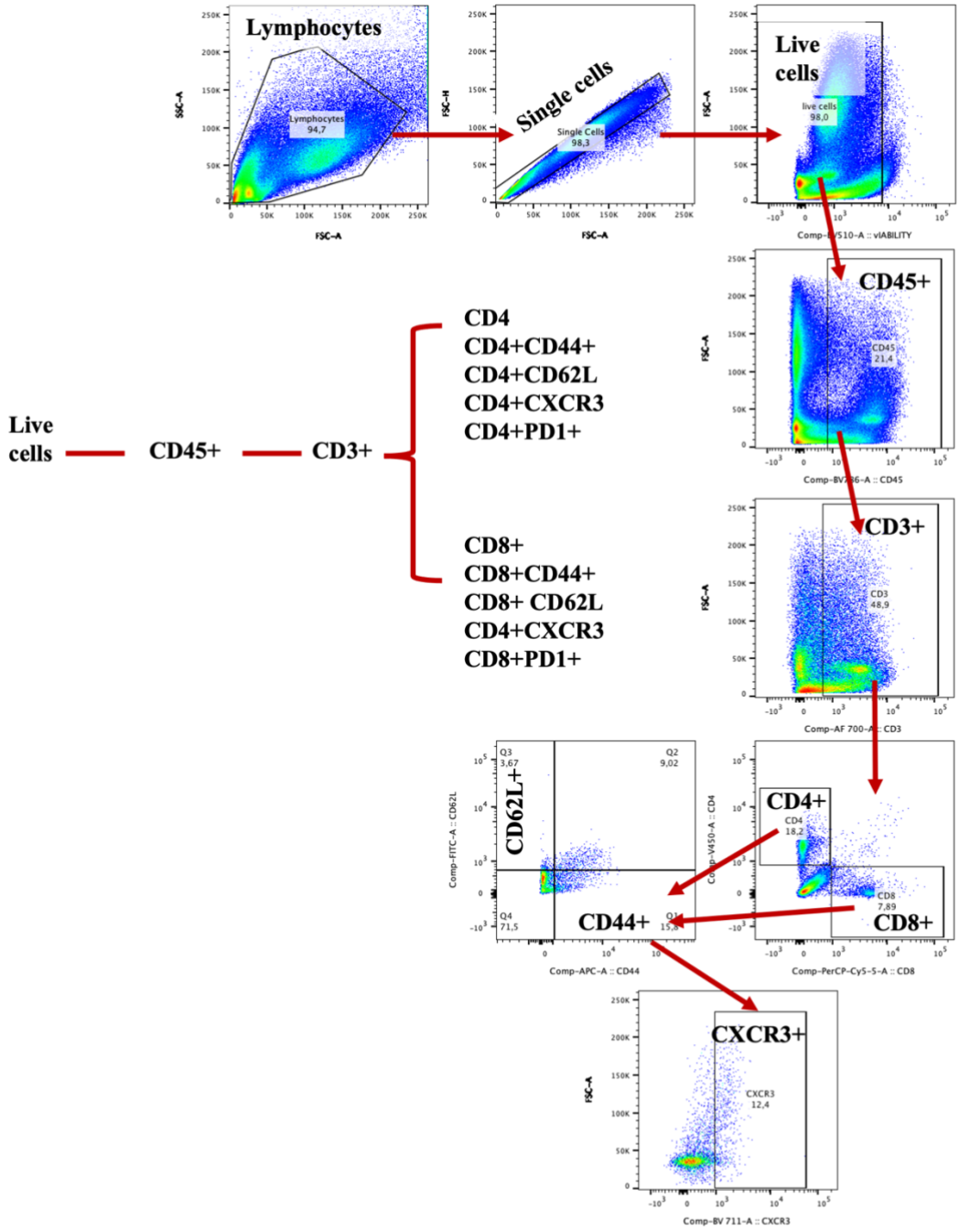


**<u>Figure S12</u>: flow cytometry gating strategy for T cell-based panel.**
Tumor infiltration leukocytes were stained with viability dye followed by Fc blocking. Cells were then stained with anti-CD45, anti-CD3, anti-CD8 and anti-CD4 antibodies as well as activation markers including CD44 and CXCR3. Cells were gated from CD45+ cells of single viable cells to include only the leukocytes. Then, T cells were gated from CD3+ subset and CD4+ cells or CD8+ cells. Each T cells subset was then gated based on the expression of various activation markers

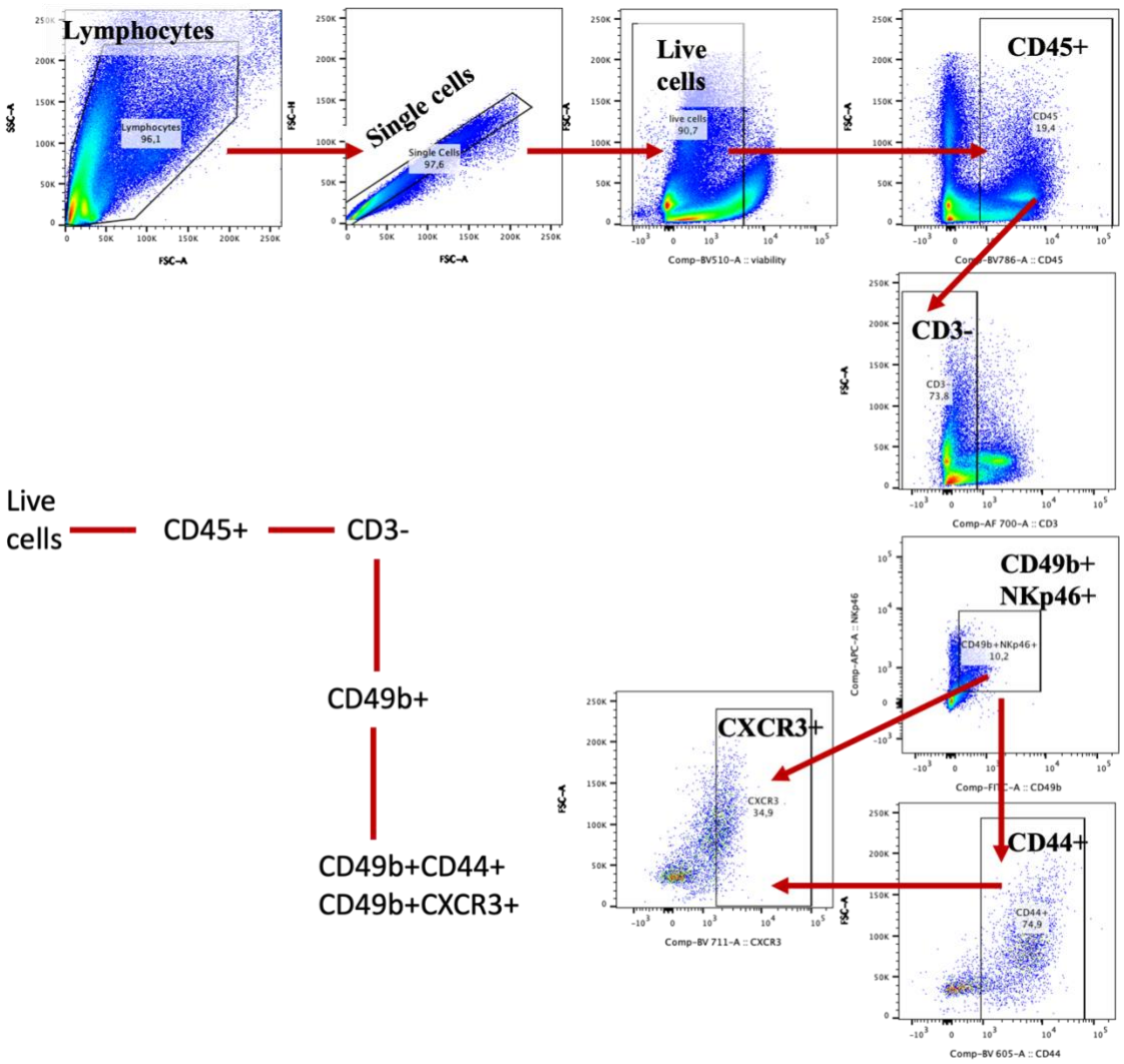


**<u>Figure S13</u>: flow cytometry gating strategy for NK cells panel.**
Tumor infiltration leukocytes were stained with viability dye followed by Fc blocking. Cells were then stained anti-CD45, anti-CD3, anti-CD49b and anti-NKp46 antibodies as well as activation markers including CD44 and CXCR3. Cells were gated from CD45+ cells of single viable cells to include only the leukocytes. NK cells were gated from CD3- subset and then CD49b+NKp46+, then gated based on the expression of various activation markers

**Table 6: T cells flow panel.**

| | Fluorochrome | Marker | Dilution |
|---|---|---|---|
| Viability | FV510 | Dead cell Stain | 1:1000 |
| CD45 | BV786 | Leukocyte marker | 1:1000 |
| CD3 | AF700 | T cell marker | 1:50 |
| CD4 | V450 | T cell marker | 1:1000 |
| CD8a | Pe.cy5.5 | T cell marker | 1:200 |
| CD44 | BV605/APC | Activation marker | 1:100 |
| CD62L | FITC | Naïve cell | 1:200 |
| CXCR3 | BV711 | Migratory cells | 1:100 |
| PD1 | APC-cy7 | Immune inhibitory marker | 1:100 |

**Table 7: NK cells flow panel.**

| | Fluorochrome | Marker | Dilution |
|---|---|---|---|
| Viability | FV510 | Dead cell Stain | 1:1000 |
| CD45 | BV786 | Leukocyte marker | 1:1000 |
| CD3 | AF700 | T cell marker | 1:50 |
| CD44 | BV605 | Activation marker | 1:100 |
| CXCR3 | BV711 | Migratory cells | 1:100 |
| PD1 | APC-cy7 | Immune inhibitory marker | 1:100 |
| CD49b | FITC | NK cell marker | 1:200 |
| NKp46 | APC | NK cell marker | 1:100 |

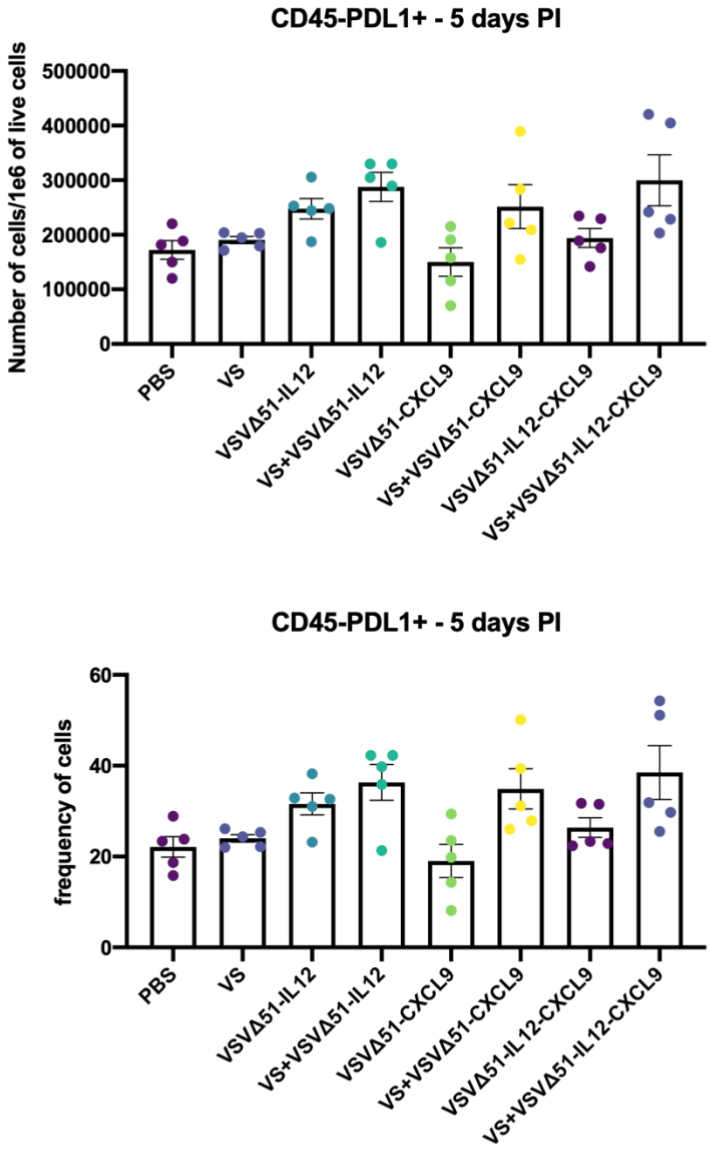


**<u>Figure S14:</u> The expression of PDL1 following treatment with VS in combination with VSVΔ51-CXCL9 and VSVΔ51-IL12-CXCL-9 5 days post-treatment.**

**(A)** Schematic representation of the treatment schedule: after 12 days, CT26WT-tumor bearing mice received three intratumorally vanadyl sulfate (50mg/kg) and VSVΔ51 expressing IL-12 (1E8 PFU) or monotherapy. Tumor were collected 5 days post-treatment. Tumors were dissected and then dissociated by Tumour dissociation kits with the gentleMACS Dissociator to analyze Tumour infiltration leukocytes (TILs). Cells were stained with a viability dye and anti-CD45 antibody. Relative proportions of PDL1-expressed cells were gated based on $CD45^{neg}$ cells of live cells . Graphs show the number and frequency of $CD45^{neg}$ $PDL1^{+}$ cells.

# Appendices

## Appendix 1: Vanadyl Sulfate-enhanced oncolytic virus immunotherapy mediates the antitumor immune response by upregulating the secretion of pro-inflammatory cytokines and chemokines.

**Nouf Alluqmani** [1,2,3], Anna Jirovec [1,2], Zaid Taha [1,2], Oliver Varette[1], Andrew Chen[1], Daniel Serrano[1], Glib Maznyi[1], Sarwat Khan[1], Nicole E. Forbes[1], Rozanne Arulanandam[1], Rebecca C. Auer[1,4], Jean-Simon Diallo[1,2*]

[1]Centre for Innovative Cancer Research, Ottawa Hospital Research Institute, Ottawa, ON, Canada
[2]Department of Biochemistry, Microbiology and Immunology, Faculty of Medicine, University of Ottawa, ON, Canada
[3]King Faisal Specialist Hospital and Research Center, Riyadh, Saudi Arabia
[4]Department of Surgery, University of Ottawa, Ottawa, Ontario, Canada.

Accepted November 2022; Published in Frontier in Immunology



https://www.frontiersin.org/articles/10.3389/fimmu.2022.1032356/full

**Author contribution**

Conceptualization, **N.A**. and J.S.D.; Methodology, **N.A**. conducted the *in vitro* and *ex vivo* experiments. **N.A.** and A.C. performed all *in vivo* experiments. R.A. contributed to the IL-12 related *in vivo* survival experiments. A.J., Z.T., and G.M. assisted with tissue processing. O.V., and S.K. contributed to the experimental design and performed the ICV experiments. **N.A.** and J.S.D. designed the experiments, performed data analyses, and wrote the paper. R.A., N. F., and D.S., helped with experimental design. **N.A**., D.S., R.A., A.J, Z.T., and J.S.D reviewed the report; Funding Acquisition, J.S.D.; Supervision, J.S.D.

frontiers | Frontiers in Immunology

TYPE Original Research
PUBLISHED 28 November 2022
DOI 10.3389/fimmu.2022.1032356



OPEN ACCESS

EDITED BY
Almohanad A. Alkayyal,
University of Tabuk, Saudi Arabia

REVIEWED BY
Lee-Hwa Tai,
Université de Sherbrooke, Canada
Carmela Passaro,
Obsidian Therapeutics, United States

*CORRESPONDENCE
Jean-Simon Diallo
jsdiallo@ohri.ca

SPECIALTY SECTION
This article was submitted to Vaccines and Molecular Therapeutics, a section of the journal Frontiers in Immunology

RECEIVED 30 August 2022
ACCEPTED 09 November 2022
PUBLISHED 28 November 2022

CITATION
Alluqmani N, Jirovec A, Taha Z, Varette O, Chen A, Serrano D, Maznyi G, Khan S, Forbes NE, Arulanandam R, Auer RC and Diallo J-S (2022) Vanadyl sulfate-enhanced oncolytic virus immunotherapy mediates the antitumor immune response by upregulating the secretion of pro-inflammatory cytokines and chemokines. *Front. Immunol.* 13:1032356. doi: 10.3389/fimmu.2022.1032356



# Vanadyl sulfate-enhanced oncolytic virus immunotherapy mediates the antitumor immune response by upregulating the secretion of pro-inflammatory cytokines and chemokines

Nouf Alluqmani[1,2,3], Anna Jirovec[1,2], Zaid Taha[1,2], Oliver Varette[1], Andrew Chen[1], Daniel Serrano[1], Glib Maznyi[1], Sarwat Khan[1], Nicole E. Forbes[1], Rozanne Arulanandam[1], Rebecca C. Auer[1,4] and Jean-Simon Diallo[1,2]*

[1]Centre for Innovative Cancer Research, Ottawa Hospital Research Institute, Ottawa, ON, Canada, [2]Department of Biochemistry, Microbiology and Immunology, Faculty of Medicine, University of Ottawa, ON, Canada, [3]Research Center, Molecular Oncology Department King Faisal Specialist Hospital and Research Center, Riyadh, Saudi Arabia, [4]Department of Surgery, University of Ottawa, Ottawa, ON, Canada

Oncolytic viruses (OVs) are promising anticancer treatments that specifically replicate in and kill cancer cells and have profound immunostimulatory effects. We previously reported the potential of vanadium-based compounds such as vanadyl sulfate (VS) as immunostimulatory enhancers of OV immunotherapy. These compounds, in conjunction with RNA-based OVs such as oncolytic vesicular stomatitis virus (VSVΔ51), improve viral spread and oncolysis, leading to long-term antitumor immunity and prolonged survival in resistant tumor models. This effect is associated with a virus-induced antiviral type I IFN response shifting towards a type II IFN response in the presence of vanadium. Here, we investigated the systemic impact of VS+VSVΔ51 combination therapy to understand the immunological mechanism of action leading to improved antitumor responses. VS+VSVΔ51 combination therapy significantly increased the levels of IFN-γ and IL-6, and improved tumor antigen-specific T-cell responses. Supported by immunological profiling and as a proof of concept for the design of more effective therapeutic regimens, we found that local delivery of IL-12 using VSVΔ51 in combination with VS further improved therapeutic outcomes in a syngeneic CT26WT colon cancer model.

KEYWORDS

**combined immunotherapy, VSVΔ51, vanadyl sulfate, antitumor immunity, IL-12, IL-6, infected cell vaccine, interferon-gamma**

## 1 Introduction

Oncolytic viruses (OVs) are versatile and tumor-selective anticancer treatment platforms. OVs are selected and/or engineered viruses that preferentially infect, replicate in, and kill cancer cells (1–3). OVs also have immunostimulatory effects that promote antitumor immune responses. They successfully interrupt the established tumor microenvironment to overcome the resistance to immunological attack and the inhibition of immune lymphoid functions (4, 5).

The field of OV therapy has reached a new level of maturity with the historical approval of Imlygic® for the treatment of advanced melanoma (6) and the more recent approval of Delytact (G47Δ; teserpaturev), a triple-mutated, replication-conditional herpes simplex virus type 1 (HSV-1) for glioblastoma (7). However, Imlygic has not achieved the anticipated level of commercial success, and most recently did not show significant clinical benefit in combination with immune checkpoint inhibitors (ICI) in phase III trials.

Beyond HSV-1, there are several promising OV platforms and opportunities for improvement of therapeutic efficacy. Among others, the efficacy of OV therapy has been shown to depend heavily on the successful delivery and spread of these agents within malignancies to redirect the immune response toward the tumor (5). Our group has discovered various small molecule enhancers of OVs that can be integrated in therapeutic regimens to potentiate the effects of OV immunotherapies. These molecules suppress and/or modulate the antiviral response thereby improving the efficacy of OVs, especially in OV-resistant tumors (8, 9). We recently uncovered the potential of vanadate and other vanadium-based compounds such as vanadyl sulfate (VS) as a unique category of immunostimulatory OV enhancers, showing high-potential for combination with RNA-based oncolytic viruses, such as the oncolytic vesicular stomatitis virus (VSVΔ51) as well as Newcastle disease virus (NDV) (10, 11).

Vanadium is a transition metal that has been shown to block protein phosphatase activity and disrupt the balance between cellular protein kinases and protein phosphatases. Vanadium compounds have diverse pharmacological activities and have been explored as insulin-mimetics in human trials owing to their capacity to inhibit protein tyrosine phosphatase 1B (PTP1B) and thereby activate the insulin receptor (12, 13). While vanadium compounds were shown to be safe and are currently used as body-building dietary supplements, they have not yet shown sufficient efficacy to be approved by regulators as treatments for diabetes. More recently, vanadium compounds have been tested as anticancer agents in a variety of cancer cell lines and animal models due to their effects as potential cancer therapeutics (14–18).

Previous studies from our group showed that sodium orthovanadate (vanadate) alters kinase/phosphatase homeostasis in VSVΔ51-infected cancer cells, leading to a shift from the traditional virus-induced antiviral type I interferon (IFN) response towards a type II IFN response (10). This shift, associated with the simultaneous downregulation of STAT2 (signal transducer and activator of transcription) and parallel activation of STAT1, results in improved virus growth and the up-regulation of many type-II IFN-regulated pro-inflammatory cytokines and leukocyte chemoattractants (e.g. CXCL9, CXCL10), a phenomenon observed in both human 786-0 and mouse CT26WT cell lines (9, 10). Recent studies have further shown that the observed effect on STAT1/STAT2 ratios involves vanadate/VSVΔ51 induced hyperactivation of the the epidermal growth factor receptor (EGFR) receptor and downstream pathways including NF-kB (Nuclear Factor Kappa B) (19). Supporting this mechanism, Gefitinib, an EGFR antagonist, abrogated the enhancing effect of vanadium *in vivo* in a syngeneic CT26WT model (19).

In several immunocompetent tumor models including but not limited to CT26WT, DBT, and 4T1, combined vanadate/VSVΔ51 improved viral spread within the tumor, delaying tumor progression and leading to both long-term remission and persistent antitumor immunity in cured animals (10). Notably, approximately 80% of DBT- (glioma) tumor-bearing mice and 20% of CT26WT (colon) tumor-bearing mice demonstrated complete remission after the combination treatment. Additionally, vanadate/VSVΔ51 combination treatment led to an enhancement in T cell recruitment to tumor sites with significantly increased interferon-gamma (IFN-γ) producing CD8+ T cells, particularly in treatment-responsive animals (10). A similarly profound therapeutic benefit was observed in another study using NDV in combination with vanadyl sulfate (VS), although in this context innate immune mechanisms predominate (11). Altogether, a better understanding of the *in vivo* immunological mechanisms involved in eliciting the improved therapeutic benefit provided by vanadium compounds is critical to inform the design of improved OV therapeutic regimens. In this study we sought to better understand the *in vivo* immunological mechanisms that lead to improved antitumor responses brought about from the combination of VS and VSVΔ51 in order to devise strategies to further drive therapeutic benefit.

## 2 Results

### 2.1 VS+VSVΔ51 combination treatment upregulates the secretion of pro-inflammatory chemokines and cytokines *in vivo*

To explore the immunological mechanisms that lead to improved antitumor responses brought about from the

combination of VS+VSVΔ51, we chose to focus on the CT26WT colon cancer model (syngeneic in Balb/C). Subcutaneously implanted CT26WT tumors are inherently resistant to VSVΔ51 and while monotherapy is not curative, improved survival can be observed using a vanadate/VSVΔ51 therapeutic combination in this model, leading to approximately 20% complete remissions (10). Improved virus spread, as measured by VSVΔ51-encoded luciferase transgene-associated luminescence using an *in vivo* imaging system (IVIS), is also observed in this model (10). To confirm that similar effects were achievable using the body building supplement VS, mice were implanted with the CT26WT cells, and when tumors reached a volume of 100 $mm^3$, three doses delivered intratumorally of VS (50 mg/kg) or PBS, followed by 1E8 plaque forming units (PFU) VSVΔ51 (encoding luciferase) or PBS were administrated over the course of 5 days (Figure 1A). In line with previous studies with vanadate, improved viral replication elicited by VS was confirmed by IVIS imaging 1 day post the first treatment (Figure 1B). The combination treatment was well-tolerated but accompanied with a limited and transient decrease in body weight followed by quick recovery within the following week (Figure S1).

A multiplex assay was subsequently performed using collected sera to evaluate the secretion of a panel of pro-inflammatory chemokines and cytokines in the blood at various time points following the treatment (Figures 1C, D, E). Pooled sera were used to map general trends in cytokine profiles over time (Figure 1C). Further analyses using sera from individual mice were carried out to confirm trends.

Our findings from these analyses revealed that, apart from increasing Interleukin-6 (IL-6) on day 1 (Figure 1D), VS had little impact on overall cytokine secretion. On the other hand, VSVΔ51 alone significantly increased the secretion of proinflammatory cytokines and chemokines including IFN-γ, CXCL9, CXCL10, CCL3, CCL4, and IL15 compared with VS and PBS groups (Figures 1D, E). Importantly, we observed significant increases in the secretion of a subset of cytokines and chemokines in the group that received the combined therapy as compared to monotherapies. Most notably, we measured a 5-fold increase in IFN-γ secretion 1-day post-infection ((Figures 1C, D), p-value=0.0001 compared to PBS and VS, and p-value=0.01 compared to VSVΔ51 alone, Figure S2). IL-6, an IFN-γ responsive cytokine, increased most significantly at 5 days post treatment (Figures 1C, D). In addition to IL-6, IFN-γ is known to upregulate the secretion of pro-inflammatory cytokines and chemokines. This includes CXCL-9 and CXCL10, which we have previously shown to be upregulated through vanadate/VSVΔ51 combination treatment in CT26WT cells *in vitro* (10). However, while average levels were highest coinciding with the peak of IFN-γ secretion, there was no statistically significant difference in CXCL9 when comparing VSVΔ51 to VSVΔ51 in combination with VS (p=0.1, Figure S2).

## 2.2 Combined VS+VSVΔ51 therapy enhances antigen-specific antitumor immune response

In conjunction with previous studies (10), the results above support a potential role of activated and IFN-γ producing T-cells in eliciting the response to combined vanadate/VSVΔ51 therapy. We next sought to investigate the impact of VS treatment in combination with VSVΔ51 on viral- and tumor antigen-specific immune responses. We assessed the antigen specific immune response against peptides for gp70 (the immunodominant antigen in CT26WT tumor model and a common murine tumor-associated antigen that is highly expressed) and VSV N following combined therapy or controls using an IFN-γ ELISPOT assay. Fourteen days post treatment, splenocytes were isolated from mice and then stimulated *ex vivo* with gp70 or VSV N peptides (Figure 2A). A significant increase in the number of IFN-γ producing splenocytes reacting to the peptide gp70 was detected in the group that received VS+VSVΔ51 when compared with monotherapy alone (Figure 2B). As expected, treatment with VSVΔ51 alone induced an antiviral immune response measured by the reaction against the VSV N peptide in comparison with the combination treatment group (Figure 2B). However, we did detect a response against the DMSO control in the VSVΔ51 group, suggesting there could be non-specific activation owing to the virus treatment. Altogether, these results suggest that VS/VSVΔ51 combination therapy can improve the tumor antigen-specific T-cell response.

## 2.3 Enhanced antigenicity driven by vanadium implicates a cancer cell autonomous mechanism

In previous studies, we showed that the treatment of cancer cells with vanadate/VSVΔ51 leads to profound changes in gene expression profiles in infected cancer cells and in particular, the up-regulation of multiple cytokines and chemokines associated to response to type II IFN (10). This profile is corroborated from cytokine profiles in Figure 1. However, given that cytokine profiles measured in the blood are representative of systemic responses, it is not possible to discern the specific impact of VS +VSVΔ51 treatment on cancer cells from its potential impact on immune cells.

To better understand whether cancer-cell autonomous mechanisms could contribute to the improved tumor antigen responses observed in the vanadate/VSVΔ51 conditions, we employed a prophylactic infected cancer cell vaccination (ICV) model to isolate the impact of vanadate/VSVΔ51 treatment *in vitro* on the immunogenicity of the same *in vivo*. As previously published (20, 21), ICVs involve irradiation of cancer cells, followed by infection with an OV *in vitro*. Administration of

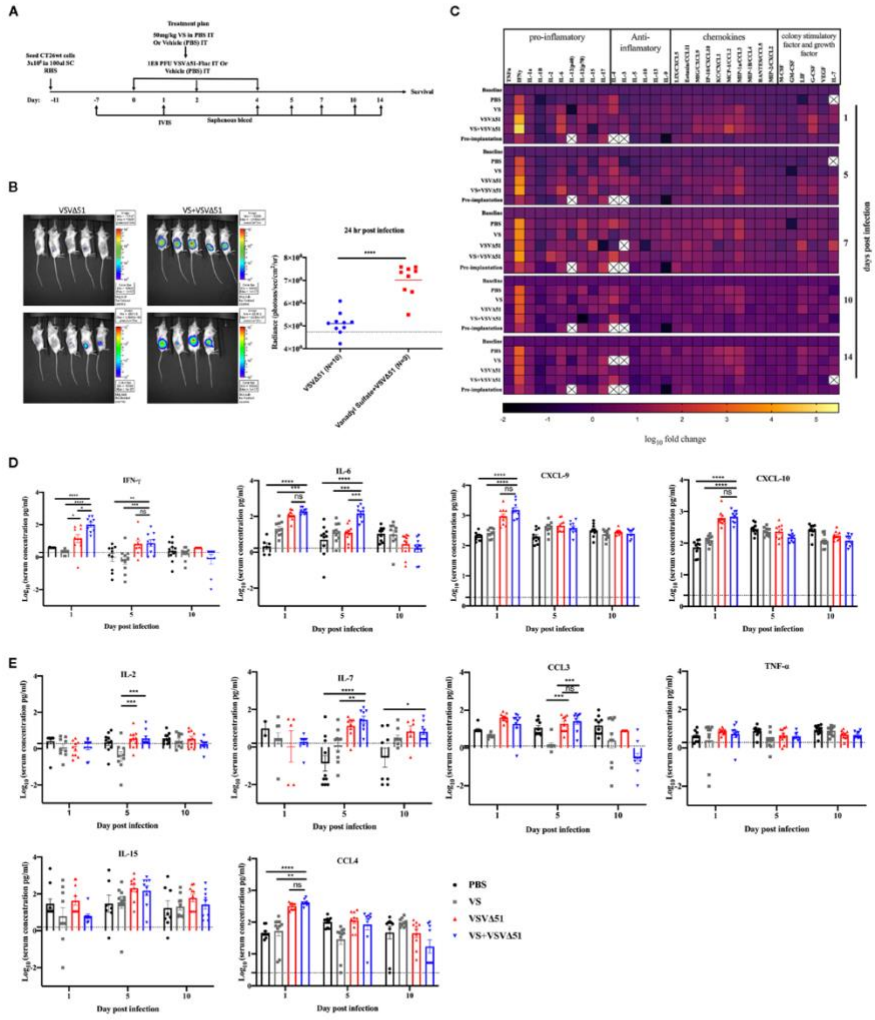


FIGURE 1
VS+VSVΔ51 co-treatment upregulates the secretion of pro-inflammatory chemokines and cytokines 1 and 5 days post the treatment. **(A)** Schematic representation of the treatment schedule: CT26WT-tumor bearing mice received a total of three doses delivered intratumorally of vanadyl sulfate (50mg/kg) and VSVΔ51-fluc (1E8 PFU) or monotreatment injections with PBS, vanadyl sulfate (50mg/kg), or VSVΔ51-fluc (1E8 PFU) alone over 5 days. **(B)** Twenty-four hours post the first treatment, viral replication was monitored by IVIS. Representative bioluminescence images of mice. Scale represented in photons, bar indicate mean. P=0.0007 as compared to mock-treated condition. **(C)** Heatmap represented the $\log_{10}$ fold change per condition of pooled sera for all the treated time points, normalized to day 7 post implantation as baseline. **(D, E)** The concentration of Cytokines and chemokines pg/ml for each group for each individual mouse, data transformed into $\log_{10}$. (n=10 per condition), line indicates the detection concentration, Mean ± SEM; * P=0.01, ** P=0.003, *** P=0.001,****P<0.0001, Two-way ANOVA.

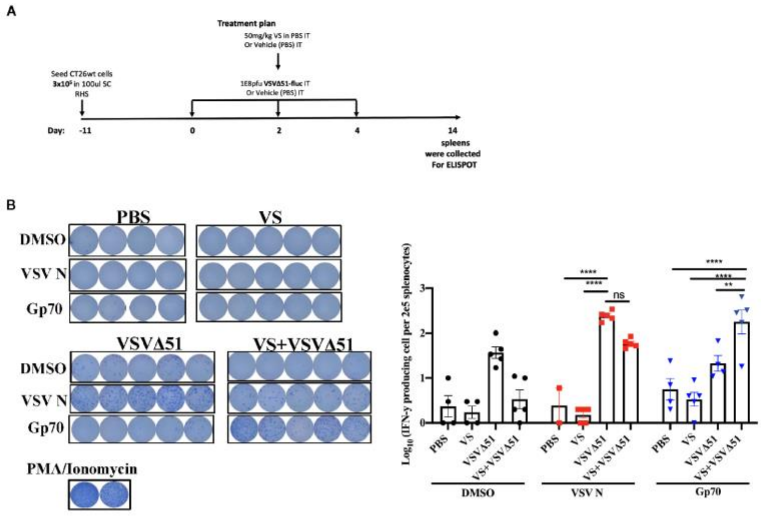


FIGURE 2
VS plus VSVΔ51 combination therapy further induces antigen specific immune response 14 days post treatment. **(A)** Schematic representation of the treatment schedule: after 12 days, CT26WT-tumor bearing mice received a total of three doses delivered intratumorally of vanadyl sulfate (50mg/kg) and VSVΔ51-fluc (1E8 PFU) or monotreatment injections with PBS, vanadyl sulfate (50mg/kg), or VSVΔ51-fluc (1E8 PFU) alone over 5 days. **(B)** Representative plates from an ELISPOT assay, splenocytes from treated mice were processed 14 days post treatment, then co-cultured with either DMSO, VSV N, or gp70 peptides for 20 hours, PMA and ionomycin were used as a positive control. Graph shows quantification of $\log_{10}$ of the number of IFN-γ producing cells per 2E5 splenocytes. N = 5 per condition, Mean ± SEM; **P=0.003, ****P<0.0001, ns, not significant, Two-way ANOVA.

ICV elicits both antitumor and anti-viral immune responses. The antitumor response can be further boosted when an initial prime with irradiated cancer cells alone is administered 7 days prior to the ICV (Figure 3) and can be measured among others by looking at the impact on tumor growth following challenge with the same cancer cells used to create the ICV.

We generated ICV preparations using 5E6 CT26WT cells infected with 5E7 PFU of VSVΔ51 (MOI=10), with or without 100μM vanadate. After collection, these were administered to Balb/C mice previously primed with irradiated CT26WT cells (5E6) intraperitoneally (i.p). On day 7 post ICV administration, mice were challenged with 5E5 CT26WT cells subcutaneously (s.c.). In Figure 3A, we monitored tumor progression following the ICV treatments. We observed that mice prophylactically treated with irradiated cells infected with VSVΔ51 in combination with vanadate developed fewer tumors with more delayed kinetics compared to the group receiving ICV made using VSVΔ51 alone (Figure 3B). In addition, ICV made using vanadate further stimulated specific killing against targeted cells loaded with gp70 peptides, as measured by *in vivo* CTL assay in vaccinated mice (p=0.0219 comparing ICV group with ICV +Vanadate group, Figure 3C). This altogether suggests that vanadate treatment of cancer cells in conjunction with VSVΔ51 infection promotes their inherent immunogenicity, independently of a direct impact of vanadate on immune cells. Given we have previously reported the increased expression of type II IFN response-induced chemo-attractants such as CXCL9 and CXCL10 following vanadate/VSVΔ51 co-treatment, we looked at whether VS+VSVΔ51 co-treatment could promote the recruitment of T-cells in a chemotaxis assay. As illustrated in Figure 4, cultured CT26WT cells were treated with PBS, VS 100μM, VSVΔ51 (multiplicity of infection (MOI)=0.01) or the combination of VS+VSVΔ51. Supernatants were collected 24h later and added to the lower chamber of Trans-well plates with 5-μm pores. A condition with CXCL9 cytokine (1 μg/ml) was included as a positive control. Mouse T-cells isolated from splenocytes were activated using anti-CD3/CD28 beads and IL-2 and then added to the top chamber. Activated cells were allowed to migrate to the bottom well containing supernatants for a period of 24h. The results of this chemotaxis assay are shown in Figure 4 and demonstrate that supernatants from VSVΔ51-infected cells co-treated with VS significantly increase

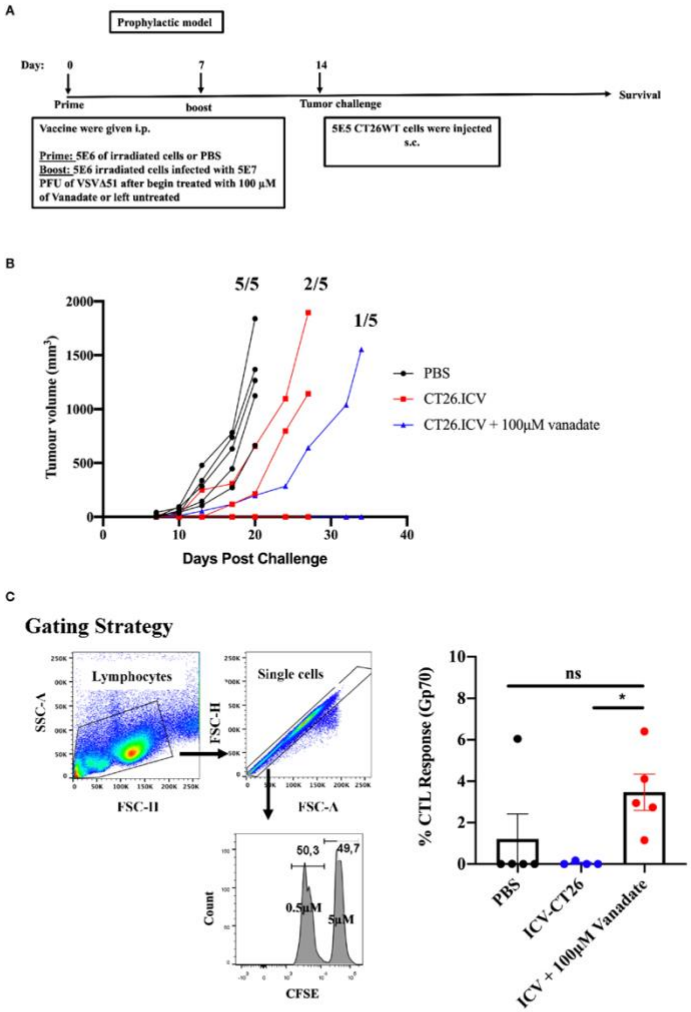


FIGURE 3
VS enhances irradiated infected cell vaccine antigenicity. **(A)** Schematic representation of the treatment schedule of prophylactic vaccine, CT26WT-tumor bearing mice injected with 5E6 irradiated CT26WT cells i.p. at day 0, and 7 days following that 5E6 irradiated CT26WT cells infected with 5E7 PFU VSVΔ51 with and without vanadate were injected i.p. At day 14, CT26WT cells were implanted s.c. **(B)** Tumor volume of each individual mouse measured over time (n=5 per condition). Fractions indicate the proportion of mice that developed tumors in each group. **(C)** following the same therapeutic regiment described in A, 7 days post the last treatment, splenocytes from immunized mice were harvested eighteen hours after injecting an equal number of $CFSE_{Hi}$ cells (that were labelled with 5µM CSFE) loaded with gp70 peptide and $CFSE_{Lo}$ cells (labelled with 0.5µM CSFE) unloaded with peptide, in equal proportions of 2E7/200µl total splenocytes intravenously (i.v.). The proportion of $CFSE_{Hi}$ and $CFSE_{Lo}$ was quantified by flow cytometry by first gating for lymphocytes using forward scatter (FSC) and side scatter (SSC) followed by single-cell gating, the $CSFE_{Hi}$ and $CFSE_{Lo}$ populations. The graph shows the percentage of specific killing against Gp70-CFSE-stained targeted cells compared to control groups. Mean ± SEM; * P = 0.02, One-way ANOVA, n = 5 per conditions. ns, not significant.

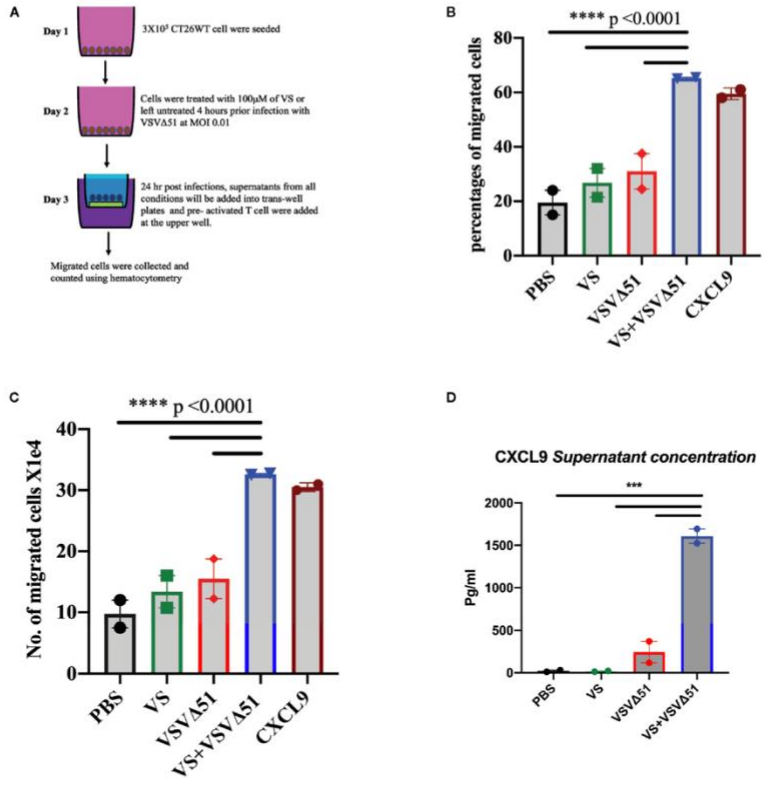


FIGURE 4
Vanadyl sulfate in combination with VSVΔ51 increases the production of T-cell chemoattractant and T-cell migration *in vitro*. **(A)** Tissue culture supernatants were collected after treating CT26WT cells with vanadyl sulfate at a concentration of 100μM for 4 hours prior infection with VSVΔ51 at MOI 0.01 or with PBS, vanadyl sulfate alone or VSVΔ51 alone for 24 hour and subsequently used for the assessment of chemokines or for performing chemotaxis assays (compared to CXCL9 control). Chemotaxis of T cells was assessed using a Trans-well system. **(B)** Migration percentage was calculated as (total number T cells in bottom chamber/total number T cell input) x 100. **(C)** The Number of migrated cells $X10^4$ with the mean of the duplicate for each condition. Mean ± SEM; ****P<0.0001, Two-way ANOVA. Representative data of the average of 2 independent experiments, n = 2 per condition. **(D)** The supernatant concentration of CXCL-9, graph shows the pg/ml. Mean ± SEM; n = 2 per condition, *** P = 0.001, Two-way ANOVA.

the migration of activated T-cells compared to single treatments, to levels exceeding the CXCL9 positive control (Figures 4B, C). The CXCL-9 concentration in the supernatants used in the migration assay was measured by ELISA. As shown in Figure 4D, treatment with VS+VSVΔ51 substantially increased the secretion of CXCL-9 compared to single treatments. Altogether, these data support the hypothesis that treatment of cancer cells with vanadium during infection increases their immunogenicity profile and promotes the migration of activated T-cells to the tumor.

## 2.4 VS in combination of VSVΔ51 encoding IL-12 further improves therapeutic efficacy

The results above implicate a role of T-cells in eliciting the enhanced therapeutic effects of VS+VSVΔ51 treatment and that is also associated with up-regulation in the secretion of pro-inflammatory cytokines and chemokines; however, the overall survival is still 20% in the CT26WT tumor model (Figure S3). We therefore considered whether therapeutic efficacy could be

further enhanced by genetically encoding complementary cytokines in VSVΔ51.

As a first candidate and proof of concept, we evaluated the impact of encoding IL-12 within VSVΔ51. IL-12 is produced by dendritic cells (DC) in response to IFN-γ secretion to enhance the activity of CD8+ cytotoxic T-cells (CTL) as well as Natural Killer cells (NK) (22, 23). Further, IL-12 is thought to be a positive regulator of IFN-γ secretion. Many OVs such as Maraba-MG-1, Adenovirus, and HSV-1 have been engineered to express IL-12, leading to improved antitumor effects in numerous murine carcinoma models by promoting both the activation of T cells and NK cells (24, 25). As a first step, multi-step and single-step viral growth kinetics were determined in CT26WT cells, and the inclusion of IL-12 as transgene had no impact on virus replication kinetics compared with parental virus VSVΔ51encoding firefly luciferase (Figure S4A). In addition, IL12 secretion was confirmed 24 hr following viral infection compared with the parental virus (around 6000pg/ml) (Figure S4B). To validate the impact of IL-12 in our system, we performed a similar therapeutic regimen as shown in Figure 1A with VSVΔ51 encoding/expressing IL12 (Figure 5A) and then monitored tumor progression and survival following the treatment. Combination treatment was well-tolerated although we did observe a slight decrease in the body weight of mice treated with VSVΔ51 encoding/expressing IL12 during the week of the treatment followed by quick recovery within the following week (Figure S1). Our data demonstrate that approximately 40% of the group receiving VS in combination with VSVΔ51-IL-12 survived compared to 20% in the VS+VSVΔ51 condition, and only 10% in the group receiving the VSVΔ51 expressing IL-12 alone (Figures 5B, D). These mice also showed rejected tumors after re-challenge with CT26WT cells. The inclusion of IL-12 to VSVΔ51 in combination with VS also further enhanced the antigen specific immune response against the gp70 peptide (Figure 5C); however, there was no apparent improvement in comparison with VS+VSVΔ51 treatment (compare Figures 2B and 5C). Cytokine profiling by multiplex assay (Figure 6A) revealed a trend towards increasing systemic IL-12 with VSVΔ51-IL12 and further with VS+VSVΔ51-IL12, which was the only condition showing a statistically significant increase in IL-12 relative to PBS (p-value=0.023, Figure S5) (Figures 6B, C, D). In contrast with results obtained in Figure 1, VS+VSVΔ51-IL12 co-treatment did not elicit a further increase in the levels of IFN-γ compared to VSVΔ51-IL12 (Figures 6B, C); however, compared to Figure 1D, it is apparent that when viruses were used alone, IFN-γ reached higher levels on day 1 with VSVΔ51-IL12 compared to VSVΔ51 (more than 200 pg/ml vs. around 100 pg/ml). On the other hand and consistent with Figure 1C, levels of IL-6 were significantly higher at day 5 following VS+VSVΔ51-IL12 combination treatment compared to the monotherapies (Figures 6B, C). Taken together, these data provide compelling evidence that further improvements in therapeutic efficacy can be achieved through genetic complementation by encoding cytokines such as IL-12 that are not otherwise up-regulated by VS/VSVΔ51 co-treatment.

## 3 Discussion

In this study, we found evidence that VS+VSVΔ51 combination treatment leads to an increase in the *in vivo* secretion of type II-IFN related cytokines, including IFN-γ and IL-6. Complementing previous studies showing increased infiltration of activated T-cells in tumors from combination-treatment responsive animals (10), we observed an increase in the number of tumor antigen-specific T-cells in the spleen. These findings were supported by the notion that treatment of cancer cells with vanadate during infection with VSVΔ51 can increase the immunogenicity of cancer cells, which is explained in part by a cancer cell autonomous driven mechanism as confirmed by the ICV and *in vitro* chemotaxis experiments.

The role of IFN-γ in the context of the antitumor immune response remains unclear based on the literature. For example, it has been reported that antigen-specific T-cells increase IFN-γ concentration in tumor tissue, which facilitates tumor clearance (26). However, IFN-γ also induces the expression of PD-L1 on lymphatic endothelial cells, negatively impacting cytotoxic T-cell activity and migration from the peritumoral space to the tumor microenvironment (27). High levels of IFN-γ can also induce apoptosis in tumor-specific T-cells and compromise antitumor immunity (28, 29). On the other hand, recent reports have suggested that tumor IFN-γ signatures are associated with greater response to immune checkpoint blockade (30), other studies have also shown that encoding IFN-γ from OVs like VSVΔ51 can improve therapeutic benefit (31).

While we observed elevated IFN-γ at early timepoints following combination treatments with VS and VSVΔ51, we did not see further increases in IFN-γ secretion when including IL-12 as a transgene, despite nearly doubling the rate of complete remissions (from 20% to 40%). While we cannot exclude the possibility that IFN-γ may negatively impact the effect of VS and VSVΔ51, this suggests that other factors must contribute to curative responses. One hypothesis that warrants further study is that an increased chemotaxis of activated and tumor antigen-specific cytotoxic T-cells to the tumor, potentially *via* chemokines such as CXCL9 and CXCL10. Indeed, this is supported by our previous studies showing more substantially elevated levels of activated T-cell in tumors in the process of regression in comparison to non-responders (10).

Interestingly, we found that IL-6 is consistently and significantly increased with VS combination treatments using either VSVΔ51 or VSVΔ51-IL12 during the first 5 days post treatment. IL-6 is an NF-kB-regulated cytokine known to inhibit T-cell apoptosis and prevent regulatory T-cell differentiation, but also plays an essential role in the differentiation of

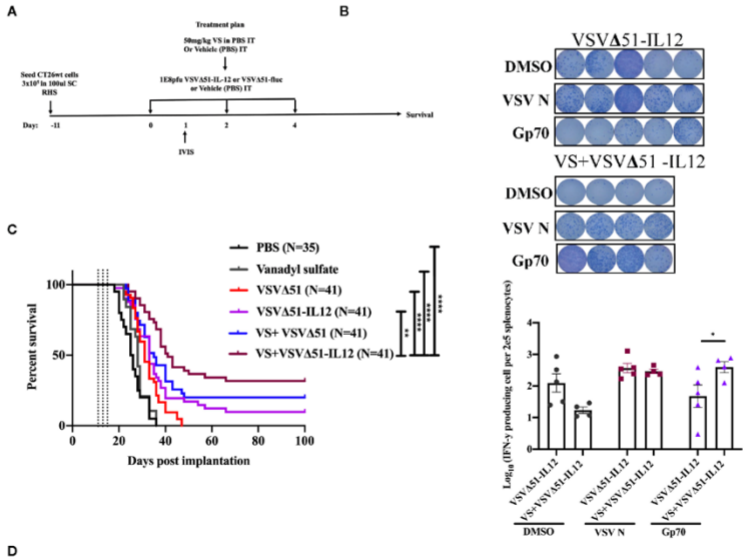


D

| | PBS | Vanadyl Sulfate | VSVΔ51 | VSVΔ51-IL12 | VS+ VSVΔ51 |
|---|---|---|---|---|---|
| PBS | X | ns | 0.0001 | <0.0001 | <0.0001 |
| Vanadyl Sulfate | ns | X | 0.006 | 0.001 | 0.0001 |
| VSVΔ51 | 0.0001 | 0.006 | X | 0.04 | 0.004 |
| VSVΔ51-IL12 | <0.0001 | 0.001 | 0.04 | X | ns |
| VS+VSVΔ51 | <0.0001 | 0.0001 | 0.004 | ns | X |
| VS+VSVΔ51-IL12 | <0.0001 | <0.0001 | <0.0001 | 0.001 | 0.08 |

FIGURE 5
Vanadyl sulfate in combination with VSVΔ51 encoding/expressing IL-12 improves the therapeutic efficacy in CT26WT-tumor model **(A)** Schematic representation of the treatment schedule: CT26WT-tumor-bearing mice received a total of three dose delivered intratumorally of vanadyl sulfate (50mg/kg) and VSVΔ51 expressing IL-12 (1E8 PFU) or with PBS, vanadyl sulfate (50mg/kg), or VSVΔ51 expressing IL-12 (1E8 PFU) alone over 5 days. **(B)** Survival was monitored over time, the percentage of survival was included for each condition, Long rank (Mantel-Cox) test indicated the significance as shown in table below. Survival data represents an aggregate of 3 independent studies. **(C)** as part of Figure 2, two additional groups received three intratumorally vanadyl sulfate (50mg/kg) and VSVΔ51 expressing IL-12 or monotreatment injections over 5 days. representative data from ELISPOT assay and Graph shows quantification of $\log_{10}$ of the number of IFN-γ producing cells per 2E5 splenocytes. Mean ± SEM; * P=0.01, ** P=0.003, ****P<0.0001, Two-way ANOVA. **(D)** Table shows the significance values using Long rank (Mantel-Cox), * P=0.01, ** P=0.003, ****P<0.0001.

monocytes to macrophages (32). As previously reported by Fisher et al. and others, IL-6 can further increase naïve and central memory T cell trafficking to the tumor (32–34). The elevated levels of IL-6 observed peaking at 5 days post treatment in this study are therefore consistent with an increase in tumor-antigen-specific T-cell response (Figure 2). This observation is also consistent with previous *in vitro* studies, implicating EGFR pathway activation as a molecular mechanism of vanadium compounds, leading to simultaneous downregulation of STAT2 and hyperactivation of both STAT1 and NF-kB (19). On the other hand, IL-6 is also suspected to play a role in tumour development (35) and some groups have found a correlation between high circulating levels of IL-6 and poor prognosis in cancer patients (36). However, in this study we observed only transiently increased levels of IL-6 returning to normal levels after day 5. The observation of complete tumor regression in this context suggests that at least transient up-regulation of IL-6 may be beneficial to generate robust anti-tumour responses.

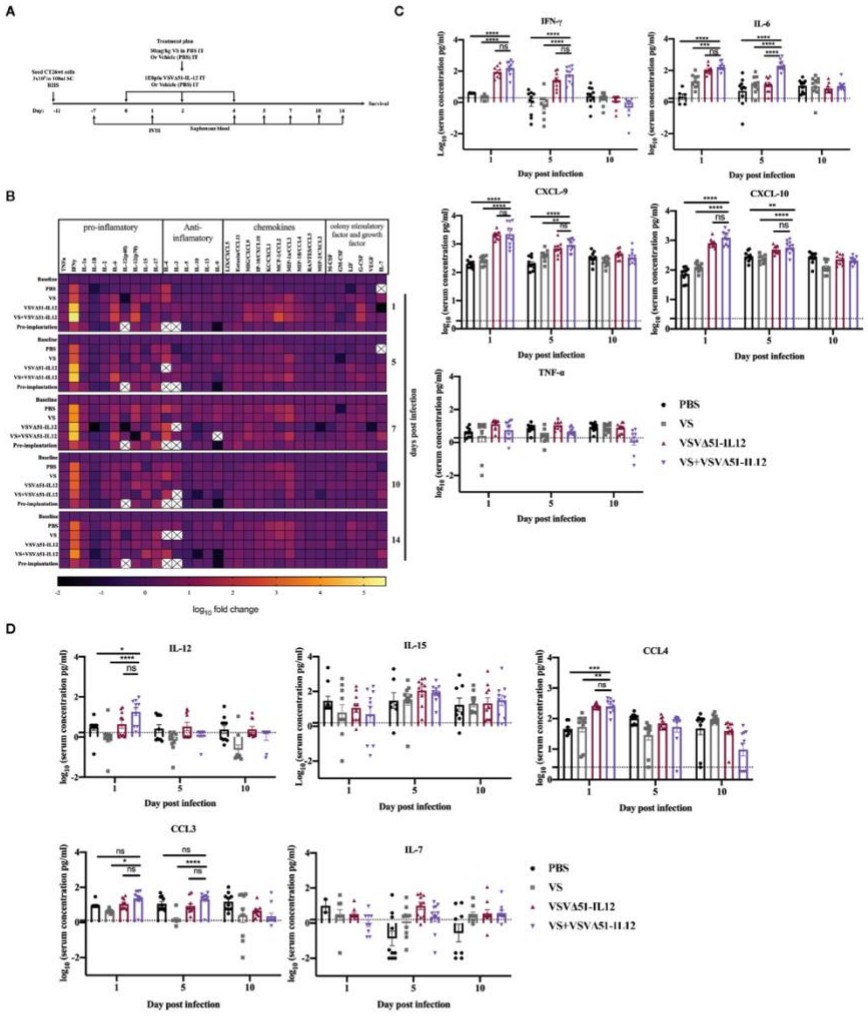


FIGURE 6
VS+VSVΔ51 encoding/ expressing IL12 co-treatment further induces the upregulation of the secretion of pro-inflammatory chemokines and cytokines 1 day and 5 days post the treatment. **(A)** CT26WTtumor bearing mice received a total of three doses delivered intratumorally of vanadyl sulfate (50mg/kg) and VSVΔ51 expressing IL-12 (1E8 PFU) or with PBS, vanadyl sulfate (50mg/ kg), or VSVΔ51 expressing IL-12 (1E8 PFU) alone over 5 days. **(B)** Heatmap of the $log_{10}$ fold change per condition of pooled sera, normalized to day 7 post implantation as baseline for all the tested time points. **(C, D)** The concentration of cytokines and chemokines pg/ml for each group for each individual mouse (n=10 per condition) was presented in each graph. Data transformed into $Log_{10}$, line indicated the detection concentration, Mean ± SEM; * P = 0.01, ** P = 0.003, *** P = 0.001, ****P < 0.0001, Two-way ANOVA. ns=not significant

We observed increased gp70 specific T-cells in the spleen of animals treated with combination regimen. While there was also a detectable increase in anti-viral immune response in the combination treatment, its magnitude was subdued compared to the increase in anti-gp70 response (Figure 2B). One possibility is that the tumor-specific antigen response is in effect a memory response since the tumors were implanted over a week prior to the first virus treatment. Supporting this idea, we find that in the ICV model, antitumor responses are significantly improved following an initial prime with irradiated CT26WT cells, followed by a boost with infected-irradiated cells a week or more later (Figure 3C). If validated, this hypothesis may further suggest a preferential impact of vanadate on memory T-cells as opposed to naïve T-cells. Further studies will be required to address this question.

In this study, IL-12 was selected for provision in cis with VSVΔ51 to enhance the therapeutic effect in combination with VS in part because it was previously shown to provide therapeutic benefit with other OVs (37–40). While it is challenging to rationalize the choice of transgene to enhance OV activity based on cytokine profiling owing to the complexity and kinetics of cytokine signaling networks, cytokine profiling in this case was helpful to rationalize IL-12 as a choice to further improve activity. IL-12 is known to drive IFN-γ expression which led us to hypothesize that inclusion of the IL-12 transgene may further drive upwards IFN-γ secretion when included within the virus. However, underscoring the complexity of cytokine networks, we did not observe increased IFN-γ secretion upon inclusion of IL-12 within VSVΔ51, despite observing improved therapeutic effects. While significantly increased at day 1 following treatment in the VS+VSVΔ51-IL12 condition compared to PBS, we found that IL-12 levels in the blood remained low (Figure 6). However, high levels of replication in the tumor as measured with VSVΔ51-Fluc in combination with VS (Figure 1), may suggest that a localized IL-12 delivery safely generates a systemic effect that induces an antitumor immunity that benefits a locally initiated immune response (41–43). It would be interesting to determine whether supplementation of cytokines and chemokines not detected to be significantly up-regulated but that could play a complementary role could further enhance activity in combination with VS when encoded in the virus either alone or potentially in combination with IL-12.

In conclusion, our results add to a growing body of evidence demonstrating the potential of vanadium compounds as viral enhancers in combination with OVs to improve their therapeutic efficacy. This study provides a new framework for understanding the immunological impacts of vanadium-VSV combinations, and provide a path forward for therapeutic regimen optimization, exemplified by the combination of VS and VSVΔ51-IL12.

# 4 Material and methods

## 4.1 Drugs

The vanadium-based compounds used in this study were sodium orthovanadate and vanadyl sulfate. Sodium orthovanadate was used for all ICV experiments ($Na_3VO_4$, Sigma-Aldrich, Cat# 450243) and was dissolved in water and pH adjusted to 10 at 100μM. Where otherwise indicated, vanadyl sulfate at 50 mg/kg ($VOSO_4$, Sigma-Aldrich, Cat# 204862) dissolved in PBS was used for *in vivo* experiments whereas 100μM was used for *in vitro* experiments.

## 4.2 Cell lines

CT26WT (murine colon carcinoma, Cat.CRL-2638) was obtained from the American Type Culture Collection (ATCC). These cells were cultured in HyQ high-glucose Dulbecco's modified Eagle's medium (DMEM; HyClone Cat#10-013) supplemented with 1% (v/v) penicillin-streptomycin (Gibco Life Technologies, Waltham, MA), and 10% (v/v) serum composed of 3-parts HyClone newborn calf serum (Thermo Fisher, Cat# SH3011803) and 1-part Fetal Bovine Serum (Gibco, Cat# 12483020). All cells were incubated at 37C in 5% CO2 humidified incubator and regularly tested to ensure they are free of mycoplasma contamination.

## 4.3 Viruses

### 4.3.1 Rhabdovirus

VSVΔ51-Fluc: The Indiana serotype of VSV used throughout this study was propagated in Vero cells and purified on 5-50% Optiprep (Sigma-Aldrich, St. Louis, MO). VSVΔ51 expressing firefly luciferase are recombinant derivatives of VSVΔ51 described previously (10).

VSVΔ51 encoding/expressing IL-12: VSVΔ51 encoding/expressing IL-12 was generated in the laboratory of Dr. Rebecca Auer using PCR amplified from pORF-mIL12 [IL12elasti(p35:p40); *In vivo*Gen] (20). Virus was produced and purified on 5-50% Optiprep (Sigma-Aldrich, St. Louis, MO) in our laboratory.

## 4.4 Mouse tumor model

Six-week-old female BALB/c mice obtained from Charles River Laboratories (Senneville, Canada) were implanted with subcutaneous tumors by injecting 3E5 syngeneic CT26WT cells, suspended in 100μl serum-free DMEM. Eleven days post implantation when tumor reached a volume of 100 $mm^3$, mice

were treated intratumorally vanadyl sulfate (dissolved in PBS) at 50mg/kg in 50µl or 50µl of PBS. Four hours later, mice were treated intratumorally with 1E8 plaque forming units (PFU) in 25µl PBS of the indicated viruses as described previously (10). Tumor sizes were measured three times a week using electronic calipers. Tumor volumes were calculated based on this equation (length$^2$ X width)/2. All *in vivo* experiments were performed in accordance with the University of Ottawa Animal Care and Veterinary service guidelines for animal care under the protocol OHRIe-2265-R5 and OHRI-2265-R4 A2.

## 4.5 Blood and serum sample processing

For blood samples, saphenous bleeds were performed in one of the legs and blood was collected in tubes containing Serum-Gel (Sarstedt Inc, Fisher Scientific, Cat. NC9315741) to allow serum separation by centrifugation (14 000 rpm) for 10 mins using Eppendorf centrifuge 5418R, then serum was used for measuring cytokine and chemokines. Serum samples were stored at –80C after collection.

## 4.6 Multiplex assay

Serum from blood samples was collected at day 7 days post implantation as a baseline, and 24 hours to 14 days post treatment. Serum was then added in duplicate for each sample in a 96-well plate, and magnetic microspheres premixed with 32-plex beads were added according to the manufacturer's recommendation (MILLIPLEX MAP Mouse Cytokine/Chemokine Magnetic Bead Panel - Premixed 32 Plex - Immunology Multiplex Assay, Millipore Sigma, Cat# MCYTMAG-70K-PX32) and incubated overnight at 4°C. A biotinylated detection antibody was added, followed by streptavidin-PE conjugate antibody incubated for 1 hr at room temperature. Plates were run in the Luminex® analyzer (MAGPIX®), using a CCD-based analysis that captures and detects components with the speed and efficiency of magnetic beads. All measurements were performed using a MAGPIX instrument (Luminex, Ottawa, CA), following the manufacturer's instructions. Data were collected using xPonent software (Luminex, Version 4.2), log transformed, and analyzed as described below in the statistical analysis section.

## 4.7 Splenocyte processing

Spleens were processed into single cell suspension by first transferring the spleen into sterile 70µm cell strainers on 50 ml conical tubes. Then, spleens were softly minced by pressing against the flat side of a syringe plunger in a circular motion. Cell strainers were washed with 5 ml of R 10 media. Tubes containing the cell suspension were topped up with media and spun at 300 g for 5 mins. Carefully, supernatants were removed without disturbing the pellet and cells resuspended by gently tapping before adding the ACK (Ammonium-Chloride-Potassium) lysing buffer (Gibco™, Cat# A1049201) for lysing red blood cells in samples for 5 mins. Cells were then washed and resuspended with R 10 media.

## 4.8 Peptides for *ex vivo* stimulation

Peptides used for *ex vivo* stimulation were gp70 tumor peptide: H-2Ld SPSYVYHQF (MBL International Corporation, Cat# SPM521) and VSV N virus peptide: H-2Ld MPYLIDFGL (CanPeptide Inc, custom peptide)

## 4.9 Mouse IFN-γ single-color enzyme-linked immune absorbent spot

Cells from spleens were processed as previously described and then resuspended in CTL media (provided with the ELISPOT kit, Immunospot, Cat# mIFNgp-1M/5) in 2E5 cells/100µl before being added to IFN-γ pre-coated plates (Immunospot, Cat# mIFNgp-1M/5) containing 100µl/well of each stimulant including either gp70 or VSV N peptides at a final concentration of 10 µM as well as unstimulated control (equivalent amount of DMSO). PMA ((Phorbol 12-myristate 13-acetate, Sigma-Aldrich, Cat# P8139)/ionomycin (Sigma-Aldric Cat# I9657) for pooled samples were used as a positive control at 2µg/ml. Plates were then incubated at 37°C for 20 hours. Following that, ELISPOT assays were developed following the manufacturer's protocol. Plates were scanned and spots were counted using CTL S6 ImmunoSpot analyzer.

## 4.10 Infected cell vaccine preparation

CT26WT cells were harvested and washed twice with Phosphate Buffered Saline (PBS; Corning, Manassas, VA), and then resuspended in DMEM at 5E7 cells/mL (± 10%). Cells were then irradiated in a Pantak HF320 X-Ray machine (OHRI, Ottawa, CA) for 60 Gy before infection with VSVΔ51 at a Multiplicity of Infection (MOI) of 10, for 2 hours in rotation before *i.p.* delivery (5 x 10$^6$ cells; 5E7 plaque forming units (PFU) of virus/mouse). Irradiated CT26WT cells (*irr)* were prepared similarly without the infection step. Cells were treated with 100µM vanadate before infecting them for some conditions.

## 4.11 Infected cell vaccine mouse model

In prophylactic treatment model: BALB/c mice were treated with 5E6 irradiated CT26WT cells on day 0 intraperitoneally (i.p.), followed by treatment with ICV on day 7 i.p (5E6 irradiated CT26WT cells infected with 5E7 PFU of VSVΔ51). At day 14 mice were challenged with 5E5 CT26WT cells s.c.

## 4.12 *In vivo* CTL assay

Donor splenocytes from naïve Balb/c mice were labelled with either a high (5μM) or low (0.5μM) concentration of carboxyfluorescein succinimidyl ester (CFSE; ThermoFisher Scientific, Waltham, MA, Cat# 65-0850-84) for 10 minutes at 37C. Each tube was then topped up with R 10 media and spun down for 5 minutes at 1500 rpm to remove excess dye. The CFSE-high ($CFSE_{Hi}$) population of naïve splenocytes is subsequently peptide-loaded with exogenous tumour gp70 tumour peptide (H2Ld-restricted, SPSYVYHQF; MBL International, Woburn, MA) at a concentration of 5μM for 45 minutes at 37°C rotated every 15 mins, whereas the CFSE-low ($CFSE_{Lo}$) population was left unloaded. Cells were washed with R 10 media to remove excess peptides and spun down for 5 minutes at 1500 rpm, then re-suspended in serum-free media. An equal number of $CFSE_{Hi}$ and $CFSE_{Lo}$ populations were combined in equal proportions of 1E7 cells/100μl each in serum-free media and a total of 2E7/200μl cells were administered intravenously (i.v.) to previously vaccinated mice. Eighteen hours later, vaccinated mice were sacrificed and splenocytes were harvested. Flow cytometry was used in order to assess the relative elimination of the tumour antigen-loaded $CFSE_{Hi}$ population compared to control groups. Percent specific lysis was calculated based on this equation Percent specific lysis= [1-[($CFSE_{Lo}$/$CFSE_{Hi}$ in PBS mice)/($CFSE_{Lo}$/$CFSE_{Hi}$ in treated mice)]]x100.

## 4.13 Migration/chemotaxis assay

CT26WT cells were pretreated with 100 μM VS or PBS for 4 hours followed by viral infection with VSVΔ51 at MOI 0.01 or mock infection. 24 hours later, cultured supernatants were collected and subsequently used for the assessment of chemokines or for performing chemotaxis assays. Chemotaxis of T cells was assessed using a Trans-well system as described previously (20). Briefly, 700μl of conditioned media from CT26WT cell cultures described above was added to the lower chamber of Trans-well plates with 5-μm pores (Costar, Corning, sigma-Aldrich, Cat# CLS3421-48EA). 5E5 activated CD3+ T cells from naïve spleen were purified by negative selection using EasySep™ mouse isolation T cell kit (Stemcell technologies, Cat# 19851) and then activated with 2μg of anti-CD3/CD28 in a precoated plate (BD Pharmingen™, CD3 Cat# 550275 and CD28 Cat# 553295) supplemented with 2ng/ml of murine recombinant IL-2 (PeproTech, Cat# 212-12) for 2 days, were added to the upper chamber, and plates were incubated for 24 hours at 37°C. After 24 hours, cells in the lower chambers were collected, stained with trypan blue and counted with a hemacytometer. Migration percentage was calculated as follows: total number of T cells in bottom chamber/total number of T cell input) x 100 (20).

## 4.14 Viral growth curves

3E5 of CT26WT Cells were seeded in 24 well plates for overnight confluency. Cells were then inoculated with VSVΔ51-Fluc at an MOI of 0.01 (multi-step growth curve) or 1.0 (single-step growth curve). Cells infected at MOI 1.0 were incubated for 60 minutes, followed by washing and replenishing with fresh medium. Cells were incubated up to 48 hours post infection (hpi), with 200 μl of supernatant collected and frozen at -80°C at the following timepoints: 0, 4, 8, 12, 24, 32, 48 hpi. Viral titer in collected supernatant was quantified by high-throughput tittering using a standard plaque assay.

## 4.15 Plaque assay

For virus titration using standard plaque assay, Vero cells African green monkey kidney cells, Cat# CCL-81) obtained from the American Type Culture Collection (ATCC) were seeded into 12-well plates at a final density of 3E5 cells per well. Infectious supernatants were serially diluted using serum-free DMEM, transferred (500μL/well) onto Vero cells and incubated at 37° C, 5% CO2 for 45 minutes, following which media was removed and replaced with 1ml/well of an agarose overlay (1:1 ratio of 1% agarose mixed with 2X DMEM containing 20% FBS). After a 24 hours incubation, plaques were fixed with methanol: glacial acetic acid in a 3:1 ratio for a minimum of 1 hour, then stained for 30 minutes with a Coomassie Blue solution (4 g Coomassie Brilliant Blue R (Sigma, Cat# B0149), 800 ml methanol, 400 ml acetic acid and 2800 ml distilled water) to visualize and count plaques.

## 4.16 IL-12 p70 Enzyme-linked immunosorbent assay

Supernatants from infected CT26WT cells with VSVΔ51 encoding Fluc or IL12 at MOI 0.1 were collected 24 hours post infection. The secretion of IL12 was measured using mouse IL-12 p70 Quantikine ELISA (Mouse IL-12 p70 Quantikine ELISA Kit, R&D system, Cat#M1270) following the manufacturer's instructions. Absorbance values at 450nM were measured on a Multiskan Ascent Microplate Reader (MXT Lab System) and corrected for plate imperfections at 540. Data were analyzed using Prism.

### 4.17 CXCL9 Enzyme-linked immunosorbent assay

CT26WT cells were pretreated with 100 μM VS or PBS for 4 hours followed by viral infection with VSVΔ51 at MOI 0.01 or mock infection. 24 hours later, cultured supernatants were collected and the concentration of CXCL9 was measured using mouse MIG/CXCL9 ELISA Kit (ELM-MIG, RayBiotech, Cat# ELM-MIG-2) following the manufacturer's instructions. Absorbance values at 450nM were measured on a Multiskan Ascent Microplate Reader (MXT Lab System) and corrected for plate imperfections at 540. Data were analyzed using Prism.

### 4.18 Statistical analysis

Statistical significance was calculated using Student's t test or one-way or two-way ANOVA tests with Sidak or Dunnett's multiple correction test was applied when groups were split on multiple independent variables and also using Tukey's multiple comparison test. Mantel-Cox log rank test was used to determine significant differences in plots for survival studies. Error bars represent standard error of the mean. Significance is based on a p value <0.05. Statistical analyses were performed using Graph-Pad Prism 8.0 (GraphPad software, LLC) and Excel. For multiplex data, the analysis software is milliplex analyst, version 5.1.0.0. VigeneTech Inc using 5 parameter curve fitting (log scale). Data were then transformed to $\log_{10}$ then normalized to the baseline values for each cytokines/chemokines for each time point to quantify the fold changes. For individual response, data transformed to $\log_{10}$ as plotted in the graphs to be able to see the significant difference. For ELISPOT analysis software is ImmunoSpot version 7.0.20.0, Flow cytometry was performed at the University of Ottawa's Flow Cytometry Core Facility using the BD LSR Fortessa (BD) or BD Celesta (BD) Flow Cytometers. Analysis of flow data was conducted using FlowJo v10 (FlowJo, LLC, Ashland, OR). For all analyses, *p < 0.05, 872 **p < 0.01, ***p < 0.001, ****p < 0.0001; n.s. = not significant.

## Data availability statement

The original contributions presented in the study are included in the article/Supplementary Material. Further inquiries can be directed to the corresponding author.

## Ethics statement

All *in vivo* experiments were performed in accordance with the University of Ottawa Animal Care and Veterinary service guidelines for animal care under the protocol OHRIe-2265-R5 and OHRI-2265-R4 A2.

## Author contributions

Conceptualization, NA and J-SD; Methodology, NA conducted the *in vitro* and *ex vivo* experiments. NA and AC performed all *in vivo* experiments. RoA contributed to the IL-12 related *in vivo* survival experiments. AJ, ZT, and GM assisted with tissue processing. OV and SK contributed to the experimental design and performed the ICV experiments. NA and J-SD designed the experiments, performed data analyses, and wrote the paper. RoA, NF, and DS, helped with experimental design. NA, DS, RoA, AJ, ZT, and J-SD reviewed the paper; Funding Acquisition, J-SD; Supervision, J-SD. All authors contributed to the article and approved the submitted version.

## Funding

J-SD is supported by funding from the Terry Fox Research Institute, TFF-122868 (J-SD) Canadian Institutes of Health Research, grant INI-147824, Canadian Institutes of Health Research, grant #705952, a Canadian Cancer Society grant supported by the Lotte & John Hecht Memorial Foundation, grant #703014 (J-SD). NA is supported by a scholarship from King Faisal Specialist Hospital and Research Center, Riyadh, Saudi Arabia (KFSHRC) representative by Saudi Arabian Cultural Bureau in Canada (SACB). ZT is funded by NSERC Alexander Graham Bell Canada Graduate Scholarship, Ontario Graduate Scholarship, and Mitacs CanPRIME Accelerate fellowship. AJ is supported by the MITACS Accelerate Canadian Partnership in Immunotherapy Manufacturing Excellence PhD Internships. OV was supported by a CIHR Master's Award.

## Acknowledgments

The Authors thank Almohand Alkayyal for his generous help with optimizing the migration assay, Alexandra Acal for her assistance with some experiments, and Stephanie Burke Schinkel for her generous help with the MAGPIX instrument. The Authors also thank Dr. Debbie C. Crans for her helpful discussion surrounding vanadium chemistry

## Conflict of interest

J-SD is co-inventor on a patent covering the use of vanadium compounds as enhancers of RNA viruses and holds shares in

Virica Biotech and Virano Therapeutics that hold licenses to this intellectual property.

The remaining authors declare that the research was conducted in the absence of any commercial or financial relationships that could be construed as a potential conflict of interest.

## Publisher's note

All claims expressed in this article are solely those of the authors and do not necessarily represent those of their affiliated organizations, or those of the publisher, the editors and the reviewers. Any product that may be evaluated in this article, or claim that may be made by its manufacturer, is not guaranteed or endorsed by the publisher.

## Supplementary material

The Supplementary Material for this article can be found online at: https://www.frontiersin.org/articles/10.3389/fimmu.2022.1032356/full#supplementary-material.

## References


1. Ilkow C, Swift S, Bell J, Diallo J. From scourge to cure: Tumour-selective viral pathogenesis as a new strategy against cancer. *PLoS Pathogens*. (2014) 10(1): e1003836. doi: 10.1371/journal.ppat.1003836

2. Russell S, Peng K, Bell J. Oncolytic virotherapy. *Nat Biotechnol* (2012) 30 (7):658–70. doi: 10.1038/nbt.2287

3. Lawler S, Chiocca E. Oncolytic virus-mediated immunotherapy: A combinatorial approach for cancer treatment. *J Clin Oncol* (2015) 33(25):2812–4. doi: 10.1200/JCO.2015.62.5244

4. Van Vloten J, Workenhe S, Wootton S, Mossman K, Bridle B. Critical interactions between immunogenic cancer cell death, oncolytic viruses, and the immune system define the rational design of combination immunotherapies. *J Immunol* (2018) 200(2):450–8. doi: 10.4049/jimmunol.1701021

5. Martinez-Quintanilla J, Seah I, Chua M, Shah K. Oncolytic viruses: overcoming translational challenges. *J Clin Invest* (2019) 129(4):1407–18. doi: 10.1172/JCI122287

6. Gangi A, Zager J. The safety of talimogene laherparepvec for the treatment of advanced melanoma. *Expert Opin Drug Saf* (2016), 2:1–5. doi: 10.1080/14740338.2017.1274729

7. Fukuhara H, Takeshima Y, Todo T. Triple-mutated oncolytic herpes virus for treating both fast- and slow-growing tumors. *Cancer Science*. (2021) 112(8):3293–301. doi: 10.1111/cas.14981

8. Diallo J, Boeuf F, Lai F, Cox J, Vaha-Koskela M, Abdelbary H, et al. A high-throughput pharmacoviral approach identifies novel oncolytic virus sensitizers. *Mol Ther* (2010) 18(6):1123–9. doi: 10.1038/mt.2010.67

9. Phan M, Watson M, Alain T, Diallo J. Oncolytic viruses on drugs: Achieving higher therapeutic efficacy. *ACS Infect Diseases*. (2018) 4(10):1448–67. doi: 10.1021/acsinfecdis.8b00144

10. Selman M, Rousso C, Bergeron A, Son H, Krishnan R, El-Sayes N, et al. Multi-modal potentiation of oncolytic virotherapy by vanadium compounds. *Mol Ther* (2018) 26(1):56–69. doi: 10.1016/j.ymthe.2017.10.014

11. McAusland T, van Vloten J, Santry L, Guilleman M, Rghei A, Ferreira E, et al. Combining vanadyl sulfate with Newcastle disease virus potentiates rapid innate immune-mediated regression with curative potential in murine cancer models. *Mol Ther - Oncolytics*. (2021) 20:306–24. doi: 10.1016/j.omto.2021.01.009

12. Pessoa J, Etcheverry S, Gambino D. Vanadium compounds in medicine. *Coordination Chem Rev* (2015) 301-302:24–48. doi: 10.1016/j.ccr.2014.12.002.

13. Thompson K, Lichter J, LeBel C, Scaife M, McNeill J, Orvig C. Vanadium treatment of type 2 diabetes: A view to the future. *J Inorganic Biochem* (2009) 103 (4):554–8. doi: 10.1016/j.jinorgbio.2008.12.003

14. León I, Butenko N, Di Virgilio A, Muglia C, Baran E, Cavaco I, et al. Vanadium and cancer treatment: Antitumoral mechanisms of three oxidovanadium(IV) complexes on a human osteosarcoma cell line. *J Inorganic Biochem* (2014) 134:106–17. doi: 10.1016/j.jinorgbio.2013.10.009

15. Kioseoglou E, Petanidis S, Gabriel C, Salifoglou A. The chemistry and biology of vanadium compounds in cancer therapeutics. *Coord Chem Rev* (2015) 301–302:87–105. doi: 10.1016/j.ccr.2015.03.010

16. Rozzo C, Sanna D, Garribba E, Serra M, Cantara A, Palmieri G, et al. Antitumoral effect of vanadium compounds in malignant melanoma cell lines. *J Inorg Biochem* (2017) 174:14–24. doi: 10.1016/j.jinorgbio.2017.05.010

17. Gamero AM, Larner AC. Vanadate facilitates interferon α-mediated apoptosis that is dependent on the Jak/Stat pathway. *J Biol Chem* (2001) 276 (17):13547–53. doi: 10.1074/jbc.M007948200.

18. Huang C, Zhang Z, Ding M, Li J, Ye J, Leonard SS, et al. Vanadate induces p53 transactivation through hydrogen peroxide and causes apoptosis. *J Biol Chem* (2000) 275(42):32516–22. doi: 10.1074/jbc.M005366200

19. Wong B, Bergeron A, Alluqmani N, Maznyi G, Chen A, Arulanandam R, et al. Dependency of EGFR activation in vanadium-based sensitization to oncolytic virotherapy. *Mol Ther Oncolytics*. (2022) 25:146–59. doi: 10.1016/j.omto.2022.04.004

20. Alkayyal AA, Tai L-H, Kennedy MA, de Souza CT, Zhang J, Lefebvre C, et al. NK-cell recruitment is necessary for eradication of peritoneal carcinomatosis with an IL12-expressing maraba virus cellular vaccine. *Cancer Immunol Res* (2017) 5(3):211–21. doi: 10.1158/2326-6066.CIR-16-0162

21. Lemay CG, Rintoul JL, Kus A, Paterson JM, Garcia V, Falls TJ, et al. Harnessing oncolytic virus-mediated antitumor immunity in an infected cell vaccine. *Mol Ther* (2012) 20(9):1791–9. doi: 10.1038/mt.2012.128

22. De Graaf JF, De Vor L, Fouchier RAM, Van Den Hoogen BG. Armed oncolytic viruses: A kick-start for antitumor immunity. *Cytokine Growth Factor Rev* (2018) 41:28–39. doi: 10.1016/j.cytogfr.2018.03.00

23. Yu J, Wei M, Becknell B, Trotta R, Liu S, Boyd Z, et al. Pro- and antiinflammatory cytokine signaling: reciprocal antagonism regulates interferon-gamma production by human natural killer cells. *Immunity*. (2006) 24(5):575–90. doi: 10.1016/j.immuni.2006.03.016

24. Thomas ED, Meza-Perez S, Bevis KS, Randall TD, Gillespie GY, Langford C, et al. IL-12 expressing oncolytic herpes simplex virus promotes antitumor activity and immunologic control of metastatic ovarian cancer in mice. *J Ovarian Res* (2016) 9(1):1–11. doi: 10.1186/s13048-016-0282-3.

25. Turner MD, Nedjai B, Hurst T, Pennington DJ. Cytokines and chemokines: At the crossroads of cell signalling and inflammatory disease. *Biochim Biophys Acta* (2014) 1843(11):2563–82. doi: 10.1016/j.bbamcr.2014.05.014

26. Castro F, Cardoso AP, Gonçalves RM, Serre K, Oliveira MJ. Interferon-gamma at the crossroads of tumor immune surveillance or evasion. *Front Immunol* (2018) 9:847. doi: 10.3389/fimmu.2018.00847

27. Lane RS, Femel J, Breazeale AP, Loo CP, Thibault G, Kaempf A, et al. IFNγ-activated dermal lymphatic vessels inhibit cytotoxic T cells in melanoma and inflamed skin. *J Exp Med* (2018) 215(12):3057–74. doi: 10.1084/jem.20180654

28. Russell L, Peng KW, Russell SJ, Diaz RM. Oncolytic viruses: Priming time for cancer immunotherapy. *BioDrugs* (2019) 33(5):485–501. doi: 10.1007/s40259-019-00367-0

29. Pai C-CS, Huang JT, Lu X, Simons DM, Park C, Chang A, et al. Clonal deletion of tumor-specific T cells by interferon-γ confers therapeutic resistance to combination immune checkpoint blockade. *Immunity* (2019) 50(2):477–92.e8. doi: 10.1016/j.immuni.2019.01.006

30. Ayers M, Lunceford J, Nebozhyn M, Murphy E, Loboda A, Kaufman DR, et al. IFN-γ-related mRNA profile predicts clinical response to PD-1 blockade. *J Clin Invest* (2017) 127(8):2930–40. doi: 10.1172/JCI91

31. Bourgeois-Daigneault M-C, Roy DG, Falls T, Twumasi-Boateng K, St-Germain LE, Marguerie M, et al. Oncolytic vesicular stomatitis virus expressing

interferon-γ has enhanced therapeutic activity. *Mol Ther Oncolytics.* (2016) 3 (16001):16001. doi: 10.1038/mto.2016.1

32. Vlaykova T, Talve L, Hahka-Kemppinen M, Hernberg M, Muhonen T, Collan Y, et al. Immunohistochemically detectable bcl-2 expression in metastatic melanoma: association with survival and treatment response. *Oncology* (2002) 62 (3):259–68. doi: 10.1159/000059574

33. Fisher DT, Chen Q, Skitzki JJ, Muhitch JB, Zhou L, Appenheimer MM, et al. IL-6 trans-signaling licenses mouse and human tumor microvascular gateways for trafficking of cytotoxic T cells. *J Clin Invest* (2011) 121(10):3846–59. doi: 10.1172/JCI44952

34. Kimura A, Naka T, Kishimoto T. IL-6-dependent and -independent pathways in the development of interleukin 17-producing T helper cells. *Proc Natl Acad Sci U.S.A.* (2007) 104(29):12099–104. doi: 10.1073/pnas.0705268104

35. Mikucki ME, Fisher DT, Ku AW, Appenheimer MM, Muhitch JB, Evans SS. Preconditioning thermal therapy:Flipping the switch on IL-6 for anti-tumour immunity. *Int J Hyperthermia.* (2013) 29(5):464–73. doi: 10.3109/02656736.2013.807440.

36. Esfandi F, Mohammadzadeh Ghobadloo S, Basati G. Interleukin-6 level in patients with colorectal cancer. *Cancer Lett* (2006) 244(1):76–8. doi: 10.1016/j.canlet.2005.12.003

37. Bramson JL, Hitt M, Addison CL, Muller WJ, Gauldie J, Graham FL. Direct intratumoral injection of an adenovirus expressing interleukin-12 induces regression and long-lasting immunity that is associated with highly localized expression of interleukin-12. *Hum Gene Ther* (1996) 7(16):1995–2002. doi: 10.1089/hum.1996.7.16-1995

38. Osada T, Berglund P, Morse MA, Hubby B, Lewis W, Niedzwiecki D, et al. Co-Delivery of antigen and IL-12 by Venezuelan equine encephalitis virus replicon particles enhances antigen-specific immune responses and antitumor effects. *Cancer Immunol Immunother.* (2012) 61(11):1941–51. doi: 10.1007/s00262-012-1248-y

39. Lyerly HK, Osada T, Hartman ZC. Right time and place for IL12: Targeted delivery stimulates immune therapy. *Clin Cancer Res* (2019) 25(1):9–11. doi: 10.1158/1078-0432.CCR-18-2819

40. Tugues S, Burkhard SH, Ohs I, Vrohlings M, Nussbaum K, Vom Berg J, et al. New insights into IL-12-mediated tumor suppression. *Cell Death Differ* (2015) 22 (2):237–46. doi: 10.1038/cdd.2014.134

41. Sangro B, Melero I, Qian C, Prieto J. Gene therapy of cancer based on interleukin 12. *Curr Gene Ther* (2005) 5(6):573–81. doi: 10.2174/156652305774964712

42. Vo JL, Yang L, Kurtz SL, Smith SG, Koppolu BP, Ravindranathan S, et al. Neoadjuvant immunotherapy with chitosan and interleukin-12 to control breast cancer metastasis. *Oncoimmunology.* (2014) 3(12):e968001. doi: 10.4161/21624011.2014.968001

43. Smith SG, Koppolu BP, Ravindranathan S, Kurtz SL, Yang L, Katz MD, et al. Intravesical chitosan/interleukin-12 immunotherapy induces tumor-specific systemic immunity against murine bladder cancer. *Cancer Immunol Immunother.* (2015) 64(6):689–96. doi: 10.1007/s00262-015-1672-x

**Appendix II: Syngeneic mouse model of human HER2+ metastatic breast cancer for the evaluation of trastuzumab emtansine combined with oncolytic rhabdovirus. Frontiers in Immunology, section Cancer Immunity and Immunotherapy.**

Zaid Taha[1,2], Mathieu J.F. Crupi[1,2], **Nouf Alluqmani[1,2]**, Faiha Fareez[3], Kristy Ng[1], Judy Sobh[1], Emily Lee[1], Andrew Chen[1], Max Thomson[1], Marcus M. Spinelli[1], Carolina S. Ilkow[1,2], John C. Bell[1,2], Rozanne Arulanandam[1†] and Jean-Simon Diallo[1,2*†]

[1]Centre for Cancer Therapeutics, Ottawa Hospital Research Institute, Ottawa, ON, Canada,
[2]Department of Biochemistry, Microbiology, and Immunology, Faculty of Medicine, University of Ottawa, Ottawa, ON, Canada,
[3]Department of Pathology and Molecular Medicine, McMaster University, Hamilton, ON, Canada

Accepted 30 March 2023; Published 19 April 2023 in Frontier in Immunology

**Author contribution**

Nouf Allumqmani contributed to *in vivo* animal investigations, flow cytometry related analyses, and virus propagation, purification and validation.
ZT, MC, **NA**, AC, MT, and MS performed and assisted with *in vivo* animal investigation. ZT, MC, and **NA** performed flow cytometry preparation and acquisition. ZT, MC, **NA**, and AC propagated, purified, and validated VSVD51.
ZT prepared the original manuscript with editorial contributions from RA, JS-D, MC, **NA**, CI, and JB.

**Appendix III: CRISPR-mediated rapid arming of poxvirus vectors enables facile generation of the novel immunotherapeutic STINGPOX**

Jack T. Whelan[1,2†,] Ragunath Singaravelu[1,2,3†,] Fuan Wang[4,5†,] Adrian Pelin[1,2†,] Levi A. Tamming[1,2], Giuseppe Pugliese[2], Nikolas T. Martin[1,2], Mathieu J. F. Crupi[1,2], Julia Petryk[2], Bradley Austin[2], Xiaohong He[2], Ricardo Marius[1,2], Jessie Duong[1,2], Carter Jones[2], Emily E. F. Fekete[1,2], **Nouf Alluqmani[1,2]**, Andrew Chen[2], Stephen Boulton[1,2], Michael S. Huh[2], Matt Y. Tang[2], Zaid Taha[1,2], Elena Scut[1,2], Jean-Simon Diallo[1,2], Taha Azad[1,2], Brian D. Lichty[4,5*,] Carolina S. Ilkow[1,2*] and John C. Bell[1,2*]

[1]Department of Biochemistry, Microbiology and Immunology, University of Ottawa, Ottawa, ON, Canada,
[2]Centre for Innovation Cancer Therapeutics, Ottawa Hospital Research Institute, Ottawa, ON, Canada, 3Public Health Agency of Canada, Ottawa, ON, Canada,
[4]McMaster Immunology Research Centre, Department of Medicine, McMaster University, Hamilton, ON, Canada,
[5]MG DeGroote Institute for Infectious Disease Research, McMaster University, Hamilton, ON, Canada

Accepted 05 December 2022; Published 13 January 2023 in Frontier in Immunology

## Author contribution

Nouf Alluqmani contributed to performing some experiments.

RS, JW, FW, AP, LT, GP, NM, MC, JP, BA, XH, RM, JD, CJ, EEFF, **NA**, AC, SB, MH, MT, ZT, and TA contributed to the design of experiments, performing experiments, and/or analysis of data.

**Appendix IV: Oncolytic virus driven T-cell-based combination immunotherapy platform for colorectal cancer.**

Mathieu J. F. Crupi[1,2], Zaid Taha[1,2], Thijs J. A. Janssen[1], Julia Petryk[1], Stephen Boulton[1,2], **Nouf Alluqmani[1,2],** Anna Jirovec[1,2], Omar Kassas[1], Sarwat T. Khan[1], Sydney Vallati[1,2], Emily Lee[1], Ben Zhen Huang[1], Michael Huh[1,3], Larissa Pikor[1,2,3], Xiaohong He[1], Ricardo Marius[1], Bradley Austin[1], Jessie Duong[1,2,3], Adrian Pelin[1,2,3], Serge Neault[1,2], Taha Azad[1,2], Caroline J. Breitbach[3], David F. Stojdl[3], Michael F. Burgess[3], Scott McComb[2,4], Rebecca Auer[1,2], Jean-Simon Diallo[1,2], Carolina S. Ilkow[1,2] and John Cameron Bell[1,2]*

[1]Centre for Innovative Cancer Research, Ottawa Hospital Research Institute, Ottawa, ON, Canada,
[2]Department of Biochemistry, Microbiology and Immunology, University of Ottawa, Ottawa,ON, Canada,
[3]Discovery Research, Turnstone Biologics Inc, Ottawa, ON, Canada, 4Human Health Therapeutics Research Centre, National Research Council, Ottawa, ON, Canada

Accepted 18 October 2022; Published 03 November 2022 in Frontier in Immunology

**Author contribution**

Nouf Alluqmani contributed to some flow cytometry experiments.
MC, ZT, TJ, NA, and SK completed and analyzed flow cytometry experiments.

**Appendix V: Identification of FDA-approved compound as SARS-CoV-2 blocking agent following a bioreporter drug screen.**

Zaid Taha,[1,2,*] Rozanne Arulanandam,[1,*] Glib Maznyi,[1] Elena Godbout,[1] Madalina E. Carter-Timofte,[4] Naziia Kurmasheva,[4] Line S. Reinert,4 Andrew Chen,1 Mathieu J.F. Crupi,[1] Stephen Boulton,[1] Geneviève Laroche,[2] Alexandra Phan,[2] Reza Rezaei,[1,2] **Nouf Alluqmani,[1,2]** Anna Jirovec,[1,2] Alexandra Acal,[1] Emily E.F. Brown,[1] Ragunath Singaravelu,[1] Julia Petryk,[1] Manja Idorn,[4] Kyle G. Potts,[5,6,7] Hayley Todesco,[5,6,7] Cini John,[5,6,7] Douglas J. Mahoney,[5,6,7] Carolina S. Ilkow,[1,2] Patrick Giguère,[2] Tommy Alain,[2,3] Marceline Côté,[2] Søren R. Paludan,[4] David Olagnier,[4] John C. Bell,[1,2] Taha Azad,[1] and Jean-Simon Diallo[1,2]

[1]Centre for Cancer Therapeutics, Ottawa Hospital Research Institute, Ottawa, ON K1H 8L6, Canada;
[2]Department of Biochemistry, Microbiology, and Immunology, Faculty of Medicine, University of Ottawa, Ottawa, ON K1H 8M5, Canada;
[3]Children's Hospital of Eastern Ontario Research Institute, Ottawa, ON K1H 8L1, Canada; 4Department of Biomedicine, Aarhus University, 8000 Aarhus C, Denmark;
[5]Alberta Children's Hospital Research Institute, University of Calgary, Calgary, AB T2N 4N1, Canada;
[6]Arnie Charbonneau Cancer Institute, University of Calgary, Calgary, AB T2N 4N1, Canada;
[7]Department of Microbiology, Immunology and Infectious Diseases, Cumming School of Medicine, University of Calgary, Calgary, AB T2N 4N1, Canada

Accepted 29 April 2022; Published in Molecular Therapy: the journal of the American Society of Gene Therapy

**Author contribution**

Nouf Alluqmani contributed to performing some experiments.
S.B., M.J.F.C., A.A., A.J., and **N.A**. assisted with experiments.

**Appendix VI: Virally programmed extracellular vesicles sensitize cancer cells to oncolytic virus and small molecule therapy.**

Wedge, M-E.*, Jennings, V.*, Crupi, M.*, Poutou, J.*, Jamieson, T., Pugliese, G., Souza, C., Petryk, J., Laight, B., Boileau, M., Taha, Z., **Alluqmani, N.,** McKay, H., Pikor, L., Tahsin Khan, S., Azad, T., Rezaei, R., Austin, B., He, X., Mansfield, D., Pelin, A., Rose, E., Brown, E., Crawford, N., Alkayyal, A., Surendran, A., Singaravelu, R., Roy, D., Migneco, G., McSweeney, B., Cottee, M.L., Jacobus, E., Keller, B., Geoffrion, M., Rayner, K., Chatterjee, A., Auer, R., Diallo, J.S., Gibbings, D., Tenoever, B., Melcher, A., Bell, J.

Accepted 07 April 2022; Published in Nature Communication

**Author contribution**

Nouf Alluqmani contributed to performing flow cytometry experiments and analyses. Z.T., **N.A.,** M.J.F.C. and S.T.K. performed flow cytometry experiments.

**Appendix VII: Dependency of EGFR activation in vanadium-based sensitization to oncolytic virotherapy.**

Boaz Wong,[1,2] Anabel Bergeron,[1,2] **Nouf Alluqmani,[1,2]** Glib Maznyi,[1] Andrew Chen,[1] Rozanne Arulanandam,[1] and Jean-Simon Diallo[1,2]

[1]Centre for Innovative Cancer Research, Ottawa Hospital Research Institute, 501 Smyth Road, Ottawa, ON K1H 8L6 Canada;
[2]Department of Biochemistry, Microbiology and Immunology, Faculty of Medicine, University of Ottawa, Ottawa, ON K1H 8M5, Canada

Accepted 13 November 2021; Published in Molecular Therapy

**Author contribution**

Nouf Alluqmani contributed to performing some of the *in vivo* experiments and assisted with the drug screen.
Investigation, B.W., A.B., R.A., **N.A.,** G.M. and A.C.

**Appendix VIII: Nanoluciferase complementation-based bioreporter reveals the importance of N-linked glycosylation of SARS-CoV-2 S for viral entry.**

Azad, T., Singaravelu, R., Taha, Z., Jamieson, T. R., Boulton, S., Crupi, M., Martin, N. T., Brown, E., Poutou, J., Ghahremani, M., Pelin, A., Nouri, K., Rezaei, R., Marshall, C. B., Enomoto, M., Arulanandam, R., **Alluqmani, N.,** Samson, R., Gingras, A. C., Cameron,D.W., Bell,J.C.

Accepted 02 June 2021; Published in Molecular Therapy: the Journal of the American Society of Gene Therapy

**Author contribution**

Nouf Alluqmani contributed to flow cytometry experiments and analyses.
Iinvestigation, T.A., R.S., Z.T., A.P., N.T.M., **N.A**., M.C., T.J., E.E.F.B., J.P., M.G., R.S., R.R., and R.A

**Appendix IX: The strategic combination of trastuzumab emtansine with oncolytic rhabdoviruses leads to therapeutic synergy.**

Arulanandam, R., Taha, Z., Garcia, V., Selman, M., Chen, A., Varette, O., Jirovec, A., Sutherland, K., Macdonald, E., Tzelepis, F., Birdi, H., **Alluqmani, N.,** Landry, A., Bergeron, A., Vanderhyden, 4 B., & Diallo, J. S.

Accepted 22 May 2020; Published in Communication Biology.

**Author contribution**

Nouf Alluqmani contributed to flow cytometry experiments and analyses.
Z.T., A.J., S.B., **N.A**., A.L. and F.T. performed flow cytometry acquisition and analysis.

# Curriculum Vitae

**AWARDS**

**2018-2023** *Received scholarship (tuition and stipend) from the **King Faisal Specialist Hospital and Research Institute for Ph.D degree** as represented by the Saudi Arabian Cultural Bureau.*

***2022*** *Received a travel award from BioCanRx to attend BioCanRx's Summit for Cancer Immunotherapy (Summit4CI).*

***2022*** *Received **a Public Health Agency of Canada Award in recognition of contributions to Canada's response to COVID-19, for Outstanding Achievements in the Protection of the Health of Canadians.***

**2021** *Received **Dr. Andrés Petrasovits Award for Excellence in Public Health** for National Advisory Committee on Immunization (NACI) Secretariat as a member of the team.*

**2011-2016** *Received scholarship (tuition and stipend) from the **Ministry of Higher Education, King Abdullah Scholarship Program, Kingdom of Saudi Arabia (KSA) for my academic English program and master's degree.***

**EDUCATION**

**May 2018- 2023** **Full-time** Ph.D. (doctorate) student in Microbiology and Immunology department at Faculty of Medicine, University of Ottawa.

- **5 years full-time program, thesis-based, Immunotherapy area specialist**
- **Supervisor:** Dr. Jean-Simon Diallo
- Required to successfully complete her Ph.D. studies 6 credits graduate courses, seminar course (MIC8366), comprehensive examination (MIC9998), and thesis (THD9999).
- **Research area:** Work on a project focusing on using small molecules in combination with oncolytic viruses to treat cancer.

**Sept 2013- Jan 2016** **Master of Science,** Department of Cell and System Biology, Specialized in immunology University of Toronto, Toronto, Canada.

- **2 years full-time program, thesis-based, immunology area specialist**
- **Thesis:** The role of glycan-binding protein Galectin-9 in B cell activation. **Supervisor:** Dr. Bebhinn Treanor
- **Area of specialist: Immunology**

**2006-2010** ***Bachelor's Degree in Laboratory Medicine with Honors***, College of Applied Medical Science, Umm Al-Qura University, Makkah, K.S.A. *All in-class studies and field work conducted in English.*

- **The First four years focus on in-class studies and labs.**
- ***Undergraduate Research***, Department of Laboratory Medicine, Umm Al-Qura University, Makkah, Practical Research Course, Faculty of Applied Medical Sciences. Project: The Effect of Cupping Therapy on The Immune System.
- **5th year internship in different clinical diagnostic departments (**Maternity and Children Hospital, Makkah, K.S.A.

**English Proficiency Test**

**Feb 2013** **IELTS final grade: 6.5 with up to 6 in each band Academic English Language Program**

**Jan 2013 – April 2013** **English Language Program**, Advance Academic Skills Course, University of Toronto.
**Sept 2012 - Dec 2012** **English Language Program**, Academic English Program, Level 60, University of Toronto.
**Jan 2012 - Mar 2012** **English Language Program**, Academic English Program, Level 50, University of Toronto.

**RESEARCH EXPERIENCES:**

**May 2018 – present** **Graduate student,** Ph.D in Microbiology and Immunology, Faculty of Medicine, University of Ottawa, Ottawa, Canada.

- 4 years full-time program, thesis based, Immunology area specialist
- Required to successfully complete her Ph.D. studies 6 credits graduate courses, seminar course (MIC8366), comprehensive examination (MIC9998), and thesis (THD9999).
- Research area: Work on a project focusing on using small molecules in combination with oncolytic viruses to treat cancer.
- Developed expertise in oncolytic virotherapy, immune responses, molecular immunology, molecular and cellular biology, T-cell activation, designing immunological-based assays, advanced optical microscopy skills, and Flow cytometry.
- Expertise in animal handling, injection procedure and dissection.
- Analysis skills: using imaging software (Volocity and ImageJ), statistical analysis using prism, and figure design using Adobe Indesign.

- Data analyses, Statistic analyses.
- Beginner in R programming and 10X genomic analyses.
- Involved in systemic review and data extraction.
- Expertise in flow cytometry analyses, multiparameter panel designing and immune profiling.
- Virus cloning and production.
- Expertise in therapeutic treatments and vaccine development.
- Expertise in oncolytic viruses.
- Expertise in immune responses.

**Sept 2013- Jan 2016** **Graduate student,** Master of Science at Cell and System Biology Department, university of Toronto.

- Doing master research in the area of immunology.
- 2 years full-time program, thesis based, specialized in immunology.
- Developed expertise in molecular immunology, molecular and cellular biology, B cell activation, advanced optical microscopy skills, artificial Lipid Bilayer, Flow cytometry, immunoblotting techniques, mass spectrometry skills, Super Resolution image techniques (SIM), expert in total internal reflection fluorescence microscopy (TIRFM), professional immunostaining techniques, working with knockout animal model, and more specialized and cutting edge techniques in biochemical and immunological field.
- Expertise in animal handling, injection procedure and dissection.
- Analysis skills: using imaging software (Volocity and ImageJ), statistical analysis using prism, and figure design using Adobe Indesign.

**2008-2009** ***Undergraduate Research***, Department of Laboratory Medicine, Umm Al-Qura University, Makkah

- Practical Research Course at fourth year, Faculty of Applied Medical Sciences. Project: The Effect of Cupping Therapy on The Immune System. Supervisor: Dr. Waheeb Alharbi.
- Full year research including collecting sample, analyzing them, analyzing data, writing thesis, and participating in committee defense.
- Immunology area specialist.

**PROFESSIONAL EXPERIENCES**

- Student analyst, **Public Health Agency of Canada | Agence de la santé publique du Canada, from Jan 2021 – Aug 2022 (Part-time).**

- Member of a team in the National Advisory Committee on Immunization (NACI) Secretariat. Track COVID-19-related updates and support with immunology-related tasks; a member of the Evidence Extraction Team for Research Analysis (EXTRA).

- Internship at **different clinical diagnostic departments and laboratories,** Maternity and Children Hospital, Makkah, K.S.A, from 2009-2010.

**PUBLICATION**

1. **Alluqmani, N.**, Jirovec, A., Taha, Z., Varette, O., Chen, A., Serrano, D., Maznyi, G., Khan, S., Forbes, N. E., Arulanandam, R., Auer, R. C., & Diallo, J. S. (**2022**). Vanadyl sulfate-enhanced oncolytic virus immunotherapy mediates the antitumor immune response by upregulating the secretion of pro-inflammatory cytokines and chemokines. *Frontiers in immunology*, *13*, 1032356.

2. Stephen Boulton; Joanna Poutou; Rida Gill; **Nouf Alluqmani**; Xiaohong He; Ragunath Singaravelu; Mathieu J.F. Crupi; Julia Petryk; Bradley Austin; Leonard Angka; Zaid Taha; Iris Teo; Siddharth Singh; Rameen Jamil; Ricardo Marius; Nikolas Martin; Taylor Jamieson; Taha Azad; Jean-Simon Diallo; Carolina S. Ilkow; John C. Bell. A T Cell-Targeted Multi-Antigen Poxvirus Vector Vaccine Generates Robust Cellular and Humoral Immunity Against SARS-CoV-2 Infection. MOLECULAR-THERAPY-D-23-00609, (Under revision), **2023**

3. Taha, Z., Crupi, M., **Alluqmani, N.,** Fareez, F., Ng, K., Sobh, J., Lee, E., Chen, A., Thomson, M., Spinelli, M. M., Ilkow, C. S., Bell, J. C., Arulanandam, R., Diallo, J.S. (**2023**). Syngeneic mouse model of human HER2+ metastatic breast cancer for the evaluation of trastuzumab emtansine combined with oncolytic rhabdovirus. Frontiers in Immunology, section Cancer Immunity and Immunotherapy.

4. Whelan, J. T., Singaravelu, R., Wang, F., Pelin, A., Tamming, L. A., Pugliese, G., Martin, N. T., Crupi, M. J. F., Petryk, J., Austin, B., He, X., Marius, R., Duong, J., Jones, C., Fekete, E. E. F., **Alluqmani, N.,** Chen, A., Boulton, S., Huh, M. S., Tang, M. Y., … Bell, J. C. (**2023**). CRISPR-mediated rapid arming of poxvirus vectors enables facile generation of the novel immunotherapeutic STINGPOX. Frontiers in immunology, 13, 1050250.

5. Crupi, M. J. F., Taha, Z., Janssen, T. J. A., Petryk, J., Boulton, S., **Alluqmani, N.,** Jirovec, A., Kassas, O., Khan, S. T., Vallati, S., Lee, E., Huang, B. Z., Huh, M., Pikor, L., He, X., Marius, R., Austin, B., Duong, J., Pelin, A., Neault, S., … Bell, J. C. (**2022**). Oncolytic virus driven T-cell-based combination immunotherapy platform for colorectal cancer. Frontiers in immunology, 13, 1029269.

6. Taha, Z.*, Arulanandam, R.*, Maznyi, G., Godbout, E., Carter-Tomofte, M.E., Karmasheva, N., Reinert, L.S., Chen, A., Crupi, M.J.F., Boulton, S., Laroche, G., Phan, A., **Alluqmani, N.,** Jirovec, A., Acai, A., Brown, E.E.F., Singaravelu, R., Petryk, J., Idorn,

M., Potts, K.G., Todesco, H., John, C., Mahoney, D.J., Ilkow, C.S., Giguère, P, Alain, T., Côté, M., Paludan, S.R., Olagnier, D., Bell, J.C., Azad, T., Diallo, J.S. Identification of FDA-approved compound as SARS-CoV-2 blocking agent following a bioreporter drug screen. The journal of the American Society of Gene Therapy, **2022**

7. Wedge, M-E.*, Jennings, V.*, Crupi, M.*, Poutou, J.*, Jamieson, T., Pugliese, G., Souza, C., Petryk, J., Laight, B., Boileau, M., Taha, Z., **Alluqmani, N.,** McKay, H., Pikor, L., Tahsin Khan, S., Azad, T., Rezaei, R., Austin, B., He, X., Mansfield, D., Pelin, A., Rose, E., Brown, E., Crawford, N., Alkayyal, A., Surendran, A., Singaravelu, R., Roy, D., Migneco, G., McSweeney, B., Cottee, M.L., Jacobus, E., Keller, B., Geoffrion, M., Rayner, K., Chatterjee, A., Auer, R., Diallo, J.S., Gibbings, D., Tenoever, B., Melcher, A., Bell, J. Virally programmed extracellular vesicles sensitize cancer cells to oncolytic virus and small molecule therapy., Nature Communications, **2022**

8. Wong B, Bergeron A, **Alluqmani N**, Maznyi G, Chen A, Arulanandam R, et al. Dependency of EGFR activation in vanadium-based sensitization to oncolytic virotherapy. Mol Ther Oncolytics. **2021**

9. Azad, T., Singaravelu, R., Taha, Z., Jamieson, T. R., Boulton, S., Crupi, M., Martin, N. T., Brown, E., Poutou, J., Ghahremani, M., Pelin, A., Nouri, K., Rezaei, R., Marshall, C. B., Enomoto, M., Arulanandam, R., **Alluqmani, N.,** Samson, R., Gingras, A. C., Cameron,D.W., Bell,J.C.(**2021**). Nanoluciferase complementation-based bioreporter reveals the importance of N-linked glycosylation of SARS-CoV-2 S for viral entry. Molecular therapy: the journal of the American Society of Gene Therapy, 29(6), 1984–2000. https://doi.org/10.1016/j.ymthe.2021.02.007

10. Arulanandam, R., Taha, Z., Garcia, V., Selman, M., Chen, A., Varette, O., Jirovec, A., Sutherland, K., Macdonald, E., Tzelepis, F., Birdi, H., **Alluqmani, N.,** Landry, A., Bergeron, A., Vanderhyden, 4 B., & Diallo, J. S. (**2020**). The strategic combination of trastuzumab emtansine with oncolytic rhabdoviruses leads to therapeutic synergy. Communications biology, 3(1), 254. https://doi.org/10.1038/s42003-020-0972-7

11. Anh Cao, **Nouf Alluqmani**, Fatima Hifza Mohammed Buhari, Laabiah Wasim, Logan K. Smith, Andrew T. Quaile, Michael Shannon, Zaki Hakim, Hossai Furmli, Dylan M. Owen, Alexei Savchenko & Bebhinn Treanor. Nature Communications, **2018**. DOI: 10.1038/s41467-018-05771-8

**CONFERENCES**

**presented a poster or presentation at each of these Conferences.**

**2019 and 2021** **Canadian Cancer Research Conference (CCRC)**

- Poster presentation

**2019, 2020, 2021, 2022 and 2023** **BMI research day**

- Oral presentation (three times)

- Poster presentation (two times)

| | |
|---|---|
| **2019, 2020 and 2021** | **Ottawa Hospital Research Institute Day (OHRI)** |

- Poster presentation

| | |
|---|---|
| **2021and 2022** | **International Oncolytic virus Conference (IOVC)** |

- Poster presentation

| | |
|---|---|
| **2021 and 2022** | **BioCanRx's Summit for Cancer Immunotherapy (Summit4CI)** |

- Poster presentation

| | |
|---|---|
| **2015** | **CSB Research Day** |

- Poster presentation

| | |
|---|---|
| **2015** | **28th Annual Spring Meeting of the Canadian Society for Immunology, Winnipeg, Manitoba, Canada.** |

- Poster presentation

**ORAL PRESENTATION:**

1. Vanadate-enhanced oncolytic virus immunotherapy mediates the anti-tumor immune response by upregulating the secretion of pro-inflammatory cytokines and chemokines**. Nouf Alluqmani**, Anna Jirovec , Zaid Taha, Rozanne Arulanandam , Andrew Chen, Daniel Serrano , Oliver Varette, Glib Maznyi , Anabel Bergeron, Sarwat Khan, Nicole Forbes, Rebecca C. Auer and Jean-Simon Diallo. **BMI day**, April **2022.**
2. Impact of vanadium-enhanced oncolytic virus immunotherapy on the anti-tumor immune response. **Nouf Alluqmani**, Anna Jirovec, Zaid Taha, Andrew Chen, Rozanne Arulanandam, Daniel Serrano, Glib Maznyi, Alexandra Acal, Nicole Forbes, Debbie C. Crans, Jean-Simon Diallo. **BMI day**, April 15, **2021**.
3. Impact of viral sensitizer-enhanced oncolytic virus immunotherapy on the anti-tumor immune response. **Nouf Alluqmani**, Anabel Bergeron, Andrew Chen, Sarwat Khan, Nicole Forbes, Rozanne Arulanandam, Christiano Souza, Debbi C. Crans , Jean-Simon Diallo. **BMI day, 2020**.

**POSTER PRESENTATION:**

1. Vanadate-enhanced oncolytic virus immunotherapy mediates the anti-tumor immune response by upregulating the secretion of pro-inflammatory cytokines and chemokines. **Nouf Alluqmani**, Anna Jirovec , Zaid Taha, Rozanne Arulanandam , Andrew Chen, Daniel Serrano , Oliver Varette, Glib Maznyi , Anabel Bergeron, Sarwat Khan, Nicole Forbes, Rebecca C. Auer and Jean-Simon Diallo. **BMI Day, February 2023**
2. Vanadate-enhanced oncolytic virus immunotherapy mediates the anti-tumor immune response by upregulating the secretion of pro-inflammatory cytokines and chemokines. **Nouf Alluqmani**, Anna Jirovec , Zaid Taha, Rozanne Arulanandam , Andrew Chen, Daniel Serrano , Oliver Varette, Glib Maznyi , Anabel Bergeron, Sarwat Khan, Nicole Forbes, Rebecca C. Auer and Jean-Simon Diallo. **BMI Scientific symposium, May 2022.**

3. Vanadate-enhanced oncolytic virus immunotherapy mediates the anti-tumor immune response by upregulating the secretion of pro-inflammatory cytokines and chemokines. **Nouf Alluqmani**, Anna Jirovec , Zaid Taha, Rozanne Arulanandam , Andrew Chen, Daniel Serrano , Oliver Varette, Glib Maznyi , Anabel Bergeron, Sarwat Khan, Nicole Forbes, Rebecca C. Auer and Jean-Simon Diallo. **IOVC, October 23-26, 2022 .**
4. Vanadyl Sulfate-enhanced oncolytic virus immunotherapy mediates the antitumor immune response by upregulating the secretion of pro-inflammatory cytokines and chemokines. **Nouf Alluqmani**, Anna Jirovec, Zaid Taha, Oliver Varette, Andrew Chen, Daniel Serrano, Glib Maznyi, Sarwat Khan, Nicole E. Forbes, Rozanne Arulanandam, Rebecca C. Auer1,4, Jean-Simon Diallo. Summit4CI, **BioCanRx, November 19-22, 2022.**
5. Impact of vanadium-enhanced oncolytic virus immunotherapy on the anti-tumor immune response. **Nouf Alluqmani**, Anna Jirovec, Zaid Taha, Andrew Chen, Rozanne Arulanandam, Daniel Serrano, Glib Maznyi, Alexandra Acal, Nicole Forbes, Debbie C. Crans, Jean-Simon Diallo**. IOVC, November 5-7, 2021.**
6. Impact of vanadium-enhanced oncolytic virus immunotherapy on the anti-tumor immune response. **Nouf Alluqmani**, Anna Jirovec, Zaid Taha, Andrew Chen, Rozanne Arulanandam, Daniel Serrano, Glib Maznyi, Alexandra Acal, Nicole Forbes, Debbie C. Crans, Jean-Simon Diallo. **CCRC, November 11-14, 2021.**
7. Impact of vanadium-enhanced oncolytic virus immunotherapy on the anti-tumor immune response. **Nouf Alluqmani**, Anna Jirovec, Zaid Taha, Andrew Chen, Rozanne Arulanandam, Daniel Serrano, Glib Maznyi, Alexandra Acal, Nicole Forbes, Debbie C. Crans, Jean-Simon Diallo. **OHRI research day, November 17-18, 2021.**
8. Impact of vanadium-enhanced oncolytic virus immunotherapy on the anti-tumor immune response. **Nouf Alluqmani**, Anna Jirovec, Zaid Taha, Andrew Chen, Rozanne Arulanandam, Daniel Serrano, Glib Maznyi, Alexandra Acal, Nicole Forbes, Debbie C. Crans, Jean-Simon Diallo. **Summit4CI, BioCanRx, November 19-22, 2021**.
9. Impact of viral sensitizer-enhanced oncolytic virus immunotherapy on the anti-tumor immune response. **Nouf Alluqmani**, Anabel Bergeron, Andrew Chen, Sarwat Khan, Nicole Forbes, Rozanne Arulanandam, Christiano Souza, Debbi C. Crans , Jean-Simon Diallo, **AAI, May 2020.**
10. Impact of viral sensitizer-enhanced oncolytic virus immunotherapy on the anti-tumor immune response. **Nouf Alluqmani**, Anna Jirovec, Zaid Taha, Andrew Chen, Rozanne Arulanandam, Daniel Serrano, Glib Maznyi, Alexandra Acal, Nicole Forbes, Debbie C. Crans, Jean-Simon Diallo. **OHRI research day, November 17-18, 2020.**
11. Impact of viral sensitizer-enhanced oncolytic virus immunotherapy on the anti-tumor immune response. **Nouf Alluqmani**, Anabel Bergeron, Andrew Chen, Sarwat Khan, Nicole Forbes, Rozanne Arulanandam, Christiano Souza, Debbi C. Crans , Jean-Simon Diallo, **IOVC, November 2019.**
12. Impact of viral sensitizer-enhanced oncolytic virus immunotherapy on the anti-tumor immune response. **Nouf Alluqmani**, Anabel Bergeron, Andrew Chen, Sarwat Khan, Nicole Forbes, Rozanne Arulanandam, Christiano Souza, Debbi C. Crans , Jean-Simon Diallo, **BMI day, May 2019.**

**TRAINING AND CERTIFICATION**

| | |
|---|---|
| **2013- present** | **Certificate in Animal Training and Care** |
| **2013-present** | **Certificate in Biosafety course** |
| **Sept 2014** | **Certificate in attending Emotional smart workshop.** |
| **2009-2010** | **Training Certificate, Department of Laboratory and Blood Bank, Maternity and Children Hospital, Makkah, K.S.A.** |
| **2009-2010** | **Certificate of Internship, Faculty of Applied Medical Sciences (Laboratory Medicine), BCs. In Med. Sciences, Umm Al-Qura University, Makkah, K.S.A** |

**VOLUNTEER EXPERIENCE AND OTHER ACTIVITIES**

**2018- present**, **Volunteer,** Terry Fox run

**2020- present, Volunteer,** Let's talk science.

**2021- present**, **Volunteer,** Let's talk cancer.

**2014- present, Volunteer,** as a photographer at some social events.

**2021- present, Member** of Cancer Therapeutic Program student committee.

**2020-2021, Member**, American Association of Immunologists (AAI)

**2013-2016, Member,** Canadian Society of Immunology (CSI)

**2011-2016, Volunteer**, Saudi Association of Toronto (Nadi Toronto), participated in different events and organized some of them.

**2012**, **Volunteer,** Canadian Breast Cancer Society, Toronto, Canada: Marketing Assistant.

**2012**, **Volunteer**, Second Kicks Foundation, Toronto, Canada: Uniform Packaging Assistant.

**2012, Volunteer,** Central Neighborhood House, Toronto, Canada: Kids Club St. Patrick's Day Breakfast-Set-up Assistant and Sever (March 2012).

**OTHER SKILLS**

- Bilingual: Arabic, English.
- Photographer.
- Sketching.
- Drawing.
- Event designer.
- Writer.
- Designer.